

© 2004 by Augusto Moita de Deus. All rights reserved

A THERMAL AND MECHANICAL MODEL OF LASER CLADDING

BY

AUGUSTO MOITA DE DEUS

B.S., Physics, University of Lisbon, 1989
M.Sc., Materials Engineering, Instituto Superior Tecnico, Lisbon, 1993

DISSERTATION

Submitted in partial fulfillment of the requirements
for the degree of Doctor of Philosophy in Mechanical Engineering
in the Graduate College of the
University of Illinois at Urbana-Champaign, 2004

Urbana, Illinois

CERTIFICATE OF COMMITTEE APPROVAL

*University of Illinois at Urbana-Champaign
Graduate College*

April 13, 2004

We hereby recommend that the thesis by:

AUGUSTO MOITA DE DEUS

Entitled:

A THERMAL AND MECHANICAL MODEL OF LASER CLADDING

Be accepted in partial fulfillment of the requirements for the degree of:

Doctor of Philosophy

Signatures:



Director of Research



Head of Department

Committee on Final Examination*



Chairperson



Committee Member



Committee Member



Committee Member

Committee Member

* Required for doctoral degree but not for master's degree

Abstract

Laser Cladding (LC) is a coating manufacturing technique, in which a laser beam is used to deposit one or several layers of a certain clad material onto a substrate, in such a way that a sound interfacial bond is formed, without significant dilution of one material into the other. LC has received considerable attention, *e.g.* in the field of Rapid Manufacturing, due to its ability to quickly produce near-net shape parts of complex geometries and flexible compositions. It is also an attractive scientific tool, as it provides the potential to produce alloys of arbitrary nominal composition.

Mathematical modeling is a useful tool to investigate the range of processing parameters that lead to successful cladding. This is done, primarily, by performing a heat transfer analysis. Nevertheless, it is convenient to also have a mechanical model of the process: thermally cycling together materials that have different compositions and/or thermal expansion reference temperatures, gives rise to residual stress, which can bring the fabricated parts to (or, near to) failure conditions. The Finite Element (FE) method provides an adequate modeling tool for LC, due to its ability to accommodate both thermal and mechanical analysis, as well as a good description of LC geometric features.

2D and 3D FE lagrangian models were developed using the AbaqusTM software. Simulation results were obtained for a system (cladding of C95600 copper on AA333 aluminum alloy) in which experiments had been successfully carried out. A simple model of dilution, *i.e.* the change in local composition due to mixing, is included. In 3D stress analysis, numerical convergence is seen to be a critical issue. A recommendation is made for modeling of LC and similar processes: 1) use 2D models to swiftly explore parameter space; 2) carry out 3D temperature simulations, with meshes matching the process geometry (curved boundaries) and; 3) perform the stress analysis with more regular meshes (with overall planar boundaries) that are more likely to lead to convergence.

Keywords: laser materials processing, laser cladding, solid freeform fabrication, rapid prototyping, rapid manufacturing, layered manufacturing, finite element method, residual stress, mathematical modeling.

To Almighty God

I wish to dedicate this thesis, first of all, to the Creator.

I sometimes like to view God as the Great Mathematician who at some point became the Great Physicist, in setting up mathematics as a language of reality, who then acted as the Great Engineer, while putting reality in motion and making things work.

To Alexandra, Filipa and Miguel

This thesis is also dedicated to the ones that I share my life with, namely my wife Alexandra, my daughter Filipa and my son Miguel.

We share a name, a home, our lives and so much more.

Acknowledgements

There are so many individuals that in one way or another merit my thankfulness that there is the risk, actually the certainty, that I am going to forget someone. So, whether named here or not, I would like to thank all that throughout the years helped me in this journey.

First of all, I want to thank my wonderful family: my wife Alexandra, whose loyal and constant support made this project possible. Was I going to write all I wanted to in this regard, it would fill so many pages; my wonderful children, Filipa and Miguel who are what I'm most proud for in life; my beloved parents, João and Eulália Moita de Deus.

Next I need to thank Professor Jyoti Mazumder for all his patient support and guidance throughout the years. I was not the easiest of students that he has had to deal with during his career, but I was certainly given the best advisor I could ever have had. Being one of the leading personalities in the Laser Materials Processing community in the world, Professor Mazumder was always available to give direction, with a keen eye to identify the essential aspects of scientific research. His words were always encouraging, making a student such as myself feel at ease and empowered with room for scientific initiative.

Special words of appreciation have to be extended to the other dissertation committee members (Professors Lawrence, Sehitoglu, Thomas) for their suggestions, patience and encouragement.

Many thanks go to my colleagues, fellow students and post-doc researchers, first at the Center for Laser Aided Materials Processing, UIUC and then at the Center for Laser Aided Intelligent Manufacturing, University of Michigan, Ann Arbor, some of which had a direct impact on my research, especially J. Choi, J. Kelly and P. Mohanty, as well as all the others with whom vital companionship was shared: M. Douglass, H. Ki, T. Asghari, T. Duffey, H. Chung, K. Nagarathnam and J. Koch. Many thanks go to all the staff (in particular, C. Snyder and K. Bryan) and faculty at the Mechanical and Industrial Engin. Dept., UIUC,

especially the Professors who taught the excellent courses I attended (Professors Georgiadis, Mazumder, Sehitoglu, Socie, Thomas, Tortorelli and Walker).

Acknowledgements are due with equal strength to many individuals back in Portugal, first of all to Professor R. Vilar, who made his Laser Materials Processing group at Instituto Superior Técnico one of the leading institutions of the kind in the world. I had joined the group from its early beginnings and later, after my return to Portugal, I was allowed to proceed with my research within it, to which I am grateful. The whole Laser Materials Processing group in Lisbon deserves my thanks, especially Rogério Colaço (who took good care of so many of my personal matters during my absence) and Amélia Almeida (whose hardwork and generosity toward the group is one of the keys of its success).

Since returning to Portugal other research was carried out, so many thanks go to Lino Costa (whose Ph.D. dissertation will in part pick up from aspects that I'm leaving behind; while doing that, he ended up having a direct impact on my research) and to Professor M. Amaral Fortes, one of the leading portuguese scientists. It's difficult to put in words how intellectually rewarding were some of our brainstorming discussions on grain growth and scaling.

A special word of acknowledgement goes to Professor O. Conde and also to A. J. Silvestre, with whom I started my scientific career. Thanks are given also to all faculty and staff at the Materials Engineering Department, Instituto Superior Técnico (the Engineering College of the Technical University of Lisbon), in particular, the Department Directive Committees. Support from staff at the Computational Mechanics Lab., Civil Engin. Dept., I.S.T., where some of the simulations were ran, is also acknowledged.

Thanks will also have to go to all who at the time were part the portuguese graduate student community in Urbana-Champaign, especially P. Ferreira. A very deep expression of gratitude goes as well to all our dear christian friends at Woodland Park and Arbor Oaks.

The research presented in this dissertation was supported through grants from FLAD (Portuguese and American Foundation for Development), grant 50/94, in the earlier stages of the project and then, after being admitted as a graduate student at the UIUC, from FCT (the portuguese Foundation for Science and Technology), grant PRAXIS XXI BD/5092/95. Their financial support is gratefully acknowledged.

Table of Contents

	Page
1. Introduction.....	1
1.1. Laser cladding: fundamentals	1
1.1.1. Definition	1
1.1.2. Techniques	3
1.1.3. Bonding and dilution.....	5
1.1.4. Scientific importance	8
1.2. Similar processes	9
1.2.1. Laser alloying.....	9
1.2.2. Laser welding.....	10
1.3. Scope of thesis research.....	10
1.3.1. The finite element method	11
1.3.2. Relevant phenomena.....	12
1.3.3. Pre-processing.....	12
1.3.4. Results.....	14
1.3.5. Issues not covered.....	14
1.4. Literature review.....	16
1.4.1. General references	16
1.4.2. Modeling of laser cladding: without stress analysis	17
1.4.3. Modeling of laser cladding: with stress analysis	19
2. A simple model for dilution in laser cladding.....	23
2.1. Introduction.....	23
2.2. Single-material system.....	23
2.3. Bi-material system	34
2.3.1. Substrate with a higher melting point	34
2.3.2. Substrate with a lower melting point	36
2.4. Model implementation.....	39
2.4.1. Interface with fixed composition	40
2.4.2. Interface with varying composition	41
3. Finite element modeling of laser cladding.....	44
3.1. Introduction.....	44
3.2. Pre-processing scheme.....	45
3.2.1. Mesh design	45
3.2.2. Nodal definitions.....	48
3.2.3. Lagrangian vs. eulerian approach	50
3.2.4. Successive addition of new elements.....	51
3.2.5. Mesh generation in 3D.....	52

3.3. Heat transfer analysis.....	53
3.3.1. Governing equations.....	53
3.3.2. Mass and heat transfer consistency.....	56
3.4. Stress analysis.....	57
3.4.1. Residual strain and stress.....	57
3.4.2. Governing equations.....	58
3.5. Materials properties.....	60
4. Results.....	64
4.1. Introduction.....	64
4.2. Element library.....	65
4.3. Mesh independence.....	67
4.4. 2D FE models.....	70
4.5. 3D FE models.....	78
5. Discussion and Conclusion.....	90
5.1. Comparison with experimental results.....	90
5.2. Summary.....	94
5.3. Conclusions.....	97
5.4. Suggestions for future research.....	98
References.....	100
Appendix A. Input file generator files.....	106
Appendix B. Materials properties.....	136
Appendix C. Sample Abaqus™ input files.....	142
Appendix D. Computer runs.....	185
Vita.....	186

List of Figures

	Page
Figure 1. Longitudinal section of typical laser clad sample.....	2
Figure 2. Transversal section of typical laser clad sample.....	2
Figure 3. Parallel clad tracks, with overlap.....	3
Figure 4. Buildup of clad tracks, forming a wall.....	4
Figure 5. Schematic of laser cladding setup.....	5
Figure 6. High dilution clad track.....	6
Figure 7. Low dilution clad track.....	6
Figure 8. Definition of dilution parameter.....	7
Figure 9. Longitudinal section of laser clad material: single-material case.....	24
Figure 10. Insufficient energy leads to unacceptably small melt pool.....	24
Figure 11. Improper location of laser beam: toward back.....	25
Figure 12. Improper location of laser beam: toward front.....	25
Figure 13. Clad cross-section, assumed cylindrical in shape.....	26
Figure 14. Moving point source: schematic of temperature field.....	27
Figure 15. Extreme proper location of laser beam: toward back.....	28
Figure 16. Improper location of laser: inconsistent location of clad melt isotherm....	28
Figure 17. Possible location of laser beam.....	29
Figure 18. Extreme proper location of laser beam: toward front.....	29
Figure 19. Definition of minimum laser power.....	29
Figure 20. Definition of dilution parameter.....	30
Figure 21. Definition of maximum laser power.....	30
Figure 22. View of (half) clad bead. Melt pool spans height and width of track.....	31
Figure 23. Top view of (half) clad bead.....	32
Figure 24. Transient stage: formation of stable clad track.....	33
Figure 25. Substrate with higher melting point: threshold condition with no mixing..	34
Figure 26. Substrate with higher melting point: good mixing.....	35
Figure 27. Substrate with higher melting point: moderate mixing and stratification...	36
Figure 28. Substrate with lower melting point: threshold condition with no mixing...	36
Figure 29. Substrate with lower melting point: little mixing.....	37
Figure 30. Substrate with lower melting point: good mixing.....	38
Figure 31. Substrate with lower melting point: mixing and stratification.....	38
Figure 32. Melt pool showing early solidification pattern on the interface.....	39
Figure 33. Definition of the interface region.....	40
Figure 34. Relationship between peak temperature and final composition.....	41
Figure 35. Thermal cycles at various depths (schematic).....	42
Figure 36. Node numbering scheme.....	49
Figure 37. Mesh activation scheme.....	51
Figure 38. Typical 2D 4-node linear element.....	66
Figure 39. Typical 3D 8-node linear element.....	66
Figure 40. Typical 3D 6-node linear element.....	67

Figure 41. Mesh independence study: mesh comparison.....	68
Figure 42. Mesh independence study: temperature.....	69
Figure 43. Mesh independence study: Von Mises stress.....	69
Figure 44. Mesh independence study: longitudinal stress.....	70
Figure 45. Two-dimensional model for temperature, prescribed interface.....	72
Figure 46. Temperature and composition index, variable interface case.....	72
Figure 47. Stress components, 2D GPS model, large thickness.....	73
Figure 48. Stress components, 2D GPS model, 25mm substrate thickness.....	73
Figure 49. Stress components, 2D GPS model, 10mm substrate thickness.....	74
Figure 50. Stress components, 2D GPS model in substrate, plane stress in clad.....	74
Figure 51. Stress components, 2D plane stress in both clad and substrate.....	74
Figure 52. Two-dimensional model for temperature, thick substrate.....	75
Figure 53. Two-dimensional mechanical model, strain components.....	76
Figure 54. Two-dimensional mechanical model, thick substrate.....	77
Figure 55. Boundary conditions for 2D stress models.....	77
Figure 56. Three-dimensional curved meshes.....	78
Figure 57. Three-dimensional model for temperature, curved mesh.....	79
Figure 58. Comparison of melt pool shapes in 3D and 2D.....	80
Figure 59. 3D model for temperature: secondary variables.....	81
Figure 60. 3D model for stress, curved shape.....	82
Figure 61. 3D model for stress, curved shape (cont'd).....	82
Figure 62. 3D model for stress, curved shape (cont'd).....	83
Figure 63. Three-dimensional model for temperature, planar mesh.....	83
Figure 64. 3D model for temperature: secondary variables.....	84
Figure 65. 3D model for stress, planar mesh.....	85
Figure 66. 3D model for stress, planar mesh (cont'd).....	86
Figure 67. Shear stress profile, top and bottom of clad, planar and curved mesh.....	88
Figure 68. Boundary conditions for 3D stress models.....	89
Figure 69. Hardness profile of laser clad track.....	90
Figure 70. Composition profile of laser clad track.....	92
Figure 71. Composition in the interfacial zone.....	92
Figure 72. Composition index profile, 3D curved shape mesh.....	94

List of Symbols

Latin symbols:

A	-absorptivity.
a, b, c	-auxiliary functions, Mori-Tanaka model for yield stress.
c_i	-composition index.
C_{ijkl}	-stiffness tensor.
c_p	-specific heat.
d	-number of digits to use per direction in the node numbering scheme.
D	-thermal diffusivity.
E	-Young's modulus.
e, f, g	-angular auxiliary functions (in the calculation of clad height).
f	-volume fraction of precipitates.
f_{dil}	-dilution parameter.
H	-hardness.
h	-heat transfer coefficient.
h_c	-clad height.
h_i	-clad melt depth, defined by the depth at which the interface region begins, with relation to the substrate surface.
k	-thermal conductivity.
L	-latent heat of melting.
n	-node number.
NDX, NDY	-node number increment along x and y .
n_j	-exterior normal to the free surfaces.
n_x, n_y	-node location along x and y axis.
P	-laser power.
P, P_p, P_m	-generic physical property, for composite, precipitate and matrix.
$PEEQ$	-equivalent plastic strain.
Q	-imposed heat flux.
r	-radial distance from the beam axis.
r_o	-laser beam radius.

$SDV1$	-composition index.
$SDV2$	-relative temperature.
$SDV5$	-cooling rate.
$SDV6$	-temperature gradient.
t	-time.
t_i	-interaction time.
T	-temperature.
T_0	-room temperature, initial temperature.
$\overline{T_c}$	-mean temperature of clad melt pool.
$T_{MAX}(x, y, z, t)$	-peak temperature.
T_m^C	-cladding melting (liquidus) temperature.
T_m^S	-substrate melting (liquidus) temperature.
T_{ref}	-CTE reference temperature.
T_∞	-remote temperature.
u_i	-displacement.
v	-laser scanning speed.
x, y, z	-cartesian coordinates.
x_i	-cartesian coordinates.
x_{in}	-initial x coordinate of laser beam.

Greek symbols:

α_T	-coefficient of thermal expansion.
ε	-emissivity.
ε_{ij}	-total strain.
ε_{ij}^{el}	-elastic strain.
ε^{pl}	-equivalent plastic strain.
ε_{ij}^{pl}	-plastic strain.
ε_{ij}^{th}	-thermal strain.
ε_{pki}	-alternating symbol.
$\dot{\varepsilon}$	-strain rate.

φ	-mass deposition rate, mass feed rate.
ν	-Poisson's ratio.
ρ	-mass density.
ρ_c	-clad mass density.
θ	-angle between the normal to the solidification front and the laser scanning direction.
θ_m	-preferred solidification direction angle.
σ	-Stefan-Boltzman constant.
σ_{ij}	-stress tensor.
σ_{Mises}	-Von Mises stress.
σ_{res}	-residual stress.
σ_Y	-yield stress.
σ_{Y0}	-value of first yield.

List of Abbreviations

2D	-Two-dimensional.
3D	-Three-dimensional.
CAD	-Computer Assisted Design.
CAM	-Computer Assisted Manufacturing.
CLAIM	-Center for Laser Aided Intelligent Manufacturing.
CLAMP	-Center for Laser Aided Materials Processing.
CTE	-Coefficient of Thermal Expansion.
DMD	-Direct Metal Deposition.
FE	-Finite Element.
GPS	-Generalized Plane Strain.
ICALEO	-International Congress on Applications of Lasers and Electro-Optics.
IFG	-Input File Generator.
IR	-Infrared.
LA	-Laser Alloying.
LC	-Laser Cladding.
LENS	-Laser Engineered Net Shaping.
LIA	-Laser Institute of America.
LW	-Laser Welding.
RP	-Rapid Prototyping.
UIUC	-University of Illinois at Urbana-Champaign.

Preface

Laser Cladding (LC) is a coating manufacturing technique, in which a laser beam is used to melt and deposit one or several layers of a certain clad material onto a substrate, in such a way that a sound interfacial bond is formed, without significant dilution of one material into the other. LC has received considerable attention in recent years, especially in the field of Rapid Manufacturing, due to its ability to quickly produce near-net shape, fully dense, metallic parts of complex geometries and flexible compositions. This latter characteristic makes it also a very attractive scientific tool, in that it provides the potential to readily produce alloys of arbitrary nominal composition. Still, for a successful laser cladding operation, there needs to be a fine tuning between the processing parameters, most prominently the laser scanning speed, the laser beam power and the clad feed rate.

Mathematical modeling is an appropriate tool to investigate the range of processing parameters that lead to successful cladding. It has been verified that the Finite Element (FE) method provides an adequate modeling framework: for example, since the procedure is additive by nature, the corresponding computation domain changes during calculation; also, the interaction zone has a curved shape and the clad beads formed have a near semi-cylindrical shape, over a substrate that is usually planar. Analytical or Finite Differences methods usually are not able to accommodate such geometric features, while in FE those aspects are modeled in a natural way.

Parametric studies for LC are conducted by performing a heat transfer analysis of the process, but in addition to that, it might be useful to also carry out a mechanical analysis. In effect, bringing together dissimilar materials and/or materials that are processed at different reference temperatures, gives rise to thermal strain (that in turn can also lead to plastic strain), so in the end there will be residual strain and, therefore, residual stress at room temperature, which in some cases can bring the fabricated parts to (or, near to) failure conditions. The FE method is quite advantageous in this regard, as it gives the flexibility to address both the thermal and mechanical problem.

In the research work that is presented in this dissertation, 2D and 3D FE lagrangian models were developed and implemented using the AbaqusTM software, for the calculation of temperature and stress/strain fields in laser cladding of dissimilar materials, in particular of C95600 copper based- on AA333 aluminum based-alloy, for which cladding experiments had been successfully carried out.

Non-trivial algorithms had to be implemented so as to generate adequate AbaqusTM input files with information on the FE mesh (with an adequate degree of refining) and the adequate boundary conditions, as a function of processing parameters. An important feature of those models is the possibility to incorporate dilution: as the melt front progresses down to the substrate, the local composition is allowed to change (using very simple assumptions for mixing), with a definite impact on thermal and mechanical behavior.

Results are presented for simulations done with different processing parameters and dimensions of the clad-substrate system. A number of 2D results are presented, featuring the mid-longitudinal plane in a single bead clad/substrate system. These results are then compared with (a more limited range of) 3D results, for which convergence issues are critical, especially in the mechanical problem.

A different type of mesh in 3D is also used, in which all the elements are cubic in shape, leading to better numerical convergence. Although there is a distinct difference in heat transfer results when the two types of 3D mesh are compared, as the problem is sensitive to a proper description of the melt front shape, the stress analysis yields similar results. This supports the following recommendation: first use 2D models to quickly explore parameter space, which will provide a guide for further calculations in 3D; then work first on the 3D heat transfer problem, using the more realistic curved shape meshes; finally, use meshes with planar boundaries to perform the stress/strain analyses.

1. Introduction

1.1. Laser cladding: fundamentals

1.1.1. Definition

In Laser Cladding (LC) one aims at depositing one or several layers of a certain clad material on top of a substrate, with the assistance of a laser beam. The clad material and a small portion of the substrate get melted together under the action of the laser beam, so there is the possibility to obtain, after solidification, a coating that shows good bonding to the substrate and that has little incorporation of substrate atoms into it, *i.e.*, has little dilution (see figures 1 and 2).

The material to be deposited is normally in the form of a powder, carried by a gas-assisted powder delivery system. Such powder gets heated by the laser beam in-flight as it crosses the radiation path and eventually will melt, either still airborne or (most likely) as it is put in contact with the laser generated melt pool, located on the surface. The thickness of the coating thus formed is typically up to the millimeter range, so a relatively thick film can be obtained in one quick elementary step.

The goal of this process is usually:

- to obtain a substrate/coating system showing an improvement in surface properties, usually chemical (*e.g.* corrosion or high temperature oxidation resistance) and/or mechanical (*e.g.* wear resistance); or,
- to deposit material in an additive fashion so as to obtain a part with a prescribed geometry in near net shape condition.

Quite frequently, the term “Laser Cladding” refers mainly to the former, while the latter has been described as Direct Metal Deposition (DMD), Laser Metal Deposition or Laser Powder Deposition.

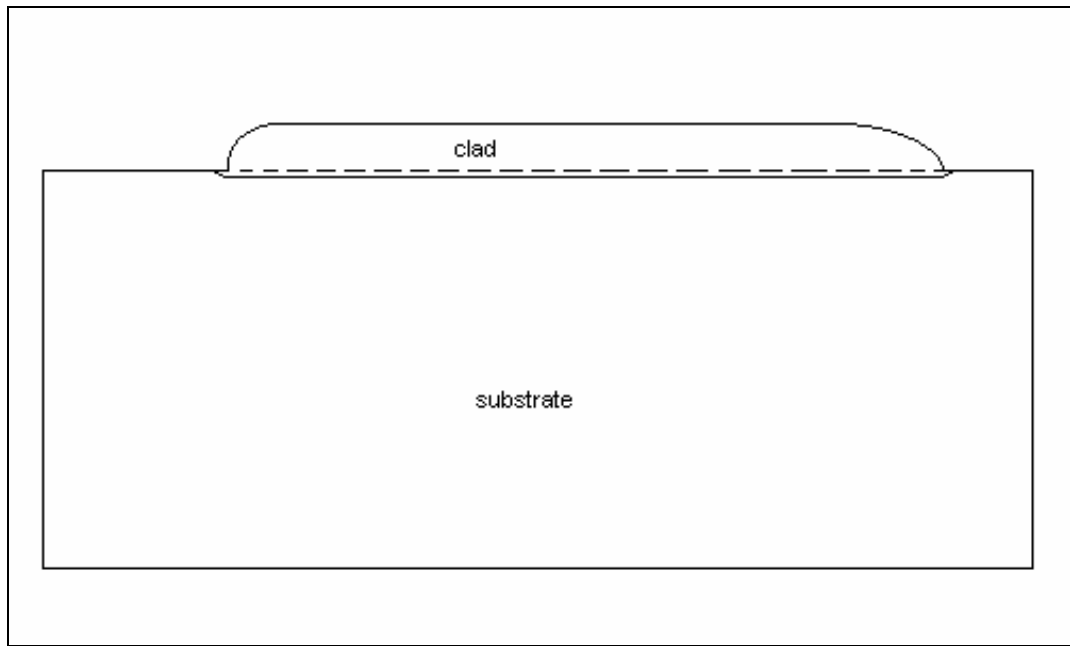


Figure 1. Longitudinal section of typical laser clad sample.

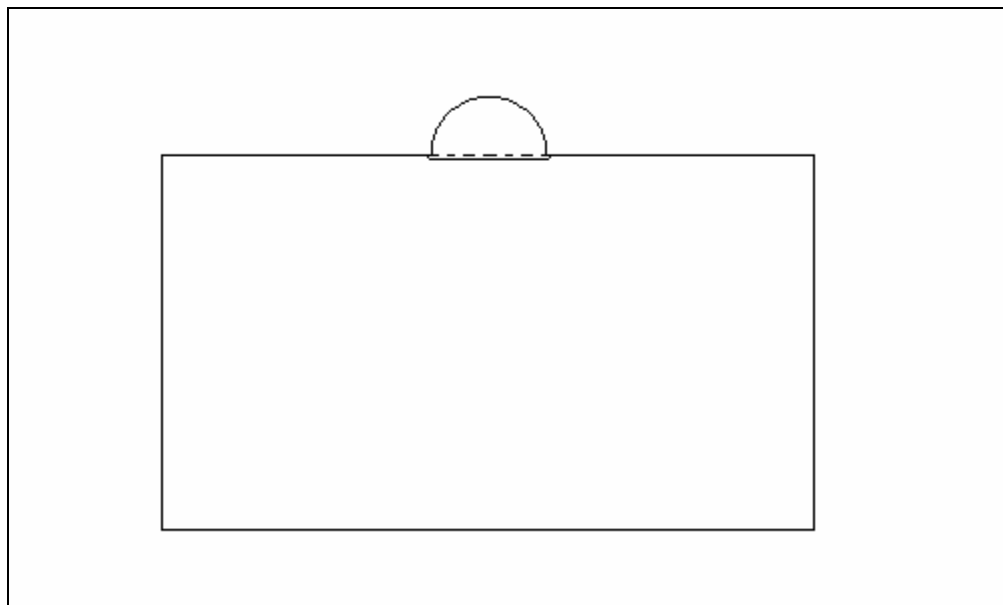


Figure 2. Transversal section of typical laser clad sample.

In LC the beam acts as a heat source, whereas the powder delivery system can be viewed as a mass source. Accuracy of deposition location will depend critically of proper design of the powder and beam delivery systems.

1.1.2. Techniques

In LC *per se* one is usually concerned with covering a surface, which is accomplished by deposition of parallel tracks, often with a certain amount of overlap (see figure 3). On the other hand, LC can be viewed as an elementary step for more elaborate manufacturing techniques. Extensions of this basic operation include DMD and *in-situ* repair.

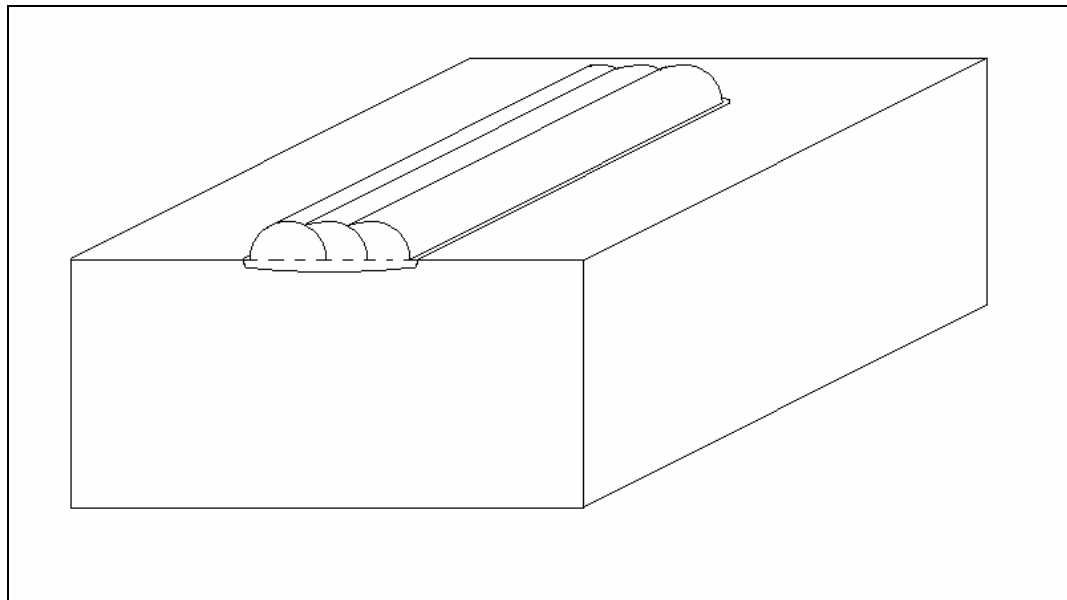


Figure 3. Parallel clad tracks, with overlap.

In the latter, one aims at restoring material that was lost in service in cost sensitive parts, such as turbine blades and injection molds. In the former, especially in the context of Rapid Prototyping (RP) and Manufacturing, the usual goal is to obtain a near-net shape part, by means of the buildup (see figure 4) of successive laser clad beads. The geometry of the part, which can be obtained from CAD software, is translated into a series of tool path commands. These will determine the relative position and speed of the substrate (placed usually on a XY-table) in relation to the laser and powder delivery systems, leading to the

manufacture of a desired part, *e.g.* a prototype. In parts of relatively small dimension (typically in the order of 10^{-1} m), this could be a one-step operation accomplished in a short period of time (for example, in the order of minutes).

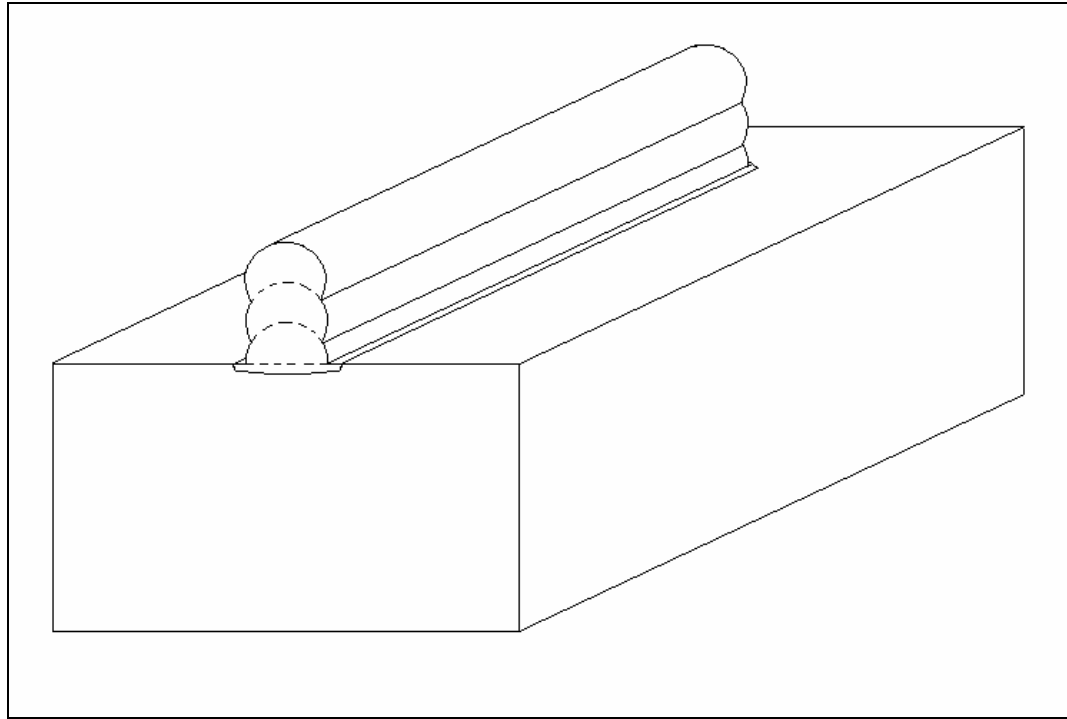


Figure 4. Buildup of clad tracks, forming a wall.

At the irradiated zone, the clad material must be brought together with the substrate and these are to undergo melting, so that a metallurgical bond forms between the two materials. For this purpose, one possibility is to pre-place the clad material in the form of a wire or a powder on top of the substrate. However, the most common procedure, known as the blown powder method, has the cladding material delivered to the substrate in the form of a powder that is injected into the laser melting pool, dragged with the help of an inert carrier gas (see schematic of laser cladding apparatus at CLAMP/UIUC [1], shown in figure 5). Further references to LC will be made in relation to this latter method, unless otherwise stated.

1.1.3. Bonding and dilution

In LC, one usually aims at obtaining a coating/substrate system showing good bonding and low dilution, two requirements that are often difficult to obtain simultaneously with conventional techniques. 'Low dilution' means that the composition of the coating is little affected by the substrate material (and *vice-versa*). As a consequence, the interface region between the clad and the base material is relatively narrow and located very close to the substrate original surface (see figures 6 and 7).

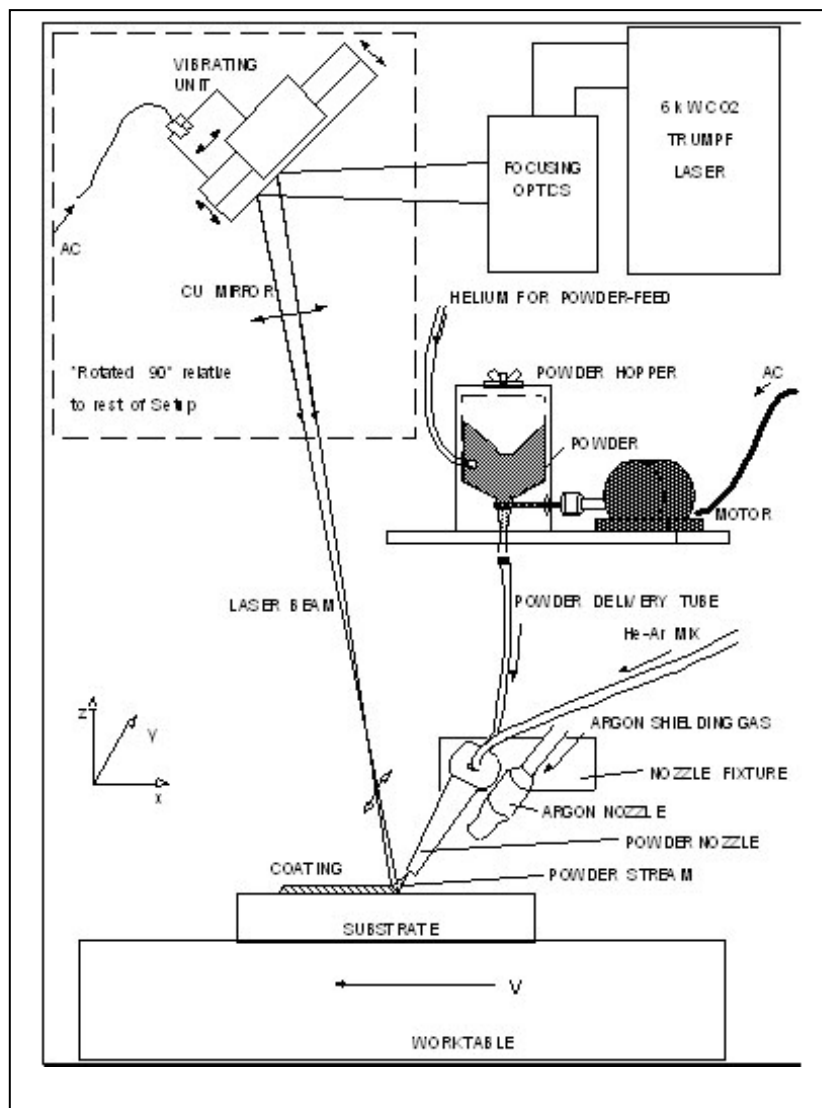


Figure 5. Schematic of laser cladding setup.

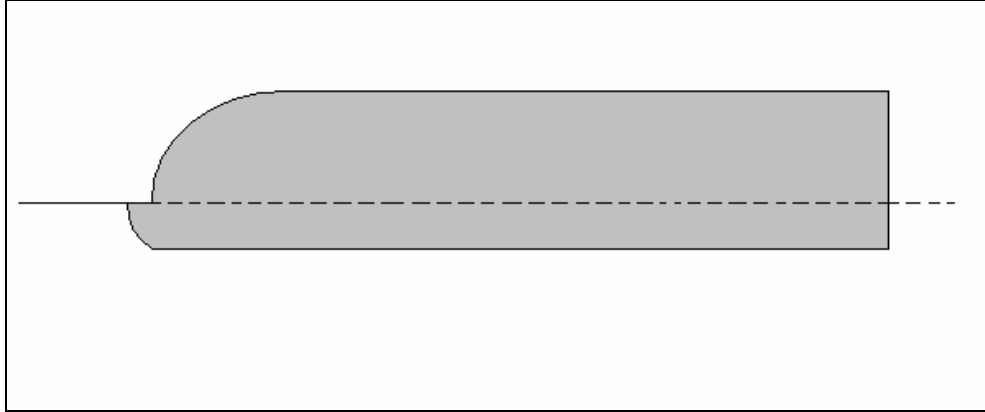


Figure 6. High dilution clad track.

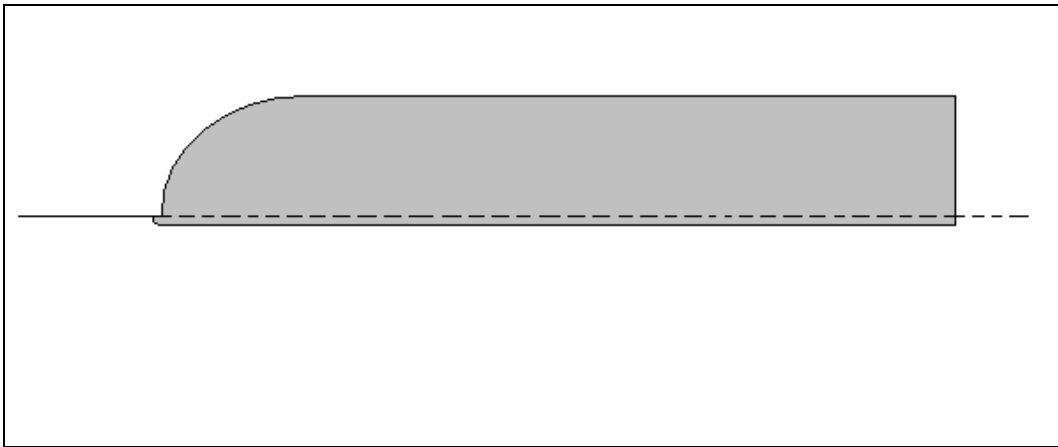


Figure 7. Low dilution clad track.

The ratio between the clad melt depth, h_i , and the clad height, h_c , is many times used as the parameter characterizing dilution, f_{dil} (figure 8):

$$f_{dil} = \frac{h_i}{h_c}. \quad (\text{eq. 1.})$$

It should be mentioned that even in a low dilution case some of the substrate material will always be present in the coating. In fact, at the beginning stages of the process (the initial transient), a melt pool has to be formed in the base material, so that the powder can be caught; particles hitting the solid portion of the substrate will obviously not be incorporated in the film. After this initial, usually very short transient —*e.g.* dozens to hundreds

milliseconds long— where composition varies significantly in the clad, the process tends to reach a quasi-steady state. During this latter stage, the catchment efficiency of the surface is high enough to allow for the formation of a continuous strip of clad material, which is desirably of homogeneous composition and height. From the transient stage to the quasi-steady state one expects that the volume of melted substrate will decrease very rapidly, but some fusion of the substrate will always have to occur, as it is a necessary condition for a metallurgical bond to be formed.

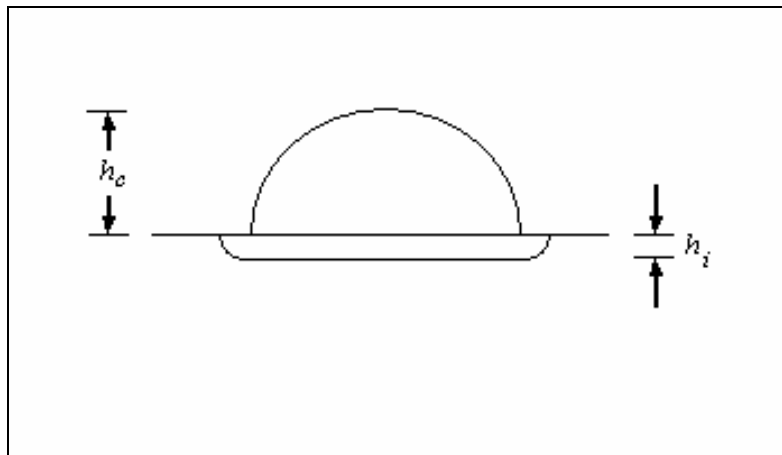


Figure 8. Definition of dilution parameter.

As a consequence of these simultaneous heat and mass transfer constraints, one has to fine tune the process parameters —most notably the laser scanning speed, laser power and the powder feed rate— so as to melt as little substrate as possible (low dilution) and at the same time as much substrate material as needed (so as to assure a strong bond). This can indeed be obtained for a good number of metallic systems, even in cases where melting points of the clad and substrate are relatively dissimilar.

If dilution is high, this means that significant melting of the substrate occurred and this introduces a certain amount of uncertainty in determining the coating composition. In contrast, in a low dilution case the composition of the coating will obviously be very close to the nominal composition generated at the powder mixing system. This is important to note, as quite often the powdered material that is available from commercial manufacturers

has already a composition that is designed for a certain purpose (for example, Stellite™ coatings, in connection with an improvement in corrosion and wear resistance). In this context, incorporation of alloy elements coming from the substrate will likely have a detrimental effect on the performance of the coating. In addition to that, having a melting powder in contact with a significantly melted substrate could lead to the formation of extensive regions of intermediate compositions, most notably intermetallic compounds, frequently showing brittle behavior, which in turn could be detrimental for the interface mechanical behavior. Although it might be true that in a limited number of systems the quantity and distribution of such phases could actually have a beneficial effect on coating behavior, as dispersions of hard particles lead to higher strengths, one can expect this not to be the general case.

1.1.4. Scientific importance

Laser cladding has been used as a valuable tool in a number of scientific studies, namely in the field of materials science. Among other fields, it provides a workbench for studies in:

Alloy design: most elements of the periodic table with interest to surface engineering applications are found in powder format. Thus, it is convenient to use LC as a tool for obtaining coatings of prescribed composition. In fact, for low dilution, that it is simply the nominal composition at the powder mixing chamber (provided there is no vaporization of one of the elements) affected by a perturbation term that is a function of the clad melt depth, h_i . Rapid alloy scanning ([2] and [3]) is another possibility: by varying continuously the proportion of powder materials, clad tracks with variable composition can be obtained. This allows for a relatively expedite study of the properties of a certain alloy system and in turn the making of design decisions. This kind of film, however, can be obtained for its own merit, as in the case of functionally graded coatings [4].

Solidification: because of the high cooling rates associated with laser processing, as well as the flexibility in defining the melt composition, LC is a procedure that has been used in both experimental and theoretical research in the field of solidification. Examples of this are studies that relate process parameters with microstructural features [5] or investigations

on extended solid solubility [6] (*i.e.*, solidification of phases with composition beyond the solubility limit predicted by the equilibrium phase diagram).

Tribology: a good number of different coatings can be produced in a relatively expedite fashion [7] and then tested for performance, for example in a wear ([1], [8]) or corrosion test [9].

1.2. Similar processes

Among the many laser assisted surface modification techniques, two can be viewed as closely related to laser cladding: laser alloying and laser welding. Similarities and differences will be briefly mentioned.

1.2.1. Laser alloying

In Laser Alloying (LA), powdered material is continuously added to a laser-melted substrate, so that in the fusion zone an alloy is obtained with a composition that is different from that of the bulk. At the same time, the addition of material is normally expected to produce only a slight variation in the height of the substrate.

Many aspects of laser alloying are similar to laser cladding. For example, material addition is frequently accomplished by means of a blown powder technique. Nonetheless, some fundamental differences can be established: for example, the typical powder feed rate is considerably smaller, as the goal is to modify an already existing surface, not to deposit a coating onto a surface. In fact, in LC the majority of the modified surface comes from the added materials (the powder) whereas in LA it comes mainly from the substrate.

If surface displacement exceeds a certain user-defined threshold, than one perhaps would no longer refer to this process as LA, as this was tending now toward being a laser cladding process. Minimal expansion can be obtained for small quantities of added material and for good solubility of elements, especially in the case of interstitial solid solutions. In view of

this, ‘ideal’ (zero dilution) LC on one side and LA on the other side can be viewed as extreme situations in the whole range of laser-assisted deposition of materials.

1.2.2. Laser welding

In Laser Welding (LW) one aims at joining together two solid materials, by using a laser beam to melt the interfacial zone, while the two portions are held in close contact. Although it is just one of the variants in the wide array of possibilities for welding, its importance has been growing, as it has become increasingly used, for example in the automotive industry.

A number of similarities exist between LW and LC. For example, in LW it is also desirable that a strong metallurgical bond exists at the interface; if a different composition filler metal is used, it is likely required that dilution is also minimal. Issues such as finding good combinations of process parameters, solidification (phase composition, microstructure selection and scale) and mechanics (residual stresses, cracking and distortion) are a common concern in the two fields. On the other hand, the two processes obviously differ in purpose, which in one case is the joining of materials and in the other is the production of a coating. Therefore, the typical geometry is different in the two processes.

1.3. Scope of thesis research

Thesis research in the field of laser cladding focused on the development of Finite Element (FE) models allowing for the estimation of temperature and stress/strain fields. For this purpose, two- and three-dimensional models for single track laser cladding were developed, for processing in the FE package AbaqusTM. In particular, pre-processor algorithms were written and implemented, allowing for the generation of ‘input files’, which contain the whole model information (*e.g.*, geometry, boundary conditions and materials properties). Parametric studies were made as well as a comparison of results with experimental data generated within the research group. The models were developed for bi-material systems (clad different from the substrate), although they can readily be applied to single-material systems. A simple model of mixing and dilution was also developed.

1.3.1. The finite element method

From a scientific standpoint, laser cladding is found to be a multi-disciplinary field –in a similar fashion as is the case of welding– as a number of different physical phenomena play a decisive role in producing the final result. Thus, a proper understanding of the process involves the simultaneous use of results derived in a number of disciplines, such as materials science, heat transfer and mechanics of materials.

In modeling a process that involves such degree of complexity and intertwining of fields, one aims to start with a simple approach, one that will still capture the main features of the physical processes taking place. At the same time, the model should be flexible enough, so that new features can be further added. The Finite Element (FE) method has proved to be such a workbench modeling tool. In addition to that, there are a number of other reasons that make the FE method a preferred one:

- a wide variety of different physical problems (mechanics, diffusion, heat transfer, etc.) can be addressed within a formally similar mathematical framework;
- great versatility in dealing with the geometric features of models;
- easy integration with other engineering tools, such as CAD/ CAM;
- widely known and available among the engineering community.

In the present thesis two- and three-dimensional models based on the FE method are described. Since the commercial software package AbaqusTM was used to perform the calculations, the modeling effort was placed in:

- a) selecting the *relevant phenomena* and incorporating such within the framework of the FE model and then carry out the appropriate computational studies;
- b) designing an automatic *pre-processing* procedure, in such a way that the processing parameters can be easily translated to the FE model.

These issues will be briefly addressed in the next two sub-sections.

1.3.2. Relevant phenomena

The following phenomena are addressed within the FE model that was developed:

Heat transfer: the laser beam acts as a moving heat source. In the model this is simulated by means of an imposed flux boundary condition, the value of which changes with time and space, at each point of the irradiated surfaces. Convective and radiation boundary conditions are also considered, namely in regards to cooling. Heat transfer in the bulk is considered to take place by conduction only. Latent heat is taken into account.

Mechanics of materials: the presence of relatively high thermal gradients and the fact that dissimilar materials are brought together in close contact, as in the case of a coating-substrate system, lead to the development of thermal strains and stresses. In fact, the coating and substrate materials will have in general different coefficients of thermal expansion (CTE) and different CTE reference (initial) temperatures. If the stress state brings a certain material point above the yield strength, plastic strain develops. So in the FE model for deformation, elastic-plastic behavior is assumed, with kinematic hardening and a Von Mises equivalent stress flow rule. No external loading is considered, and constraints are applied so as to prevent rigid body motion.

1.3.3. Pre-processing

A number of issues received particular attention in the establishment of a pre-processing strategy:

Processing parameters: among the many quantities affecting the process of laser cladding, three are considered to be the most important: laser power (P), scanning speed (v) and mass deposition rate (ϕ), also known as feed rate. These are considered in the model by means of:

- *Boundary conditions:* for example, the magnitude of the imposed flux is proportional to laser power; also, the location of the laser beam depends on the speed.

- *The definition of the overall geometry:* for example, the clad layer height is a function of feed rate and scanning speed.

It is verified that, while changes in laser power result in a simple change in the FE input file, modifications in the other two parameters result in non-trivial changes in the model, bringing about the need for a so-called ‘input file generator’ (IFG), an algorithmic procedure to generate automatically such changes. Such an algorithm must also accommodate the need to obtain successively refined meshes, so as to find the numerical solution of the problem, as well as produce meshes that are more refined at the zones where the variables are expected to vary more strongly.

Curved geometry: the calculation domain that is used in the model must match as closely as possible the geometry of the part that is being fabricated by laser cladding. For example, the free surface –where most of the heat and mass input is being deposited into the system– is observed to show a curved shape, which in turn will affect by itself the temperature and stress fields. So, in designing a FE mesh to model this process it is desirable that nodes be located in points allowing for the definition of such curved surfaces. These node generation “trajectories” are also a function of process parameters and thus are also to be calculated within the IFG framework.

Evolving geometry: laser cladding is a manufacturing technique that involves addition of material, thus the geometry of the material is constantly changing. Therefore, a desirable feature of a model of laser cladding is to be able to accommodate this geometry change. In a lagrangian description of the model (*i.e.*, one that has the reference frame fixed to the base material) this can be accomplished in a discrete fashion. The idea is to assume that a certain geometry is valid during a small time step, solve the equations and then take the state at the end of the time step as the initial condition for the next step, for which a number of new elements is to be added to the domain. This element generation procedure is, again, a function of processing parameters and requires a great deal of care in the labeling rationale of nodes and elements. For example, some surfaces that up to a certain time step are “exposed” (where heat transfer boundary conditions are to be applied, for example) are now “covered” by the new elements.

As mentioned, the IFG must also include a suitable mesh labeling strategy. While in 2D such labeling strategy is straightforward, in 3D the problem is considerably harder to solve, due to the topological constraints involved in matching zones with cylindrical- (the coating) with ones with cartesian-like symmetry (the substrate).

1.3.4. Results

The 2D and 3D models were run and results are presented in chapter 3. The numerical research that is presented in this thesis was made at early stages parallel with an experimental study at the Center for Laser Assisted Materials Processing, CLAMP, at the University of Illinois at Urbana-Champaign. The results of such research were included on a M.Sc. thesis [1], and some of the major findings have been published elsewhere [10]. The parametric studies made therein provided the validation guidelines for the FE models that were developed.

Besides primary variables, such as temperature, or stress components, some other secondary variables of interest received attention. For example, cooling rates and temperature gradients allow for the estimation of the primary and secondary arm spacing, which could also be compared with experimental results. Also, a calculation scheme is presented so as to directly obtain the dilution as well as to estimate the local composition changes due to mixing. As a result, melt pool shapes that take into consideration the variation of liquidus temperature from the clad to the substrate zone are also obtained. The systematic approach that leads to such analysis, based on a simple picture of mixing, is found in chapter 2.

1.3.5. Issues not covered

As pointed before, LC is a very interesting technology from the viewpoint of basic science, because a number of phenomena occur simultaneously, all playing an important role in the process, with important process understanding coming from different disciplines. Some of those areas are not to be considered in the scope of the present research, although they play a very important role in the process. Some examples are as follows:

Kinetics: Obtaining the transient temperature and stress field is important in itself and also an essential preliminary step in other studies, such as kinetics. Phenomena such as grain growth, precipitate coarsening, recrystallization or decomposition of metastable phases are all thermally activated (and eventually also affected by the stress/strain field). Still, such issues are not directly addressed in this thesis, despite collaborations held in which kinetics was a crucial element, for example involving tempering effects in steel parts produced by laser cladding ([11] and [12]), or investigations on the fundamentals of grain growth [13].

Failure: in a bi-material system subject to thermal cycling there is the possible occurrence of failure of a clad/substrate ensemble by cracking and/or debonding, so knowledge of the stress field is obviously critical, as well as the temperature (if not for other reason, because strength is temperature dependent).

Laser delivery: in LC the heat source is a laser beam, usually of the CO₂ type, with wavelength equal to 10.6 μm, which is in the infrared (IR) region of the spectrum. More recently, systems are being employed that use Nd-YAG lasers, also in the IR (1.06 μm). The beam is delivered to the part being treated by means of a system of lenses and mirrors. Practical issues such as mode, proper alignment and focusing of the beams are verified to play an important role in the process.

Powder delivery: in LC with the blown powder technique, the material is deposited in the laser generated melt pool, carried by an inert gas through a properly designed nozzle. This design must take into consideration factors such as the presence of the laser beam and the typical feed rates that are going to be utilized. Also, the mean powder size of the powdered material is important, because usually one requires that powders melt/dissolve completely as they enter the melt pool (unless a particle reinforced surface composite is required).

Fluid mechanics: laser cladding always involves production of a zone that is in the liquid state and where strong thermal gradients are expected to be found. Thus, convection is expected to play a very important role in heat and mass transfer. The estimation of velocity fields in laser materials processing has been done extensively, using Finite Differences/

Finite Volume and Finite Element techniques, but was not attempted in this research, where the focus was on the estimation of residual stress fields. From that viewpoint, the details of the temperature field in the melt pool (which is a stress-free zone), *i.e.* in the region where convection will play a direct role are perhaps not as important as having a reasonably good estimate of the temperature field in the solid phase, where heat is transported by conduction only. Therefore, having the ability to model the overall geometry of the melt pool using conduction-only models seemed to be an adequate strategy, in particular if one is concerned mainly with the mechanical problem. This approach is especially valid in materials with high thermal conductivity, such as copper and aluminum alloys.

1.4. Literature review

An overview of published literature in laser cladding, with emphasis on modeling, will be presented.

1.4.1. General references

The first references to laser cladding appeared in the literature in the mid 70's, in reports from Gnanamuthu ([14] and [15]). Then, in the early 80's, both basic LC processes (pre-placed and blown powder) were described by Steen and co-authors ([16] and [17], respectively in 1980 and 1983). The blown powder method was reported [18] as being used in production at Rolls Royce since 1981. In the meantime, patents were filed ([19] and [20]). From then on, literally hundreds of papers have been published, reporting advances in applications, materials used, processing and monitoring equipment, etc., which will not be reviewed here. Nonetheless, it is worth mentioning that the main source for references in this field are the Proceedings of the ICALEO (International Congress on Applications of Lasers and Electro-Optics), sponsored annually by the Laser Institute of America (LIA), as well as the Journal of Laser Applications, which is also published by the LIA. In addition, review papers in the area of LC have been published by Vilar ([21] and [22]). The several variants of LC were therein described, the blown powder (or, powder injection) method

receiving special attention. Alloy and microstructure development, equipment design and applications were also described in detail.

1.4.2. Modeling of laser cladding: without stress analysis

Earlier efforts in modeling of laser cladding focused mainly on heat transfer, with a few considering also mass transfer and fluid flow. An overview of such papers is presented next.

Weerasinghe and Steen [23] used a 3D finite differences model to calculate the temperature field. The circular bead section was modeled as a stepped Cartesian grid. The shadowing effect (attenuation of the laser power at the workpiece due to the gas-powder jet) was considered. Clad dimensions were computed as a function of process parameters, both for single and also for multiple track cases.

Kar and Mazumder ([24], [25] and [26]) and **Agrawal *et al.*** [27] solved analytically the one-dimensional heat and mass transfer (coupled) equations, for binary systems. The goal was to calculate the composition of the extended solid solution that is formed by rapid cooling. Parametric studies were also included, correlating variables such as laser power, P , beam radius, traverse speed, v , clad thickness, h_c , feed rate, ϕ , and film composition. A semi-cylindrical clad shape was assumed for the overall mass and heat balances, thus the relationship between processing parameters could be obtained. A lumped heat transfer analysis gave:

$$h_c = \sqrt{\frac{2AP}{\left(\overline{T_c} - T_0\right) c_p + L} \pi v \rho} \quad (\text{eq. 2.})$$

where $\overline{T_c}$ is the mean temperature of the clad melt pool, T_0 is the initial temperature (usually room temperature), c_p is the specific heat, A is the absorptivity, ρ is the mass density and L is the latent heat of melting.

Overall mass balance gave, in turn:

$$\varphi = \frac{1}{2} \pi h_c^2 v \rho. \quad (\text{eq. 3.})$$

Portions of non-equilibrium phase diagrams (such as Al-Ni, Ni-Hf and Al-Nb) were also proposed, as an application of the rapid solidification scheme for extended solid solubility that was therein developed.

Hoadley and Rappaz [28] used a 2D FE model for the calculation of the quasi-steady state temperature field. An idealized problem, in which almost no melting occurs in the substrate, was taken as the basis for defining a successful cladding operation. Mixing was assumed to distribute the powder instantaneously in the melt, giving a volumetric heat source term associated with the latent heat. The free surface was considered to be an arc of a circle and the temperature of the powder particles was estimated. The calculation procedure involved determination of the laser beam position that is consistent with the requirements of the idealized problem. A parametric study involving laser power, processing speed and clad thickness was included.

Picasso and Hoadley [29] used the FE method to solve for the stationary heat transfer and fluid flow problem on a 2D geometry. The model considered the deformation of the gas-liquid interface and the forces associated with the powder injection into the melt pool, and the powder was assumed to melt instantaneously as it hits the liquid surface.

Picasso et al. [30] used an iterative procedure, based on a 3D analytical model for temperature, for obtaining process parameters such as scanning speed and powder feed rate as a function of laser power, beam radius, powder jet geometry and clad height. The shadowing effect and the dependence of the absorption coefficient on the angle of incidence of laser radiation into the melt pool were also considered.

Kim and Peng ([31] and [32]) used an adaptive mesh FE 2D scheme to obtain the temperature field in the case of LC with wire feeding. The authors chose for their analysis a transversal plane located near the end of the melt pool, *i.e.*, near the solidifying front. The height of the clad was assumed constant, and the width of the clad continually adjusted so

that the melting temperature is attained at the clad/substrate intersection. Melt pool shape and dilution were studied as a function of laser power and scanning speed.

One aspect of modeling in LC that has also received attention is the interaction between the laser beam and the powdered material while in flight. Papers by Marsden *et al.* [33], Neto and Vilar [34], Lin ([35] and [36]), Fu *et al.* [37], have addressed this important issue.

1.4.3. Modeling of laser cladding: with stress analysis

Recent modeling of laser cladding began to feature not only thermal aspects but also the mechanical problem, namely the generation of residual stresses associated with thermal expansion. An overview of such papers is presented next. Models developed within the context of DMD are also featured. Most of the papers use the FE method, but a few analytical models are also presented.

Deus and Mazumder [38] developed a 2D FE model for temperature and stress/strain, developed within the AbaqusTM software package. The longitudinal mid-plane was chosen to perform the analysis. The clad front was modeled as an arc of a circle. A lagrangian reference frame (fixed to the material) was chosen. The addition of powdered material was modeled by mesh generation, *i.e.*, elements were automatically added to the domain at appropriate times during the computations. The temperature analysis was performed first and was then used as an input to the thermal stress analysis. Generalized plane strain was assumed in the 2D mechanical problem. As for plasticity, the Von Mises criterion with no hardening was utilized. Results were presented for cladding of C95600 on AA333 alloys, namely the temperature, longitudinal stress, plastic strain magnitude and displacement fields. Computations showed that the highest absolute values for longitudinal stress are located at the transition zone between the substrate and the clad.

Nickel *et al.* [39] studied the effect of deposition patterns on residual stresses and strains. FE software AbaqusTM was used and the calculation results were compared with experimental observations, namely of the deflections that were observed on samples produced by DMD. Nevertheless, material deposition *per se* is not considered in the model,

so in fact the paper basically analyses the stress and strain fields associated with laser treatment of materials, not the case where material is being added to the substrate. Laser heating is modeled by a constant flux boundary condition applied simultaneously in the whole track where the treatment is to be applied, whereas in the experiments the laser scans such track. Such boundary condition is applied during some time, then the material is allowed to cool down, and then the process is repeated for the next line, until the desired pattern is completed.

In the thermal problem, thermal conductivity, specific heat and density were assumed to be temperature independent, and radiation, convection and latent heat effects were not considered. In the mechanical problem, Young's modulus, Poisson's ratio and thermal expansion coefficients are temperature independent. The yield strength is assumed to vary linearly from its room temperature value to 10% of that at the melting temperature. The authors conclude that the principal stress in the direction of laser treatment (σ_{xx}) is always higher than the corresponding σ_{yy} component (the XY plane is the deposition plane). Another conclusion is that the highest stresses are found where the last lines are remelted.

Dai and Shaw [40] used a 3D FE model based on the software package AnsysTM to obtain temperature and stress fields in Multi-Material Laser Densification, a RP procedure that shows many similarities to the cladding and DMD processes. Simple bi-material geometries were modeled and elements of cubic shape were considered. Element addition and laser processing occur alternately and the laser source is modeled by means of a localized fixed temperature boundary condition. The fabrication sequence is verified to play a determining role in the value of residual stress components. As expected, the mismatch of the coefficients of thermal expansion is verified to have a direct impact on residual stresses and distortion; similarly, higher laser scanning speeds are seen in general to lead to higher residual stresses.

Kahlen and Kar [41] developed a 1D analytical model for the estimation of temperature and residual stress fields in laser deposition processes. The temperature model takes into account the laser beam absorption that occurs in the metal vapor-plasma plume above the

workpiece, where metal powder is being blown into the substrate. The approach for the estimation of residual stresses is said to be a very simple one and is as follows. The residual stress is taken as

$$\sigma_{res} = E \dot{\epsilon} t_i , \quad (\text{eq. 4.})$$

where E is the Young's modulus, t_i is the interaction time and $\dot{\epsilon}$ is the strain rate, estimated as being proportional to the steady state temperature gradient

$$\dot{\epsilon} = \alpha_T \left(\frac{\partial T}{\partial x} \right) v \cos(\theta - \theta_m) , \quad (\text{eq. 5.})$$

where α_T is the coefficient of thermal expansion, v is the laser scanning speed, θ is the angle between the normal to the solidification front and the laser scanning direction and θ_m is the preferred solidification direction angle. Considering that the interaction time is

$$t_i = \frac{2 r_o}{v} , \quad (\text{eq. 6.})$$

where r_o is the beam radius, a simple expression for the residual stress is obtained

$$\sigma_{res} = 2 \alpha_T E r_o \left(\frac{\partial T}{\partial x} \right) \cos(\theta - \theta_m) . \quad (\text{eq. 7.})$$

Vasinonta *et al.* ([42] and [43]) developed process maps in the context of laser deposition of thin-walled structures, in particular with the Laser Engineered Net Shaping (LENSTM) process. In one study [42], a 2D FEM using AbaqusTM was used in order to obtain operation curves relating process variables, namely the normalized wall height, melt pool length and melting temperature of the wall material. The effect of pre-heating temperature, laser power and scanning speed were also evaluated. Although such maps were produced with constant properties, a strategy is outlined for producing such maps with temperature dependent properties. In the other paper [43], operation curves involving the normalized temperature gradient, temperature at the top surface and wall height were obtained. Results for the maximum stress as a function of temperature gradient and pre-heating temperature were also featured.

Costa *et al.* ([11] and [12]) developed a 3D model for temperature and phase content evolution in the case of laser powder deposition of steels, using the AbaqusTM FE software.

The evolution of mechanical properties, namely hardness, was accomplished by means of kinetics equations, an approach that is quite common in the study of phase transformations, for example to model processes such as quenching and tempering of steel. Within that framework, the temperature field provided the input for the calculation of martensite content (by means of the Koistinen-Marburger equation) and the hardness evolution (through the Dorn parameter). The calculation is performed in the same mesh than the temperature problem, by means of user defined variables and subroutines, a feature of the AbaqusTM software. Such analysis allows the calculation of the final distribution of hardness in the material, taking into account the tempering effect caused by thermal cycling associated with the buildup of successive clad layers.

Labudovic *et al.* [44] developed a 3D FE model based on the software package AnsysTM to simulate the temperature and stress fields in the laser metal powder deposition process. Cubic shaped elements were used. Fusion zone sizes and residual stress magnitudes were calculated with the model and then compared with experimental results in the case of deposition of Monel 400 on AISI 1006 steel.

2. A simple model for dilution in laser cladding

2.1. Introduction

In order to ascertain if a certain cladding operation is feasible, one has to evaluate the joint effect of the process parameters (mainly the laser scanning speed v , laser power P and the powder feed rate φ) in the possibility of establishing a stable melt pool in a clad material with melting temperature T_m^C which is to be deposited over a substrate with melting temperature T_m^S . This evaluation is best performed assuming the system is in a quasi-steady state; nonetheless, the issue of establishing such a state is not a trivial one and will be addressed at the latter portion of the following section.

The case of LC in which the substrate and cladding materials are the same (single-material system) will be addressed first. This is the situation that arises more often in DMD and In-situ Repair.

2.2. Single-material system

At steady state the mid-plane of a single-bead clad and substrate system should be as shown in figure 9. In order to assure that the clad adheres to the substrate, the melting isotherm should enter into the substrate. In addition to that, it is expected that the whole clad material undergoes melting, so the melt pool in the clad should span the whole height (and width) of the clad zone.

In figures 10-12 unacceptable configurations can be seen. In all cases there would be a layer in the clad never undergoing melting, which is not possible. In order to avoid these situations:

- a) laser scanning speed, laser power, powder feed rate and melting temperature T_m^C must be such that the melting pool has a depth equal or higher than the expected clad height (figure 10);
- b) the location of the laser source must be such that the melt pool is not shifted too much toward the back (figure 11) or to the front (figure 12) of the interaction zone (*i.e.*, the zone where laser beam, powder and melt pool are coming in contact).

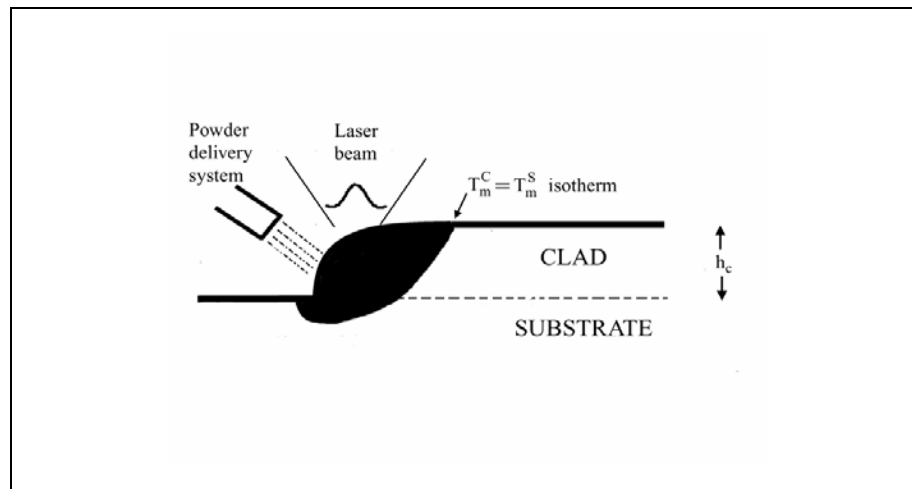


Figure 9. Longitudinal section of laser clad material: single-material case.

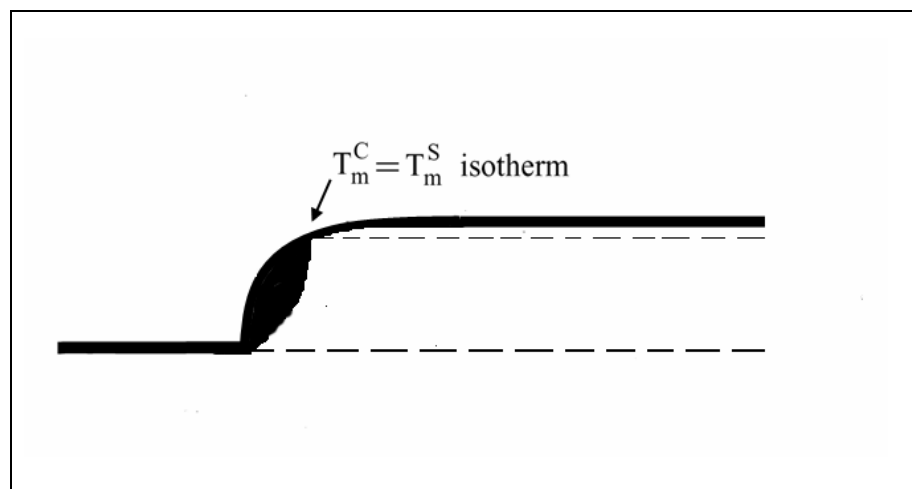


Figure 10. Insufficient energy leads to unacceptably small melt pool.

Item a) relates mainly to whether there is enough energy in the system. A rough estimate of this condition can be made using a global balance of heat and mass, eventually with the

assistance of a heat transfer analytical solution (such as the Rosenthal solution for a moving point source [45] or the Ashby-Easterling [46] solution for a line source of heat).

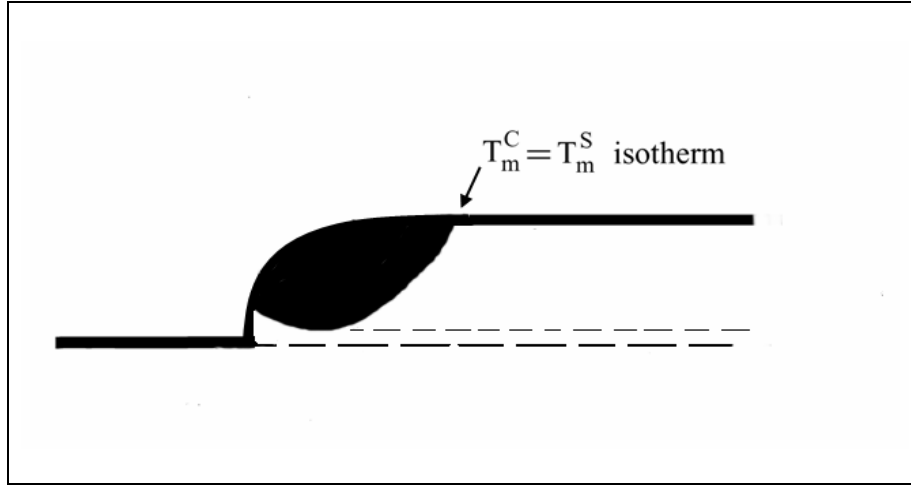


Figure 11. Improper location of laser beam: toward back.

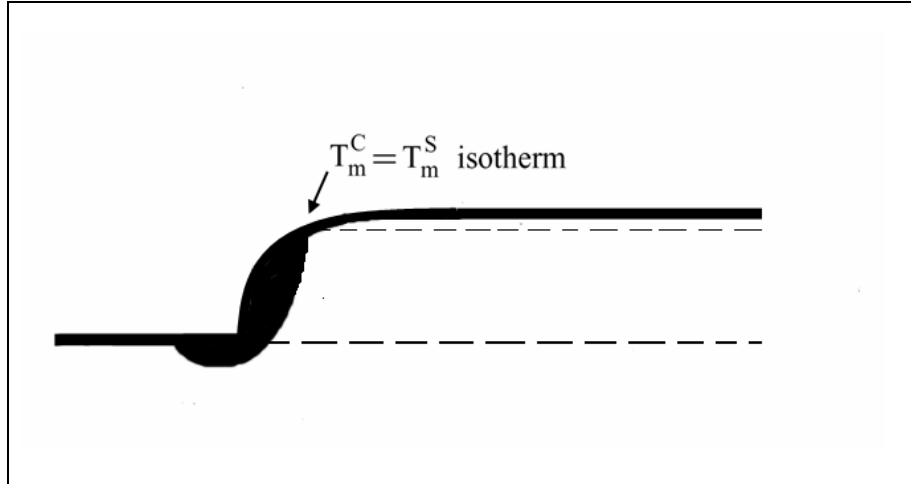


Figure 12. Improper location of laser beam: toward front.

For that purpose, we can estimate the clad height as a function of v , φ and the clad density ρ_c (assuming the clad strip is a half-cylinder of radius equal to the height, h_c , figure 13). For a time interval Δt :

$$\frac{\pi}{2} h_c^2 \rho_c v \Delta t = \varphi \Delta t \quad (\text{eq. 8.})$$

giving

$$h_c = \sqrt{\frac{2}{\pi} \frac{\varphi}{\rho_c v}} \quad (\text{eq. 9.})$$

Then we evaluate if there is enough energy to heat up a portion $v \Delta t$ of the cylindrical strip from room temperature T_0 up to the melting temperature T_m^C :

$$\frac{\pi}{2} h_c^2 \rho_c v \Delta t \left[L + \bar{c}_p (T_m^C - T_0) \right] < P \Delta t \quad (\text{eq. 10.})$$

or (with $\Delta T_m = T_m^C - T_0$):

$$P > \left(L + \bar{c}_p \Delta T_m \right) \varphi \quad (\text{eq. 11.})$$

where L is the latent heat of melting and \bar{c}_p is the (clad) mean specific heat in that temperature range, assuming the clad portion of length $v \Delta t$ underwent a full thermal cycle during $v \Delta t$, in which the laser energy $P \Delta t$ was transformed into thermal energy. This is basically the lumped heat analysis presented by Kar and Mazumder [24].

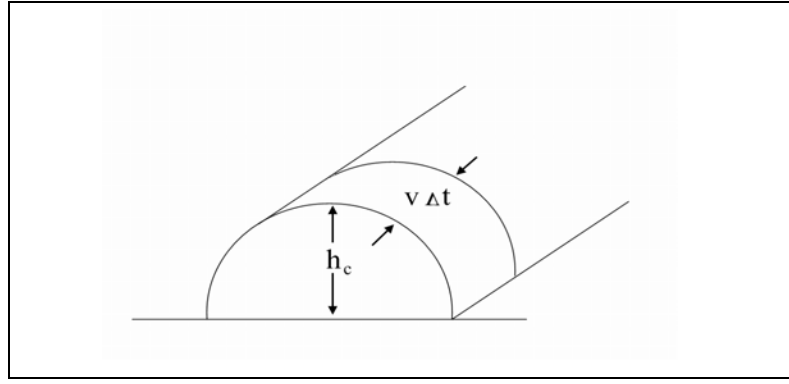


Figure 13. Clad cross-section, assumed cylindrical in shape.

Since at steady state there is heat conduction into the substrate, an alternative evaluation might be made as follows: we can use a 2D solution for a semi-infinite geometry, *e.g.* the Rosenthal solution [45]:

$$\Delta T = \frac{P}{2 \pi k r} \exp\left(-\frac{v(x+r)}{2D}\right), \quad r = \sqrt{x^2 + y^2 + z^2}. \quad (\text{eq. 12.})$$

Talking $x = z = 0$, we can check the temperature increase ΔT at $y = r = h_c$, where h_c is calculated from equation 9. Thus we impose (see figure 14):

$$\frac{P}{2 \pi k h_c} \exp\left(-\frac{v h_c}{2D}\right) > \Delta T_m \quad (\text{eq. 13.})$$

or

$$P > 2\pi k h_c \Delta T_m \exp\left(\frac{v h_c}{2D}\right). \quad (\text{eq. 14.})$$

Since h_c is given by equation 9, we thus obtain a single relation involving the three important processing parameters (the laser scanning speed v , the laser power P and the powder feed rate ϕ).

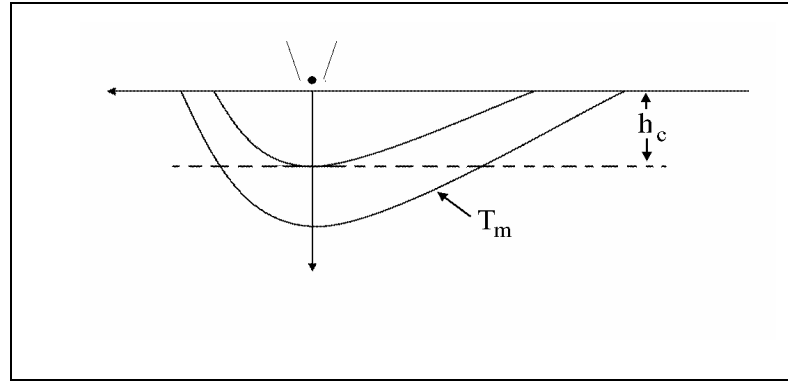


Figure 14. Moving point source: schematic of temperature field.

Estimates based on analytical models are expected to be crude in nature, although they may provide important preliminary insight on the range of processing parameters that will be used on a given system. Nevertheless, a numerical (*e.g.*, FE) model, performed in a realistic domain, might allow for a more accurate estimation of those parameters.

An approach might be to start with a given v and ϕ (which define a clad height) and then adjust P such that a melt pool of height $h > h_c$ is seen developing at steady state. In this, it is important to properly define the position of the heat source in relation to the clad advance front (*i.e.*, the interaction zone). Since it is often required that we get as less melting in the substrate as possible, it might be a good criterion to match the location of the front of the clad with the front of the T_m^C isotherm (figure 15), which for a given P and v will define a position of the heat source in relation to the clad front, which in this case is the farthest allowable position of the laser beam in relation to the clad front (laser beam thus located toward the back of the melt pool).

Note that if the position of the laser source is such that it is farther from the clad front, we get a case that might be inconsistent with the heat transfer overall requirements mentioned before (figure 16), while if we bring the laser closer to the clad leading edge, we might still obtain a consistent cladding operation (figures 17 and 18; the latter features the extreme laser position toward the front of the melt pool). The fact that, besides a range of parameters, there is a range of laser positions allowing for a successful cladding operation reflects the real-life situation that exists in the laboratory.

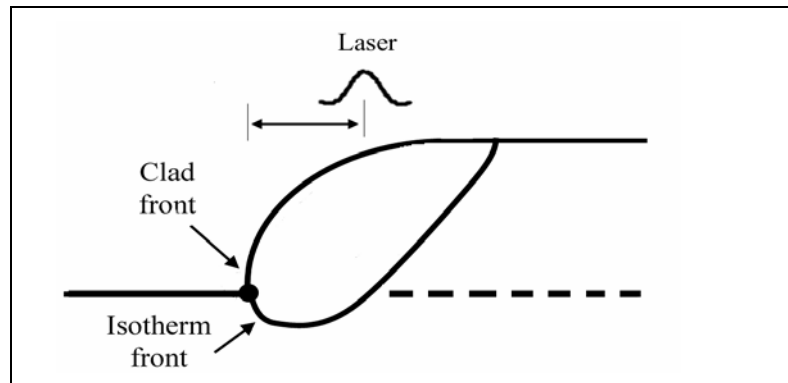


Figure 15. Extreme proper location of laser beam: toward back.

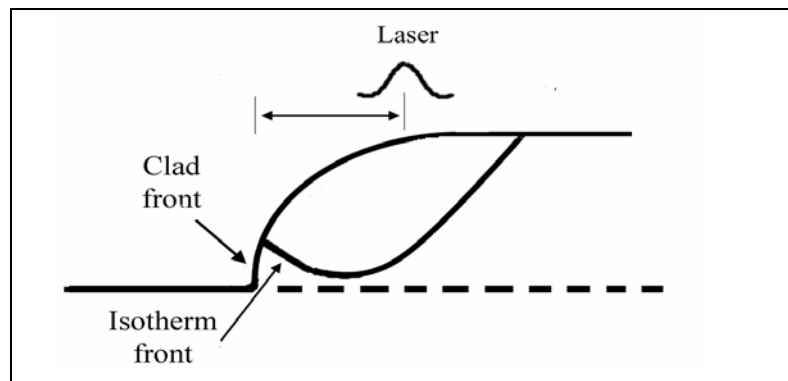


Figure 16. Improper location of laser: inconsistent location of clad melt isotherm.

As a reference “threshold” problem (or, an “idealized” problem, as discussed by Hoadley and Rappaz [28]), one could do as follows: adjust both the laser power and the location of the laser beam so that the melting isotherm touches both the clad front and the leading edge

of the top portion of the clad (figure 19) This would give the minimum power to achieve a successful cladding operation.

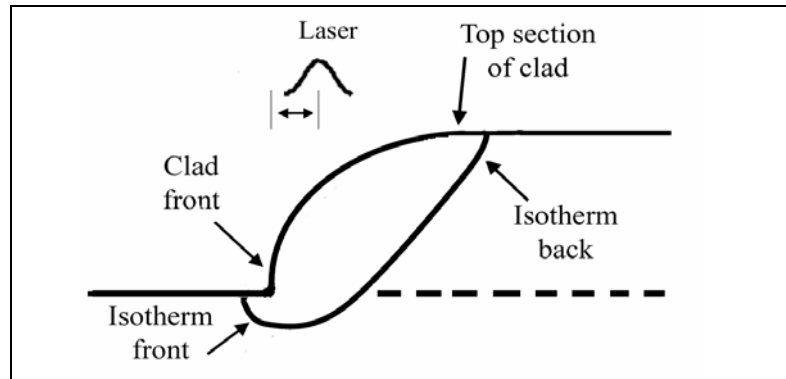


Figure 17. Possible location of laser beam.

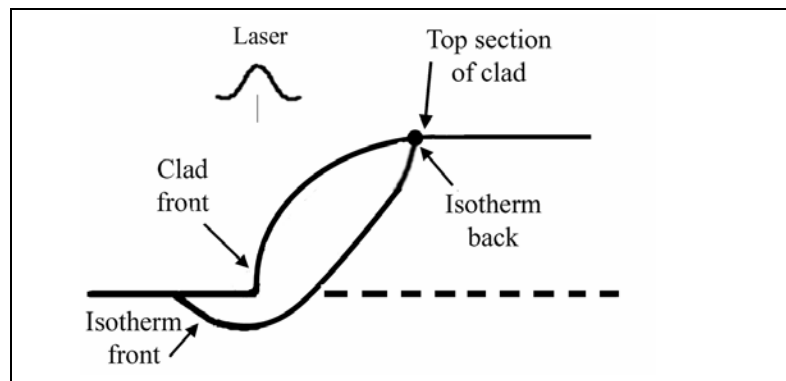


Figure 18. Extreme proper location of laser beam: toward front.

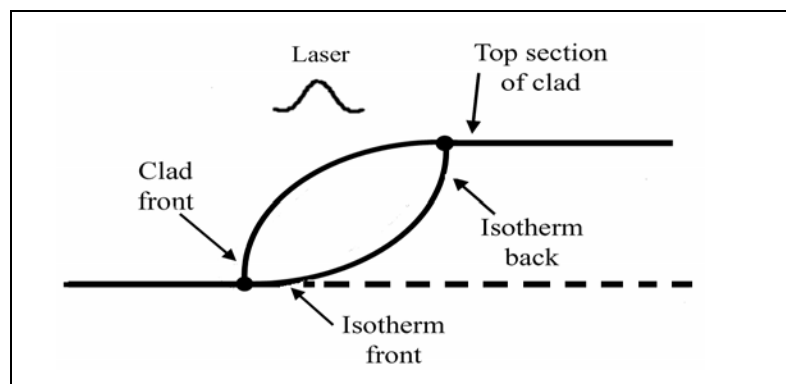


Figure 19. Definition of minimum laser power.

To find out the maximum acceptable power one has first to define a maximum allowable dilution parameter, which (as seen before) could be defined as the ratio between the depth of the melt layer in the substrate, h_i , and the clad height, h_c (figure 20):

$$f_{dil} = \frac{h_i}{h_c}. \quad (\text{eq. 1.})$$

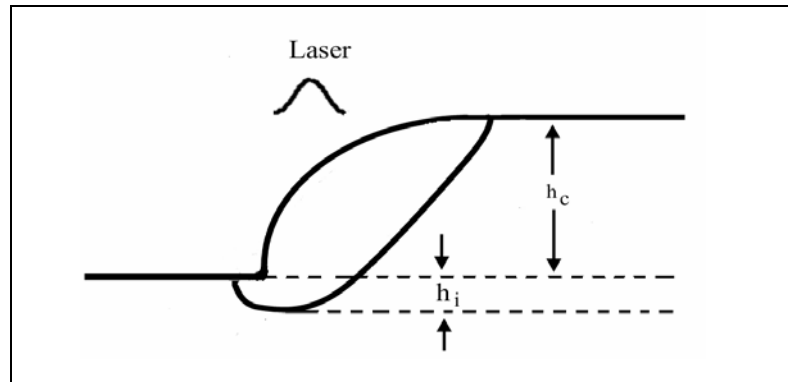


Figure 20. Definition of dilution parameter.

For a given f_{dil} (*i.e.*, for a given maximum h_i) the maximum power can be found using similar lines of reasoning as before; that value of P is expected to be associated with a laser beam positioning toward the back of the melt pool (figure 21).

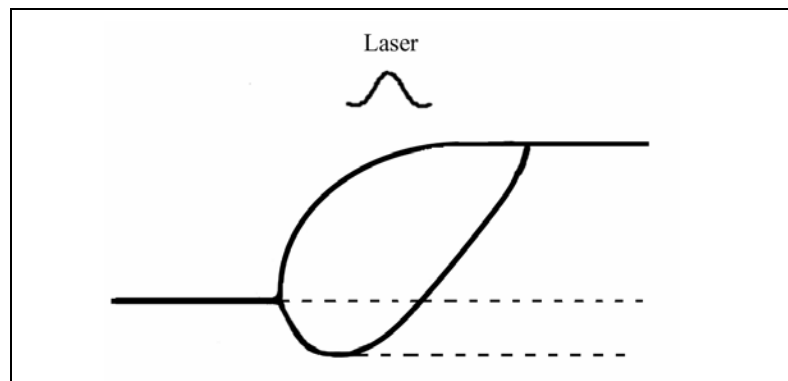


Figure 21. Definition of maximum laser power.

To obtain estimates of power, we can use equation 10 and use the value $h_i + h_c$ instead of h_c , giving:

$$P < \left(L + \overline{c_p} \Delta T_m \right) (1 + f_{dil})^2 \varphi \quad (\text{eq. 15.})$$

or using the Rosenthal equation:

$$P < 2 \pi k h_c (1 + f_{dil}) \Delta T_m \exp\left(\frac{v h_c (1 + f_{dil})}{2 D}\right). \quad (\text{eq. 16.})$$

Thus, for given v and φ and a stipulated maximum allowable dilution parameter f_{dil} (typically up to 10%), it is usually possible to make a rough estimate of the range of laser powers that lead to a successful laser cladding operation. This range of parameters, although still narrow, is usually manageable to achieve in the laboratory.

The analysis that was done focused on the longitudinal mid plane but the reasoning should be of course applied to the whole clad bead front (figure 22). In fact, the steady-state melt pool must span the whole width of the clad bead (figures 22 and 23), so as to exist mass and heat transfer consistency (all clad material must undergo melting).

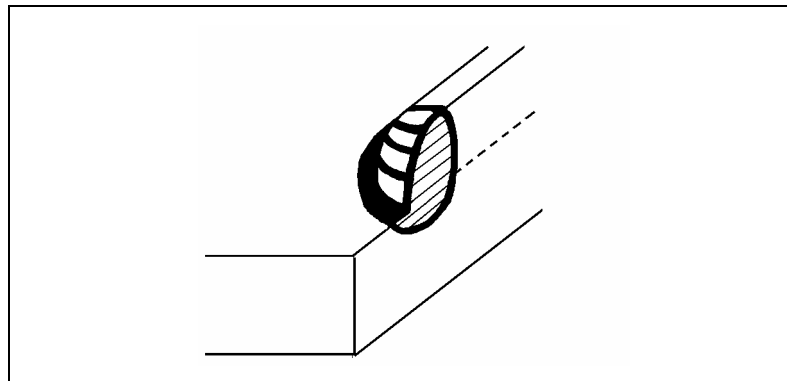


Figure 22. View of (half) clad bead. Melt pool spans height and width of track.

An important remark should be made in connection with the laser beam position with respect to the melt pool. Although the theoretical range of power for cladding might be estimated first using the matching of the melting isotherm with the clad front (figures 19 and 21), it is usually expected that the melt pool reaches to some distance ahead of the clad front. This usually leads to a better powder catchment efficiency, than with the case where the melt pool is totally shifted toward the back.

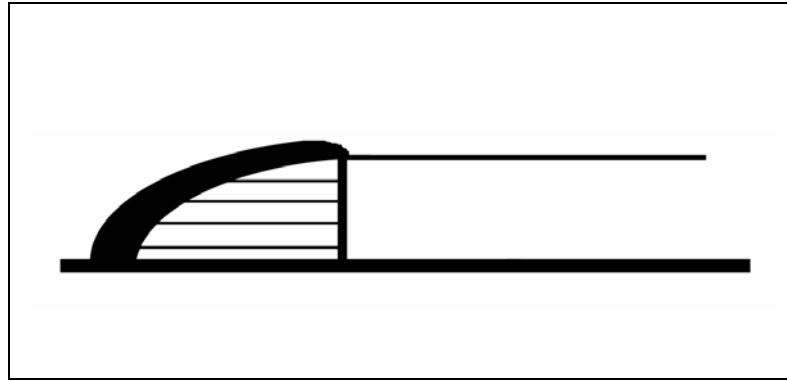


Figure 23. Top view of (half) clad bead.

Actually, the issue of powder catchment efficiency (percentage of powdered material that becomes clad material) is a central one in the possibility of establishing a steady state in LC. Powder particles that hit and enter the already existing melt pool will be included in the clad bead, whereas the ones that impinge on the solid portion of the system will be lost (although it is desirable that they are recycled, for example recaptured by a pneumatic device and placed back in the powder delivery system).

This issue of powder catchment is critical, in particular, at the beginning of the process. During that transient phase, a melt pool must form first in the substrate so as to catch the powder that will in turn melt and then solidify, leading to a clad bead that grows higher and higher up to a stable height, the steady-state clad length h_c (figure 24).

It should be noted that during the transient period, the remelt depth (thus also the dilution) can be higher than its allowable steady-state value, although this can be minimized by, for example, ramping up the value of the laser power at those early stages. (In multi-material laser cladding, composition will also tend to vary down to a deeper layer in the substrate, compared with the steady state situation, because of the increased local dilution. Nevertheless, for a successful clad bead, that initial transient tends to be relatively short when compared with the track length).

The steady state is established once the power absorption efficiency (absorptivity) and the powder catchment efficiency (function of melt pool size and powder delivery system alignment, carrier gas speed distribution, etc) attain approximately constant values –thus, if there is heat and mass transfer consistency, the system will tend naturally to such a stable steady state. On the other hand, if heat and mass delivery are not properly matched (for example too little power is present in the system for the amount of powder present), the system will be unstable, in that whatever bead that starts to form will not grow uniformly, leading to incipient clad formation, many times with no adhesion to the substrate, or to a clad bead that is wobbly in nature (similar to a succession of differently sized contacting spherical droplets).

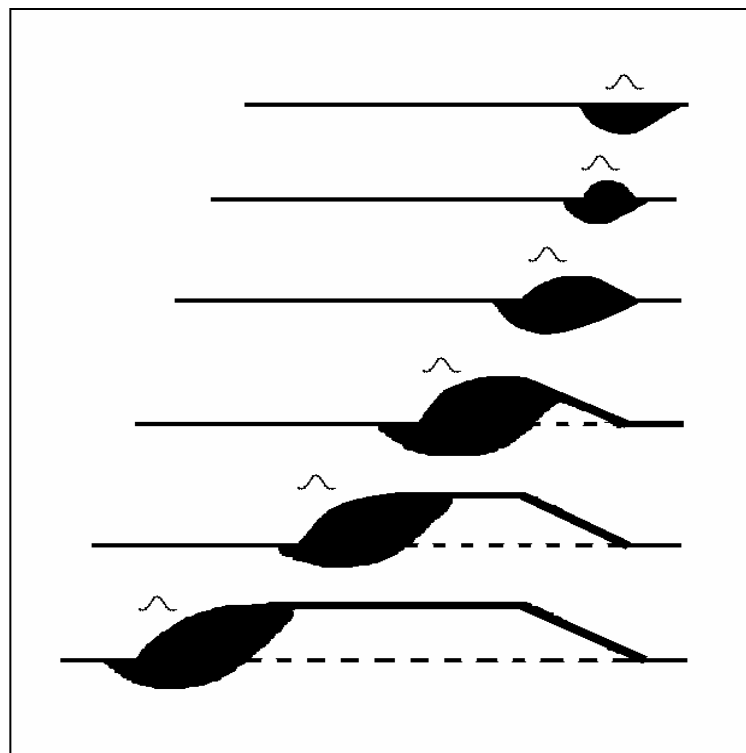


Figure 24. Transient stage: formation of stable clad track.

Interestingly, if a stable melt pool forms in the substrate and the powder feed rate is very small then there might exist good conditions for laser alloying, provided there is solubility potential for the powder elements to be incorporated into the substrate, whether in solid solution form and/or as precipitates.

2.3. Bi-material system

In LC one frequently aims at depositing a coating onto a substrate of different composition, so as to improve the surface properties of the latter. Since melting points of such materials are in general different, sometimes it is difficult to obtain such systems by conventional methods (*e.g.* casting or similar processes), especially in view of the fact that a close metallurgical bond usually involve melting of both materials at the contact zone (an exception to that is friction stir welding).

In this regard, laser processing is an appropriate technique, as heat gets deposited into the material in a localized fashion, allowing the user to gauge the amount of energy to be applied and its location. Still, the issues of mixing of dissimilar materials have to be addressed, namely the different melting points of the materials involved, the forming of new phases (either in bulk or on a matrix with precipitates), and the homogeneity of the melt pool (dependent upon the mixing efficiency in the liquid).

2.3.1. Substrate with a higher melting point

In the ideal low power threshold situation we would have, were we to assume that no mixing takes place, the situation depicted in figure 25, in which the melt pool would only reside in the clad. The liquid clad would be in contact with a substrate that is below its melting point.

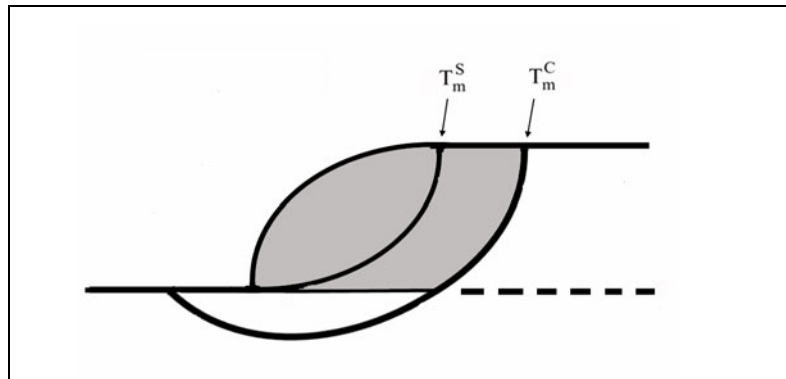


Figure 25. Substrate with higher melting point: threshold condition with no mixing.

Allowing for the substrate melting isotherm to drop slightly below the substrate surface, as required in laser cladding, will lead to mixing of the substrate and clad materials. The melt will have a different melting point, which we will assume to be higher, without loss of generality (but that will obviously depend on the relevant phase diagrams), than the corresponding value for the pure clad material. At steady state, with good mixing, the composition in the melt pool is expected to approach the one of this new alloy thus formed, except at the melting front in the substrate region, where a solid with the substrate composition is being transformed into liquid. If the overall composition is uniform, with the exception just mentioned, the melt pool would look like figure 26.

If the mixing effect is felt mainly at the interface, with a certain degree of stratification (local composition dependent on depth), one can obtain a configuration such as in figure 27, where the local melting point would also vary with depth and the melt pool limits would span the isotherms.

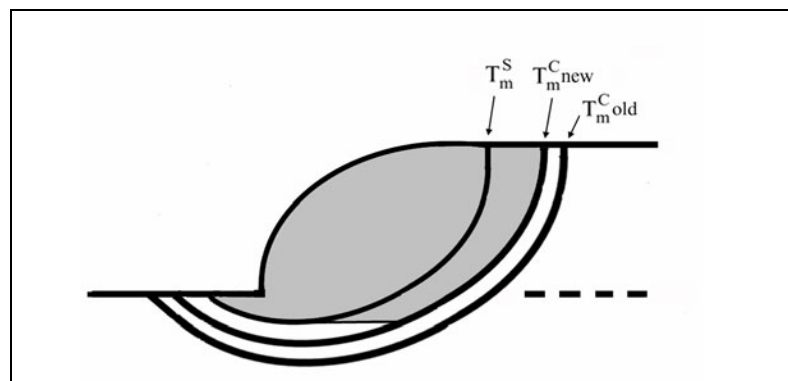


Figure 26. Substrate with higher melting point: good mixing.

In the case where the substrate has a higher melting point, it might be possible to obtain a clad with low dilution with relative ease. In effect, the melt front in the substrate tends to be shallow. On the other hand, in the case where the substrate has a lower melting point the situation gets reversed and there is greater tendency for higher dilutions. This latter case is more common: in many applications one uses a coating that is harder than the substrate, so in general the clad melting point is indeed higher. This situation will be now addressed in more detail.

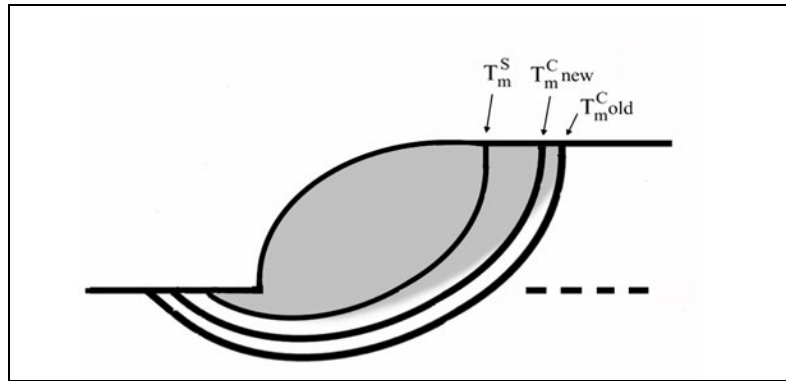


Figure 27. Substrate with higher melting point: moderate mixing and stratification.

2.3.2. Substrate with a lower melting point

Looking again first to the ideal low power threshold situation with no mixing, we would have the configuration depicted in figure 28, in which the melt pool would be divided in two zones. Of course, this situation is highly unlikely, not only because it is an unstable threshold condition but also because the melt pool in the substrate would lead to catchment of clad powder particles, leading to dilution therein. It is just a first step, though, in forming a picture of mixing in such systems. The next step is to consider the modification of such configuration if little mixing is considered, in such a way that the almost independent melt pools in the clad and substrate regions see their melting points slightly affected (figure 29).

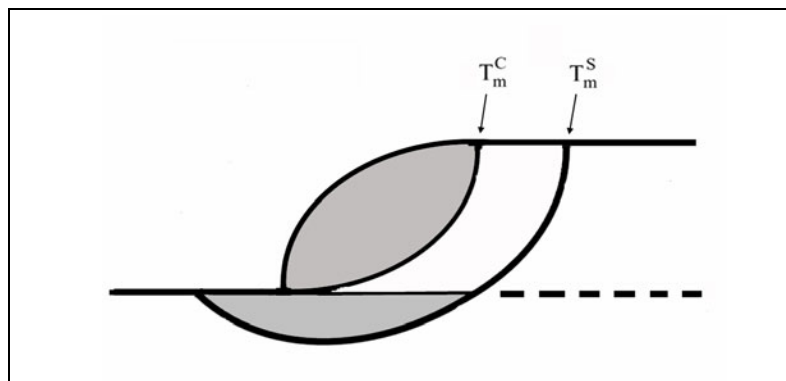


Figure 28. Substrate with lower melting point: threshold condition with no mixing.

In this situation we see a melt pool that would have, by assumption, a zone on top with composition close to the clad and on lower depths a region similar in composition to the substrate. These liquids have different melting points and the pool geometry reflects that: the melt would tend to get slightly extended toward in the lower depths of the substrate (due to steady state conditions, the upper portion of the substrate region would solidify with the clad material melting point).

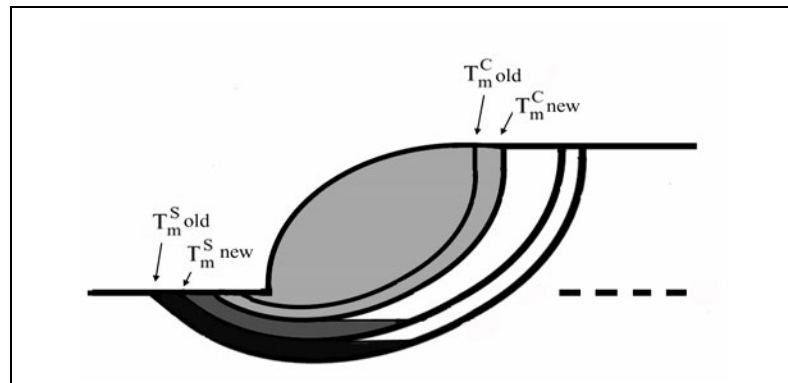


Figure 29. Substrate with lower melting point: little mixing.

Since these two fluids are in contact and there is convection in the fluid, the composition is expected to tend to homogenization. We can assume that the melt pool as a whole has a for the most part a homogeneous composition, but again there must be always a transition zone between that liquid and the substrate-rich just-melted material, just as in the case of the previous section. It is noteworthy that such region, with lower melting point, has the tendency to extend backwards (figure 30).

Assuming that some stratification in the composition takes place, this behaviour will likely persist (figure 31). Note that the convection pattern in such enclosure, which is very near the substrate melting front, might tend to keep its composition near to that of the substrate, with a tendency to keep that enclosure in a stable compositional condition.

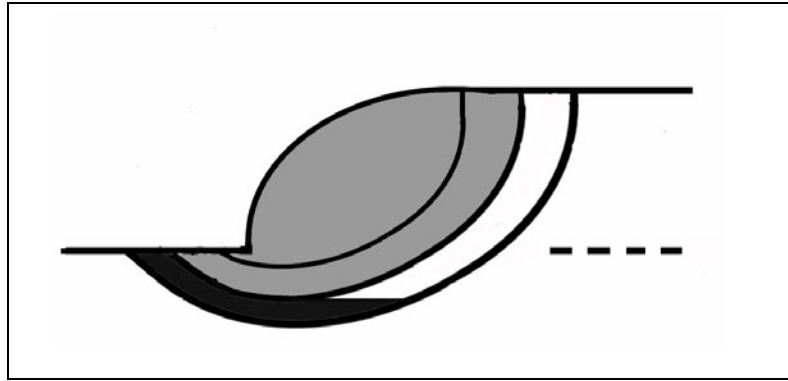


Figure 30. Substrate with lower melting point: good mixing.

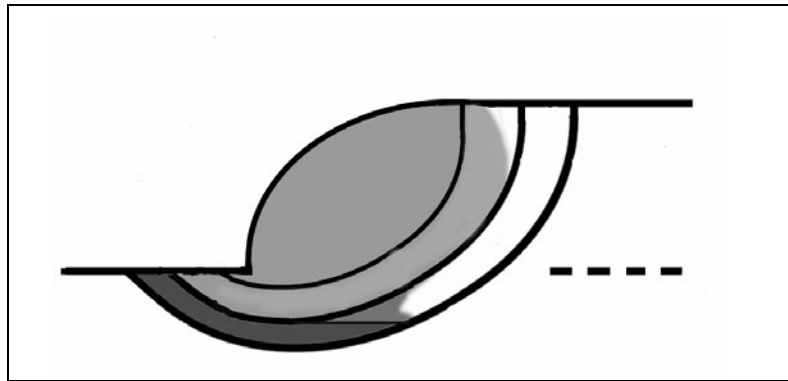


Figure 31. Substrate with lower melting point: mixing and stratification.

This morphology would also likely be seen if in the interface zone intermetallic compounds would tend to form. These would generally solidify at higher temperatures and otherwise act as nucleation sites for the surrounding melt, bringing the local solidification boundary toward the front, in contrast with the lower regions of the substrate (figure 32). The unusual microstructures that sometimes occur in laser cladding and alloying, in which solidifying fronts are seen to grow at considerably different angles due to such stratification, were studied in detail elsewhere [47] and were, in particular, observed in the experimental work that ran parallel to this dissertation [1].

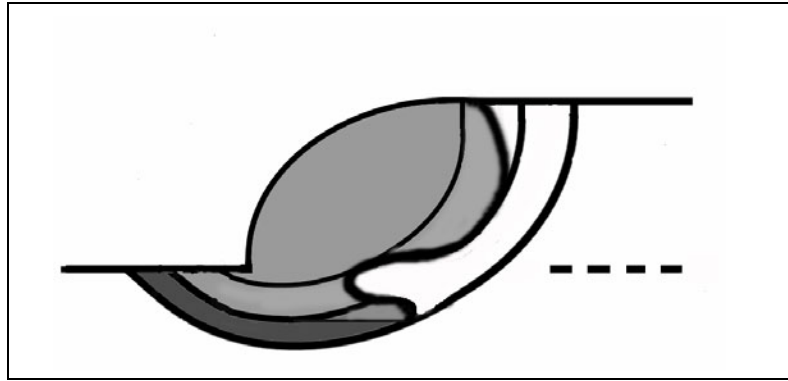


Figure 32. Melt pool showing early solidification pattern on the interface.

2.4. Model implementation

For the system we are considering in this dissertation, the substrate, aluminium-based alloy AA333, has a lower melting point ($T_m^S = 585\text{ }^\circ\text{C}$) than the clad, copper-based alloy C95600 ($T_m^C = 950\text{ }^\circ\text{C}$), so we should consider the conditions of section 2.3.2.

In the model implementation we assume that the clad zone maintains its original composition (when the material is on the powdered condition). This should be the more correct the smaller is the dilution parameter f_{dil} . As to the substrate zone, especially its top portion that will be referred to as the interface (figure 33), two possibilities were considered:

1. The domain is considered to remain filled with the same material throughout the simulation;
2. The composition of such domain can, alternatively, be allowed to evolve, determined by the evolution of the temperature field and assuming a very simple model for mixing.

2.4.1. Interface with fixed composition

In this case, there is the possibility to assign to the interface layer the properties of the appropriate material that is seen to be the most suitable in regards to the processing conditions. For example, for cladding with a non-zero dilution, the interface zone can be assumed to be made of the clad material. Or, it can be assigned the properties of a metal matrix composite, with the substrate material as the matrix and the appropriate precipitate(s) as the reinforcement. The depth of such interface zone should be matched with the depth of the appropriate melting isotherm. On the other hand, if one wants to find out the minimum power threshold condition, then the composition of such layer should be assigned to the substrate material; thus, there is no separate interface region.

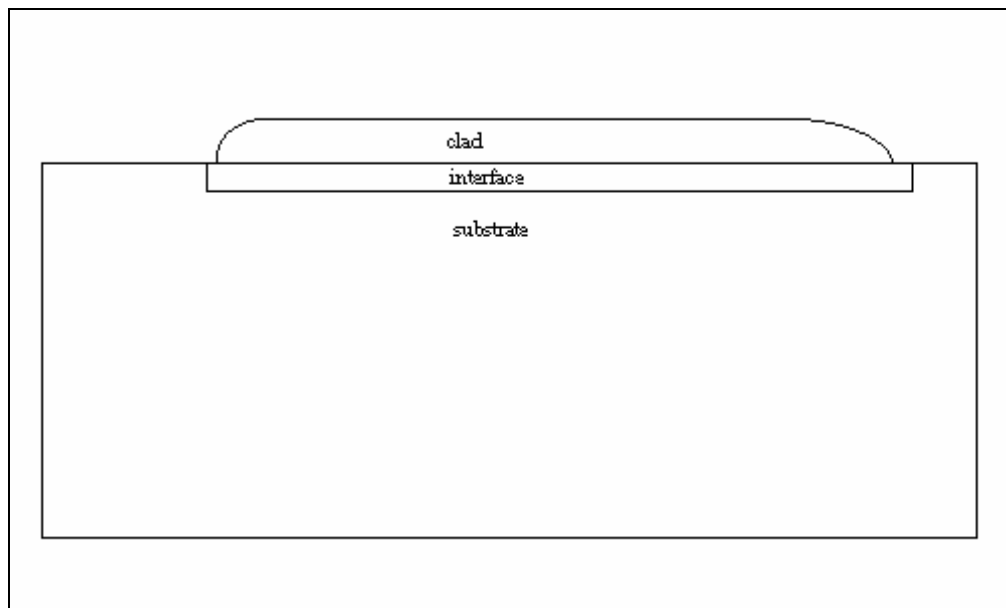


Figure 33. Definition of the interface region.

It's admittedly difficult to ascertain the properties of that zone, when viewed as a composite. Experimental data of composition and hardness can be very helpful in guiding the modeling assumptions for that situation. One possibility is to assume that there is a predominant precipitate (in the experimental study, that was found to be Al_2Cu) and also that its average volume fraction can be estimated (although kept relatively small, typically up to a volume fraction of 20%) and then utilize usual methods to estimate the properties of such composite.

2.4.2. Interface with varying composition

The local composition in the interface region can be allowed to evolve as a function of temperature. While it is assumed that the composition of the clad zone is not altered, the substrate can change its local composition (most notably in the interface zone) according to the thermal history of each point; more specifically, in a simple model for mixing, a composition variable (or index) will be determined by the peak temperature that was attained at each point. The relevance of the peak temperature has to do with the steady state nature of the process: using the situation depicted in figure 34, we see that the clad and substrate isotherms plough through the substrate material, up to a depth that is the lowest point of the respective isotherms, leaving behind a solid material that has a composition corresponding to such melting isotherm. From the viewpoint of a fixed point on the substrate, therefore, its final composition depends upon the peak temperature therein attained:

- if it is above the clad melting temperature, the solidified material will be of clad composition;
- if it is below the substrate melting point, the composition is unaltered;
- if it is intermediate between those two melting points, then the composition will likely be also found to lie between the one of the clad and the one of the substrate material.

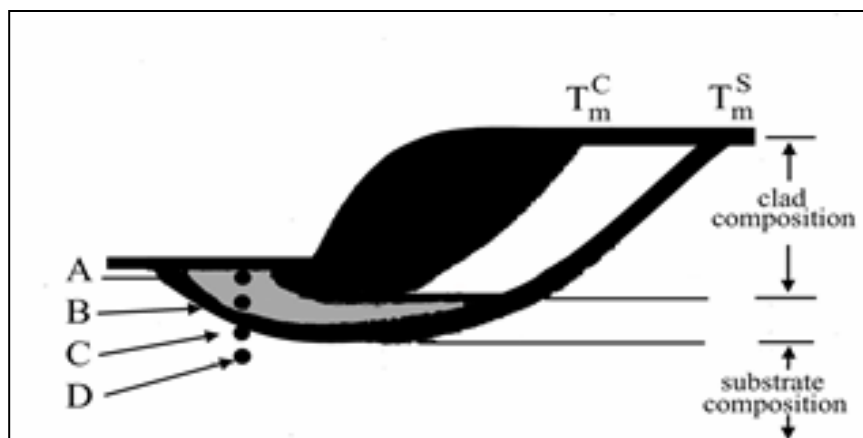


Figure 34. Relationship between peak temperature and final composition.

This is represented in figure 35, where we see the typical thermal cycles suffered by the points shown in figure 34 (the schematic in figure 35 is actually a plot of the Rosenthal solution [45], used here for argument sake only). For example we see that point A, already in the liquid state, that has a composition that is close to the substrate's. But as the clad front advances, point A is swept by the clad melting isotherm, thus the composition of point A changes from the one of the substrate to the one of the clad. On the other hand, the peak temperatures of points B and C are lower than T_m^C but higher than T_m^S . This means that those points will have a composition that is intermediate between the clad and the substrate. Since B remained in the liquid state longer, and since it is closer to the clad, we expect B to have a composition closer to the clad than C. On the other hand, the composition of point D remains constant.

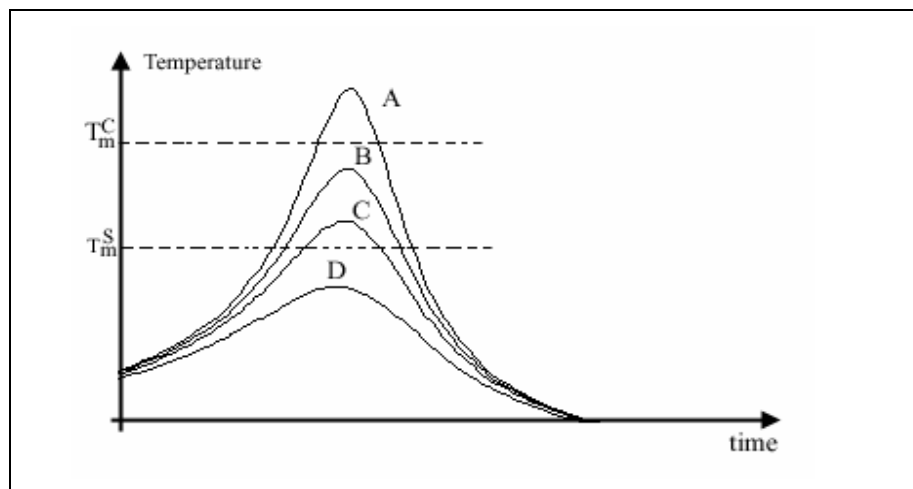


Figure 35. Thermal cycles at various depths (schematic).

We see that under the assumptions of this simple model for mixing, the stratification that was mentioned before is tied with this peak temperature analysis and therefore is a consequence of the steady state temperature field. Nevertheless, such model assumes that only moderate convection is taking place, enough to assure that some necessary mixing happens, but not as violent so as to distort dramatically the isotherms and the composition iso-lines within the melt pool.

It seems convenient to define a composition index, c_i , that is a function of the local peak temperature, $T_{MAX}(x, y, z, t)$ and of the melting points of substrate and clad:

$$c_i = \frac{T_{MAX}(x, y, z, t) - T_m^S}{T_m^C - T_m^S}. \quad (\text{eq. 17.})$$

The composition index is thus the reduced peak temperature. If $c_i \geq 1$ we consider that we have clad material and if $c_i \leq 0$ we have substrate material. For $0 < c_i < 1$, we have “interface” material, that we must characterize. Please note that c_i is a function of time, as it is expected to vary during heating. For example point A in figure 34 has $0 < c_i < 1$, whereas it is clear that after the cladding front passes by c_i will become $c_i(A) > 1$.

While c_i might vary in a nearly linear fashion, the real composition (*e.g.* the amount of one of the elements in the clad and substrate material, per unit volume) is expected to vary more drastically. Still, with this scheme one is able to determine the location of the boundaries of the interfacial zone and, therefore, characterize dilution in a quantitative fashion.

This simple model of mixing is a feature of some of the FE simulations described in the following chapter. In this regard, we will be concerned with calculating the composition index for its own merits, as a descriptor of dilution, but also because it is a field variable assumed to be univocally tied (though not expected to be in a linear relationship) with the local composition, thus affecting the properties of the material. So, in the FE models for temperature and stress, the properties will be a function of both the temperature and the composition index.

3. Finite element modeling of laser cladding

3.1. Introduction

Laser cladding is a process that is three-dimensional in essence. This becomes evident when one looks at the applications of this technique. For example, the goal might be to deposit a coating of a certain height over an area, which is usually accomplished by the side-by-side deposition and overlapping of successive tracks. From a geometric standpoint, it might be difficult to translate such multi-bead clad process into a 2D equivalent model. Another example lies in DMD, in the context of Rapid Prototyping: since the goal is to fabricate a part with a geometry possessing a fair degree of generality, it is obvious that only a 3D modeling approach can adequately address the problem.

Nonetheless, in analyzing single track laser cladding, it seems appropriate to start with the simple approach of taking a two-dimensional description of the problem, namely by choosing for calculation domain the longitudinal mid-plane of the sample (which is a symmetry plane, provided that the deposition takes place symmetrically, in regards to the substrate). Of course, since it is common that the width of the clad bead is usually close to the height of the track, a large width approximation (for which constancy of results in parallel planes could be assumed) is not expected in this case, making it desirable a 3D analysis of the problem.

Advantages of the 2D approach, as compared with a 3D one are especially the smaller computation times and an overall easier approach to the problem, namely in mesh generation and in the application of boundary conditions. Thus, one could use a 2D model to obtain a preliminary perception of the problem, especially in view of the obvious fact that single-track LC is the basic element for multi-track LC as well as DMD.

In addition to that, one can establish a correspondence between 2D and 3D models ([48], [49]), by carefully establishing proper translation schemes (for example, an adequate

correspondence of boundary conditions from 2D to 3D). That being done, one can use 2D models to perform quick parametric studies, which may provide initial values for the processing parameters in a 3D analysis, as well as a valuable first picture of the distribution of temperature. Actually, both 2D or 3D approaches are to be validated by experimental results, so it could be that 2D results are found to be reasonable within the experimental error limits, as well as within the limitations imposed by the common scarce knowledge of the values of properties at high temperature (which tend to limit the accuracy of numerical modeling, no matter how “close” the model is from reality).

In this chapter we will first address issues that apply to both heat transfer and mechanics calculations, especially the pre-processing, *i.e.* the mesh generation scheme that was developed. Then particulars to heat transfer and deformation analyses will be discussed, including the governing equations for the phenomena.

3.2. Pre-processing scheme

3.2.1. Mesh design

A critical issue in a Finite Element model is mesh design [50]. By “mesh” we understand the set of points (“nodes”) that are used to discretize the calculation domain and/or the set of elements formed by assemblies of such nodes. The mesh:

- needs to match the geometry of the real object under study,
- should be fine enough, so as to give reasonably accurate results, while at the same time containing the minimum number of elements possible, to minimize computation time; and
- should be generated in a way that enables a straightforward integration of process parameters information into the model, *e.g.* in the ability to easily update the values of boundary conditions.

In a FE model of laser cladding, the computation domain will change based on two related but distinct reasons:

- a) each cladding operation, with its own process parameters, will determine the overall geometric features (such as the clad height and width, or the interface/transition zone location and size);
- b) in a lagrangian description of the process, the cladding zone changes with time during processing, making it necessary to periodically update features such as clad length or the description of the outer surfaces, subjected to boundary conditions.

Each of these issues poses a number of challenges in translating the process parameter information into a workable FE model. A proper strategy is proposed as follows:

- Task 1: Based on the expected final geometry, quantify geometric features (*e.g.* clad height, width, etc.) as a function of process parameters, such as feed rate and scanning speed.
- Task 2: Identify a set of “parent” (“seed”) points, from which the whole domain is going to be constructed, by means of mesh generation. The coordinates of such points should be obtained using equations derived at the previous stage.
- Task 3: Perform the mesh generation procedure, with prescribed grid coarseness. This includes the generation, from the seed points, of characteristic lines and surfaces (and volumes in 3D), up to the definition of the whole mesh.
- Task 4: Keep track of the sub-domains where materials are expected to be different in composition and, also, of the surfaces where boundary conditions are to be imposed. Note that, as material gets added to the domain, its surface will obviously change, too: the clad surface area increases, while the substrate exposed surface decreases. This means that some portions in the substrate zone –as well as the clad zone– that had exposed surfaces before material addition will now have those surfaces incorporated in the bulk after the arrival of new clad material.

To accomplish the mesh generation procedure, a number of software packages exist (*e.g.*, Hypermesh™ or Patran™) that are usually quite versatile, namely in performing task 3 above. Nevertheless, it seemed that, in relation to the overall requirements of a lagrangian

description of laser cladding, *i.e.*, one that has the reference frame tied to the material to be processed, it would be appropriate to fully develop a pre-processing scheme, even if simple, oriented toward laser processing in general and LC in particular. This approach has some advantages:

- the development of an original scheme, implemented in an accessible framework that allows for discussion and improvements;
- the possible suggestion of alternative strategies for meshing in a number of related problems, for example involving moving boundaries or in the field of fracture mechanics;
- the establishment of rules that might be useful in obtaining complex meshes (*e.g.* for DMD) from mathematical relations derived for simple geometries;
- the development of strategies that are useful not only in modeling, but also for example in the full automation of the process, namely in the ability to calculate tool paths as a function of processing variables;
- the lower degree of dependency on third party software, allowing for a closer control on the part of the user regarding the research, instead of being fully dependent of a series of non-open software products.

As regards the latter point, it could be argued that the present analysis is already dependent on proprietary software (the Abaqus™ package) being available. But to undertake the task of building a suitable FE complete code for temperature and deformation would be an independent project in itself, which was not chosen to be specifically covered in the current research, as FE packages (and quite notably Abaqus™) are indeed available in the generality of universities, research centers and engineering departments of many companies. Thus, the processing and post-processing parts of the analysis are done within the framework of Abaqus™, while the pre-processing scheme is fully developed within the present research. It is believed that the overall scheme is easily translatable to the syntaxes of other FE packages.

In accord with the above, the idea was to implement the pre-processing operations in an appropriate ‘environment’. Because of simplicity, the choice was to perform such

calculation and text editing tasks on a worksheet form (Microsoft Excel™), one that virtually all potential users are familiar with, which perhaps wouldn't be the case with script languages *per se* such as Perl, Tcl or Python. (The disadvantages of not using a computer language can be circumvented by the use of so-called 'macros'). Such the environment file is called the "input file generator" (IFG).

So, we now attempt to describe some of the main points of such approach. This can be used as a manual for the use and/or modification of worksheet files, or as a set of guidelines for implementation on a more formal script language formalism.

Some of the programming steps take advantage of simple Abaqus™ commands, for example in generating new sets of nodes as a function of pre-existing ones. And the programming strategy is fully oriented toward conformity with Abaqus™ syntax rules. Nevertheless, the node generation scheme hereby shown can be easily adapted to yield other sorts of output (such as full listings of node numbers and coordinates, element numbers and respective nodes) or to conform to other syntaxes.

3.2.2. Nodal definitions

For the discussion that will follow, a 2D mesh is assumed, although the generalization of the node numbering scheme to 3D is straightforward. A base Cartesian reference frame is set in such a way that the node with lowest node number lies at the origin (for example, node 101, see figure 36). Since we will be interested in counting nodes in rows and columns, the numbering scheme counts nodes in each direction, locally identified with cartesian coordinates (x,y) , starting at 1 (unfortunately, Abaqus™ doesn't work with a zero as a node number). Since quadrangular elements only are used in our 2D analysis, the mapping of nodes using rectangular coordinates seems to be appropriate, thus a node can be identified by its column and row numbers (n_x, n_y) . In 3D, and for the most part, 8-node brick elements are used, so a cartesian mapping will also be followed in that case.

Assuming the maximum node number in each direction is lower than 10^d , we can assign d digits in the node numbering scheme to each direction and to obtain the node number as:

$$n = n_x + 10^d n_y \quad (\text{eq. 18.})$$

The value of d is typically 2 or 3. Different node incrementation values can be used (this can be useful, for example in mesh refining studies):

$$n = n_x NDX + 10^d n_y NDY \quad (\text{eq. 19.})$$

where NDX and $10^d NDY$ are the node number increments in the x and y directions (the notation that is used in the Microsoft Excel™ script files is being kept).

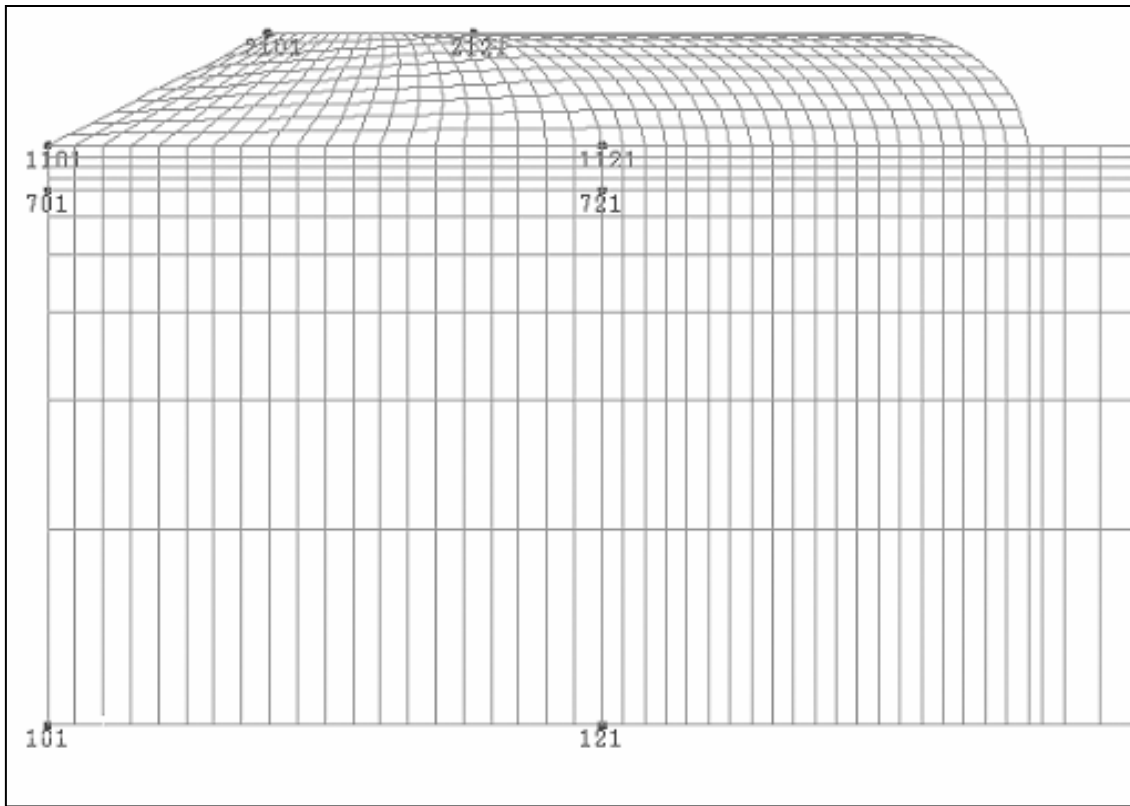


Figure 36. Node numbering scheme.

The node number obtained by means of this scheme enables easy location of nodes in the domain. Of course, these node numbers are to be viewed as labels, because the software performs internal renumbering, so as to minimize bandwidth and thus cpu time.

Mesh construction involves the definition of a number of so-called “parent” nodes, from which all others will be obtained. These can be seen in figure 36 for a particular 2D mesh. The location of such points is a function of substrate (h_s) and clad height (h_c), the latter

being a function of process parameters, such as feed rate φ and scanning speed v , as well as of properties (clad density ρ and clad/substrate dynamical contact angle θ):

$$f(\theta) = \frac{1}{\tan \theta} + \sqrt{1 + \frac{1}{\tan^2 \theta}} \quad (\text{eq. 20.})$$

$$g(\theta) = \frac{1}{2} (1 + f^2(\theta)) \quad (\text{eq. 21.})$$

$$e(\theta) = f(\theta) \sqrt{g^2(\theta) - f^2(\theta)} + g^2(\theta) \arcsin\left(\frac{f(\theta)}{g(\theta)}\right) + 2 f(\theta) (1 - g(\theta)) \quad (\text{eq. 22.})$$

$$h_c = \sqrt{\frac{\varphi}{e(\theta) \rho v}} \quad (\text{eq. 23.})$$

where e , f , and g are angular auxiliary functions. The clad melt front is assumed to be a spherical cap. These equations can be derived based on the model by Colaço *et al* [51].

Further details of the IFG can be ascertained by checking its printouts, which can be found in Appendix A.

3.2.3. Lagrangian vs. eulerian approach

In laser cladding, as in other laser processing procedures, the process can be considered to take place at quasi-steady state, this happening after an initial —usually very short— transient period. From the viewpoint of the temperature problem, it would seem that the natural approach would be to study the laser cladding process in an eulerian reference frame, *i.e.*, fixed to the heat source. Computationally, that is more efficient than a lagrangian coordinate frame (*i.e.* fixed to the substrate). This is so because, for the eulerian case, mesh refinement needs only to be performed at a very limited zone (the irradiated part of the top surface), as opposed to having the same degree of refinement for the whole top surface in the lagrangian case. But on the other hand, the deformation problem, which includes inelastic deformation, is usually defined on a lagrangian basis, because the mechanical behavior of a certain control volume depends on the stress-strain history at that location. An eulerian formulation for stress analysis would be something to be looked for, and some work has been done in that field [52], but such formulation is not readily

available, namely in AbaqusTM. Therefore, in the present work a lagrangian procedure was followed. This has the added advantage of accommodating situations such as cladding near the edges of the substrate, or cladding of overlapping tracks.

3.2.4. Successive addition of new elements

In the cladding process, mass is constantly being added to the workpiece; this event needs to be simulated in the lagrangian procedure. That was accomplished by means of successive discrete addition of new elements to the computational domain (see figure 37) throughout the calculation. That procedure had been adopted before in the case of welding [53].

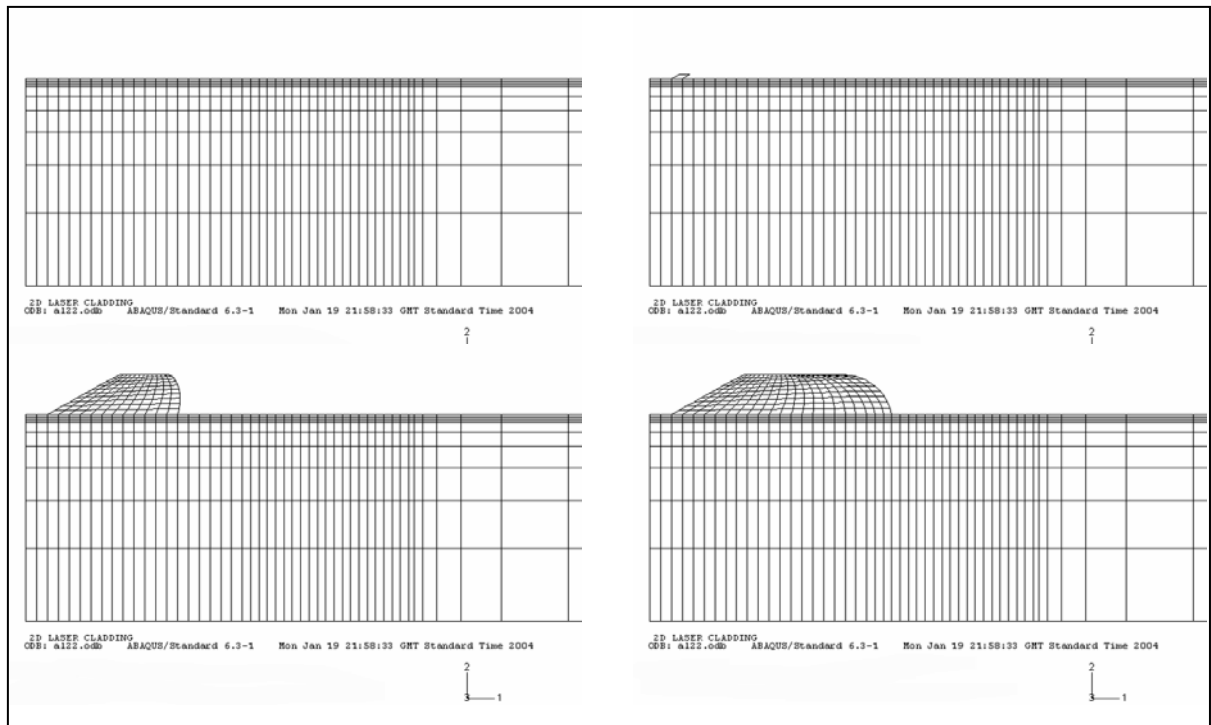


Figure 37. Mesh activation scheme.

These elements are generated either at room temperature (which will have a cooling effect on the pre-existing melt pool), at clad melting point or at an estimated steady state surface temperature. In all cases, there will be a heat redistribution period, which is usually very short as compared with the time elapsed between two element generation procedures.

Assuming that the elements are activated at room temperature has the advantage that the cooling effect of the powder on the whole melt pool is handled by means of heat conduction—that is, in a way which is consistent with conservation of energy. On the other hand, such assumption: a) doesn't take into account the fact that the powder is expected to heat up considerably while in flight; b) leads to oscillating behavior in the results of nearby elements (due to such cooling effect combined with the ever present laser heating); and c) assigns the generated elements an initial temperature that is not the adequate one for thermal strain analysis.

The element activation must be synchronized with the time dependent profile of the boundary condition that refers to the laser. In the present case, the center of the laser beam is always impinging at the clad front.

3.2.5. Mesh generation in 3D

The challenge of designing an IFG scheme in 3D that preserves the round shape of the clad front cannot be overstated. For one thing, it is very desirable to have such a geometry, especially in the heat transfer calculations—as shall be shown in the results section, where simulations using planar shaped clad beads are compared with meshes that preserve round shapes. On the other hand, a number of difficulties arise:

- The definition and labeling of nodes, elements and exposed surfaces (that will be subjected to boundary conditions) and their respective sets is a much more complicated process in 3D than in 2D.
- During the transient phase, the clad not only grows in height but also in length, so the IFG must accommodate this feature; the mesh has to “grow” upward and laterally in a synchronous fashion, so as to obtain the prescribed values of steady-state height and width. Ramping of the mesh, as it was done in 2D did not seem straightforward, so the addition of elements forming steps was the choice, with its own challenges in free surface labeling.
- In the node labeling rationale we now have to accommodate in a consistent fashion a region that has cartesian geometry (the substrate) with one that has approximately cylindrical symmetry (the clad). In trying to maintain a cartesian logic for the node

numbering, the clad zone can be seen as a succession of nodal planes which (instead of being parallel as in the case of the substrate) are obtained, one to the next, by rotation about the axis of the cylindrical clad bead. The nodes on those planes are incremented in a similar fashion than the ones in the substrate. Since, for a more straightforward generalization between 2D and 3D, we took the 2D mesh as the typical starting point for the 3D one, we had to find out how to properly match the surface substrate nodes that are immediately below clad nodes, namely in the construction of the elements that share clad and substrate nodes.

3.3. Heat transfer analysis

3.3.1. Governing equations

The standard transient nonlinear heat conduction equation was solved, with no source term other than the latent heat consumption and release. A more complete study should include convection in the melt pool, as it influences the overall heat and mass transfer (including mixing, which as it was stated before, affects the composition of the melt and consequently its properties). Nevertheless, the error involved in not taking convection into account generally decreases with increasing thermal conductivity; in many cases, considering conduction only can still provide a good idea on how the process parameters affect the temperature field. On the other hand, it can be argued that, from the deformation calculation standpoint, the location of the solid-liquid (S-L) interface is more important than the details of the temperature field inside the melt pool, as this is essentially a stress-free zone. Then, in the remainder of the domain, which is solid, we do have conduction only.

The heat conduction equation with no source term is:

$$\rho c_p \frac{\partial T}{\partial t} = \nabla(k \nabla T) \quad (\text{eq. 24.})$$

where T is the temperature, t is the time, ρ is the density, c_p is the specific heat at constant pressure and k is the thermal conductivity. The frontiers of the domain will be subject to boundary conditions of one or more of the following forms:

- Prescribed heat flux:

$$-k \nabla T = Q(x, y, z, t) \quad (\text{eq. 25.})$$

- Insulated surface (symmetry condition):

$$-k \nabla T = 0 \quad (\text{eq. 26.})$$

- Convection:

$$-k \nabla T = h(T - T_\infty) \quad (\text{eq. 27.})$$

- Radiation:

$$-k \nabla T = \varepsilon \sigma \left((T + 273.15)^4 - (T_\infty + 273.15)^4 \right) \quad (\text{eq. 28.})$$

where Q is the imposed heat flux, h is the heat transfer coefficient, ε is the emissivity and σ is the Stefan-Boltzman constant. Temperatures are in degrees Celsius, so the radiation expression, which features absolute temperatures, is adjusted accordingly. T_∞ is the temperature of the remote medium exchanging heat with the surface.

The imposed heat flux will correspond to the power density of the laser beam. Assuming a gaussian mode laser beam, we have in 3D:

$$Q(x, y, z, t) = \frac{2 A P}{\pi r_o^2} \exp\left(-2 \left(\frac{r}{r_o}\right)^2\right) \quad (\text{eq. 29.})$$

where A is the absorptivity, P is the laser power, r_o is the laser beam radius (for a focused beam, this radius has to be defined at the y coordinate of the surface under irradiation) and r is the radial distance from the beam axis, which for a beam moving with velocity v in the x direction is:

$$r(x, z, t) = \sqrt{(x - vt - x_{in})^2 + z^2} \quad (\text{eq. 30.})$$

The initial coordinates of the laser beam center are $(x_{in}, y, 0)$, assuming that the trajectory of the laser axis coincides with the mid longitudinal plane of the material, for which $z=0$.

In 2D the imposed heat flux will have the same form:

$$Q(x, y, t) = \frac{2 A P}{\pi r_o^2} \exp\left(-2 \left(\frac{r}{r_o}\right)^2\right) \quad (\text{eq. 31.})$$

$$r(x, t) = |x - vt - x_{in}| \quad . \quad (\text{eq. 32.})$$

If the same value of laser power is used, the 2D and 3D expressions should give the same value of heat flux for points in the mid longitudinal plane, which is a convenient common ground for comparing 2D and 3D simulations. Nevertheless, when comparing such situations, care has to be exercised: the 2D boundary condition means the heat flux is constant for all planes parallel to the 2D domain, whereas in 3D the heat flux decays in the perpendicular direction. Thus, if the same value of power is used, the total energy absorbed in the 2D case is expected to be higher than in 3D.

Results are generated for fixed values of absorbed power during each computer run. This is an approximation, because the amount of energy imparted to the workpiece varies with time, by means of the absorptivity dependence on surface temperature [54]. Nevertheless, since the process is taking place at steady-state for the most part, one can assume that an average absorptivity can be defined; it can be calculated—for each particular experimental setup— by calibrating the model with the help of experimental results. Then the total power, which is an important process parameter, can be accessed. Of course, a complete description for the total process should include the dependencies of the absorptivities (clad and substrate) on temperature and angle of incidence, plus the losses associated with the beam focusing optics and also from the interaction between the beam and the traveling particles. The latter results in a shadowing effect, in which the clad material particles partially block laser irradiation of the melt pool, while in turn get themselves heated by it. To account for this, one needs to know particle size, shape and distribution in the jet; a full discussion should include energy absorption at each particle and also account for multiple reflections between particles and from particles to the melt pool ([33], [34]).

Besides the laser beam, which is modeled by means of an imposed flux boundary condition on the top surface, the radiation boundary condition is considered for all surfaces except for the bottom substrate surface. Also included is the convective boundary condition. A higher

value of the heat transfer coefficient was taken at the melt pool (during irradiation), consistent with the presence of forced convection, associated with the powder carrier gas; on the rest of the domain surface, natural convection was assumed. Typical values were considered, although a more complete procedure would involve calculation of Nusselt numbers for a particular setup.

3.3.2. Mass and heat transfer consistency

Emphasis will be placed on imposing the location of the S-L interface as it conforms with the overall mass transfer. Namely, at steady state, the liquidus isotherm of the clad material has to completely span from the bottom of the interface zone to the top of the clad layer, as discussed in chapter 2. If in a computer run this condition is not achieved, this means that the available laser energy is not enough to produce a clad layer of the previously assumed thickness. Therefore, in keeping the same clad height (which, for a given speed, corresponds to a certain powder feed rate) the laser power has to be adjusted accordingly. On the other hand, if this isotherm drops considerably to the substrate, this would mean that the clad layer would become diluted, so power has to be decreased. This iterative process should continue, until the laser power value is within the two acceptable limits (between the zero and the maximum allowable dilution conditions) Therefore, a parametric study can be undertaken, in such a way that a region of successful cladding can be defined in the {absorbed power, absorbed feed rate, scanning speed} parameter space, for a certain experimental setup (i. e. optical and powder delivery systems) and clad-substrate materials.

As for the mesh itself, after an initial buildup period, the total amount of mass added in each step, which corresponds to the generated elements, is constant, being a function of the steady state net powder feed rate. This corresponds to the assumption of a constant average catchment efficiency throughout the process. It is known that this parameter (the ratio between the total mass of particles that get incorporated in the melt pool per unit time and the nominal feed rate) varies throughout the process, increasing from zero (at the time the substrate begins to melt) to a steady state value, as it depends most notably on the melt pool size, other parameters remaining the same. The steady state value can be determined by knowing the nominal feed rate, the processing time and the weight increase of the

workpiece. The dependence of catchment efficiency on process parameters is discussed in reference [51].

3.4. Stress analysis

3.4.1. Residual strain and stress

In the mechanical analysis it will be assumed that no body forces or surface tractions are applied. The only loading comes from the application of a transient thermal field in a bi-material system. Such thermal loading will induce thermal strain: that will not be uniform throughout the domain: a) the two materials held in contact have coefficients of thermal expansion (CTE) that are different; b) they have initial temperatures that are different and; c) there are strong temperature gradients associated with laser processing, so even within a single material domain thermal strain will vary.

Such thermal strain field will eventually lead to plastic strain, as each material volume constrains (and gets constrained by) its surroundings. Also, there are the constraints associated with the boundary conditions: even if the material rests apparently unconstrained in the laboratory, the presence of symmetry planes leads to constraint. Also, at least a point in the domain is to be kept highly constrained (with several fixed degrees of freedom), so as to prevent rigid body motion.

Even if plastic strain is not present, the formation and processing of clad material at high temperature (where it is placed in contact with a substrate material that was at room temperature at the beginning of the process) will lead to residual strain at room temperature and therefore residual stress. The stress field has the property [55]:

$$\int \sigma_{ij} dV = 0 \quad (\text{eq. 33.})$$

where the integration is done over the whole domain. The definition of residual stresses is tied to this property: “residual stresses are the self-equilibrating internal stresses existing in a free body at equilibrium with no externally imposed surface tractions” ([55], [56]).

Therefore, in contour plots of a particular stress component, zones in compression and in tension tend to be almost equally represented.

3.4.2. Governing equations

The governing equations are as follows:

- In the absence of body forces, the equilibrium equation is:

$$\frac{\partial \sigma_{ij}}{\partial x_j} = 0 \quad . \quad (\text{eq. 34.})$$

- In the absence of surface tractions:

$$\sigma_{ij} n_j = 0 \quad (\text{eq. 35.})$$

where n_j is the exterior normal to the free surfaces.

- The strain-displacement relation is written:

$$\varepsilon_{ij} = \frac{1}{2} \left(\frac{\partial u_i}{\partial x_j} + \frac{\partial u_j}{\partial x_i} \right) \quad (\text{eq. 36.})$$

where u_i is the displacement and ε_{ij} is the total strain tensor.

- The total strain is subject to compatibility equations:

$$\varepsilon_{pki} \varepsilon_{qlj} \frac{\partial^2 \varepsilon_{ij}}{\partial x_k \partial x_l} = 0 \quad (\text{eq. 37.})$$

where ε_{pki} is the alternating symbol.

- The total strain, in the present case, has three components:

$$\varepsilon_{ij} = \varepsilon_{ij}^{el} + \varepsilon_{ij}^{pl} + \varepsilon_{ij}^{th} \quad (\text{eq. 38.})$$

where the components refer to elastic, plastic and thermal strain, respectively.

- Stress and elastic strain are primarily connected through the elastic moduli (or, stiffness) tensor, C_{ijkl} :

$$\sigma_{ij} = C_{ijkl} (\varepsilon_{kl} - \varepsilon_{kl}^{pl} - \varepsilon_{kl}^{th}). \quad (\text{eq. 39.})$$

For an isotropic material, the components of the stiffness tensor are a function of Young's modulus, E , and of Poisson's ratio, ν .

- The strain and stress field are also connected through the evolution of plastic strain. For that purpose, kinematic hardening, in conjunction with the Von Mises yield criterion, is assumed. This is valid for the clad, substrate and interface regions of the domain. In the latter, work hardening resulting from the presence of precipitates was considered. In all cases, the yield stress decreases exponentially with temperature, tending to zero as the liquidus temperature is approached. At the same time, the Young's modulus is taken as (near) zero as temperature reaches the melting temperature, so as to make the melt a stress free zone. In addition, AbaqusTM uses the 'anneal temperature' feature, which resets to zero the stress and strain components above a certain value of ('anneal') temperature.

- As to thermal strain, the secant formulation (used in AbaqusTM) gives:

$$\varepsilon_{ij}^{th}(T) = \alpha_T(T)(T - T_{ref}) - \alpha_T(T_o)(T_o - T_{ref}) \quad (\text{eq. 40.})$$

where α_T is the coefficient of thermal expansion, T_{ref} is the respective reference temperature (the starting temperature for the experimental data from which CTE values were obtained) and T_o the initial temperature.

- As to boundary conditions, depending on the simulations, we will have either fully constrained nodes (zero displacement and zero rotation degrees of freedom), or partially constrained ones (see schematics of 2D and 3D cases in chapter 4). The general idea is to fully constrain one node in the lower edge of the domain and keep the other extremities (three in 3D and one in 2D) of that edge with some mobility but still on the same horizontal plane. The mid-longitudinal plane in 3D is a symmetry plane, so there cannot be displacement or rotation bringing material through it.

A more complete model should include other components of strain, such as transformation strain arising from phase transformation, or creep strain, and phenomena such as tempering or grain growth, but it is believed that even such a simple model can capture the essentials of the relevant sequence of events, namely, thermal expansion of substrate, formation of compatible clad material at high temperature, followed by dissimilar contraction of both materials, resulting in residual stress. In all that, plastic deformation will likely occur also, especially due to (but not limited to) the low strength at high temperature.

For stress-strain behavior in 2D, both generalized plane strain and plane stress were considered. In generalized plane strain, deformations can be defined in the transverse direction although in a limited way. Still, these assumptions will have to be used with some reservations, as the thermal strain is essentially triaxial in nature, so that essential feature is not captured accurately in those simple 2D assumptions for stress-strain.

3.5. Materials properties

It is an obvious statement the fact that the quality of materials property data critically determines the results in numerical modeling. In other words, it is not enough to develop a good numerical scheme: it is essential to feed the model with property values that accurately reflect the behavior of the material. Unfortunately, many times it is difficult to find in the literature the needed values for the properties, especially at temperatures other than room temperature.

This is especially true in the case of alloys: apart from widely used systems, lack in data leads users to rely on estimations based on the major elements present in the alloy and/or on the values of those properties for similar systems. Generally speaking, this procedure is usually considered valid, although that might be, rather, because it is the only one that leads to the obtaining of any results at all. Of course, even in cases where there is uncertainty as to the accuracy of the results, one can usually rely on the overall picture that emerges from

the model, and thus develop a better insight of the process. In addition to that, tendencies can be established, as to the influence of certain parameters on the final result.

Of course, new sets of “better” properties can always be added as they become available. Besides, one can perform design sensitivity analyses, to check how crucial a certain variable might be. And, most important, modeling results are to be compared with experimental data, which can thus be used to calibrate the model, especially in regard with parameters and/or properties whose definition might be more difficult.

In the context of laser cladding, the use of numerical methods to calculate the temperature and stress-strain fields can be justified not only because of the geometric features of the process –analytical methods usually deal only with very simple geometries– but also because of the non-linearity associated with the properties. For example, for heat transfer, geometry, boundary conditions and properties determine the temperature field, which in turn affects back the properties and boundary conditions. Therefore, the numerical scheme must perform suitable iteration procedures to deal with these issues.

In view of the above, special attention is given to the definition of the properties as a function of temperature. AbaqusTM input files require properties to be entered in a tabular form, where pairs property/temperature are prescribed (if the property depends on other variables, such as plastic strain, or a field variable such as composition, those are also to be included). Since linear interpolation is performed for intermediate values of temperature, the properties, will be defined by a piecewise linear function. Due to the above mentioned scarcity of property data, in many cases only the values at room temperature and at the melting point are entered (the latter sometimes obtained by estimation), thereby resulting in properties which are linear functions in the temperature range of interest.

We now discuss some details pertaining to the most relevant materials properties that are used in the simulations. In particular, it is important to define the properties in the zone where there is mixing, *i.e.*, the interface between the mostly uniform clad and the mostly uniform substrate.

Since experimental results of composition indicate the presence of precipitates in the interfacial zone, the model was developed considering the presence of such, and that its volume fraction can be estimated. Generally speaking, a rule of mixtures is used for the metal matrix composite that is thereby considered to be present in the substrate zone:

$$P = f P_p + (1 - f) P_m \quad . \quad (\text{eq. 41.})$$

where P is a generic physical property of such composite and f is the volume fraction of precipitate (the indexes p and m refer to the precipitate and matrix, respectively).

A notable exception to this rule of mixtures is the yield stress, for which the strengthening effect caused by the presence of precipitates is evaluated using a micromechanics model. This is justified by the fact that, from experiment, the hardness is seen to be higher at the interface, when compared with the clad and substrate values. Of course, caution is needed in: a) interpreting hardness data in materials that possess a distribution of residual stresses, and b) assuming a hardness to strength equivalence, especially in view of the fact that the material, and in particular the interfacial region, is heterogeneous.

The behavior of the interface composite is then modeled using Tanaka-Mori theory, as found in Mura [56], where the following equations are given (Poisson's ratio, ν , of matrix and precipitate assumed to be the same):

$$c = \frac{7 - 5\nu}{E_p (8 - 10\nu) + E_m (7 - 5\nu)} \quad (\text{eq. 42.})$$

$$a = \frac{3 E_p E_m c}{2 (1 + \nu)} \quad (\text{eq. 43.})$$

$$b = c (E_p - E_m) \quad (\text{eq. 44.})$$

$$\sigma_{Y0} = \frac{(1 - f) \sigma_{Ym}}{1 - f (1 + b)} \quad (\text{eq. 45.})$$

$$\sigma_Y = \sigma_{Y0} + \frac{f \varepsilon^{pl} a}{1 - f (1 + b)} \quad (\text{eq. 46.})$$

where, a , b , c are auxiliary functions, E is the Young's modulus, σ_Y is the yield stress and σ_{Y0} is the value of first yield, *i.e.*, yield stress at zero equivalent plastic strain, ε^{pl} .

The matrix is assumed to be the substrate material and a maximum volume fraction of precipitate of 20% is considered (see chapter 5 for details on such assumption). In the interface zone, the properties vary linearly as a function of the composition index defined in chapter 2 (equation 17), from the clad material ($c_i = 1.0$) to the composite with the maximum precipitate contents ($c_i = 0.9$; see chapter 5 for details) then to the substrate ($c_i = 0.0$). The composition indexes are truncated to 1.0 and 0.0 in the clad and substrate materials, respectively.

The data used in the simulations can be found in appendix B. For the plastic properties (yield stress, *i.e.*, strength as a function of equivalent plastic strain) data is taken from Metals Handbook [57]. For the Young's modulus, data can be found in references [56], [57], [58], [59] and [60]. For CTE the basic reference is Touloukian [61]. For density, references [57], [62] and [63] were used (volumetric contraction was estimated based on CTE data). In the case of specific heat, the references were [57], [59], [63] and [64].

Other references were used for latent heat [65], thermal conductivity ([63], [66]), heat transfer coefficient and emissivity [67], although the respective values for the precipitate were estimated.

4. Results

4.1. Introduction

In this chapter, results of simulations done for 2D and 3D FE models of laser cladding will be presented. For each simulation, identified usually by a two-letter two-digit code, the main characteristics will be highlighted. Listings of representative input files are found in Appendix C. A more detailed set of parameters pertaining to each simulation is presented in Appendix D. Animation movies of some of the results featured in this dissertation, as well as the color pictures of this section, will be available at:

<http://www.eecs.umich.edu/~dedeus/>.

Details of the finite element formulation are not included, as they were not a matter of research for the present dissertation. Such information is readily available in AbaqusTM manuals [68]. Although most of the development of the FE model was done in AbaqusTM versions 5.4 through 5.8, the final calculations were done in version 6.3. Calculations were performed on both a SGITM OctaneTM running Irix64TM release 6.5 6.5.16m with a single MIPSTM R10000TM 250 MHz processor and on a CompaqTM PresarioTM 2100 running Windows xpTM with IntelTM CeleronTM 2.00 GHz processor.

Some parameters are kept constant, such as laser beam radius, r_o , scanning speed, v , average absorptivity, A , and powder effective feed rate, φ :

- $r_o = 1$ mm.
- $v = 12.5$ mm/s.
- $A = 25\%$.
- $\varphi = 0.2757$ g/s.

In numerical studies emphasis was placed on:

- mesh independence studies;
- geometry variations, *i.e.*, different dimensions for clad and substrate;

- properties dependent on temperature only or also a function of composition;
- different assumptions for 2D stress-strain;
- comparison between 2D and 3D results;
- comparison between different mesh types in 3D.

The variables that are more prominently featured are the temperature T (in degrees Celsius in all simulations) and stress σ_{ij} , especially the longitudinal stress σ_{11} , the shear stress σ_{12} and the Von Mises stress, σ_{Mises} (all in Pa). Temperature gradient ($^{\circ}\text{C}/\text{m}$), cooling rate ($^{\circ}\text{C}/\text{s}$), composition index, local relative temperature, thermal strain and plastic strain are also featured. Time is in seconds. Distances can be inferred from dimensions presented in Appendix D.

4.2. Element library

A number of elements were used, from the element library made available by AbaqusTM. All of the elements featured are linear, as they are the most straightforward output possible out of the Input File Generator.

4-node rectangular shaped elements were used in 2D. In figure 38 a typical element is featured, along with its nodes. In the scheme that was adopted, the element number is always the lowest of the node numbers contributing to the element. In accord with each analysis type and/or assumption the elements utilised are:

- 2D temperature: element DC2D4;
- 2D generalized plane strain: element CPEG4;
- 2D plane stress: element CPS4.

8-node brick elements were used for the most part in 3D. In the 3D curved mesh 6-node triangular prism are used about the axis of symmetry of the clad bead. Typical elements are shown in figures 39 and 40. The respective element types are as follows:

- 3D temperature: elements DC3D8 and DC3D6;
- 3D stress-strain: elements C3D8 and C3D6.

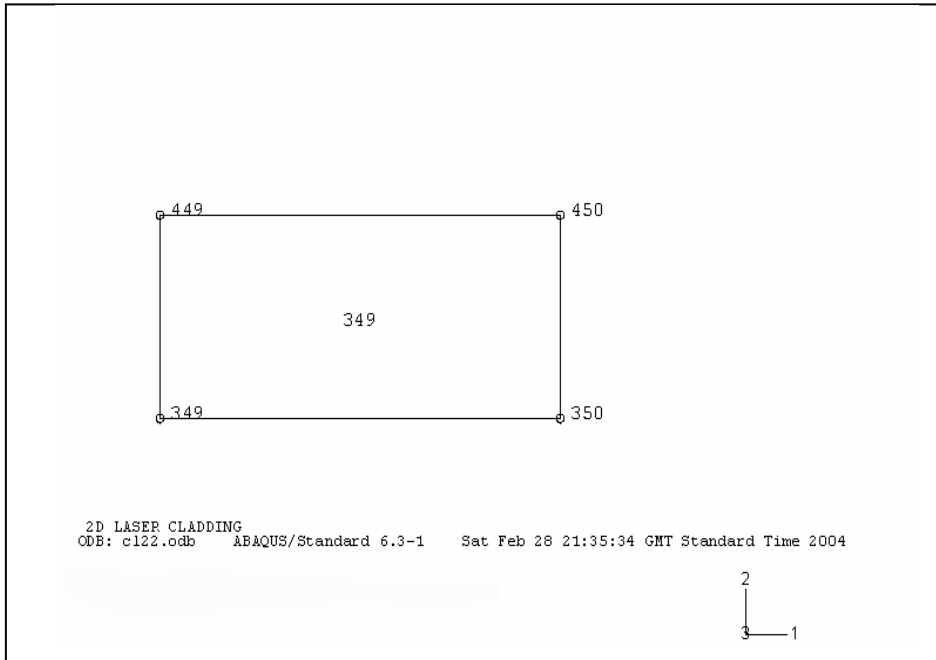


Figure 38. Typical 2D 4-node linear element.

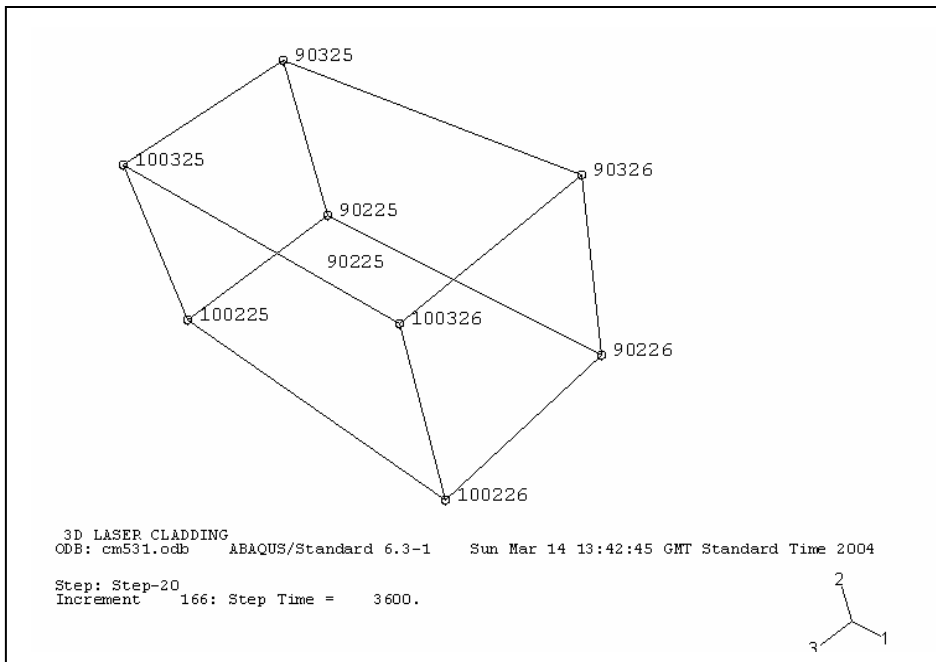


Figure 39. Typical 3D 8-node linear element.

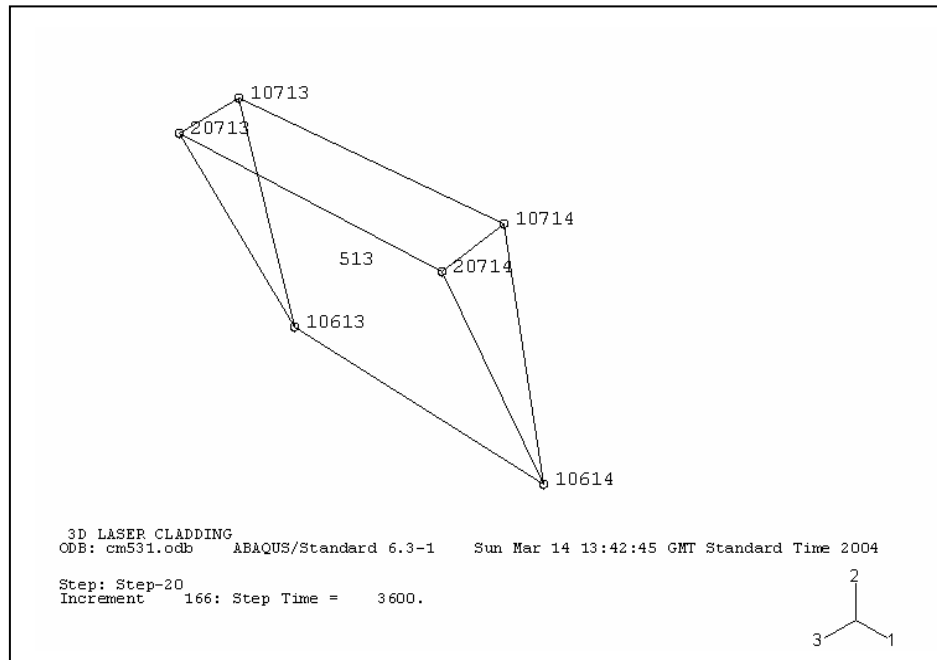


Figure 40. Typical 3D 6-node linear element.

4.3. Mesh independence

The numerical results should indeed be independent on the degree of mesh refinement, if one is to find the numerical solution to the problem. A study in mesh independence was done in 2D on a simple domain, with substrate only. That was chosen so as to check the dependence of mesh size in a simple geometry. If two meshes hold similar results, that means one can undertake further calculations in the coarser among the two, in order to save computation time. In fact, that degree of adequate refinement is expected to hold (at least approximately) for other geometries, in particular in the cases of interest, where we have laser cladding. In addition, the featured situation is verified to be a model for laser alloying, as an interfacial zone is defined up to a certain depth with the properties of a ‘modified’ material (in this case we use the clad material, C95600 copper alloy) surrounded by the substrate (AA333 aluminum alloy), so a comparison can be established between the two situations.

In figure 41 we have the three meshes that were investigated, corresponding to runs al120 (coarse), al220 (mid-grade) and al320 (fine; detail in interfacial zone is also shown). Temperature profiles are presented in figure 42 for these 3 meshes, as well as a mid-grade mesh for different dimensions (cl220). Von Mises stress (figure 43) and longitudinal stress (figure 44) are also shown (runs bl120, bl220, bl320 and dl220).

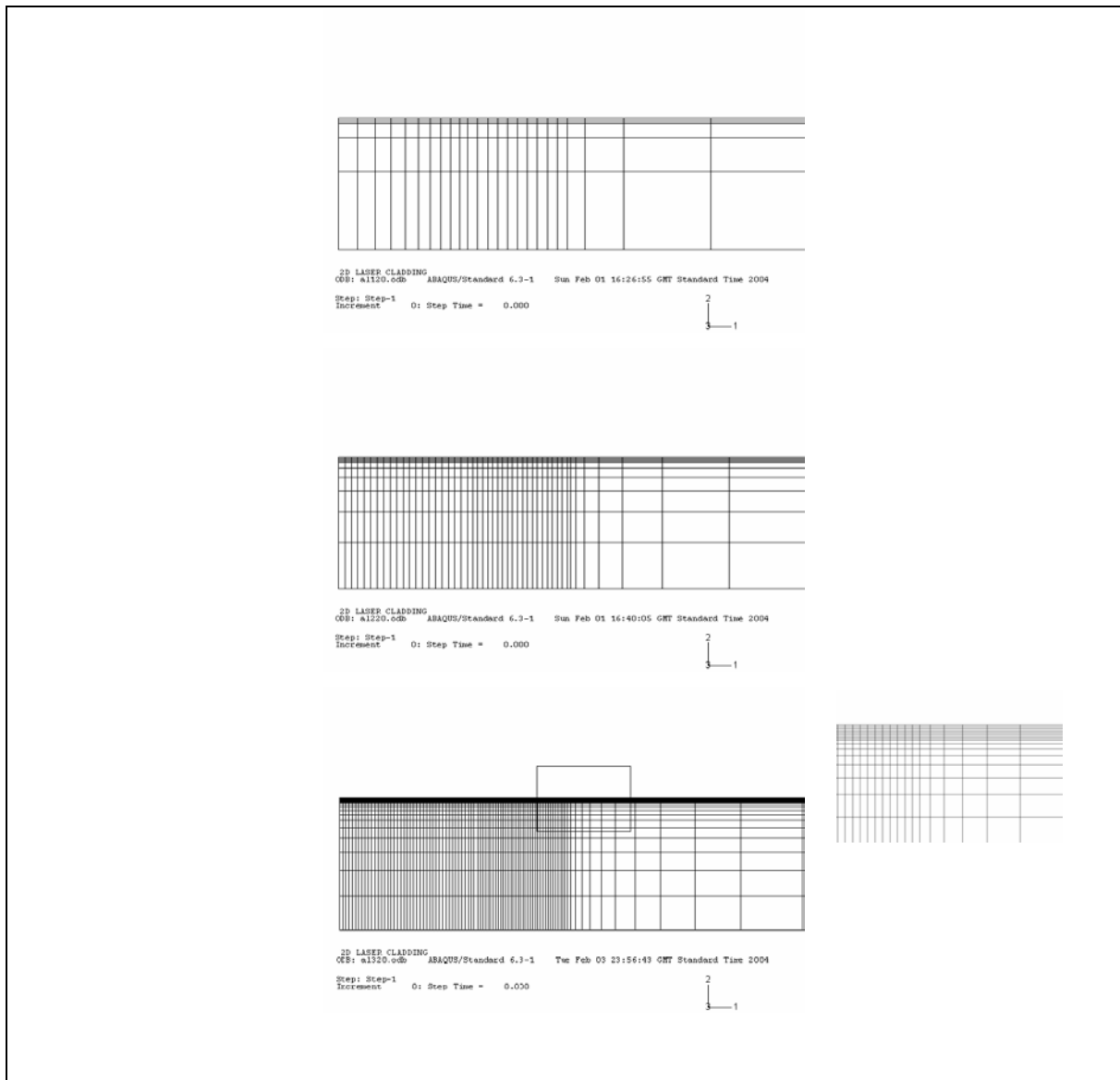


Figure 41. Mesh independence study: mesh comparison.

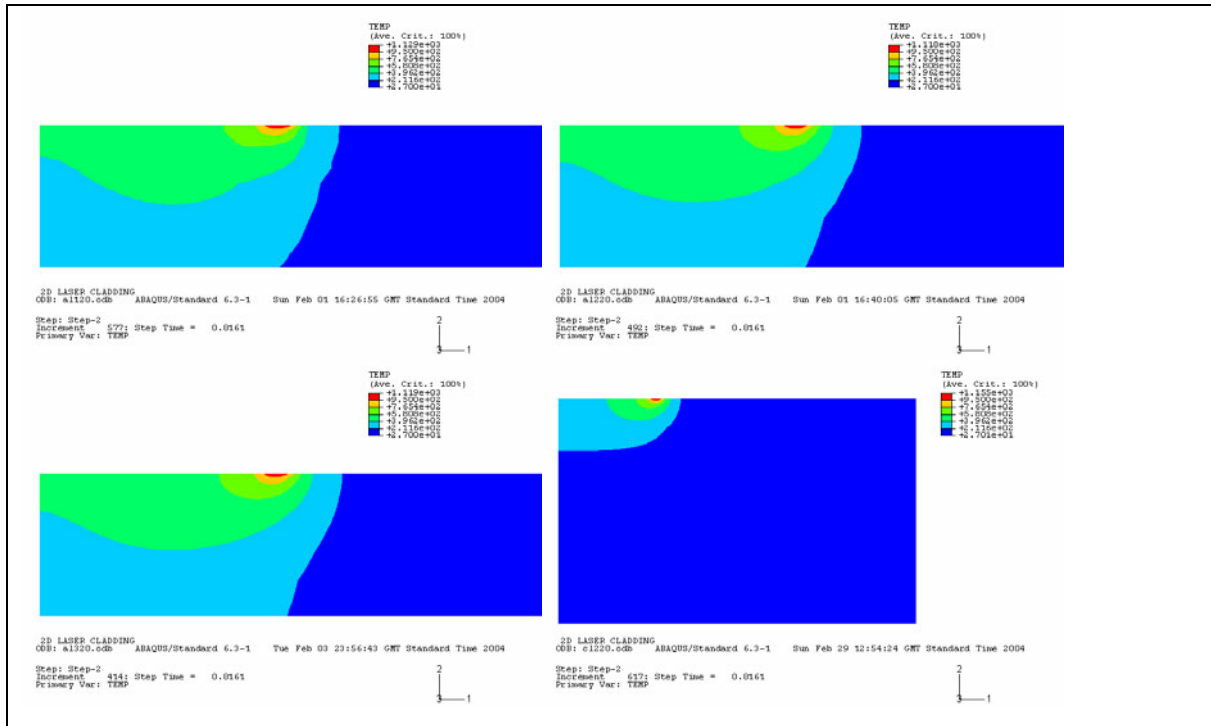


Figure 42. Mesh independence study: temperature.

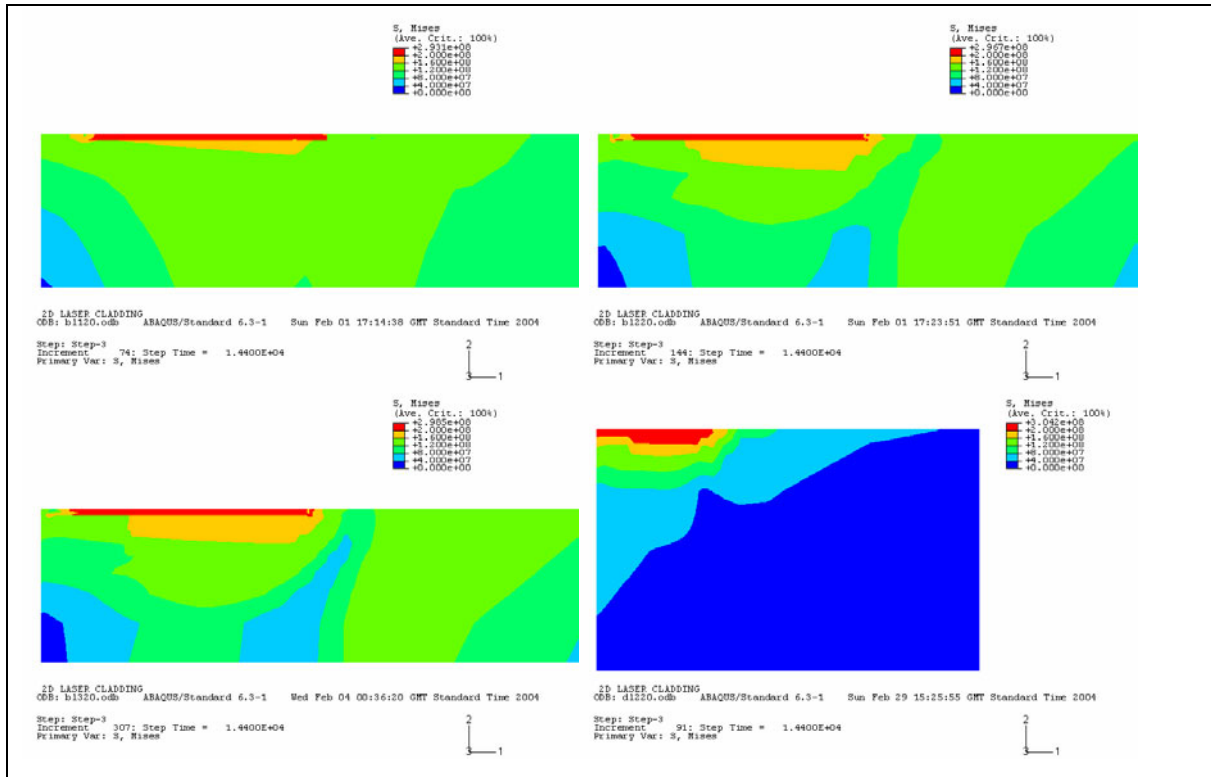


Figure 43. Mesh independence study: Von Mises stress.

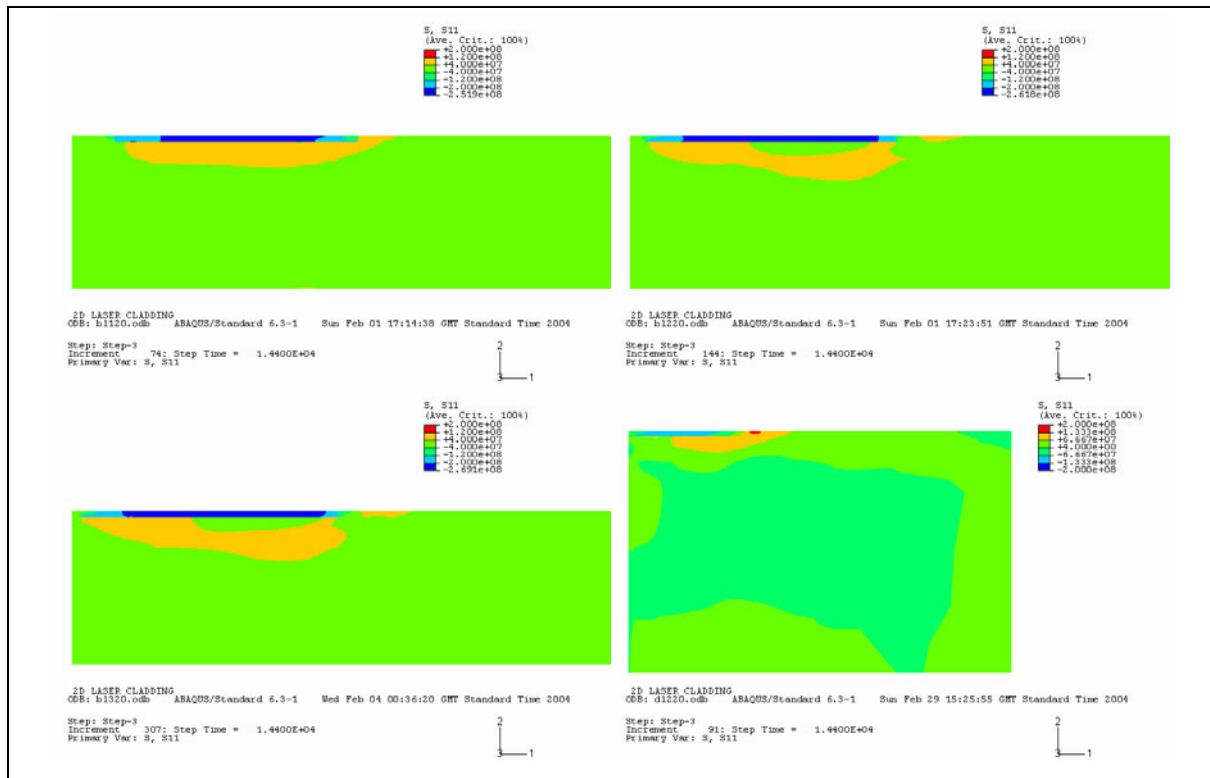


Figure 44. Mesh independence study: longitudinal stress.

The mid-grade and fine meshes do yield similar results for temperature and stress fields, so we proceed using similar meshes to the mid-grade one (if it were for temperature only, the coarse mesh could also be used). Also, we notice that the stress field is rather different when dimensions of the substrate vary. The interface zone is constrained differently when the dimensions of the substrate vary. The alloyed layer is in compression (figure 44), because the Cu alloy has a lower CTE than the Al based substrate. Thus, the Cu alloy is forced by its surroundings to shrink more than its mere unconstrained thermal contraction.

4.4. 2D FE models

We first feature models with fixed interface depth and composition (temperature runs al22, al23 and al24) with laser power and clad initial temperature adjusted so as to obtain threshold conditions for laser cladding; then simulations with variable composition (al25 and al26) where laser power decreases. In figure 45 a) and b) we see the quick development

of a steady state temperature field for the case where the interface is made of substrate material. This corresponds to a clad melting isotherm dropping slightly down to the substrate. If the interface is made of clad material or metal matrix composite (substrate with precipitates), then the assigned depth of such layer must coincide with the clad melt isotherm, as seen in figures 45 c) and d).

In figure 46 the temperature and composition index profiles are displayed. The power was relatively high on purpose, to highlight the composition modification. Of course, being a very high dilution case, the overall composition of the clad material is expected to be quite different from its initial (nominal) composition. The model could accommodate such composition change, as a function of melt pool size, but that was not attempted in this case.

Results from the 2D mechanical models are shown in figures 47 through 51 (runs bl22, bc22, bh22, bi22 and bk22). The Von Mises stress and the components of the stress tensor are featured.

We see that the normal components σ_{11} and σ_{33} are negative in the clad. The mismatch in CTE accounts for that: there is an abrupt variation (in the '2' direction) of the CTE due to the change in composition, so the differential shrinking behavior of the clad top portion of the sandwich-like material (that is what we are assuming in such 2D stress-strain models) leads to compressive components in the normal stresses perpendicular to the interface. These normal components are sometimes smaller near the extremities of the clad, as those zones undergo shrinking near a free surface, thus with less constraint. The σ_{22} component is not represented, as it is near zero for the whole domain. The σ_{12} component is usually small, except at the two extremities of the clad front, which is interesting to note because that is where debonding usually occurs, often with rotation in the detached portion of the clad. It is noted that the sort of 2D stress-strain assumption does affect the results, even the dimensions assumed for the depth of the domain.

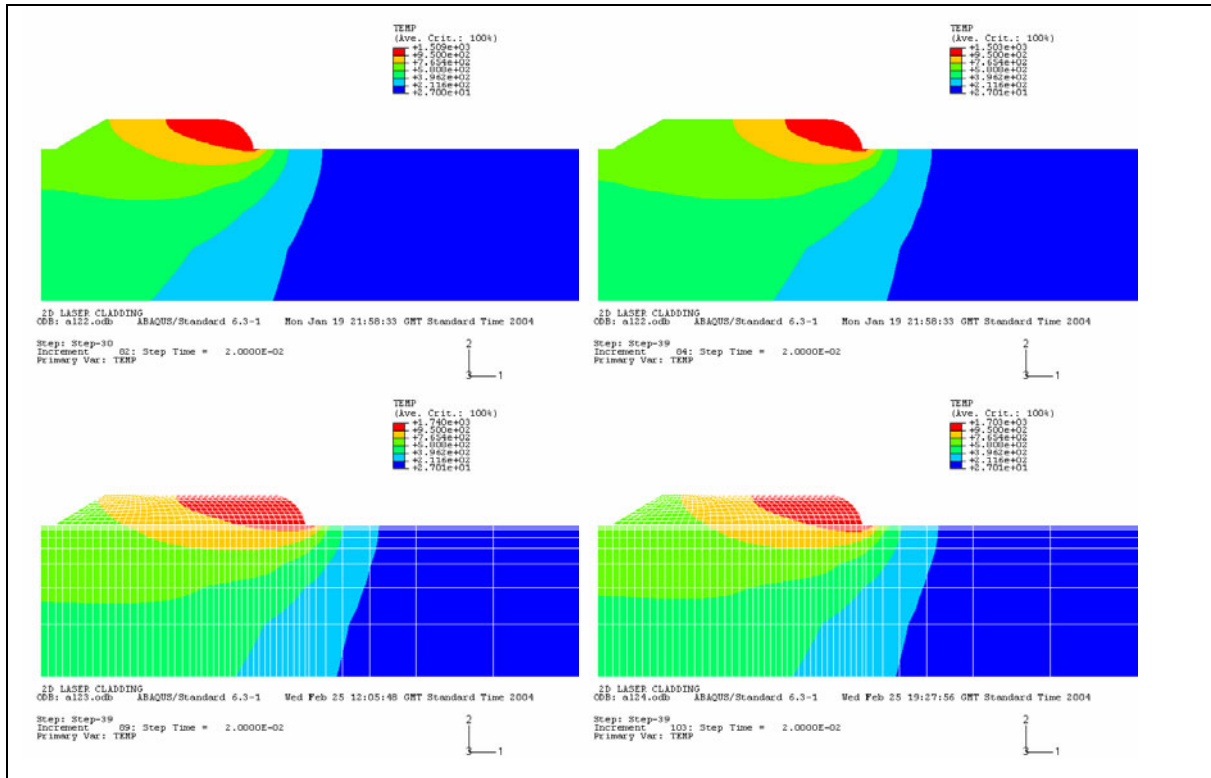


Figure 45. Two-dimensional model for temperature, prescribed interface.

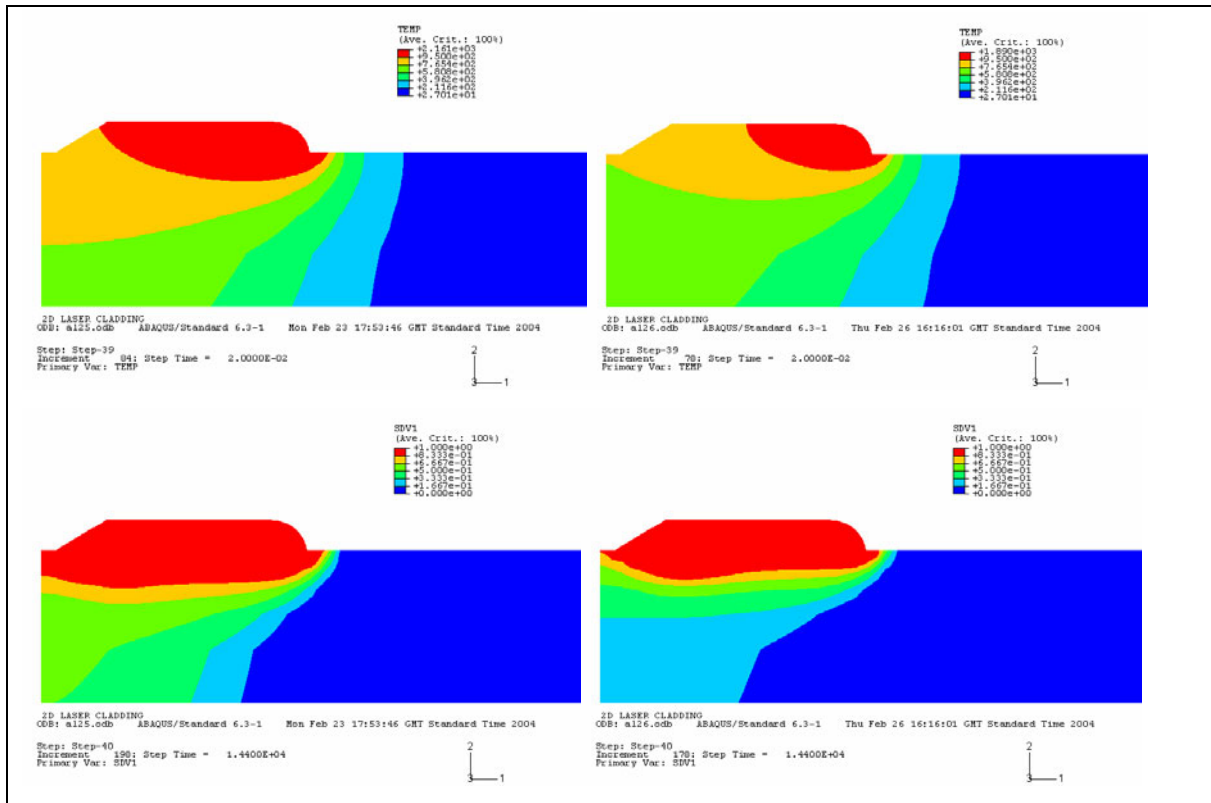


Figure 46. Temperature and composition index, variable interface case.

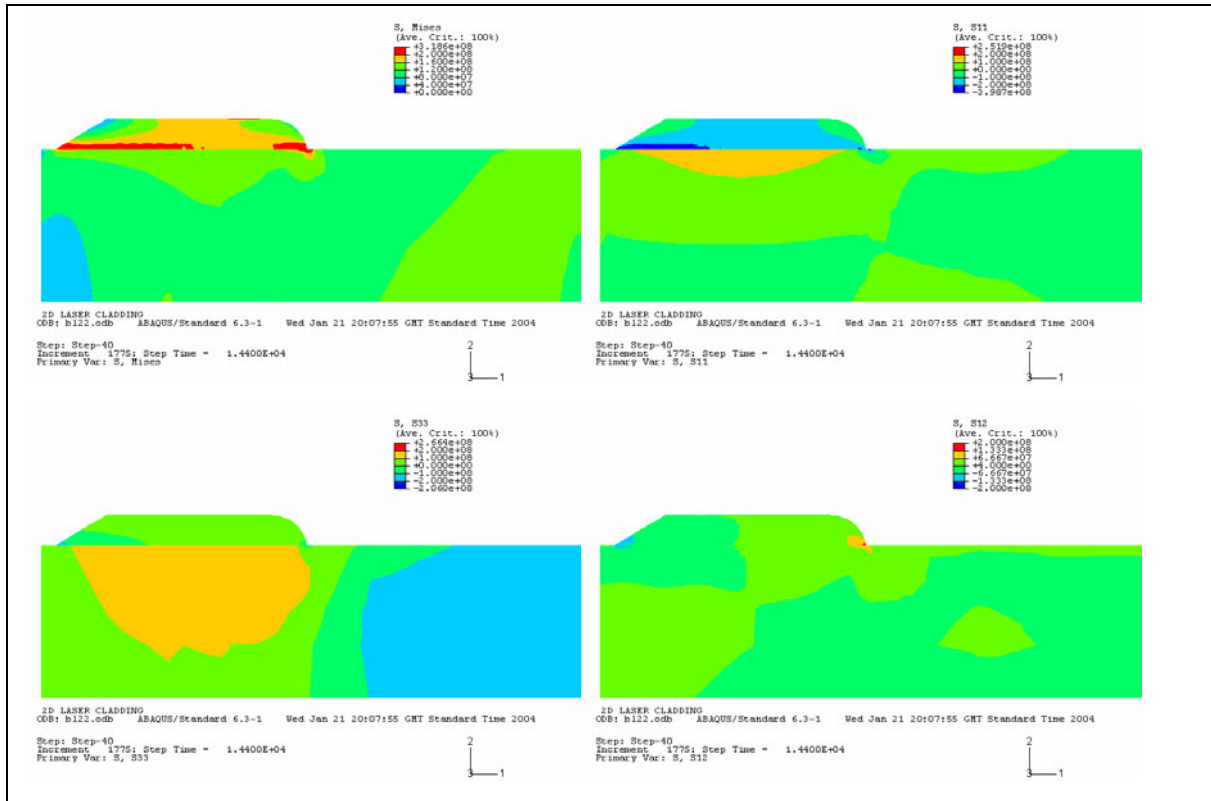


Figure 47. Stress components, 2D GPS model, large thickness.

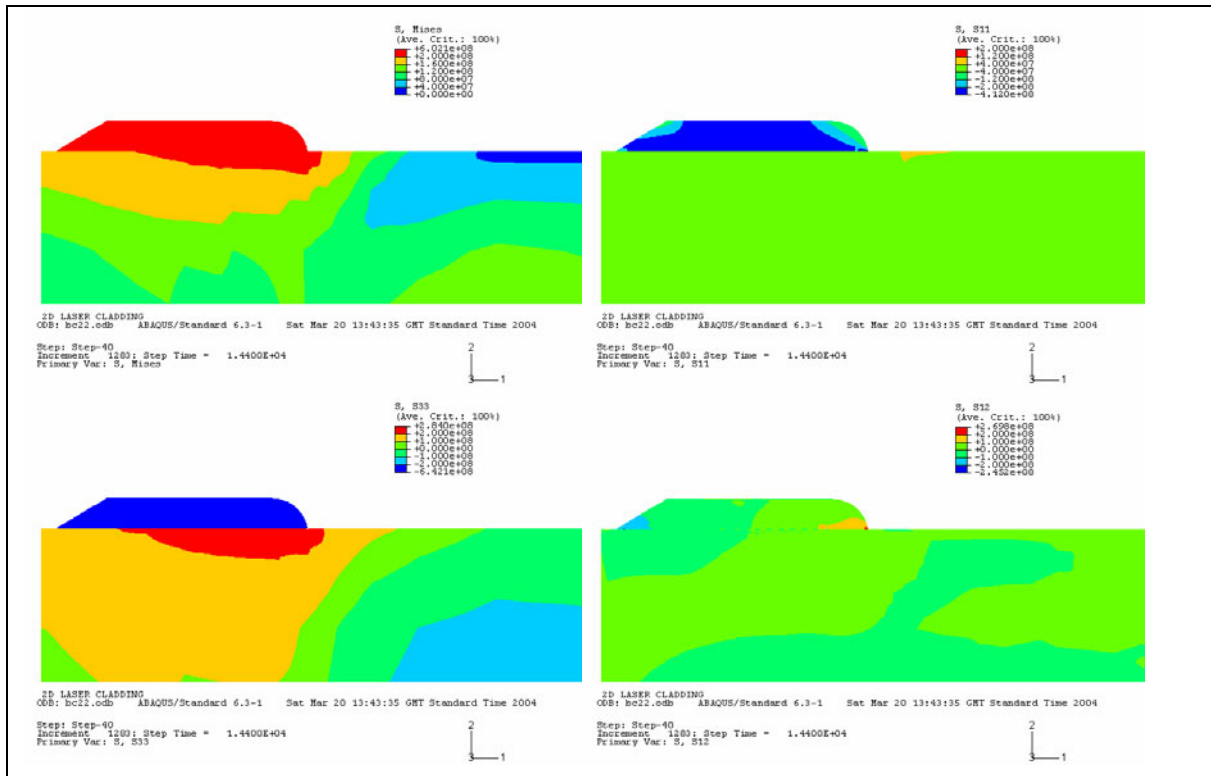


Figure 48. Stress components, 2D GPS model, 25mm substrate thickness.

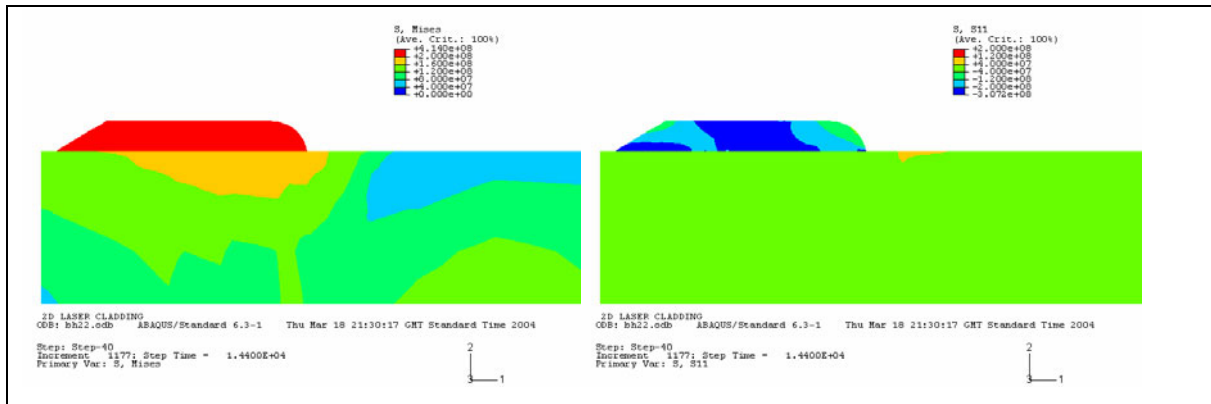


Figure 49. Stress components, 2D GPS model, 10mm substrate thickness.

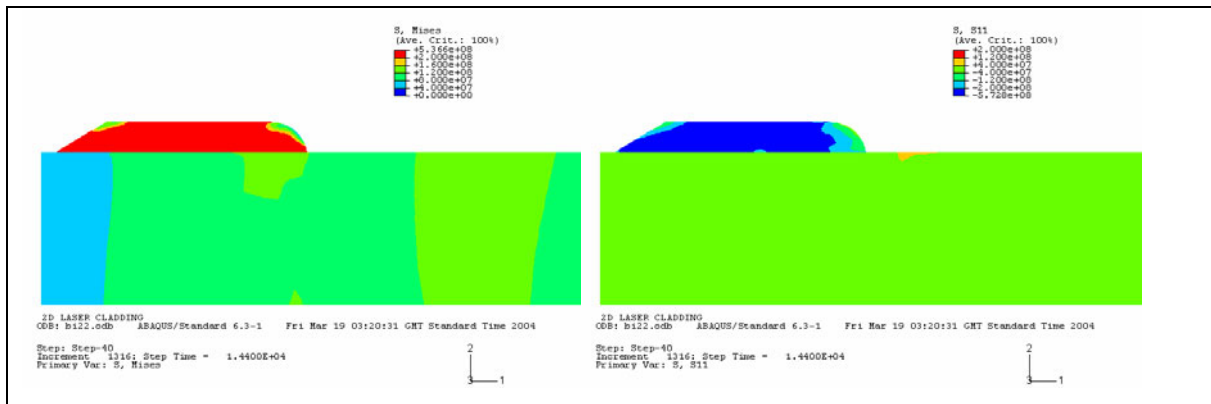


Figure 50. Stress components, 2D GPS model in substrate, plane stress in clad.

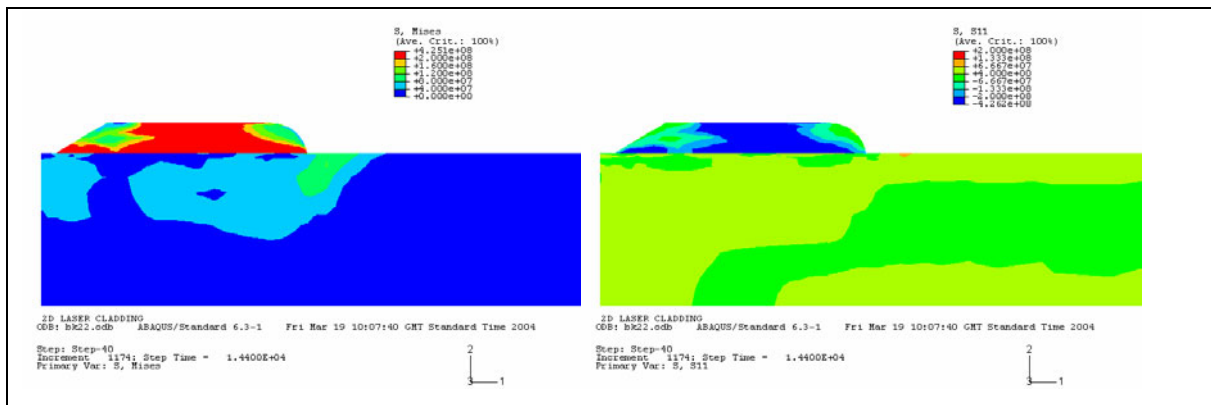


Figure 51. Stress components, 2D plane stress in both clad and substrate.

If the dimensions of the substrate and clad material change, the temperature profile is seen to be little affected, but the stress profiles show distinct differences. In the case of temperature, comparing the shorter with the longer bead cases (for the two threshold conditions), we see that steady state conditions are present in the system even when the clad bead is still small (figure 52, featuring runs cl22, el22, cl24, el24). In fact such steady state gets established typically after 4-5 beam diameters of laser travel.

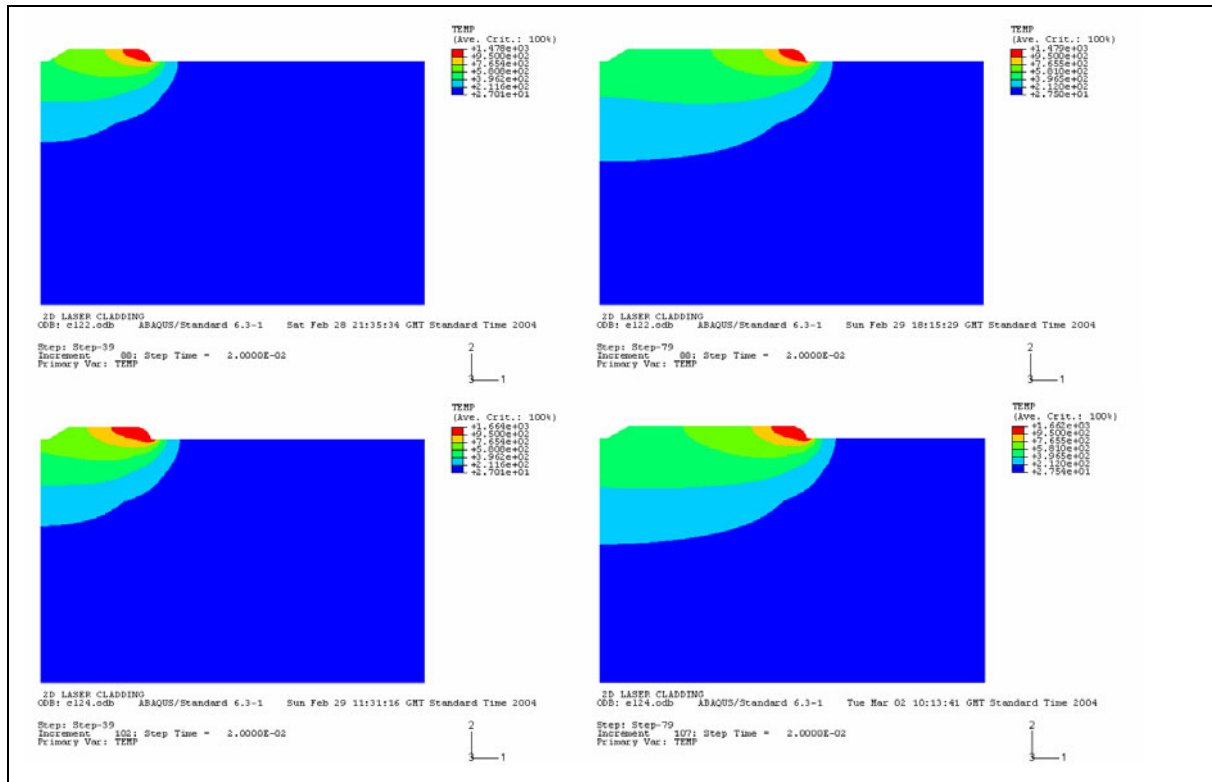


Figure 52. Two-dimensional model for temperature, thick substrate.

On the other hand, it is noted that the melting isotherm of the substrate (boundary between the two shades of green in color plots) is obviously over-represented. Such temperature field would necessarily lead to very large dilution. On the other hand, this behavior is expected in 2D, as in such model there is no cooling in the perpendicular direction, in contrast with the real 3D geometry, where heat loss from the clad bead is radial in nature.

Results from the respective mechanical models (calculations dl22, dl24, fl24) are shown in figure 53 and 54. Strain components are included: the final thermal strain is in good accord with the expected values from equation 40. The value in the substrate is uniform and very near zero, as expected, and the clad value reflects thermal strain associated with shrinking from an initial higher processing temperature. The non-uniformity in that domain reflects the fact that when new elements are activated, the already existing nodes retain their temperature and only the new ones are created at the imposed temperature, which means that the initial (or its natural reference) temperature varies within each element in the usual interpolated fashion, that is at the core of the FE method. As to the plastic strain equivalent ($PEEQ$), the ‘anneal temperature’ feature in AbaqusTM forces such variable (and, similarly, backstress in the kinematic hardening model) to zero when an ‘anneal’ (in our case: melting) temperature is reached. For points not undergoing melting, $PEEQ$ about keeps accumulating, thus explaining the behavior in the substrate. In regards to the stress components, it is clear that the stress field depends very much upon the geometry of the clad-substrate system, although the previously mentioned trends are, generally speaking, kept.

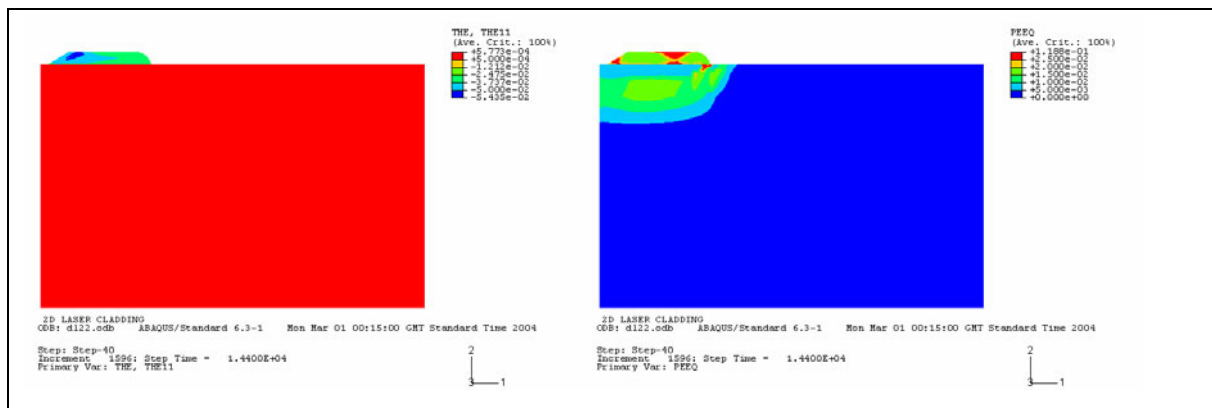


Figure 53. Two-dimensional mechanical model, strain components.

At the end of this 2D results section, the boundary conditions for the mechanical models are shown (figure 55).

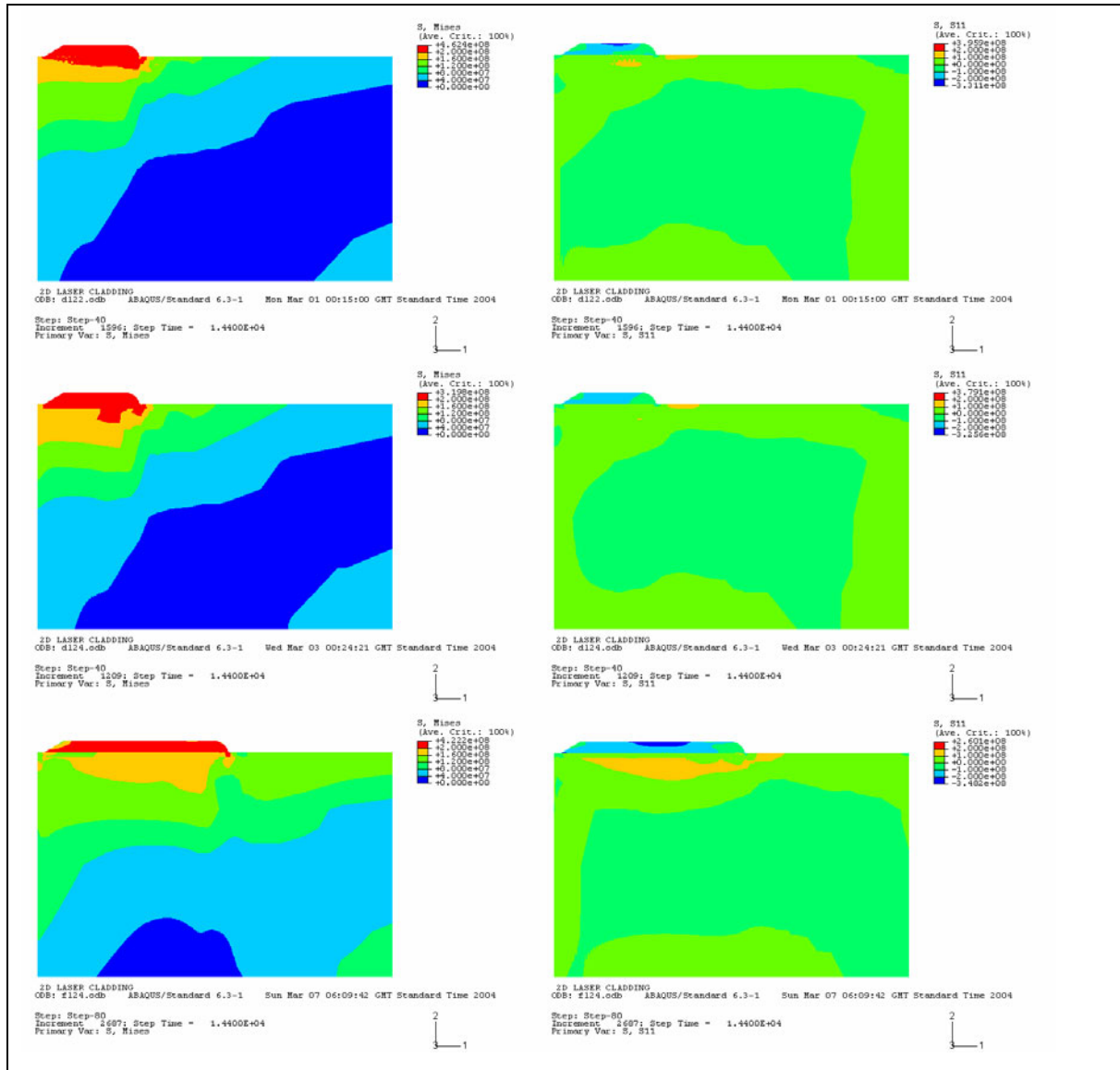


Figure 54. Two-dimensional mechanical model, thick substrate.

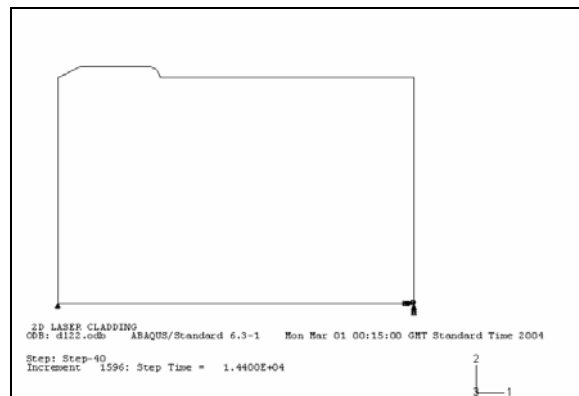


Figure 55. Boundary conditions for 2D stress models.

4.5. 3D FE models

A number of 3D models will be featured, in two variants, either with curved or planar shape external boundaries. The minimum power threshold condition (*i.e.*, when the interface composition coincides with the substrate's) is considered for the prescribed interface cases. The values that are used for laser power are slightly less than the ones strictly given by such condition; they were chosen so as to facilitate the stress calculation. Simulations with the variable composition model are also included. The curved shape meshes that were used are shown in figure 56, where changes in the dimensions of the substrate were operated.

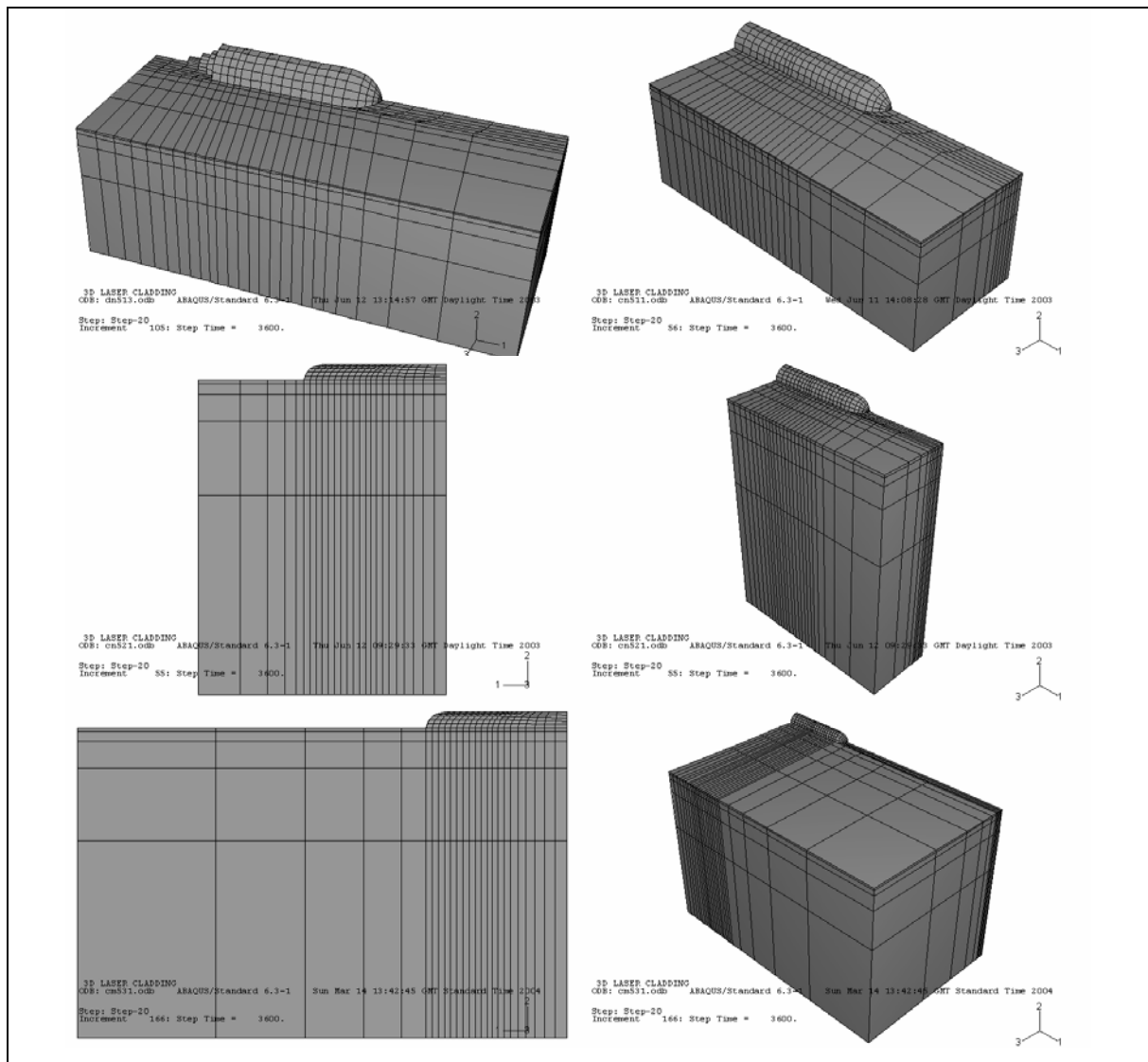


Figure 56. Three-dimensional curved meshes.

Temperature profiles are featured in figure 57 (runs cn511, cn521 and cg533), where we see the substrate melt pool now correctly displayed, in accord to what is expected in laser cladding, as outlined in chapter 2. (Newer versions of Abaqus™ post-processor display by default the full mesh, even the inactive elements, so a few of the results are shown in that fashion).

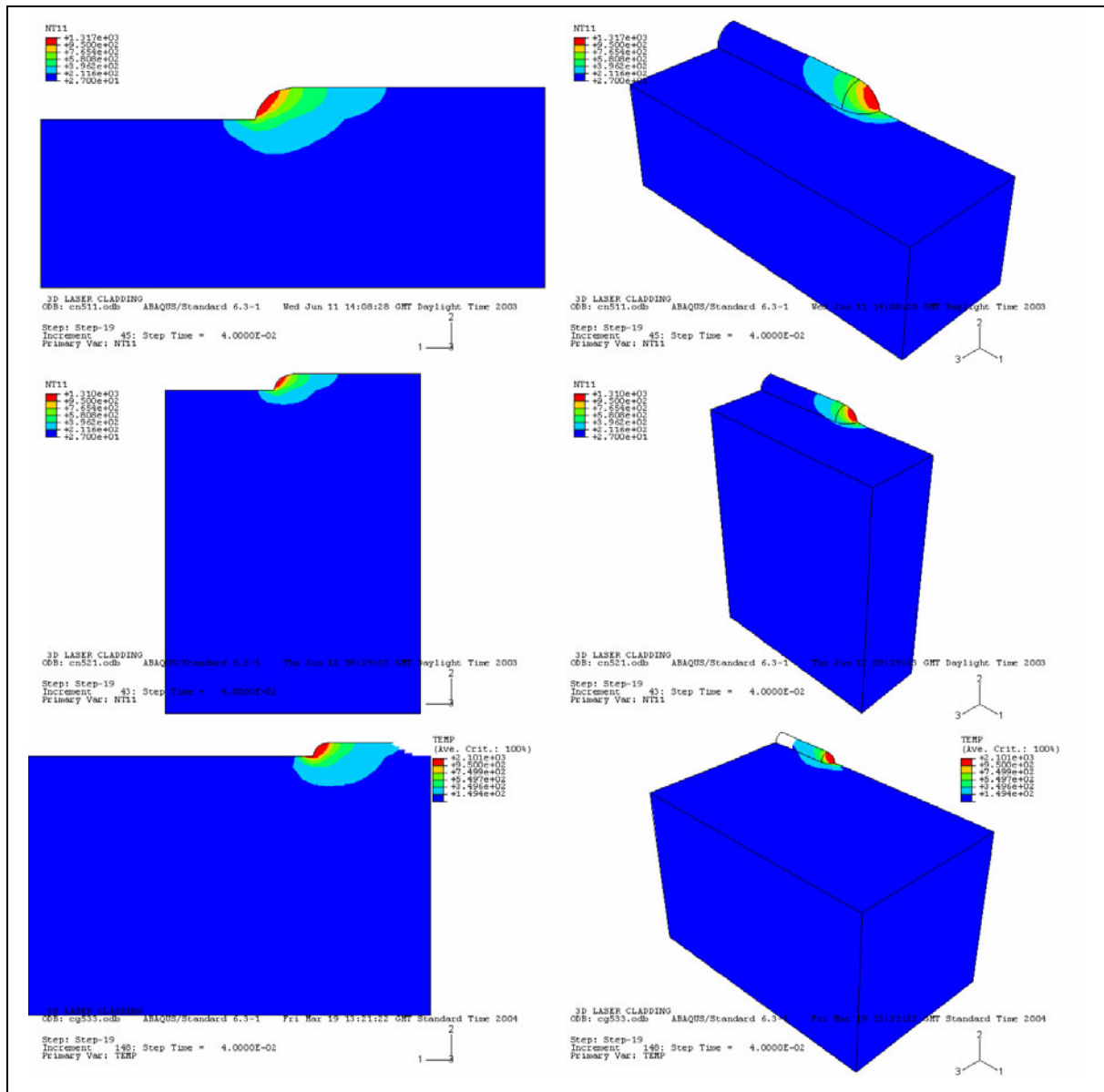


Figure 57. Three-dimensional model for temperature, curved mesh.

A comparison of melt pool shape in 3D and 2D can be made with the help of figure 58, where we see detail of the melt fronts shown in figures 57e and 52c (clad melt pool is defined in red and substrate melting isotherm is defined by the outer envelope of the green region). Heat loss from the clad bead side, and not just from the top, accounts for greater efficiency in heat extraction in 3D and thus a more compact set of isotherms.

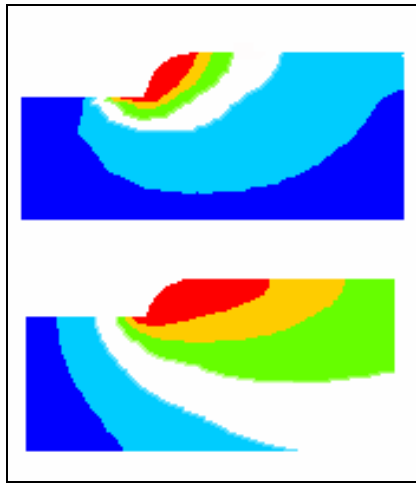


Figure 58. Comparison of melt pool shapes in 3D and 2D.

In figure 59 the variable composition case is featured (run cg533) and secondary variables are shown, such as the composition index ($SDV1$), the relative temperature ($SDV2$, the ratio between local temperature rise and local melting temperature), the cooling rate ($SDV5 = -\frac{\Delta T}{\Delta t}$) and the temperature gradient ($SDV6$). In the case of the relative temperature, the isoline equaling 1.0 stands for the local melting isotherm, so this model predicts the melt pool shapes extending back into the substrate, as discussed in chapter 2. The cooling rate and thermal gradient are among typical values for laser cladding and are within the limits predicted by microstructure measurements presented in the experimental parallel work [1].

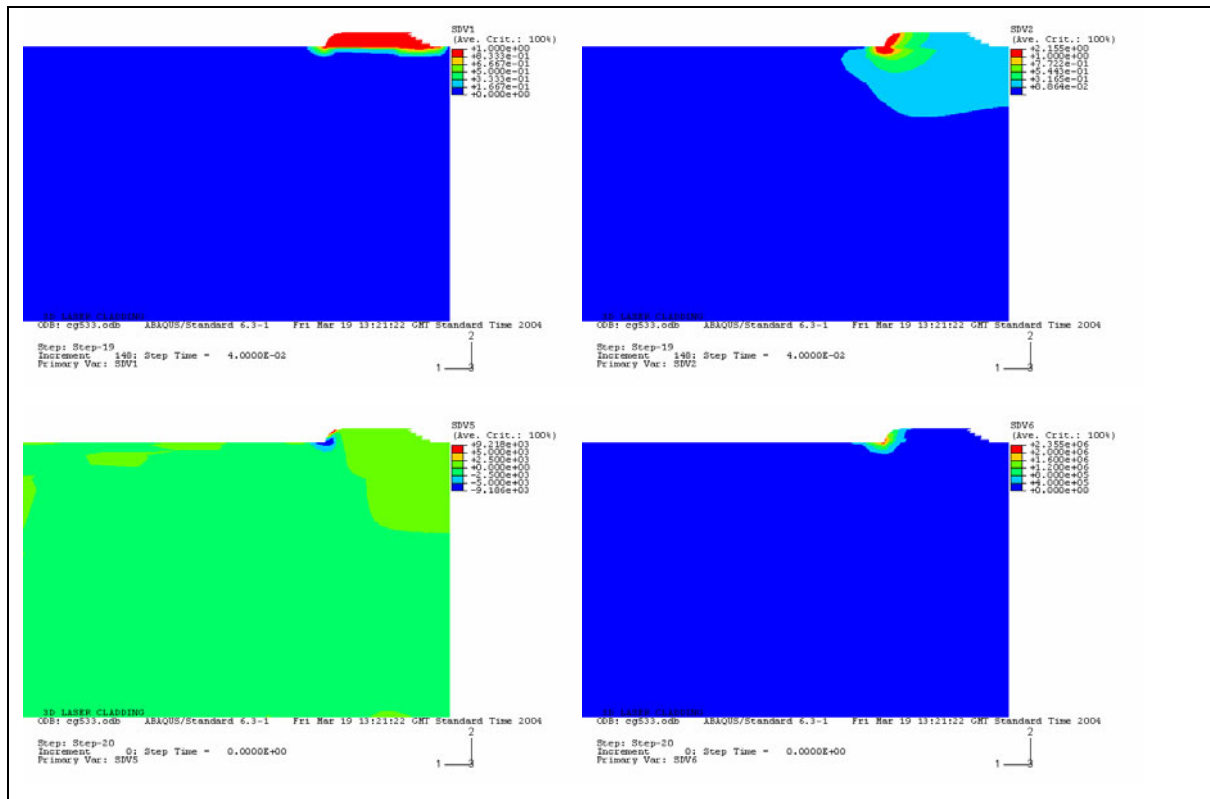


Figure 59. 3D model for temperature: secondary variables.

In figures 60 through 62 we see the corresponding results for stress (computer runs dn513, dn523, dn531). It should be mentioned that, with the mesh that was produced, numerical convergence is an issue. It is acknowledged that it is difficult to produce in a speedy fashion a number of such 3D simulations. Still, the numerical output is expected to show what the parametric tendencies are; as it will be seen, those results compare well with similar data obtained from a planar shaped mesh.

In figure 63 we see the temperature profiles for planar shaped meshes (runs lc141 and lc131). The elements are activated in the domain along straight lines. The curved shape of the melt front is not featured and that is seen to yield an important consequence: all other parameters being the same, the laser power that has to be employed is considerably higher, in order to obtain a melt pool spanning the whole clad height. The melt pool size is thus overestimated and at steady state a higher value of energy is needed in order to keep such liquid zone in a stable condition.

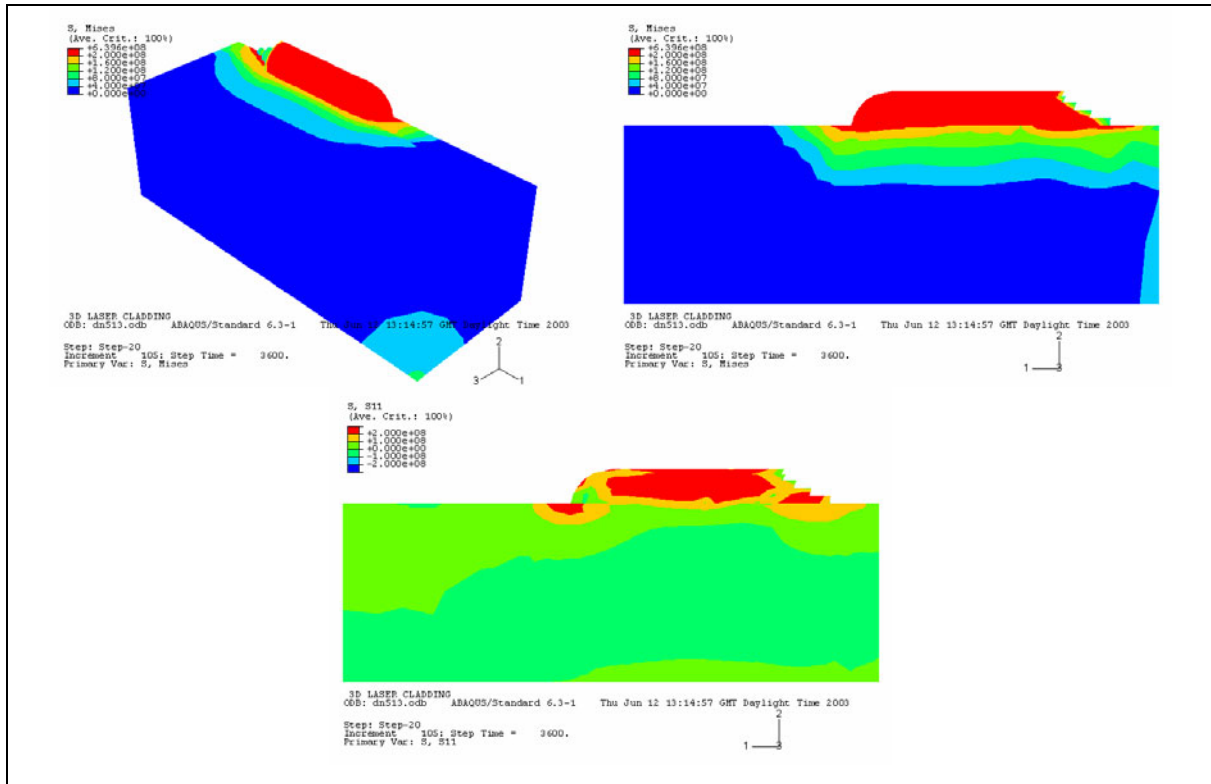


Figure 60. 3D model for stress, curved shape.

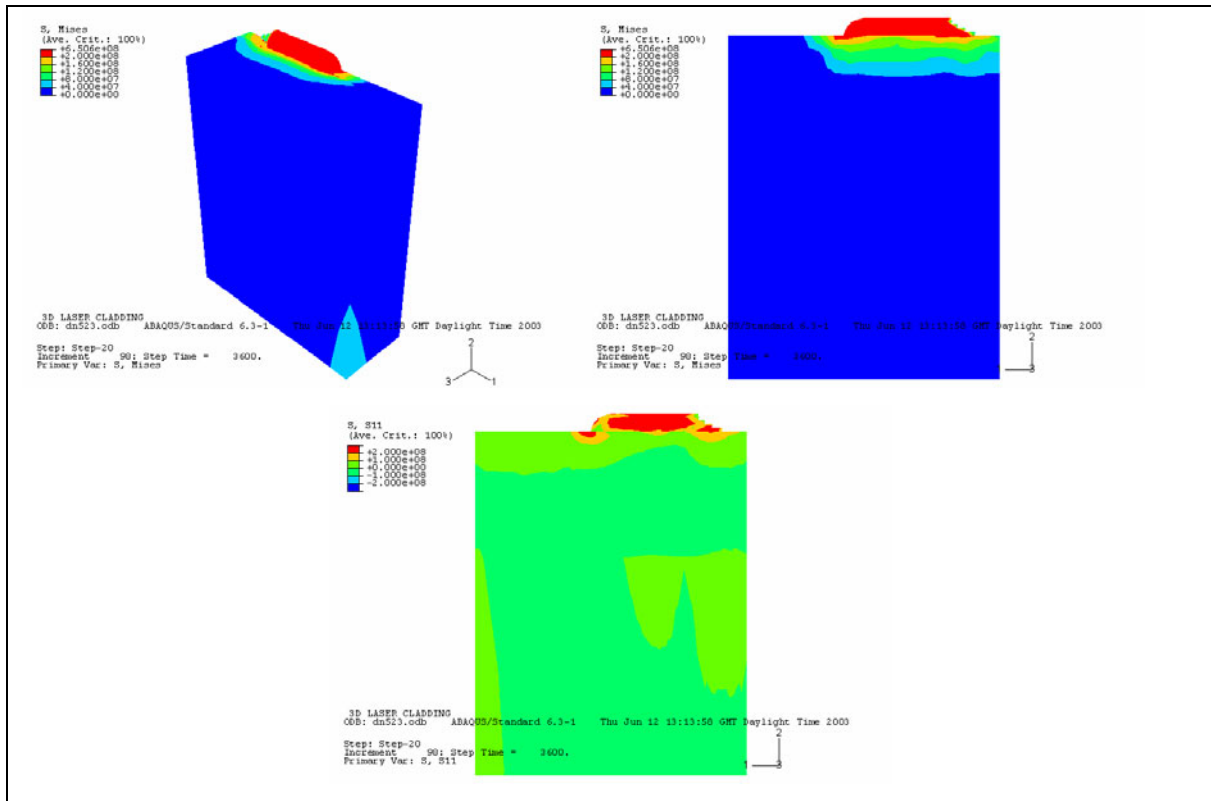


Figure 61. 3D model for stress, curved shape (cont'd).

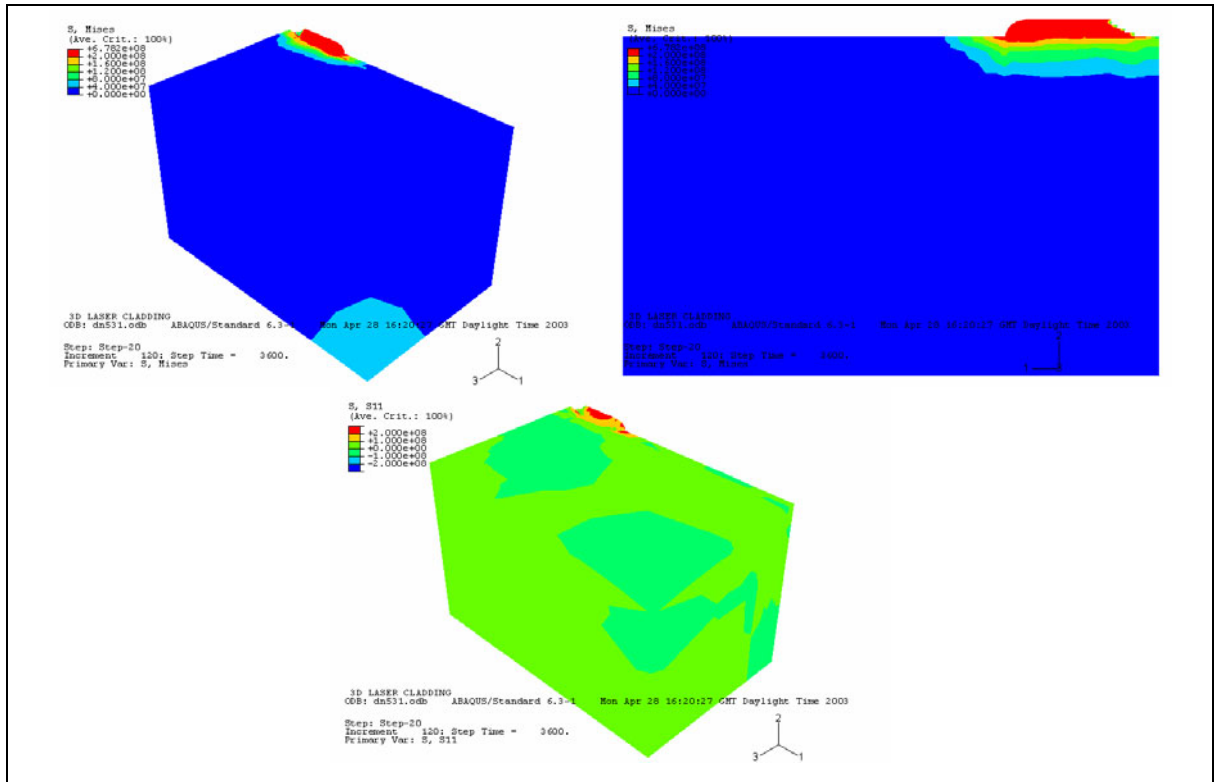


Figure 62. 3D model for stress, curved shape (cont'd).

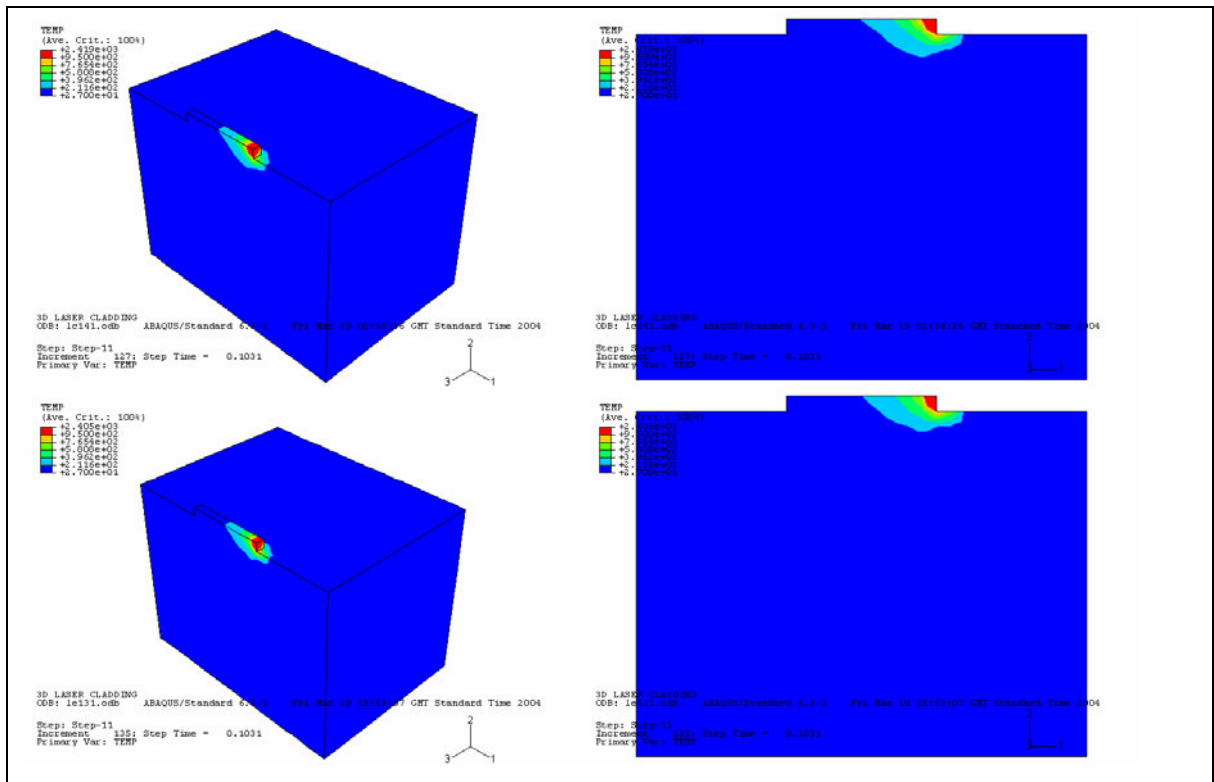


Figure 63. Three-dimensional model for temperature, planar mesh.

One should mention, however, that the overall requirement is the same (the melting isotherm reaching down to the substrate and up to the top of the clad); that is the essential condition for heat transfer modeling of laser cladding, despite the particular value of laser power (P) obtained, which actually will be affected by an average absorptivity, A . So, the modeling approach allows to obtain the product $A P$, which is to be subject to calibration through experimental results. That is an iterative procedure, as modeling will often give the very initial estimates of processing parameters, allowing for earlier tests that in turn produce data that can be fed into the model.

In figure 64 secondary variables obtained from the variable composition model are displayed, and results are seen to be comparable to the curved shape values.

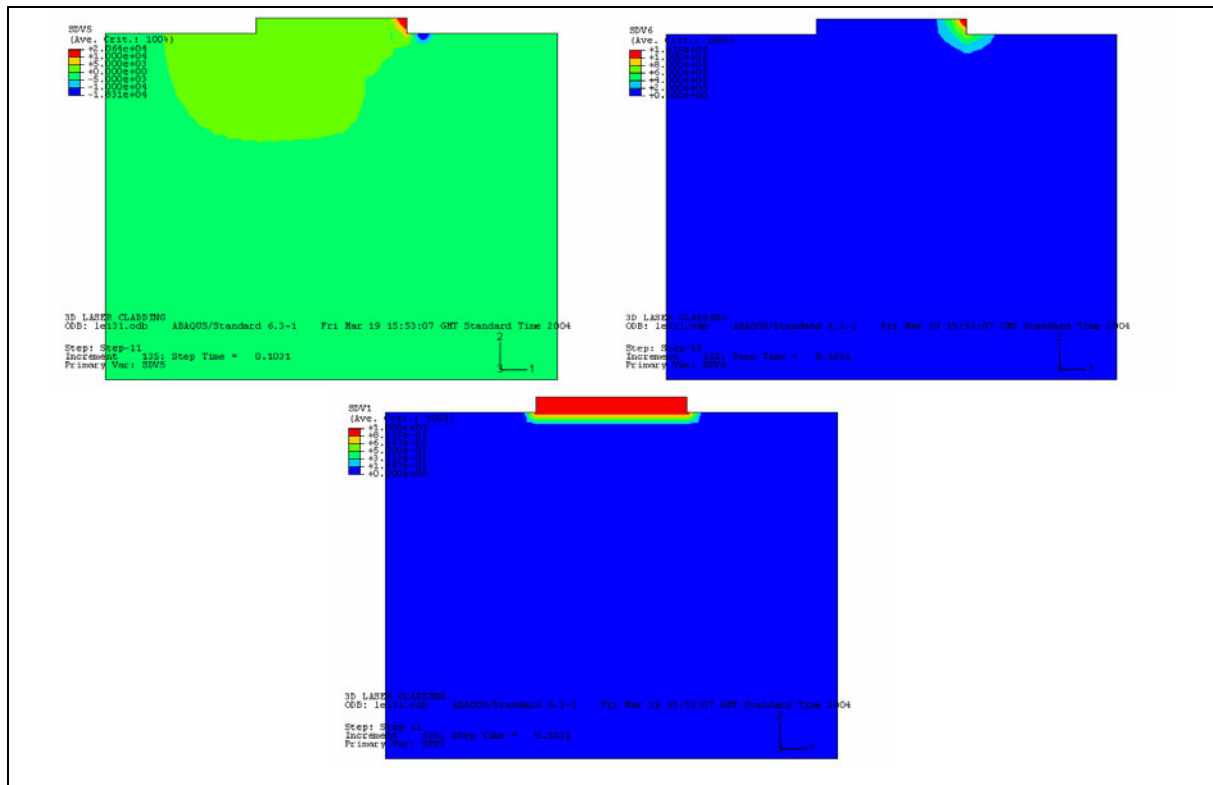


Figure 64. 3D model for temperature: secondary variables.

In figures 65 and 66 we have results from the mechanical model (runs mc141 and me131), which numerically converges well. Von Mises stress is seen to be higher in the clad (the stronger material which will be subjected to the highest load) as well in the interfacial zone.

Longitudinal stress, σ_{11} , is seen to remain at a high tensile value in the clad, and the other normal components are usually smaller.

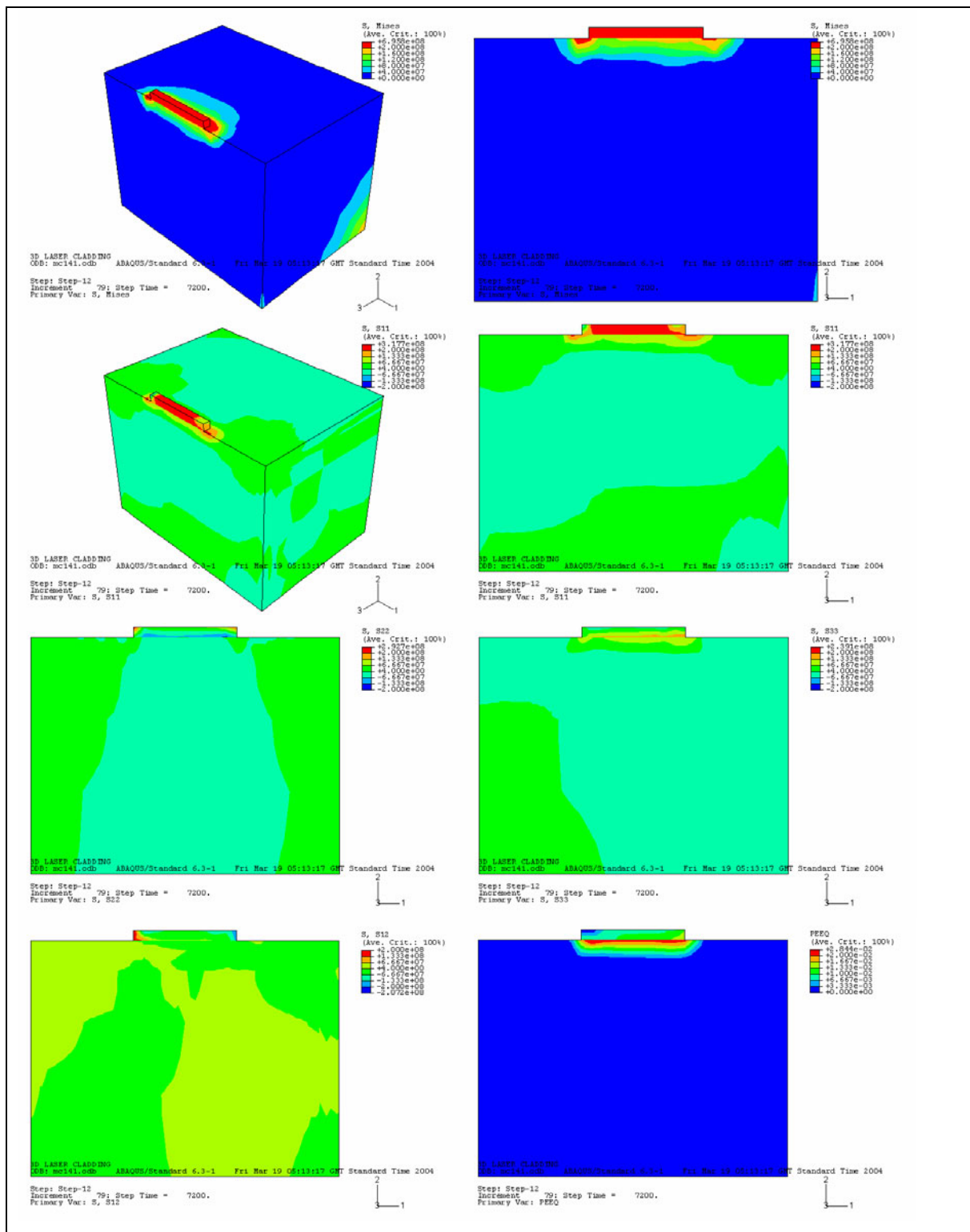


Figure 65. 3D model for stress, planar mesh.

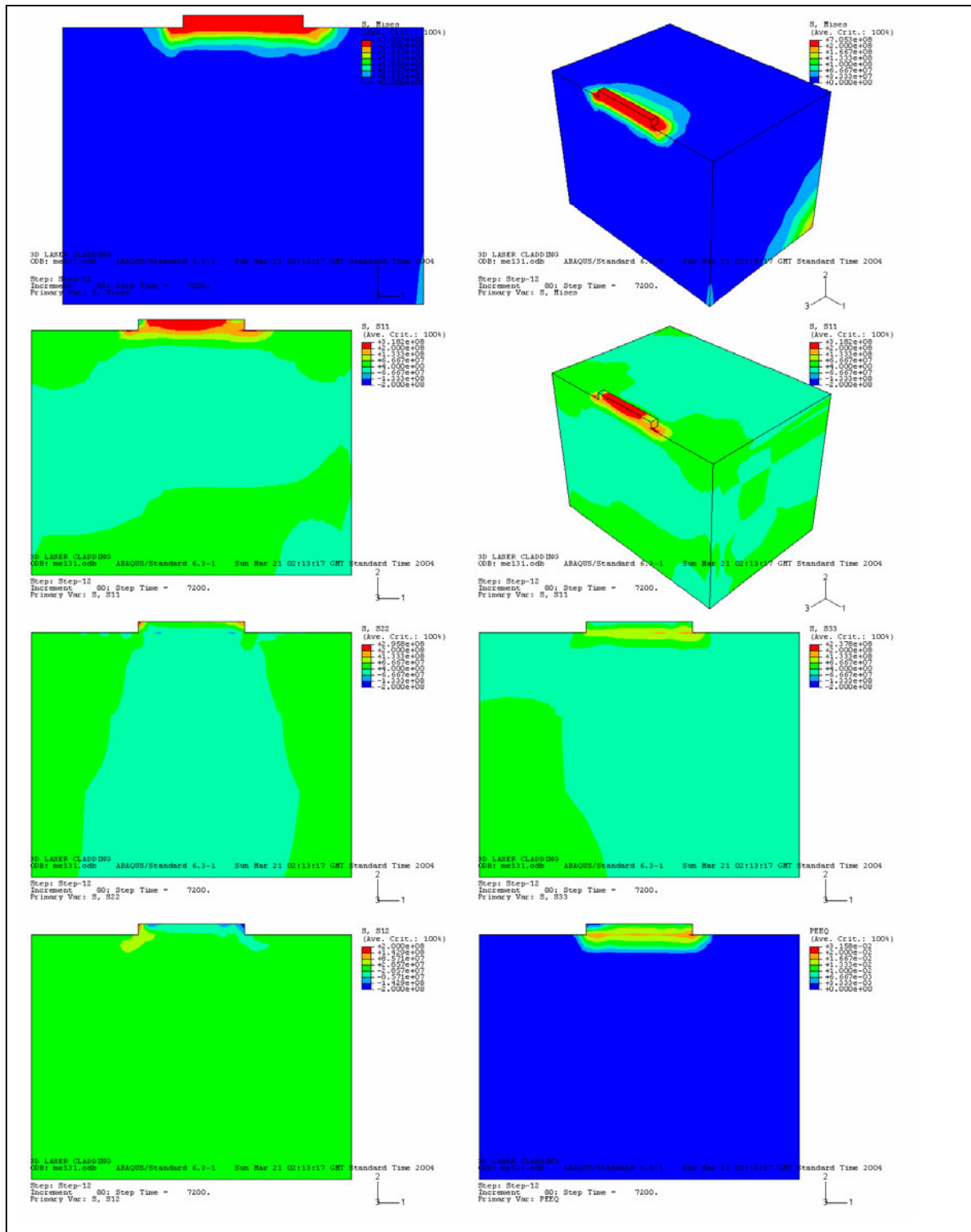


Figure 66. 3D model for stress, planar mesh (cont'd).

The longitudinal stress shows a good resemblance with the corresponding result for the curved meshes. The clad is seen to be in tension, which is more detrimental to the behavior in service, as it facilitates failure by fracture (in fact precipitates or other inhomogeneities present in the clad or the interface zone lead to stress concentrations in a stress state that could already be near failure conditions). It is interesting to note that in the parallel experimental study, a number of similar composition copper alloys were used but discarded, due to the tendency for the films to debond and/or show fracture. The copper alloy that was used, C95600 yielded good results, but is likely to lie within the same tendency as other copper alloys that were used.

A tensile stress state can be understood in view of the fact that, in 3D and for that geometry, the composition variation is no longer the determining factor, but the fact that the clad material, and the underlying strip of interfacial material, have a reference CTE temperature that is high. That zone, whose volume is very small, will have as a whole a strong tendency to contract, doing that against a large substrate that overall stays cold. That overall shrinking tendency is hindered by the substrate (in a 3D fashion), which is seen to apply to the clad a tensile stress state (especially in the longitudinal direction, where already cold clad further constrain the cooling hot portion of it). Was the coefficient of thermal expansion mismatch to be higher, there would be there a possibility for the composition effect to prevail and thus obtain a compressive state in the substrate. This shows the usefulness of a modeling approach in such a complex case where thermal strain is associated with different causes (namely CTE compositional mismatch, the presence of thermal gradients and different coefficient of thermal expansion reference initial temperatures).

Plots of the shear stress component, σ_{12} , are featured (figure 67), for the variable composition planar mesh (me131, featured in figure 66g) as well as for the fixed composition curved shape mesh (dn513). Data is taken from the symmetry plane, either at the top of the clad (*i.e.*, at the highest row of nodes) or at its bottom. We see that such stress component becomes steeply high at the clad extremities, showing a sharp variation from a low value at the mid clad regions, which is in harmony with the expected behavior for a

thin film on a thick substrate [69]. Such high shear stresses can lead to delamination; in laser clad tracks, when such phenomena occurs, it is seen to start precisely at such locations. The shear stress profile is verified to depend on the shape of the film, also in harmony with the above mentioned reference, although results for the bottom of the clad are relatively close. Results are different at the top of the clad, because that is precisely the region where the two meshes are different.

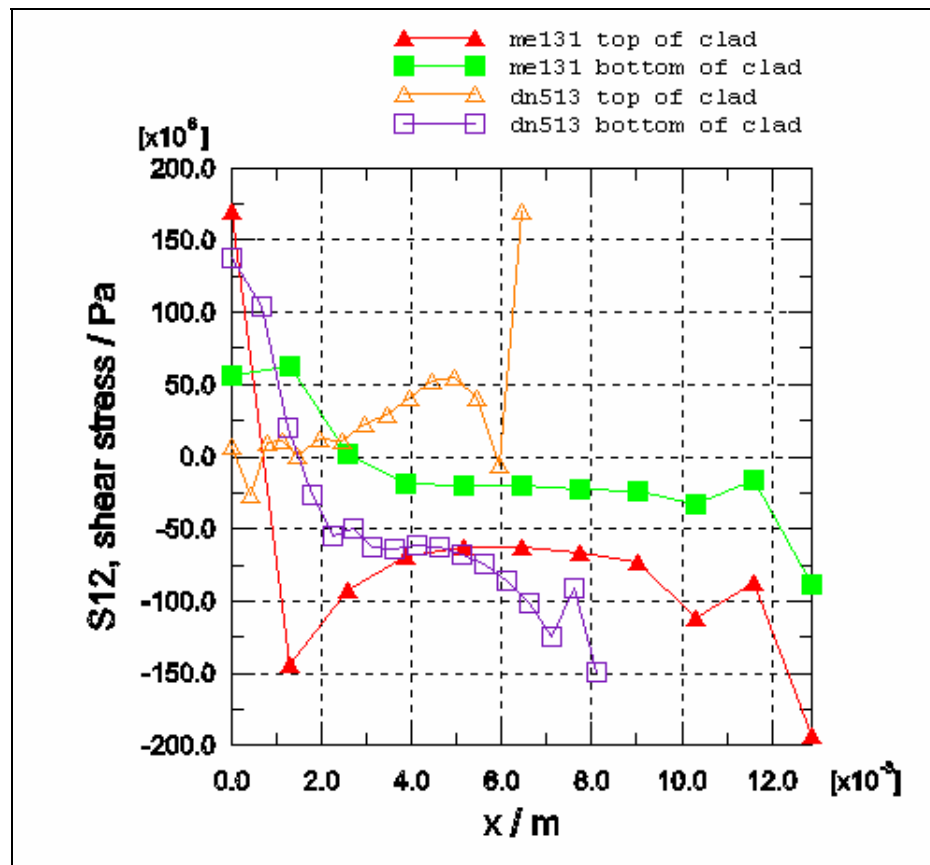


Figure 67. Shear stress profile, top and bottom of clad, planar and curved mesh.

Finally, the boundary conditions for the 3D mechanical models are shown in figure 68.

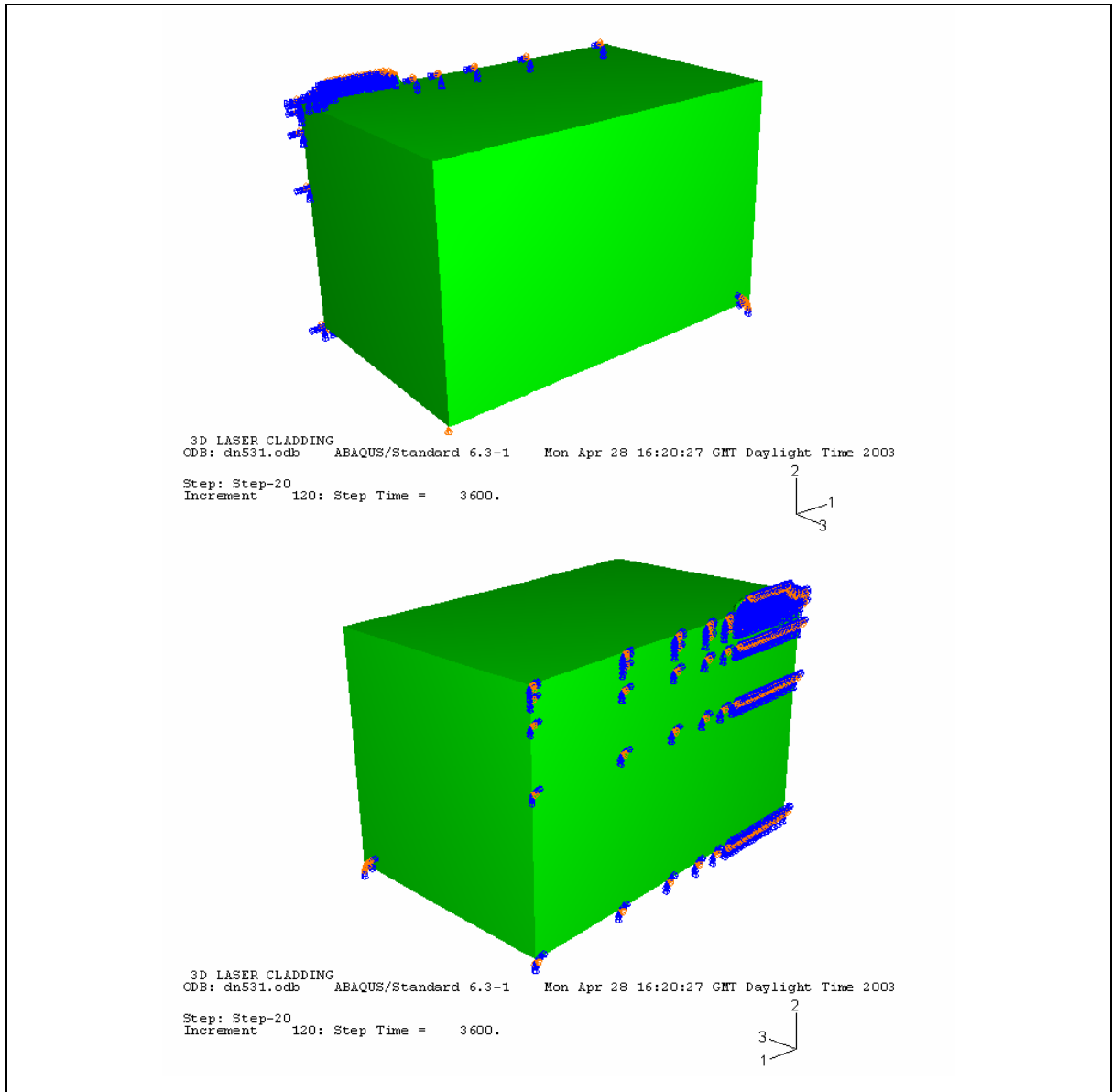


Figure 68. Boundary conditions for 3D stress models.

5. Discussion and Conclusion

5.1. Comparison with experimental results

We compare now the simulations with some experimental results obtained in the parallel experimental work referred to previously [1]. Hardness, H , results are shown in figure 69. One can identify: a) a coating zone with an approximately constant value of hardness, b) an interface region (with depth approximately 100 μm) with considerably higher values of H and c) a transition zone in the substrate, where hardness decays from the interface result to the aluminum alloy characteristic value.

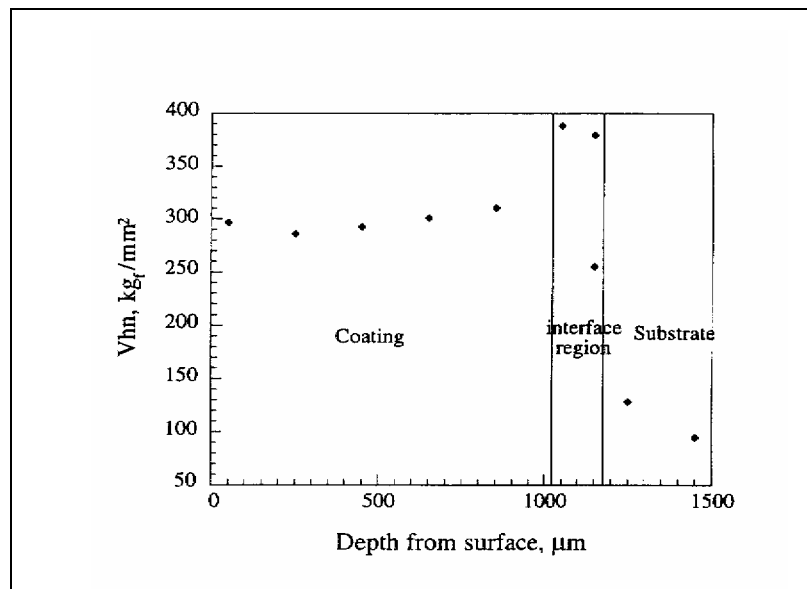


Figure 69. Hardness profile of laser clad track.

The higher value of hardness at the interface reflects the expected hardening behavior associated with the presence of precipitates. This in turn would suggest that residual stresses are to be more intense in that zone: not only the yield stress could be seen as being higher there ($H = 3 \sigma_Y$), thus the potential for high residual (elastic) stress would exist, but also it is precisely the zone which separates the two regions with different coefficients of thermal expansion, and consequently where residual stress has to play its role to accomplish compatibility and equilibrium. But one has to be careful, because when

hardness testing is performed in a material with residual stress, the applied stress state associated with the indenter superimposes with the residual stress state, making the situation more difficult to analyze.

Taking a 1D analogy, if local residual stress is tensile, then the applied stress has to overcome it and then yield in compression is attained at a higher load, giving a higher hardness (or: smaller depth of indentation for constant load); on the other hand, if residual stress is compressive, the indenting load will be smaller (or: higher depth of indentation for constant load), giving a lower hardness, from its value for the unstressed state in the same material. Generally speaking those effects might change the apparent hardness value, but most likely to a limited degree: for a not too small indentation, each material point within it suffers plastic deformation and plastic strain energy being transferred to the material by indentation should be much larger than elastic strain energy present as a result of residual stress. So the total deformation energy will likely be affected by the residual stress field to a small (though perhaps measurable) degree and the same conclusion can then be taken for the indentation depth and the hardness.

So, further study would be needed, although it can be stated with reasonable confidence that the hardness profile is in good harmony with stress results, as Mises stress was seen to be high precisely in the clad and interface regions.

The composition profile (figure 70) shows a fairly abrupt drop in the interface region, from a region (to the right) of fairly uniform composition, which is evidence of good mixing in the clad melt pool and an indirect indication of little dilution. In fact, the copper contents, for example, decreases slightly from 75% (which is its nominal composition) to an almost uniform value, 70%, therefore still within little dilution.

The interface region is seen to have a finite dimension, where composition in fact changes sharply (steeper gradients are found in a 50-75 μm band). Although few points are represented, its distribution appears to be linear, which is assumed in the composition index formulation that was used in some of the simulations. In the interfacial zone, the Al_2Cu

intermetallic is reported to be present (figure 71), which gave the basis for using that precipitate in calculating the properties of the interface.

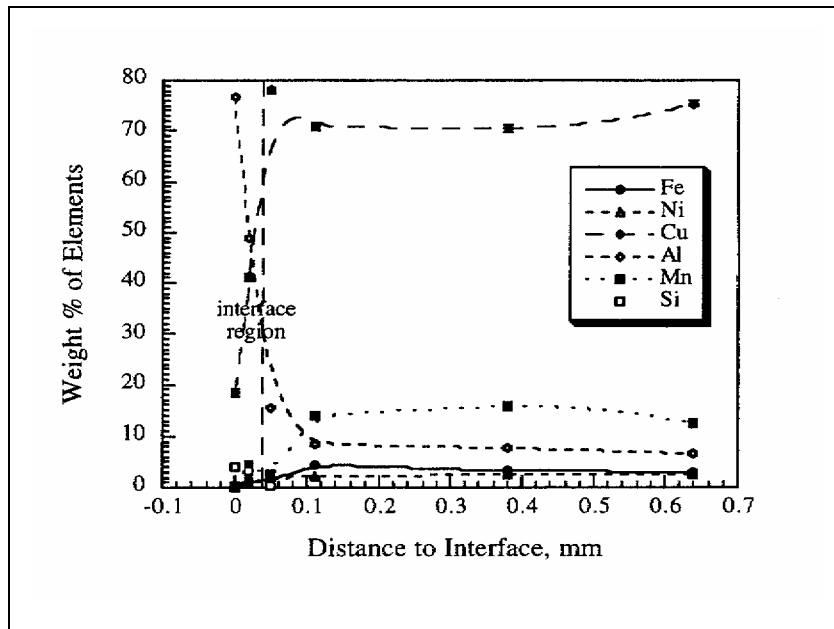


Figure 70. Composition profile of laser clad track.

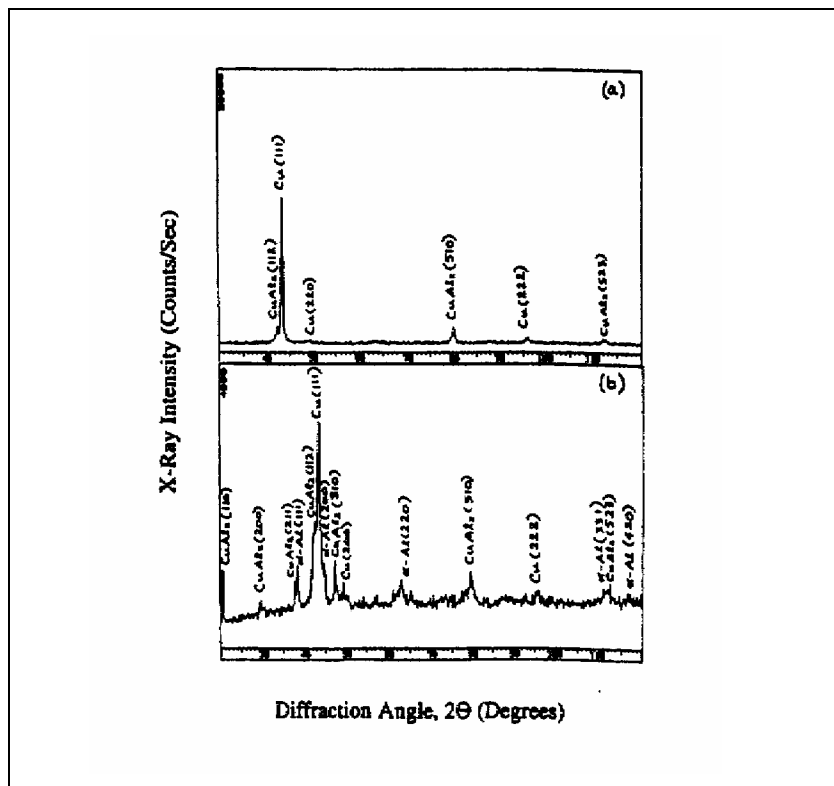


Figure 71. Composition in the interfacial zone.

A plot of the composition index is also presented (figure 72), for comparison with the hardness (figure 69) and the composition profiles (figure 70), showing good agreement and therefore providing validation for the dilution model that is proposed. The profile is taken at the symmetry plane of the curved mesh (run cg533) in the mid region of the clad bead (*i.e.* away from its extremities). At the top of the plot, the boundaries seen in the hardness result are featured.

The composition index is approximately 0.9 at around 50 μm depth (counted from the clad zone) and, from the composition plot, the copper content is seen to be approximately 14% at that depth. So the value of the volume fraction of Al_2Cu precipitates is calculated for that location, assuming substrate material as the matrix, the result being $f = 20\%$, which is precisely the value that was used in the materials properties used in the simulations (for the composite material found at the composition index 0.9 isoline).

AbaqusTM uses a linear interpolation scheme for all independent variables, including field variables such as the composition index, therefore, a smaller value of c_i will give a smaller value of yield stress, and that will correspond to a smaller value of f . In fact, the volume fraction of precipitates is expected to decrease along the depth, likely in a steep fashion, as suggested by the hardness plot, where the high hardness zone is around 100 μm deep. As it was mentioned at the end of chapter 2, the composition index is a descriptor of dilution and is expected to be univocally tied to the composition profile -and therefore to the variation of volume fraction as well- although certainly not in a linear fashion. Mixing that is driven by diffusion and convection, as well as the solidification conditions, determine the microstructure (*e.g.* the amount and composition of precipitates) and the overall composition profile.

The peak temperature/composition index approach is, therefore, expected to give a simplified description of such composition profile, with the ability to catch, however, some of its main features, as suggested by figure 72, especially in its ability to affect the calculation of materials properties by a variable directly related to composition, actually

doing that iteratively during a FE temperature calculation, as well as in the capability it offers to estimate the location of the interface and substrate transition zones.

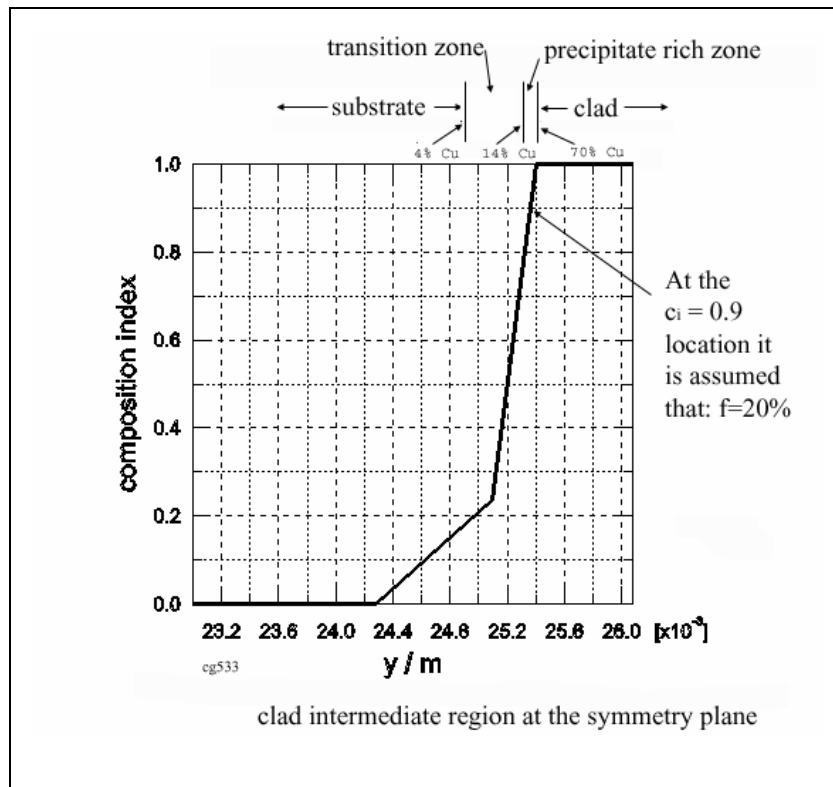


Figure 72. Composition index profile, 3D curved shape mesh.

5.2. Summary

From the research work included in the present dissertation a number of aspects can be summarized:

- An overall picture of dilution in laser cladding was outlined, for single and bi-material systems. With a simple model for mixing, that lead to a scheme for the estimation of the composition distribution along the depth of a laser clad track, and thus quantitatively address the dilution problem, as a function of process parameters.

- The feasibility of a Finite Element modeling approach to laser cladding, both 2D and 3D, was established. For that purpose, an algorithmic procedure, the Input File Generator, was developed, so as to obtain FE input files containing information of the processing parameters, geometrical and mesh requirements, as well as materials properties, *i.e.*, an adequate pre-processing procedure.
- Two-dimensional temperature models of laser cladding were seen to be useful in order to explore parameter space and get an overall picture of the phenomenon. Nevertheless, in 2D the temperature field (for example the clad and substrate melt pool sizes) tends to be over-represented, as there is absence of heat loss in the perpendicular direction to the 2D domain. In fact, heat transfer in laser cladding is 3D in nature, as the material loses heat by convection and radiation along the whole half-cylinder shaped clad bead and not just through its top portion.
- Two-dimensional stress models seem also not to be fully adequate to represent the real situation in laser cladding, as the common assumptions (plane strain, generalized plane strain and plane stress) don't seem to accommodate the geometrical features of the process:
 - Thermal strain is triaxial in nature;
 - The clad (and even the substrate) does not have a large width, which would be required for generalized- and simple- plane strain cases.
 - Although the clad is thin, its contraction leads to non-zero stress across its width, making plane strain not applicable.
- Still, from a 2D stress analysis, it can be seen that the clad and substrate dimensions affect very much the stress field, as expected from a film-substrate system.
- A three dimensional FE approach to LC is thus proposed. For the temperature field, a domain that matches the geometry of the process is verified to be very important. In fact, the melt pool, which must span the whole clad height at the leading edge of the clad, will have a certain volume, which at steady state is related both with the

process parameters and the thermal properties of the material. So, unless that melt front shape is modeled correctly, that liquid zone is not going to be correctly characterized.

- For example, if instead of having a spherical cap shape, the melt front was to be planar, the melt pool size that leads to total melting throughout the clad height is seen to be roughly double in volume, which alters considerably the steady state heat transfer conditions for the existence of such a stable melt pool; for example, laser power would be overestimated in such a case.
- Although the 3D FE model for temperature that is implemented with the curved shape mesh shows good numerical convergence, the corresponding mechanical model shows, at times, a degree of difficulty in attaining convergence in the AbaqusTM processor.
 - Part of that could perhaps be attributed to the mesh generation scheme, which leads to some elements with non-optimal aspect ratios.
- In the mechanical problem the shape of the clad front is now seen not to be as critical as in the case of temperature. Even if there is an extra amount of material in the melt pool, that is expected to impose little additional constraint in the rest of the domain. This is especially true in the case of the normal components of stress. In the case of the shear components, the results are also similar in the regions common to the two meshes.
- Therefore, it seems reasonable to undertake more accurate temperature simulations in curved shaped meshes, then repeat those (using higher values of laser power) in planar boundary shaped meshes, the latter providing an input to a stress analysis in such regular mesh, giving the overall stress state, that is seen to be particularly dependent on the dimensions of clad and substrate.

5.3. Conclusions

In the published literature there are a few models for laser cladding, especially FE models as seen in chapter 1, but these are either 2D with curved front shape or 3D with planar front and usually for single system cladding. So a contribution is made in this dissertation, in particular in the following aspects:

- A three-dimensional transient thermal and mechanical FE model for laser cladding in accord with the process geometry was developed, it is believed, for the first time. The model takes into account both the additive nature of the process and the curved shape of the melting front. The composition of the computation domain is arbitrary, so the model accommodates both single and bi-material cladding. The model also allows for the transient change of local composition due to mixing.
- In addition, three kinds of similar FE models for temperature and stress are being simultaneously proposed:
 - 2D curved-shape model;
 - 3D curved-shape model;
 - 3D planar-shape model.
- Such models can be used either independently or following the following proposed sequence:
 1. 2D temperature model, for quick survey of parameter space;
 2. 3D temperature curved-shape model, for better characterization of the temperature field;
 3. 3D temperature planar-shape model, allowing for easier generalization in the case of more complex geometries;
 4. 3D stress planar-shape model, for characterization of stress field;
 5. 3D stress- curved shape model, for better characterization of the stress field.

- Results of simulations performed for cladding of C95600 copper alloy on AA333 aluminum alloy are in good accord with the experimental results:
 - Temperature models give good account of the steady state nature of the process, especially in 3D. The parameters used are similar to the ones used in the experiments.
 - The stress model is in good accord with the expected behavior in such system, namely by predicting a relatively intense tensile longitudinal stress state in the clad, as well as the occurrence of peaks in the clad shear stress, near the extremities of the film.
 - The composition index approach for dilution gives results that compare well with hardness and composition profile results.

5.4. Suggestions for future research

The number of questions generated by scientific research is often larger than the number of questions it was supposed to answer in the first place. In accord with that, a number of suggestions for future research, a few of which are already underway, are proposed:

- Modify the dilution model to accommodate the overall composition change due to the incorporation of substrate material into the melt pool.
- The translation between 2D and 3D temperature results, and between 3D curved- and 3D planar- shaped meshes merit further investigations.
- A meshing procedure that leads to a better quality 3D mesh is to be looked for, eventually with the use of commercial software, so as to easily obtain stress results in curved shaped meshes.
- Temperature and stress field in situations other than single bead cladding are to be studied with planar shaped meshes; for example, cladding of an extended surface

with some overlap, or multipass cladding, leading to the buildup of clad material, which are more common applications of the LC technique.

- The model can be applied to furnish data for studies in other areas:
 - Tempering and grain growth kinetics, as these are affected by the temperature field and eventually the stress field also;
 - Failure, including fracture mechanics studies;
 - Solidification analysis; etc.

- The overall stress field will affect phenomena at grain size and even at lattice size level, so a correct picture of the relationship between stresses of these three kinds, by means of micromechanics, will lead to better understanding of phenomena such as recrystallization, grain growth, phase transformations, precipitate coarsening or enhanced solid solubility in laser cladding.

References

- [1] Kelly, J.K., "*Laser cladding of cast aluminum alloys: bronze alloys for seizure and wear resistance*", M.Sc. thesis, University of Illinois at Urbana-Champaign, 1998.
- [2] Carvalho, P.A., N. Braz, R. Vilar, M.M. Pontinha, M.G.S. Ferreira, "*Characterization of Co-Ni-Al alloys obtained by variable powder feed rates laser cladding*", Proceedings of LAMP '92, Nagaoka, Japan, June 1992, pp. 825-830.
- [3] Sexton, C.L., G. Byrne, K.G. Watkins, "*Alloy development by laser cladding: an overview*", Journal of Laser Applications, 13(1), (2001) pp. 2-11.
- [4] Pei, Y.T., J.T.M. De Hosson, "*Functionally graded materials produced by laser cladding*", Acta Materialia, 48 (2000) pp. 2617-2624.
- [5] Frenk, A., N. Henchoz, W. Kurz, "*Laser cladding of a cobalt-based alloy: processing parameters and microstructure*", Zeitschrift für Metallkunde, 84(12) (1993) pp. 886-892.
- [6] Mazumder, J., A. Kar, "*Solid solubility in laser cladding*", Journal of Metals, (February 1987) pp. 18-23.
- [7] Colaço, R., R. Vilar, "*Development of new coating materials using a laser rapid alloy prototyping technique*", Materials Science Forum, 414-415 (2003) pp. 57-62.
- [8] Colaço, R., Ph.D. dissertation, Instituto Superior Técnico, Technical University of Lisbon, 2002.
- [9] Carvalho, P.A., N. Braz, M.M. Pontinha, M.G.S. Ferreira, W.M. Steen, R. Vilar, K.G. Watkins, "*Automated workstation for variable composition laser cladding- its use for rapid alloy scanning*", Surface and Coatings Technology, 72 (1995) pp. 62-70.
- [10] Kelly, J., K. Nagarathnam, J. Mazumder, "*Laser cladding of cast aluminum-silicon alloys for improved dry sliding wear resistance*", Journal of Laser Applications, 10(2) (1998) pp. 45-54.
- [11] Costa, L., T. Reti, A.M. Deus, R. Vilar, "*Simulation of layer overlap tempering kinetics in steel parts deposited by laser cladding*", Proceedings of 2002 International Conference on Metal Powder Deposition for Rapid Manufacturing, San Antonio, TX, USA, April 2002, ed. D. Keicher *et al.*, pp. 172-179.

- [12] Costa, L., A.M. Deus, T. Reti, R. Vilar, "*Simulation of layer overlap tempering in steel parts produced by laser cladding*", Proceedings of RPD 2002 Advanced Solutions and Development, Marinha Grande, Portugal, October 2002, ed. J. Jorge *et al.*
- [13] Deus, A.M., M.A. Fortes, P.F. Ferreira, J.B. Vander Sande, "*A general approach to grain growth driven by energy density differences*", Acta Materialia, 50 (2002) pp. 3317-3330.
- [14] Gnanamuthu, D.S., "*Surface alloying and transformation hardening using an industrial laser*", JOM Journal of Metals, 27(12) (1975) p. A61.
- [15] Seaman, F.D., D.S. Gnanamuthu, "*Using industrial laser to surface harden and alloy*", Metal Progress, 108(3) (1975) p. 67.
- [16] Steen, W.M., C.G.H. Courtney, "*Hardfacing of Nimonic 75 using a 2 kW CW CO₂ laser*", Metals Technology, June 1980, pp. 232-237.
- [17] Weerasinghe, V. M., W.M. Steen, "*Laser cladding with pneumatic powder delivery*", Proceedings 2nd International Conference 'Laser Material Processing', Los Angeles, CA, USA, January 1983, pp. 166-175.
- [18] McIntyre, R.M., "*Laser hardsurfacing of turbine blade shroud interlocks*", Proceedings 2nd International Conference 'Laser Material Processing', Los Angeles, CA, USA, January 1983, pp. 230-240.
- [19] Rolls-Royce Ltd.: "*Laser application of a hard surface alloy*", UK Patent GB 2052566A, 1980.
- [20] Powell, J., Steen, W. M. (inventors), Control Laser Ltd.: "*Fusing cladding material to a substrate*", UK Patent GB 2090873A, 1982.
- [21] Vilar, R., "*Laser cladding*", Journal of Laser Applications, 11(2) (1999) pp. 64-79.
- [22] Vilar, R., "*Laser cladding*", The International Journal of Powder Metallurgy, 37(2) (2001) pp. 31-48.
- [23] Weerasinghe, V. M., W.M. Steen, "*Computer simulation model for laser cladding*", in Transport Phenomena in Materials Processing, ASME H.T.D., 29 (1983) pp. 15-23.

- [24] Kar, A., J. Mazumder, "One-dimensional diffusion model for extended solid solution in laser cladding", Journal of Applied Physics, 61(7) (1987) pp. 2645-2655.
- [25] Kar, A., J. Mazumder, "One-dimensional finite-medium diffusion model for extended solid solution in laser cladding of Hf on nickel", Acta Metallurgica, 36(3) (1988) pp. 701-712.
- [26] Kar, A., J. Mazumder, "Extended solid solution and nonequilibrium phase diagram for Ni-Al alloy formed during laser cladding", Metallurgical Transactions A, 20A (1989) pp. 363-371.
- [27] Agrawal, G., A. Kar, J. Mazumder, "Theoretical studies on extended solid solubility and nonequilibrium phase diagram for Nb-Al alloy formed during laser cladding", Scripta Metallurgica et Materialia, 28(11) (1993) pp. 1453-1458.
- [28] Hoadley, A. F. A., M. Rappaz, "A thermal model of laser cladding by powder injection", Metallurgical Transactions B, 23B (1992) pp. 631-642.
- [29] Picasso, M., A.F.A. Hoadley, "Finite element simulation of laser surface treatments including convection in the melt pool", International Journal Numerical Methods Heat Fluid Flow, 4 (1994) pp. 61-83.
- [30] Picasso, M., C.F. Marsden, J.D. Wagniere, A. Frenk, M. Rappaz, "A simple but realistic model for laser cladding", Metallurgical and Materials Transactions B, 25B (1994) pp. 281-291.
- [31] Kim, J.D., Y. Peng, "Melt pool shape and dilution of laser cladding with wire feeding", Journal of Materials Processing Technology, 104 (2000) pp. 284-293.
- [32] Kim, J.D., Y. Peng, "Time-dependent FEM simulation of dilution control of laser cladding by adaptative mesh method", KSME International Journal, 14(2) (2000) pp. 177-187.
- [33] Marsden, C.F., A. Frenk, J.D. Wagniere, "Power absorption during the laser cladding process", in *Laser Treatment of Materials*, ed. B. L. Mordike, DGM, Oberursel, 1992, pp. 375-380.
- [34] Neto, O.O.D., R. Vilar, "Physical-computational model to describe the interaction between a laser beam and a powder jet in laser surface processing", Journal of Laser Applications, 14(1) (2002) pp. 46-51.

- [35] Lin, J., “*Temperature analysis of the powder streams in coaxial laser cladding*”, Optics & Laser Technology, 31 (1999) pp. 565-570.
- [36] Lin, J., “*Numerical simulation of the focused powder streams in coaxial laser cladding*”, Journal of Materials Processing Technology, 105 (2000) pp. 17-23.
- [37] Fu, Y., A. Lored, B. Martin, A.B. Vannes, “*A theoretical model for laser and powder particles interaction during laser cladding*”, Journal of Materials Processing Technology, 128 (2002) pp. 106-112.
- [38] Deus, A.M., J. Mazumder, "Two-dimensional thermo-mechanical finite element model for laser cladding", Proceedings of ICALEO '96, Orlando, FL, USA, 1996, pp. B/174-B/183.
- [39] Nickel, A.H., D.M. Barnett, F.B. Prinz, “*Thermal stresses and deposition patterns in layered manufacturing*”, Materials Science and Engineering, A317 (2001) pp. 59-64.
- [40] Dai, K., L. Shaw, “*Thermal and stress modeling of multi-material laser processing*”, Acta Materialia, 49 (2001) pp. 4171-4181.
- [41] Kahlen, J.K., A. Kar, “*Residual stresses in laser-deposited metal parts*”, Journal of Laser Applications, 13(2) (2001) pp. 60-69.
- [42] Vasinonta, A., J.L. Beuth,, M.L. Griffith, "Process maps for laser deposition of thin-walled structures", Proceedings 1999 Solid Freeform Fabrication Symposium, Austin, TX, USA, August 1999, ed. D.L. Bourell, *et al.*, pp. 383-391.
- [43] Vasinonta, A., J.L. Beuth,, M.L. Griffith, "Process maps for controlling residual stress and melt pool size in laser-based SFF processes", Proceedings 2000 Solid Freeform Fabrication Symposium, Austin, TX, USA, August 2000, ed. D.L. Bourell, *et al.*, pp. 383-391.
- [44] Labudovic, M., D. Hu, R. Kovacevic, “*A three dimensional model for direct laser metal powder deposition and rapid prototyping*”, Journal of Materials Science, 38(1) (2003) pp. 35-49.
- [45] Rosenthal, D., “*The theory of moving sources of heat and its application to metal treatments*”, Transactions ASME, 68 (1946) pp. 849-866.

- [46] Ashby, M.F., K.E. Easterling, "The transformation hardening of steel surfaces by laser beams – I. Hypo-eutectoid steels", Acta Metallurgica, 32 (1984) pp. 1935-1948.
- [47] Carvalho, P.A., A.M. Deus, R. Colaço, R. Vilar, "Laser alloying of zinc with aluminum: solidification behavior", Acta Materialia, 46 (1998) pp. 1781-1792.
- [48] Lindgren, L.E., "Finite element modeling and simulation of welding part I: increased complexity", Journal of Thermal Stresses, 24 (2001) pp. 141-192 (in particular, p. 161).
- [49] Kamala, V., J.A. Goldak, "Error due to two dimensional approximation in heat transfer analysis of welds", Welding Research Supplement, (September 1993) pp. 440s-446s.
- [50] Thilmany, J., "Making a mesh of things", Mechanical Engineering ASME, (September 2003) pp. 54-56.
- [51] Colaço, R., L. Costa, R. Guerra, R. Vilar, "A simple correlation between the geometry of laser cladding tracks and the process parameters", in *Laser Processing: Surface Treatments and Film Deposition*, ed. J. Mazumder *et al.*, Kluwer, Dordrecht, Netherlands, 1996, pp. 421-429.
- [52] Balagangadhar, D., G.A. Dorai, D.A. Tortorelli, "A displacement-based reference frame formulation for steady-state thermo-elasto-plastic material processes", International Journal of Solids and Structures, 36 (1999) pp. 2397-2416.
- [53] Choi, J., "Three dimensional transient finite element model for residual stress and solidification in the GMAW process for AISI 304 stainless steel", Ph.D. dissertation, University of Illinois at Urbana-Champaign, 1994.
- [54] Deus, A.M., R. Vilar, "One-dimensional thermal model including the dependence of absorptivity on temperature using Hagen-Rubens equation", in *Laser Processing: Surface Treatments and Film Deposition*, ed. J. Mazumder *et al.*, Kluwer, Dordrecht, Netherlands, 1996, pp. 195-201.
- [55] Noyan, I.C., T.C. Huang, B.R. York, "Residual stress/strain analysis in thin films by x-ray diffraction", Critical Reviews in Solid State and Materials Science, 20(2) (1995) pp. 125-177.

- [56] Mura, T., *Micromechanics of Defects in Solids*, 2nd ed. rev., Kluwer, Dordrecht, Netherlands, 1993 (in particular pp. 1, 217, 218, eq. 25.56 and 25.58).
- [57] *Metals Handbook*, vol. 2, ASM, Metals Park, OH, USA, 1990, pp. 161, 386.
- [58] Pao, Y. H., "*A nonlinear and time dependent finite element analysis of solder joints in surface mounted components under thermal cycling*", in *Materials Research Society Symposium. Proceedings*, vol. 226 (1991) p. 25.
- [59] Holt, John M., C.Y. Ho, eds., *Structural Alloys Handbook*, CINDAS/Purdue University, West Lafayette, IN, USA, 1996.
- [60] Otterloo, J.L.M., D. Bagnoli, J.T.M. De Hosson, "*Enhanced mechanical properties of laser treated Al-Cu alloys: a microstructural analysis*", *Acta Metallurgica et Materialia*, 43 (1995) pp. 2649-2656.
- [61] Touloukian, Y. S. *et al.*, *Thermophysical Properties of Matter*, vol. 12, IFI/Plenum, New York, NY, USA, 1975, pp. 77, 422, 658.
- [62] TAPP 2.2, *Database of Thermochemical and Physical Properties*, E. S. Microware Inc., Hamilton, OH, USA, 1995.
- [63] SAE Information Report, "*General information -chemical compositions, mechanical and physical properties of SAE aluminum casting alloys*", SAE J452 (January 89), pp. 10.10-10.11.
- [64] Touloukian, Y.S., Buyco, E.H., *Thermophysical Properties of Matter*, vol. 4, IFI/Plenum, New York, NY, USA, 1970, pp. 325, 513.
- [65] Poirier, D.R., G.H. Geiger, *Transport Phenomena in Materials Science*, TMS, Warrendale, PA, USA, 1994, p. 615.
- [66] Touloukian, Y.S. *et al.*, *Thermophysical Properties of Matter*, vol. 1, IFI/Plenum, New York, NY, USA, 1970, p. 533.
- [67] Incropera, F.P., D.P. DeWitt, *Fundamentals of Heat and Mass Transfer*, 4th. ed., Wiley, New York, USA, 1996, pp. 8, 851.
- [68] Hibbitt, Karlsson & Sorensen, Inc., *ABAQUS Standard Users' Manual and ABAQUS Theory Manual*, version 5.8, Pawtucket, RI, USA, 1998 (these manuals are also available online, along with AbaqusTM Standard, for version 6.3).
- [69] Alaca, B.E., M.T.A. Saif, H. Sehitoglu, "*On the interface debond at the edge of a thin film on a thick substrate*", *Acta Materialia*, 50 (2002) pp. 1197-1209.

Appendix A. Input file generator files

IFG for 2D temperature analysis

Value	Variable	comment	
			4
			5
7530	DEN	density of clad	6
0.0125	V	scanning speed	7
0.0002756	FEE	feed rate	8
			9
81.28	CA	contact angle IN DEG	10
1.418604	THE	contact angle IN RAD	11
			12
		auxiliary angular functions	13
1.165073	f	= cotan(THE) + sqrt(cotan^2(THE)+1)	14
1.178697	g	= (1+f^2)/2	15
			16
		important lengths	17
		(write form ula here)	18
0.001289	HC	= fHC	19
0.001502	S	= gHC	20
0.001519	R	= R -HC	21
0.000230	D	= R -HC	22
			23
			24
			25
c31		temperature file name	26
			27
1	NDX	node # increm . in x-direction	28
100	NDY	node # increm . in y-direction	29
20	NYS	# elements in y-dir. in substrate	30
20	NYC	# elements in y-dir. in clad	31
			32
			33
P1		name of point	34
101	NO	node # of origin	35
0.000000	XP1	x-coordinate of origin (must be 0)	36
0.000000	YP1	y-coordinate of origin (must be 0)	37
0.006670	HS	substrate height	38
			39
P2		name of point	40
2101	NP2	= NO + NYS NDY	41
0.0	XP2	= HS	42
0.006670	YP2	= HS	43
			44
0.001289	HC	= (calculated above)	45
2.00	TF1	translation factor	46
			47
P3		name of point	48
4101	NP3	= NO + (NYS + NYC) NDY	49
0.002578	XP3	= TF1 HC	50
0.007959	YP3	= HS + HC	51
			52
0.005000	DLP	initial clad length (section 1)	53
40	NX1	# elements in x-dir. in section 1	54
			55
P4		name of point	56
4141	NP4	= NO + (NYS + NYC) NDY + NX1 NDX	57
0.005000	XP4	= DLP	58
0.007959	YP4	= HS + HC	59
			60
0.001502	S	= (calculated above)	61
			62
			63
P5		name of point	64
2141	NP5	= NO + NYS NDY + NX1 NDX	65
0.006502	XP5	= S + DLP	66
0.006670	YP5	= YP2	67
			68
			69
			70
P6		name of point	71
141	NP6	= NO + NX1 NDX	72
0.006502	XP6	= XP5	73
0.000000	YP6		74
			75
			76
8	NI	# of element rows in the interface (NI < NYS	77
0.00052	DYI	interface depth	78

```

*HEADING
2D LASER CLADDING
**
** c31
**
**
**
** MESH GEN
**
** *NODE NSET= P1
101 , 0.000000 , 0.000000
**
**
** *NODE NSET= P2
2101 , 0.000000 , 0.006670
**
**
** *NODE NSET= P3
4101 , 0.002578 , 0.007959
**
**
** *NODE NSET= P4
4141 , 0.005000 , 0.007959
**
**
** *NODE NSET= P5
2141 , 0.006502 , 0.006670
**
**
** *NODE NSET= P6
141 , 0.006502 , 0.000000
**
**
**
**
**
**

```

P7 name of point
 1341 NP7 = NO + NX1 NDX + (NYS-NI)NDY
 0.006502 XP7 = XP5
 0.006150 YP7 = YP5 -DYI

P8 name of point
 1301 NP8 = NO + (NYS-NI)NDY
 0.000000 XP8 = XP2 = 0
 0.006150 YP8 = YP7

1 NDX = (given above)
 100 NDY = (given above)
 20 NYS = (given above)
 20 NYC = (given above)

100 NDY = (given above)
 P5 = (given above)
 ROT1 name of line
 19 NRO = NYC -1

0.000230 D = (given above)
 0.006670 HS = (given above)
 81.280000 CA = (given above)

0.005000 XR = XP4
 0.006440 YR = HS -D
 3.80 DTH element rotation, close to value below
 4.064000 DTH = CA /NYC

new node set ->
 previously defined node set(s) ->
 new node set ->
 previously defined node set(s) ->
 20 NYC = (given above)
 100 NDY = (given above)

new node set ->
 bias factor #1A
 previously defined node set(s) ->
 = NYS -NI
 1.50 B1A
 12 NDY = (given above)
 100

new node set ->
 = (given above)
 previously defined node set(s) ->
 = NYS -NI
 1.50 B1A
 12 NDY = (given above)
 100

new node set ->
 bias factor #1B
 previously defined node set(s) ->
 = NI
 1.00 B1B
 8 NDY = (given above)
 100

new node set ->
 bias factor #1B
 previously defined node set(s) ->
 = NI
 1.00 B1B
 8 NDY = (given above)
 100

new node set ->
 previously defined node set(s) ->
 new node set ->
 previously defined node set(s) ->

```

79 **
80 *NODE NSET=
81 1341 , 0.006502 , 0.006150
82 **
83 **
84 **
85 *NODE NSET=
86 1301 , 0.000000 , 0.006150
87 **
88 **
89 **
90 **
91 **
92 **
93 **
94 **
95 **
96 **
97 **
98 **
99 **
100 *NCOPI CHANGE NUMBER= 100  LDSET= P5
101 MULTIPLE= 19
102 **
103 **
104 **
105 **
106 **
107 **
108 0.0,0.
109 0.005000 , 0.006440 ,0.,
110 **
111 **
112 **
113 **
114 **
115 **
116 *NSET NSET=R 1
117 ROT1 P4 P5
118 *NFLL NSET=R 2
119 P2 P3 , 20 , 100
120 **
121 **
122 **
123 **
124 *NFLL NSET=R 3A BIAS= 1.50
125 **
126 P6 P7 , 12 , 100
127 **
128 **
129 **
130 **
131 *NFLL NSET=R 4A BIAS= 1.50
132 **
133 P1 P8 , 12 , 100
134 **
135 **
136 **
137 **
138 *NFLL NSET=R 3B BIAS= 1.00
139 **
140 P7 P5 , 8 , 100
141 **
142 **
143 **
144 *NFLL NSET=R 4B BIAS= 1.00
145 **
146 P8 P2 , 8 , 100
147 **
148 **
149 **
150 **
151 *NSET NSET=R 3
152 R 3A R 3B
153 **
154 **
155 *NSET NSET=R 4
156 R 4A R 4B
157 **
158 **
159 **
160 **
161 **
162 *NSET NSET=R 5
163 R 1 R 3
164 *NSET NSET=R 6
165 R 2 R 4

```

```

166 **
167 *NFILLNSET=S1,BIAS= 1.00
168 **
169 R6R5, 40, 1
170 **
171 **
172 **
173 **
174 **
175 *NCOPY CHANGE NUMBER = 40,OLDSET=R5,SHIFT NEW SET=R7
176 **
177 **
178 **
179 0.005000 DLB buildup chd length (section 2) 0.005000,0.
180 0.,0.,0.,0.,0.1,0.
181 **
182 **
183 *NFILLNSET=S2
184 R5R7, 40, 1
185 **
186 **
187 **
188 **
189 **
190 **
191 *NCOPY CHANGE NUMBER = 95,OLDSET=R6,SHIFT NEW SET=R8
192 **
193 **
194 **
195 0.050000 DLS substate length (section 1,2 & 3) 0.050000,0.
196 0.,0.,0.,0.,0.1,0.
197 **
198 **
199 *NFILLNSET=S3,BIAS= 0.60
200 **
201 R7R8, 15, 1
202 **
203 **
204 **
205 **
206 **
207 **
208 **
209 **
210 **
211 **
212 **
213 *NSET NSET=SUB,GENERATE
214 2101, 2196, 1
215 **
216 **
217 **
218 **
219 **
220 **
221 **
222 **
223 **
224 **
225 *NSET NSET=CLD,GENERATE
226 4101, 4196, 1
227 **
228 **
229 **
230 **
231 **
232 **
233 **
234 *NSET NSET=ALL
235 SUB CLD
236 *ELEMENT,TYPE=DC2D4
237 101, 101, 102, 202
238 **
239 **
240 **
241 **
242 **
243 **
244 2101, 2101, 2102, 2202
245 **
246 **
247 **
248 **

```

new node set->
1.00 B2 bias factor#2
previously defined node set(s) ->
40 NX1 = (given above)
1 NDX = (given above)
40 NX2 # elements in x-dir. in section 2
40 NR7 = NX2 NDX
previously defined node set(s) ->
new node set->
0.005000 DLB buildup chd length (section 2)
new node set->
40 NX2 = (given above)
1 NDX = (given above)
15 NX3 # elements in x-dir. in section 3
95 NR8 = (NX1 + NX2 + NX3) NDX
previously defined node set(s) ->
new node set->
0.050000 DLS substate length (section 1,2 & 3)
new node set->
0.60 B3 bias factor#3
previously defined node set(s) ->
15 NX3 = (given above)
1 NDX = (given above)

Cycle:	from	
0	to	
20	NYS	

20 STOP! <-status /current i
2101 NO + iNDY
2196 NO + iNDY + (NX1+NX2+NX3)NDX
1 NDX

Cycle:	from	
1	to	
20	NYC	

20 STOP! <-status /current i
4101 NO + (i+ NYS)NDY
4196 NO + (i+ NYS)NDY + (NX1+NX2+NX3)NDX ->
1 NDX

101 NO = (given above)
101 NO = (given above)
102 = NO + NDX
202 = NO + NDX + NDY
201 = NO + NDY

2101 NOC = NO + NDY NYS
2101 = NO + NDY NYS
2102 = NO + NDY NYS + NDX
2202 = NO + NDY NYS + NDX + NDY
2201 = NO + NDY NYS + NDY

101	NO	= (given above)	249	**			
95	NXT	= NX1 + NX2 + NX3	250	**			
1	NDX	= (given above)	251	**			
1	NDX	= (given above)	252	** #####			
20	NYS	= (given above)	253	** elementsets			
100	NDY	= (given above)	254	**			
100	NDY	= (given above)	255	** ELGEN ELSET=SUB			
			256	** 101 , 95 , 1 , 1			
			257	**			
			258	**			
			259	**			
			260	**			
			261	**			
			262	**			
			263	**			
			264	**			
			265	** ELGEN ELSET=CLD			
2101	NOC	= (given above)	266	** 2101 , 80 , 1 , 1			
80		= NX1 + NX2	267	**			
1	NDX	= (given above)	268	**			
1	NDX	= (given above)	269	**			
20	NYC	= (given above)	270	**			
100	NDY	= (given above)	271	**			
100	NDY	= (given above)	272	**			
			273	**			
			274	**			
2	NB	= # elem . in subst. before clcd buldup	275	**			
78	NC	= NX1 + NX2 -NB	276	** #####			
			277	**			
2001		= NO + (NYS-1)NDY	278	** ELSET ELSET=SUBU GENERATE			
2002		= NO + (NYS-1)NDY + (NB-1)NDX	279	** 2001 , 2002 , 1			
1		= NDX	280	** 2081 , 2095 , 1			
2081		= NO + (NYS-1)NDY + (NB+NC)NDX	281	**			
2095		= NO + (NYS-1)NDY + (NXT-1)NDX	282	**			
1		= NDX	283	**			
			284	**			
			285	**			
			286	**			
			287	**			
			288	**			
			289	**			
			290	** ELSET ELSET=SUBD GENERATE			
101		= NO	291	** 101 , 195 , 1			
195		= NO + (NXT-1)NDX	292	**			
1		= NDX	293	**			
			294	**			
			295	**			
			296	**			
			297	** ELSET ELSET=SUBW GENERATE			
101		= NO	298	** 101 , 2001 , 100			
2001		= NO + (NYS-1)NDY	299	**			
100		= NDY	300	**			
			301	**			
			302	**			
			303	**			
			304	** ELSET ELSET=SUBE GENERATE			
195		= NO + (NXT-1)NDX	305	** 195 , 2095 , 100			
2095		= NO + (NXT-1)NDX + (NYS-1)NDY	306	**			
100		= NDY	307	**			
			308	**			
			309	**			
			310	**			
			311	**			
			312	**			
			313	**			
			314	**			
			315	**			
1	OK	<-status /cument i	316	** ELSET ELSET=U 1 GENERATE			
2003		NO+(NYS-1)NDY+(NB+i-1)NDX	317	** 2003 , 2080 , 1			
2080		NO+(NYS-1)NDY+(NB+NC-1)NDX	318	**			
1		NDX	319	**			
			320	**			
			321	**			
			322	** ELSET ELSET=U 78			
78	NC	cument i	323	** 2080			
2080		NO+(NYS-1)NDY+(NB+i-1)NDX	324	**			
			325	**			
			326	**			
			327	**			
			328	** ELSET ELSET=E 2			
1		<-status /cument i\#1 ->	329	** 2103			
2103		NO+NYS NDY+(NB+i-1)NDX	330	**			
			331	**			

Cycle:	from	to
1	NI	
8		


```

8 STOP! <-status /cument i
1303 NO+(NYS-iNDY+NB NDX
1381 NO+(NYS-iNDY+(NB+NC NDX
1 NDX

```

Cycle:	from	to
1	NI	
8		


```

8 STOP! <-status /cument i
1301 NO+(NYS-iNDY
1302 NO+(NYS-iNDY+(NB-1 NDX
1 NDX
1382 NO+(NYS-iNDY+(NB+NC+1 NDX
1395 NO+(NYS-iNDY+(NXT-1 NDX
1 NDX

```

Cycle:	from	to
9	NYS	
20		


```

20 STOP! <-status /cument i
101 NO+(NYS-iNDY
195 NO+(NYS-iNDY+(NXT-1 NDX
1 NDX

```

```

insertproperties ->

```



```

0.1 STI pre-heating time
0.001 XL inserts initialx-coordinate
0.0125 V (given above)
0.001502 S (given above)
0.005000 DLP (given above)
2 NB (given above)
40 NX1 (given above)

```

```

410 **
411 **
412 **
413 **
414 **
415 **
416 *ELSET,ELSET=INT,GENERATE
417 1303 , 1381 , 1
418 **
419 **
420 **
421 **
422 **
423 **
424 **
425 **
426 **
427 **
428 **
429 **
430 **
431 *ELSET,ELSET=BAS,GENERATE
432 1301 , 1302 , 1
433 **
434 **
435 1382 , 1395 , 1
436 **
437 **
438 **
439 **
440 **
441 **
442 **
443 **
444 **
445 **
446 **
447 *ELSET,ELSET=BAS,GENERATE
448 101 , 195 , 1
449 **
450 **
451 **
452 **
453 **
454 **
455 ** *****
456 **
457 **
458 **
459 *PHYSICAL CONSTANTS, ABSOLUTE ZERO = -273.
460 *INITIAL CONDITIONS, TYPE=TEMPERATURE
461 SUB 27.
462 CLD 27.
463 **INITIAL CONDITIONS, TYPE=MASS FLOW RATE
464 **SUB ,75.42
465 **CLD ,49.25
466 **MATERIALS PROPERTIES
467 **
468 *SOLID SECTION, ELSET=BAS, MATERIAL=ALBAS
469 *SOLID SECTION, ELSET=INT, MATERIAL=INTER
470 *SOLID SECTION, ELSET=CLD, MATERIAL=CUBAS
471 **
472 ** insertproperties
473 **
474 *RESTART WRITE FREQUENCY=1000
475 **
476 **
477 ** *****
478 **
479 **
480 **
481 **
482 **
483 **
484 **
485 **
486 **
487 **
488 **
489 **

```

10000 MNI maximum # of increments
 200. DMX temperature tolerance
 0.000001 DTN initial time increment
 0.046006 = STB (NB (DLP+S)(NX1)-XIL)/V

```

490 **-----BEGINNING OF STEP 1-----
491 *STEP,NC= 10000
492 *HEAT TRANSFER DELTM X= 200.
493 0.000001 , 0.046006
494 *MODEL CHANGE REMOVE
495 CLD
496 **
497 **FFFFFFFFFFFFFFFFFFFFFFFFFFFFFFF
498 ** F
499 *FILM OP=NEW
500 **SUBD:reduced heat loss due to
501 **contact with ground
502 SUBD F1,27,.1.
503 SUBU F3,27,.10.
504 SUBW F4,27,.10.
505 SUBE F2,27,.10.
506 **
507 U1 F3,27,.10.
508 ** F
509 **FFFFFFFFFFFFFFFFFFFFFFFFFFFFFFF
510 **
511 **
512 **RRRRRRRRRRRRRRRRRRRRRRRRRRRRRRRRRR
513 ** R
514 *RAD RATE OP=NEW
515 SUBU R3,27,.0.2268E-8
516 SUBW R4,27,.0.2268E-8
517 SUBE R2,27,.0.2268E-8
518 **
519 U1 R3,27,.0.2268E-8
520 ** R
521 **RRRRRRRRRRRRRRRRRRRRRRRRRRRRRRRRRR
522 **
523 **SSSSSSSSSSSSSSSSSSSSSSSSSSSSSSSSSS
524 ** S
525 *DFLUX OP=NEW
526 SUBU S3NU
527 **
528 U1 S3NU
529 ** S
530 **SSSSSSSSSSSSSSSSSSSSSSSSSSSSSSSSSS
531 **
532 **OUTPUT
533 *NODE FILE
534 NT
535 *NODE PRINT,FREQUENCY=0
536 *EL PRINT,FREQUENCY=0
537 **
538 *END STEP
539 **-----END OF STEP 1-----
540 **
541 **#####
542 **
543 **
544 **
545 **
546 **
547 **
548 **
549 **
550 **
551 **
552 **-----BEGINNING OF STEP 2-----
553 *STEP,NC= 10000
554 *HEAT TRANSFER DELTM X= 200.
555 0.000001 , 0.013003
556 *MODEL CHANGE ADD
557 E 2 , V 2
558 **
559 **FFFFFFFFFFFFFFFFFFFFFFFFFFFFFFF
560 ** F
561 *FILM OP=NEW
562 **SUBD:reduced heat loss due to
563 **contact with ground
564 SUBD F1,27,.1.
565 SUBU F3,27,.10.
566 SUBW F4,27,.10.
567 SUBE F2,27,.10.
568 **
569 U 2 F3,27,.10.
570 V 2 F3,27,.10.
571 E 2 F2,27,.100.
572 W 2 F4,27,.10.
573 **En:enhanced heat transfer due to
574 **shielding gas

```

40 NX2 (given above)
 0.005000 DLB (given above)

Cycle:	from
2	to
21	NYC+1

2 OK <- status /step number
 10000 MNI (given above)
 200. DMX (given above)
 0.000001 DTN (given above)
 0.013003 = (DLP+S)/(NX1 V)

Cycle:	from	
22	NYC+2	
39	NX1-NB+1	

19	OK	<- status /step number
10000	MNI	(given above)
200.	DMX	(given above)
0.000001	DTN	(given above)
0.013003		= (DLP+S)/(NX1 V)

```

575 **
576 **           F
577 **FFFFFFFFFFFFFFFFFFFFFFFFFFFF
578 **
579 **
580 **RRRRRRRRRRRRRRRRRRRRRRRRRRR
581 **           R
582 *RADATE,OP=NEW
583 SUBU R3,27,.0.2268E-8
584 SUBW R4,27,.0.2268E-8
585 SUBE R2,27,.0.2268E-8
586 **
587 U           2           R3,27,.0.2268E-8
588 V           2           R3,27,.0.2268E-8
589 E           2           R2,27,.0.2268E-8
590 W           2           R4,27,.0.2268E-8
591 **           R
592 **RRRRRRRRRRRRRRRRRRRRRRRRRRR
593 **
594 **SSSSSSSSSSSSSSSSSSSSSSSSSSSS
595 **           S
596 *DFLUX,OP=NEW
597 SUBU S3NU
598 **
599 U           2           S3NU
600 V           2           S3NU
601 E           2           S2NU
602 W           2           S4NU
603 **           S
604 **           S
605 **SSSSSSSSSSSSSSSSSSSSSSSSSSSS
606 **
607 **OUTPUT
608 *NODE FILE
609 NT
610 *NODE PRINT,FREQUENCY=0
611 *EL PRINT,FREQUENCY=0
612 **
613 *END STEP
614 **-----END OF STEP
615 **
616 **#####
617 **
618 **
619 **-----BEGINNING OF STEP
620 **
621 **
622 **
623 **-----BEGINNING OF STEP
624 *STEP,NC= 10000
625 *HEAT TRANSFER DELTMX= 200.
626           0.000001 ,           0.013003
627 *MODEL CHANGE ADD
628 E           19
629 **
630 **FFFFFFFFFFFFFFFFFFFFFFFFFFFF
631 **           F
632 *FILM,OP=NEW
633 **SUBD: reduced heat loss due to
634 **contact with ground
635 SUBD F1,27,.1.
636 SUBU F3,27,.10.
637 SUBW F4,27,.10.
638 SUBE F2,27,.10.
639 **
640 U           19           F3,27,.10.
641 V           19           F3,27,.10.
642 E           19           F2,27,.100.
643 W           19           F4,27,.10.
644 **En: enhanced heat transfer due to
645 **shielding gas
646 **
647 **           F
648 **FFFFFFFFFFFFFFFFFFFFFFFFFFFF
649 **
650 **
651 **RRRRRRRRRRRRRRRRRRRRRRRRRRR
652 **           R
653 *RADATE,OP=NEW
654 SUBU R3,27,.0.2268E-8
655 SUBW R4,27,.0.2268E-8
656 SUBE R2,27,.0.2268E-8
657 **
658 U           19           R3,27,.0.2268E-8
659 V           19           R3,27,.0.2268E-8
660 E           19           R2,27,.0.2268E-8
661 W           19           R4,27,.0.2268E-8
662 **           R
663 **RRRRRRRRRRRRRRRRRRRRRRRRRRR

```

Cycle:		from	
40	NX1-NB+2		NX1-NB+2
78	NX1+NX2-NB		NX1+NX2-NB

38	OK	<- status / step number
10000	MNI	(given above)
200.	DMX	(given above)
0.000001	DTN	(given above)
0.010000		= DLB/(NX2 V)

```

664 **
665 **SSSSSSSSSSSSSSSSSSSSSSSSSSSSSSSSSS
666 ** S
667 *DFLUX,OP=NEW
668 SUBU,S3NU
669 **
670 U 19 S3NU
671 V 19 S3NU
672 E 19 S2NU
673 W 19 S4NU
674 ** S
675 ** S
676 **SSSSSSSSSSSSSSSSSSSSSSSSSSSSSSSSSS
677 **
678 **OUTPUT
679 *NODE FILE
680 NT
681 *NODE PRINT,FREQUENCY=0
682 *EL PRINT,FREQUENCY=0
683 **
684 *END STEP
685 **-----END OF STEP 19
686 **
687 *#####
688 **
689 **
690 **
691 **
692 **
693 **
694 **
695 **
696 **-----BEGINNING OF STEP 38
697 *STEP,NC= 10000
698 *HEAT TRANSFER DELTMX= 200.
699 * 0.000001 , 0.010000
700 *MODEL CHANGE,ADD
701 E 38
702 **
703 *FFFFFFFFFFFFFFFFFFFFFFFFFFFFFF
704 ** F
705 *FILM,OP=NEW
706 **SUBD:reduced heat loss due to
707 ** contact with ground
708 SUBD,F1,27,.1.
709 SUBU,F3,27,.10.
710 SUBW,F4,27,.10.
711 SUBE,F2,27,.10.
712 **
713 U 38 F3,27,.10.
714 V 38 F3,27,.10.
715 E 38 F2,27,.100.
716 W 38 F4,27,.10.
717 **En:enhanced heat transfer due to
718 ** shielding gas
719 **
720 ** F
721 *FFFFFFFFFFFFFFFFFFFFFFFFFFFFFF
722 **
723 **
724 **RRRRRRRRRRRRRRRRRRRRRRRRRRRRRRRRR
725 ** R
726 *RATE,OP=NEW
727 SUBU,R3,27,.0.2268E-8
728 SUBW,R4,27,.0.2268E-8
729 SUBE,R2,27,.0.2268E-8
730 **
731 U 38 R3,27,.0.2268E-8
732 V 38 R3,27,.0.2268E-8
733 E 38 R2,27,.0.2268E-8
734 W 38 R4,27,.0.2268E-8
735 ** R
736 **RRRRRRRRRRRRRRRRRRRRRRRRRRRRRRRRR
737 **
738 **SSSSSSSSSSSSSSSSSSSSSSSSSSSSSSSSSS
739 ** S
740 *DFLUX,OP=NEW
741 SUBU,S3NU
742 **
743 U 38 S3NU
744 V 38 S3NU
745 E 38 S2NU
746 W 38 S4NU
747 ** S
748 ** S
749 **SSSSSSSSSSSSSSSSSSSSSSSSSSSSSSSSSS

```


IFG for 3D temperature analysis

Value	Variable	Comment	
			4
			5
7690	DEN	density of clad	6
0.0125	V	scanning speed	7
0.0002815	FEE	feed rate	8
			9
81.28	CA	contact angle N DEG	10
1.418604	THE	contact angle N RAD	11
			12
		auxiliary angular functions	13
1.165073	f	= cotan(THE) + sqrt(cotan^2(THE)+1)	14
1.178697	g	= (1+f^2)/2	15
			16
		important lengths	17
0.001289	HC	= SQRT(FEE/DEN*V)/(PSQRT(g/g-FEE)+g/g*SIN(Eg)*2*(1-g))	18
0.001502	S	= f*HC	19
0.001519	R	= g*HC	20
0.000230	D	= R -HC	21
			22
			23
			24
			25
			26
			27
			28
			29
			30
			31
			32
			33
			34
			35
			36
			37
			38
			39
			40
			41
			42
			43
			44
			45
			46
			47
			48
			49
			50
			51
			52
			53
			54
			55
			56
			57
			58
			59
			60
			61
			62
			63
			64
			65
			66
			67
			68
			69
			70
			71
			72
			73
			74
			75
			76
			77
			78
			79
			80
			81
			82
			83
			84
			85
			86
			87


```

180 **
181 **
182 **
183 **
184 **
185 **
186 **
187 **
188 **
189 **
190 **
191 **
192 **
193 **
194 **
195 **
196 **
197 **
198 **
199 **
200 **
201 **
202 **
203 **
204 **
205 **
206 **
207 **
208 **
209 **
210 **
211 **
212 **
213 **
214 **
215 **
216 **
217 **
218 **
219 **
220 **
221 **
222 **
223 **
224 **
225 **
226 **
227 **
228 **
229 **
230 **
231 **
232 **
233 **
234 **
235 **
236 **
237 **
238 **
239 **
240 **
241 **
242 **
243 **
244 **
245 **
246 **
247 **
248 **
249 **
250 **
251 **
252 **
253 **
254 **
255 **
256 **
257 **
258 **
259 **
260 **
261 **
262 **
263 **
264 **
265 **
266 **
267 **
268 **
269 **

```

Cycle:	from	to
1	1	5
5	NYC	

```

1 OK <-status /current i
10701 NO + (i+ NYS)NDY
10721 NO + (i+ NYS)NDY + (NX1+NX2)NDX ->
1 NDX

```

```

5 NZC number of layers in clad in zz direction
10000 NDZ = (given above)
CLD = (given above)
ROT2 name of new set
4 NRP = NZC -1
0.000000 XP2 = (given above)
0.006670 YP2 = (given above)
0.000000 ZP2 = (given above)
0.006502 XP5 = (given above)
0.006670 YP5 = (given above)
0.000000 ZP5 = (given above)
18.00 DT2 elem entarotation, cbse to value below
18.000 DT2 = CA / NYC

```

```

new node set ->
previously defined node set(s) ->

```

Cycle:	from	to
1	1	5
5	NYC	

```

1 OK <-status /current i
10701 NO + (i+ NYS)NDY
10721 NO + (i+ NYS)NDY + (NX1+NX2)NDX ->
1 NDX = (given above)

```

Cycle:	from	to
1	1	5
5	NYC	

```

1 OK <-status /current i
9900 i (NDZ -NDY)
0.000000 XP2 = (given above)
0.006670 YP2 = (given above)
0.000000 ZP2 = (given above)
0.006502 XP5 = (given above)
0.006670 YP5 = (given above)
0.000000 ZP5 = (given above)

```

Cycle:	from	to
1	1	5
5	NYC	

```

5 STOP! <-status /current i
500 NYS NDY
0.006670 HS = (given above)
2.30 BIL = (given above)
5 NYS = (given above)
100 NDY = (given above)
5 NZS number of layers in subst in zz direction
100000 = NDZ (NZS + NZC)
0.007500 DW S Substrate half width

```



```

362 **
363 **
364 ** #####
365 **      elementsets
366 **
367 *ELGEN ELSET=SB
368   10101 ,          25 ,          1 ,          1
369 **
370 **
371 **
372 **
373 **
374 **
375 **
376 **
377 **
378 **
379 **
380 **
381 **
382 *ELGEN ELSET=CD1
383   10701 ,          20 ,          1 ,          1
384 **
385 **
386 **
387 **
388 **
389 **
390 **
391 **
392 **
393 **
394 **
395 **
396 **
397 **
398 **
399 **
400 **
401 *ELEMENT,TYPE=DC3D8
402 **
403   20601 ,          20601 ,          20602 ,          50702
404 **
405 **
406 **
407 **
408 **
409 **
410 **
411 **
412 **
413 *ELEMENT,TYPE=DC3D6
414   101 ,          10601 ,          50701 ,          20601
415 **
416 **
417 **
418 **
419 **
420 **
421 **
422 **
423 **
424 **
425 **
426 **
427 **
428 **
429 **
430 **
431 **
432 **
433 **
434 **
435 **
436 **
437 **
438   201 ,          10601 ,          40701 ,          50701
439 **
440 **
441 **
442 **
443 **
444 **
445 **
446 **
447 **
448 **
449 **

```

10101 NO = (given above)
25 NXT = NX1 + NX2 + NX3
1 NDX = (given above)
1 NDX = (given above)
5 NYS = (given above)
100 NDY = (given above)
100 NDY = (given above)
10 = NZS + NZC
10000 NDZ = (given above)
10000 NDZ = (given above)

10701 NOC = (given above)
20 = NX1 + NX2
1 NDX = (given above)
1 NDX = (given above)
4 = NYC -1
100 NDY = (given above)
100 NDY = (given above)
4 = NZC -1
10000 NDZ = (given above)
10000 NDZ = (given above)

Cycle:	from	
	2	to
	5	NZC

2 OK <-status /current i

20601 = NO + NDY NYS + NDZ (i-1)
20601 = NO + NDY NYS + NDZ (i-1)
20602 = NO + NDY NYS + NDZ (i-1) + NDX
50702 = NO + NDY (NYS+i-1) + NDZ (NZC-1) + NDX
50701 = NO + NDY (NYS+i-1) + NDZ (NZC-1)
30601 = NO + NDY NYS + NDZ i
30602 = NO + NDY NYS + NDZ i + NDX
50802 = NO + NDY (NYS+i) + NDZ (NZC-1) + NDX
50801 = NO + NDY (NYS+i) + NDZ (NZC-1)

101 NOO
10601 = NO + NDY NYS
50701 = NO + NDY (NYS+1) + NDZ (NZC-1)
20601 = NO + NDY NYS + NDZ
10602 = NO + NDY NYS + NDX
50702 = NO + NDY (NYS+1) + NDZ (NZC-1) + NDX
20602 = NO + NDY NYS + NDX + NDZ

362 **
363 **
364 ** #####
365 ** elementsets
366 **
367 *ELGEN ELSET=SB
368 10101 , 25 , 1 , 1
369 **
370 **
371 **
372 **
373 **
374 **
375 **
376 **
377 **
378 **
379 **
380 **
381 **
382 *ELGEN ELSET=CD1
383 10701 , 20 , 1 , 1
384 **
385 **
386 **
387 **
388 **
389 **
390 **
391 **
392 **
393 **
394 **
395 **
396 **
397 **
398 **
399 **
400 **
401 *ELEMENT,TYPE=DC3D8
402 **
403 20601 , 20601 , 20602 , 50702
404 **
405 **
406 **
407 **
408 **
409 **
410 **
411 **
412 **
413 *ELEMENT,TYPE=DC3D6
414 101 , 10601 , 50701 , 20601
415 **
416 **
417 **
418 **
419 **
420 **
421 **
422 **
423 **
424 **
425 **
426 **
427 **
428 **
429 **
430 **
431 **
432 **
433 **
434 **
435 **
436 **
437 **
438 201 , 10601 , 40701 , 50701
439 **
440 **
441 **
442 **
443 **
444 **
445 **
446 **
447 **
448 **
449 **

Cycle: from		450	**
2	to	451	**
5	NZC	452	**
2 OK <-status /cument i		453	**
20601 = NO + NDY NYS + NDZ (i1)		454	**
20 = NX1 + NX2		455	**
1	NDX = (given above)	456	*ELGEN_ELSET=CD
1	NDX = (given above)	457	20601 , 2 , 1 , 1
		458	**
		459	**
		460	**
		461	**
		462	**
		463	**
Cycle: from		464	**
1	to	465	**
5	NZC	466	**
5 STOP! <-status /cument i		467	**
501 = NOO + (i1)NDY		468	**
20 NXT = NX1 + NX2		469	*ELGEN_ELSET=CT
1	NDX = (given above)	470	501 , 5 , 1 , 1
1	NDX = (given above)	471	**
		472	**
		473	**
		474	**
		475	**
		476	**
Cycle: from		477	**
1	to	478	**
5	NZC	479	**
1 OK <-status /cument i		480	**
		481	**
		482	*ELSET_ELSET=CD
		483	CD , 1 , CT , 1
		484	**
		485	**
		486	**
		487	**
		488	**
		489	**
		490	**
		491	**
		492	**
		493	**
		494	**
		495	**
2	NB = # elem . in subst. before cad buildup	496	**
18	NC = NX1 + NX2 -NB	497	**#####
		498	**
		499	*ELSET , ELSET=SUBU , GENERATE
10501	= NO + (NYS-1)NDY	500	
10502	= NO + (NYS-1)NDY + (NB-1)NDX	501	SUBU See file"Elemsets3"
1	= NDX	502	Un See file"Elemsets3"
10521	= NO + (NYS-1)NDY + (NB+NC)NDX	503	SUBD See file"Elemsets4"
10525	= NO + (NYS-1)NDY + (NXT-1)NDX	504	SUBN See file"Elemsets4"
1	= NDX	505	SUBS See file"Elemsets4"
		506	SUBE See file"Elemsets4"
		507	SUBW See file"Elemsets4"
		508	**
		509	**
		510	**
		511	*ELSET , ELSET=SUBD , GENERATE
10101	= NO	512	**
10125	= NO + (NXT-1)NDX	513	**
1	= NDX	514	**
		515	**
		516	**
		517	**
		518	*ELSET , ELSET=SUBW , GENERATE
10101	= NO	519	**
10501	= NO + (NYS-1)NDY	520	**
100	= NDY	521	**
		522	**
		523	**
		524	**
		525	*ELSET , ELSET=SUBE , GENERATE
10125	= NO + (NXT-1)NDX	526	**
10525	= NO + (NXT-1)NDX + (NYS-1)NDY	527	**
100	= NDY	528	**
		529	**
		530	**
Cycle: from		531	**
1	to	532	**
17	NC-1	533	**
		534	**
		535	**

17	STOP!	<-status /currenti	536	**			
10519		NO+NYS-1NDY+NB+i1NDX	537	*ELSET,ELSET=U	17	GENERATE	
10520		NO+NYS-1NDY+NB+NC-1NDX	538				
1		NDX	539	**			
			540	**			
			541	**			
			542	**			
18	NC	currenti	543	*ELSET,ELSET=U	18		
10520		NO+NYS-1NDY+NB+i1NDX	544				
			545	**			
			546	**			
			547	**			
			548	**			
1		<-status /currenti\i1 ->	549	*ELSET ELSET=E	2		
10603		NO+NYS NDY+NB+i1NDX	550	10603			
			551	**			
			552	**			
			553	**			
			554	**			
			555	**			
			556	**			
5	STOP!	<-status /currenti\i1 ->	557	*ELSET ELSET=E	6	GENERATE	
10607		NO+NYS NDY+NB+i1NDX	558	10607 ,	11007 ,	100	
11007		NO+NYS NDY+NB+i1NDX+(i1NDY	559	**			
100		NDY	560	**			
			561	**			
			562	**			
			563	**			
			564	**			
			565	**			
			566	**			
18	STOP!	<-status /currenti\i1 ->	567	*ELSET ELSET=E	19	GENERATE	
10620		NO+NYS NDY+NB+i1NDX	568	10620 ,	11020 ,	100	
11020		NO+NYS NDY+NB+i1NDX+(NYC-1NDY	569	**			
100		NDY	570	**			
			571	**			
			572	**			
			573	**			
			574	**			
			575	**			
			576	**			
1		<-status /currenti\i1 ->	577	*ELSET ELSET=V	2		
10603		NO+NYS+i1NDY+NBNDX	578	10603			
			579	**			
			580	**			
			581	**			
			582	**			
			583	**			
			584	**			
5	STOP!	<-status /currenti\i1 ->	585	*ELSET ELSET=V	6	GENERATE	
11003		NO+NYS+i1NDY+NBNDX	586	11003 ,	11007 ,	1	
11007		NO+NYS+i1NDY+NB+i1NDX	587	**			
1		NDX	588	**			
			589	**			
			590	**			
			591	**			
			592	**			
			593	**			
			594	**			
7	OK	<-status /currenti\i1 ->	595	*ELSET ELSET=V	8	GENERATE	
11003		NO+NYS+NYC-1NDY+NBNDX	596	11003 ,	11009 ,	1	
11009		NO+NYS+NYC-1NDY+NB+i1NDX	597	**			
1		NDX	598	**			
			599	**			
			600	**			
			601	**			
			602	**			
1		<-status /currenti\i1 ->	603	*ELSET ELSET=W	2		
10603		NO+NYS NDY+NBNDX	604	10603			
			605	**			
			606	**			
			607	**			
			608	**			
			609	**			
			610	**			
5	STOP!	<-status /currenti\i1 ->	611	*ELSET ELSET=W	6	GENERATE	
10603		NO+NYS NDY+NBNDX	612	10603 ,	11003 ,	100	
11003		NO+NYS+I1NDY+NBNDX	613	**			
100		NDY	614	**			
			615	**			
			616	**			
			617	**			
			618	**			
			619	**			
			620	**			
6	OK	<-status /currenti\i1 ->	621	*ELSET ELSET=W	7	GENERATE	
10603		NO+NYS NDY+NBNDX	622	10603 ,	11003 ,	100	
11003		NO+NYS+NYC-1NDY+NBNDX	623	**			
100		NDY	624	**			

	625	**
	626	**
2 NI # of elem entrows in the interface (NI< NYS)	627	**
	628	**
	629	**
	630	**
Cycle: from	631	**
1 to	632	**
2 NI	633	**
	634	**
	635	**
	636	**
2 STOP! <-status /current i	637	**ELSET ELSET=NT,GENERATE
10403 NO + (NYS -iNDY+NB NDX	638	10403 , 10421 , 1
10421 NO + (NYS -iNDY+NB+NC NDX	639	**
1 NDX	640	**
	641	**
	642	**
	643	**
	644	**
	645	**
Cycle: from	646	**
1 to	647	**
2 NI	648	**
	649	**
	650	**
	651	**
2 STOP! <-status /current i	652	**ELSET ELSET=BAS,GENERATE
10401 NO + (NYS -iNDY	653	10401 , 10402 , 1
10402 NO + (NYS -iNDY+NB-1 NDX	654	**
1 NDX	655	**
10422 NO + (NYS -iNDY+NB+NC+1 NDX	656	10422 , 10425 , 1
10425 NO + (NYS -iNDY+NB+NC+1 NDX	657	**
1 NDX	658	**
	659	**
	660	**
	661	**
Cycle: from	662	**
3 to	663	**
5 NYS	664	**
	665	**
	666	**
	667	**
5 STOP! <-status /current i	668	**ELSET ELSET=BAS,GENERATE
10101 NO + (NYS -iNDY	669	10101 , 10125 , 1
10125 NO + (NYS -iNDY+NB-1 NDX	670	**
1 NDX	671	**
	672	**
	673	**
	674	**
	675	**
	676	** #####
	677	**
	678	**
	679	**
	680	**PHYSICAL CONSTANTS,ABSOLUTE ZERO=-273.
	681	**INITIAL CONDITDNS,TYPE=TEMPERATURE
	682	SUB,27.
	683	CLD,27.
	684	**INITIAL CONDITDNS,TYPE=MASS FLOW RATE
	685	**SUB,-75.42
	686	**CLD,-49.25
	687	**MATERIALS PROPERTIES
	688	**
	689	**SOLD SECTDN ELSET=BAS MATERIAL=ALBAS
	690	**SOLD SECTDN ELSET=INT MATERIAL=INTER
	691	**SOLD SECTDN ELSET=CLD MATERIAL=CUBAS
	692	**
	693	** insertproperties
	694	**
	695	**RESTART WRITE FREQUENCY=10
	696	**
	697	**
	698	** #####
	699	**
	700	**
	701	**
0.1 STI pre-heating time	702	**
0.001 XIL users initial-coordinate	703	**
0.0125 V (given above)	704	**
0.001502 S (given above)	705	**
0.005000 DLP (given above)	706	**
2 NB (given above)	707	**
10 NX1 (given above)	708	**
	709	**
	710	**

10000 MNI maximum # of increments
 200. DMX temperature tolerance
 0.000001 DTN initial increment
 0.124027 = STP (NB (DLP+S)/(NX1)-XL)/V

```

711 ** -----BEGINNING OF STEP 1 -----
712 *STEP ,NC= 10000
713 *HEAT TRANSFER DELTMAX= 200.
714 0.000001 , 0.124027
715 *MODEL CHANGE REMOVE
716 CLD
717 **
718 **FFFFFFFFFFFFFFFFFFFFFFFFFFFFFF
719 ** F
720 *FILM OP=NEW
721 ** SUBD : reduced heat loss due to
722 ** contact with ground
723 SUBD F1,27,.1.
724 SUBU F3,27,.10.
725 SUBW F4,27,.10.
726 SUBE F2,27,.10.
727 **
728 U1 F3,27,.10.
729 ** F
730 **FFFFFFFFFFFFFFFFFFFFFFFFFFFFFF
731 **
732 **
733 **RRRRRRRRRRRRRRRRRRRRRRRRRRRRRRRRRR
734 ** R
735 *RADATE OP=NEW
736 SUBU R3,27,.0.2268E-8
737 SUBW R4,27,.0.2268E-8
738 SUBE R2,27,.0.2268E-8
739 **
740 U1 R3,27,.0.2268E-8
741 ** R
742 **RRRRRRRRRRRRRRRRRRRRRRRRRRRRRRRRRR
743 **
744 **SSSSSSSSSSSSSSSSSSSSSSSSSSSSSSSSSS
745 ** S
746 *DFLUX OP=NEW
747 SUBU S3NU
748 **
749 U1 S3NU
750 ** S
751 **SSSSSSSSSSSSSSSSSSSSSSSSSSSSSSSSSS
752 **
753 **OUTPUT
754 *NODE FILE
755 NT
756 *NODE PRINT,FREQUENCY=0
757 *EL PRINT,FREQUENCY=0
758 **
759 *END STEP
760 ** -----END OF STEP 1 -----
761 **
762 **#####
763 **
764 **
765 **
766 **
767 **
768 **
769 **
770 **
771 **
772 **
773 ** -----BEGINNING OF STEP 9 -----
774 *STEP ,NC= 10000
775 *HEAT TRANSFER DELTMAX= 200.
776 0.000001 , 0.052014
777 *MODEL CHANGE ADD
778 E 9 , V 9
779 **
780 **FFFFFFFFFFFFFFFFFFFFFFFFFFFFFF
781 ** F
782 *FILM OP=NEW
783 ** SUBD : reduced heat loss due to
784 ** contact with ground
785 SUBD F1,27,.1.
786 SUBU F3,27,.10.
787 SUBW F4,27,.10.
788 SUBE F2,27,.10.
789 **
790 U 9 F3,27,.10.
791 V 9 F3,27,.10.
792 E 9 F2,27,.100.
793 W 9 F4,27,.10.
794 ** En: enhanced heat transfer due to
795 ** shielding gas
796 **
797 ** F
798 **FFFFFFFFFFFFFFFFFFFFFFFFFFFFFF
799 **
800 **

```

10 NX2 (given above)
 0.005000 DLB (given above)

Cycle:	from
2	to
6	NYC+1

9 STOP ! <- status / step number
 10000 MNI (given above)
 200. DMX (given above)
 0.000001 DTN (given above)
 0.052014 = (DLP+S)/(NX1 V)

```

801 **RRRRRRRRRRRRRRRRRRRRRRRRRRRRRRRRRRRR
802 ** R
803 *RADATE,OP=NEW
804 SUBU R 3,27,.0,2268E-8
805 SUBW R 4,27,.0,2268E-8
806 SUBE R 2,27,.0,2268E-8
807 **
808 U 9 R 3,27,.0,2268E-8
809 V 9 R 3,27,.0,2268E-8
810 E 9 R 2,27,.0,2268E-8
811 W 9 R 4,27,.0,2268E-8
812 ** R
813 **RRRRRRRRRRRRRRRRRRRRRRRRRRRRRRRRRRRR
814 **
815 **SSSSSSSSSSSSSSSSSSSSSSSSSSSSSSSSSSSS
816 ** S
817 *DFLUX,OP=NEW
818 SUBU S3NU
819 **
820 U 9 S3NU
821 V 9 S3NU
822 E 9 S2NU
823 W 9 S4NU
824 ** S
825 ** S
826 **SSSSSSSSSSSSSSSSSSSSSSSSSSSSSSSSSSSS
827 **
828 **OUTPUT
829 *NODE FILE
830 NT
831 *NODE PRINT,FREQUENCY=0
832 *EL PRINT,FREQUENCY=0
833 **
834 *END STEP
835 **-----END OF STEP 9-----
836 **
837 **#####
838 **
839 **
840 **
841 **
842 **
843 **
844 **-----BEGINNING OF STEP 9-----
845 *STEP,NC= 10000
846 *HEAT TRANSFER DELTMX= 200.
847 0.000001, 0.052014
848 *MODEL CHANGE ADD
849 E 9
850 **
851 **FFFFFFFFFFFFFFFFFFFFFFFFFFFFFFFF
852 ** F
853 *FILM,OP=NEW
854 **SUBD: reduced heat loss due to
855 **contact with ground
856 SUBD F1,27,.1.
857 SUBU F 3,27,.10.
858 SUBW F 4,27,.10.
859 SUBE F 2,27,.10.
860 **
861 U 9 F 3,27,.10.
862 V 9 F 3,27,.10.
863 E 9 F 2,27,.100.
864 W 9 F 4,27,.10.
865 **En: enhanced heat transfer due to
866 **shielding gas
867 **
868 ** F
869 **FFFFFFFFFFFFFFFFFFFFFFFFFFFFFFFF
870 **
871 **
872 **RRRRRRRRRRRRRRRRRRRRRRRRRRRRRRRRRRRR
873 ** R
874 *RADATE,OP=NEW
875 SUBU R 3,27,.0,2268E-8
876 SUBW R 4,27,.0,2268E-8
877 SUBE R 2,27,.0,2268E-8
878 **
879 U 9 R 3,27,.0,2268E-8
880 V 9 R 3,27,.0,2268E-8
881 E 9 R 2,27,.0,2268E-8
882 W 9 R 4,27,.0,2268E-8
883 ** R
884 **RRRRRRRRRRRRRRRRRRRRRRRRRRRRRRRRRRRR
885 **
886 **SSSSSSSSSSSSSSSSSSSSSSSSSSSSSSSSSSSS

```

Cycle:	from
7	NYC+2
9	NX1-NB+1

```

9 STOP! <-status / step number
10000 MNI (given above)
200. DMX (given above)
0.000001 DTN (given above)
0.052014 = (DLP+S)/(NX1 V)

```

```

887 ** S
888 *DFLUX OP=NEW
889 SUBU S3NU
890 **
891 U 9 S3NU
892 V 9 S3NU
893 E 9 S2NU
894 W 9 S4NU
895 ** S
896 ** S
897 ** SSSSSSSSSSSSSSSSSSSSSSSSSSSSSSSSSSSSS
898 **
899 **OUTPUT
900 *NODE FILE
901 NT
902 *NODE PRINT,FREQUENCY=0
903 *ELPRNT,FREQUENCY=0
904 **
905 *END STEP
906 ** -----END OF STEP 9 -----
907 **
908 *#####
909 **
910 **
911 **
912 **
913 **
914 **
915 **
916 **
917 ** -----BEGINNING OF STEP 18 -----
918 *STEP,NC= 10000
919 *HEAT TRANSFER DELTM X= 200.
920 0.000001 , 0.040000
921 *MODEL CHANGE ADD
922 E #
923 **
924 *#####
925 ** F
926 *FILM OP=NEW
927 **SUBD :reduced heat loss due to
928 **contact w th ground
929 SUBD F1,27,.1.
930 SUBU F3,27,.10.
931 SUBW F4,27,.10.
932 SUBE F2,27,.10.
933 **
934 U # F3,27,.10.
935 V # F3,27,.10.
936 E # F2,27,.100.
937 W # F4,27,.10.
938 **En:enhanced heat transfer due to
939 **shielding gas
940 **
941 ** F
942 *#####
943 **
944 **
945 *#####
946 ** R
947 *RADIATE OP=NEW
948 SUBU R3,27,.0.2268E-8
949 SUBW R4,27,.0.2268E-8
950 SUBE R2,27,.0.2268E-8
951 **
952 U # R3,27,.0.2268E-8
953 V # R3,27,.0.2268E-8
954 E # R2,27,.0.2268E-8
955 W # R4,27,.0.2268E-8
956 ** R
957 *#####
958 **
959 ** SSSSSSSSSSSSSSSSSSSSSSSSSSSSSSSSSSSSS
960 ** S
961 *DFLUX OP=NEW
962 SUBU S3NU
963 **
964 U # S3NU
965 V # S3NU
966 E # S2NU
967 W # S4NU
968 ** S
969 ** S
970 ** SSSSSSSSSSSSSSSSSSSSSSSSSSSSSSSSSSSSS
971 **
972 **OUTPUT
973 *NODE FILE
974 NT
975 *NODE PRINT,FREQUENCY=0
976 *ELPRNT,FREQUENCY=0
977 **
978 *END STEP
979 ** -----END OF STEP 18 -----

```

Cycle:	from	
10	NX1-NB+2	NX1-NB+2
18	NX1+NX2-NB	NX1+NX2-NB

18	STOP!	<- status / step num ber
10000	MNI	(given above)
200.	DMX	(given above)
0.000001	DTN	(given above)
0.040000		= DLB / (NX 2 V)

Cycle:	from	
19	X1+NX2-NB	NX1+NX2-NB+1
19	X1+NX2-NB	NX1+NX2-NB+1

19 STOP! <- status / step number
 10000 MNI (given above)
 200. DMX (given above)
 0.000001 DTN (given above)
 0.040000 = DLB / (NX2 V)

```

980 **
981 ** #####
982 **
983 **
984 **
985 **
986 **
987 **
988 **
989 ** -----BEGINNING OF STEP                19 -----
990 *STEP,NC= 10000
991 *HEAT TRANSFER DELTMX= 200.
992 0.000001 , 0.040000
993 *MODEL CHANGE ADD
994 E #
995 **
996 **FFFFFFFFFFFFFFFFFFFFFFFFFFFFFFFF
997 ** F
998 *FILM OP=NEW
999 **SUBD: reduced heat loss due to
1000 ** contact with ground
1001 SUBD F1,27,.1.
1002 SUBU F3,27,.10.
1003 SUBW F4,27,.10.
1004 SUBE F2,27,.10.
1005 **
1006 V # F3,27,.10.
1007 E # F2,27,.100.
1008 W # F4,27,.10.
1009 **En: enhanced heat transfer due to
1010 ** shielding gas
1011 **
1012 ** F
1013 **FFFFFFFFFFFFFFFFFFFFFFFFFFFFFFFF
1014 **
1015 **
1016 **RRRRRRRRRRRRRRRRRRRRRRRRRRRRRRRRRRRR
1017 ** R
1018 *RADIATE OP=NEW
1019 SUBU R3,27,.0.2268E-8
1020 SUBW R4,27,.0.2268E-8
1021 SUBE R2,27,.0.2268E-8
1022 **
1023 V # R3,27,.0.2268E-8
1024 E # R2,27,.0.2268E-8
1025 W # R4,27,.0.2268E-8
1026 ** R
1027 **RRRRRRRRRRRRRRRRRRRRRRRRRRRRRRRRRRRR
1028 **
1029 **SSSSSSSSSSSSSSSSSSSSSSSSSSSSSSSSSS
1030 ** S
1031 *DFLUX OP=NEW
1032 SUBU S3NU
1033 **
1034 V # S3NU
1035 E # S2NU
1036 W # S4NU
1037 ** S
1038 ** S
1039 **SSSSSSSSSSSSSSSSSSSSSSSSSSSSSSSSSS
1040 **
1041 **OUTPUT
1042 *NODE FILE
1043 NT
1044 *NODE PRINT,FREQUENCY=0
1045 *EL PRINT,FREQUENCY=0
1046 **
1047 *END STEP
1048 ** -----END OF STEP                19 -----
1049 **
1050 ** #####
1051 **

```

Cycle:	from	
20	X1+NX2-NB	NX1+NX2-NB+2
20	X1+NX2-NB	NX1+NX2-NB+2

20 STOP! <- status / step number
 10000 MNI (given above)
 200. DMX (given above)
 0.000001 DTN (given above)
 3600. CTM cooling time

```

1052 **
1053 **
1054 **
1055 **
1056 **
1057 ** -----BEGINNING OF STEP                20 -----
1058 *STEP,NC= 10000
1059 *HEAT TRANSFER DELTMX= 200.
1060 0.000001 , 3600.
1061 **
1062 **
1063 **

```

```

1064 ****
1065 ** F
1066 *FILM,OP=NEW
1067 **SUBD: reduced heat loss due to
1068 **contact with ground
1069 SUBD F1,27,.1.
1070 SUBU F3,27,.10.
1071 SUBW F4,27,.10.
1072 SUBE F2,27,.10.
1073 **
1074 V # F3,27,.10.
1075 E # F2,27,.10.
1076 W # F4,27,.10.
1077 **En: no more enhanced heat transfer due to
1078 **shielding gas
1079 **
1080 ** F
1081 ****
1082 **
1083 **
1084 ****
1085 ** R
1086 *RAD,ATE,OP=NEW
1087 SUBU R3,27,.0.2268E-8
1088 SUBW R4,27,.0.2268E-8
1089 SUBE R2,27,.0.2268E-8
1090 **
1091 V # R3,27,.0.2268E-8
1092 E # R2,27,.0.2268E-8
1093 W # R4,27,.0.2268E-8
1094 ** R
1095 ****
1096 **
1097 ****
1098 ** S
1099 *DFLUX,OP=NEW
1100 **
1101 ** S
1102 ** S
1103 ****
1104 **
1105 **OUTPUT
1106 *NODE FILE
1107 NT
1108 *NODE PRINT,FREQUENCY=0
1109 *EL PRINT,FREQUENCY=0
1110 **
1111 *END STEP
1112 ** ----- END OF STEP
1113 **
1114 ****
1115 **

```

Auxiliary files for 3D IFG

File "elemsets"

Step **5**

SET	AA	5	Side 3	5 _ n	n = 3 ... 6	AA	5	503	506	, 1							
J=	1	Yes	AB	5	Side 1	10	7	_	n	n = 4 ... 6	AB	5	10704	10706	, 1		
	1	2	Yes	AB	5	Side 1	10	8	_	n	n = 5 ... 6	AB	5	10805	10806	, 1	
	...	3	Yes	AB	5	Side 1	10	9	_	n	n = 6 ... 6	AB	5	10906	10906	, 1	
	3	4	No	AB	5	Side 1	10	10	_	n	n = 7 ... 6	AB	5	11007	11006	, 1	
			BA	5	Side 2	m	_	6		m = 1 ... 5	BA	5	106	506	, 100		
			BB	5	Side 4	1	_	m	_	6	m = 7 ... 9	BB	5	10706	10906	, 100	
			BB	5	Side 4	2	_	m	_	6	m = 7 ... 9	BB	5	20706	20906	, 100	
			BB	5	Side 4	3	_	m	_	6	m = 7 ... 9	BB	5	30706	30906	, 100	
			BB	5	Side 4	4	_	m	_	6	m = 7 ... 9	BB	5	40706	40906	, 100	
			BB	5	Side 4	L	0	6	_	6	L = 2 ... 4	BB	5	20606	40606	, 10000	
			CA	5	Side 4,1	m	_	3		m = 1 ... 5	CA	5	103	503	, 100		
J=	1	Yes	CB	5	Side 6,5	L	7	_	4	L = 1 ... 4	CB	5	10704	40704	, 10000		
	1	2	Yes	CB	5	Side 6,5	L	8	_	5	L = 1 ... 4	CB	5	10805	40805	, 10000	
	...	3	Yes	CB	5	Side 6,5	L	9	_	6	L = 1 ... 4	CB	5	10906	40906	, 10000	
	3	4	No	CB	5	Side 6,5	L	10	_	7	L = 1 ... 4	CB	5	11007	41007	, 10000	
J=	1	Yes	CC	5	Side 6,2	2	0	6	_	4		CC	5	20604			
	1	2	Yes	CC	5	Side 6,2	3	0	6	_	5		CC	5	30605		
	...	3	Yes	CC	5	Side 6,2	4	0	6	_	6		CC	5	40606		
	3	4	No	CC	5	Side 6,2	5	0	6	_	7		CC	5	50607		

File "elemsets2"

Step **19**

SET	AA	19	Side 3	5 _ n	n = 3 ... 20	*ELSET,ELSET:AA 19 , GENERATE 503 , 520 , 1												
J=	1	Yes	AB	19	Side 1	10	7	_	n	n = 4 ... 20	*ELSET,ELSET:AB 19 , GENERATE 10704 , 10720 , 1					Yes		
	1	2	Yes	AB	19	Side 1	10	8	_	n	n = 5 ... 20	10805 , 10820 , 1					Yes	
	...	3	Yes	AB	19	Side 1	10	9	_	n	n = 6 ... 20	10906 , 10920 , 1					Yes	
	4	4	Yes	AB	19	Side 1	10	10	_	n	n = 7 ... 20	11007 , 11020 , 1					Yes	
			BA	19	Side 2	m	_	20		m = 1 ... 5	*ELSET,ELSET:BA 19 , GENERATE 120 , 520 , 100							
			BB	19	Side 4	1	_	m	_	20	m = 7 ... 10	*ELSET,ELSET:BB 19 , GENERATE 10720 , 11020 , 100						
			BB	19	Side 4	2	_	m	_	20	m = 7 ... 10	20720 , 21020 , 100						
			BB	19	Side 4	3	_	m	_	20	m = 7 ... 10	30720 , 31020 , 100						
			BB	19	Side 4	4	_	m	_	20	m = 7 ... 10	40720 , 41020 , 100						
			BB	19	Side 4	L	0	6	_	20	L = 2 ... 5	20620 , 50620 , 10000						
			CA	19	Side 4,1	m	_	3		m = 1 ... 5	*ELSET,ELSET:BC 19 BA 19 , BB 19							
			CA	19	Side 4,1	m	_	3		m = 1 ... 5	*ELSET,ELSET:CA 19 , GENERATE 103 , 503 , 100							
J=	1	Yes	CB	19	Side 6,5	L	7	_	4	L = 1 ... 4	*ELSET,ELSET:CB 19 , GENERATE 10704 , 40704 , 10000					Yes		
	1	2	Yes	CB	19	Side 6,5	L	8	_	5	L = 1 ... 4	10805 , 40805 , 10000					Yes	
	...	3	Yes	CB	19	Side 6,5	L	9	_	6	L = 1 ... 4	10906 , 40906 , 10000					Yes	
	4	4	Yes	CB	19	Side 6,5	L	10	_	7	L = 1 ... 4	11007 , 41007 , 10000					Yes	
J=	1	Yes	CC	19	Side 6,2	2	0	6	_	4		*ELSET,ELSET:CC 19 , GENERATE 20604 , 20604 , 1					Yes	
	1	2	Yes	CC	19	Side 6,2	3	0	6	_	5		30605 , 30605 , 1					Yes
	...	3	Yes	CC	19	Side 6,2	4	0	6	_	6		40606 , 40606 , 1					Yes
	4	4	Yes	CC	19	Side 6,2	5	0	6	_	7		50607 , 50607 , 1					Yes

File "elemsets3"

				*ELSET,ELSET=SUBU		,GENERATE
SUBU	1 05 _ n	n = 21 ... 25	10521	, 10525	, 1	
	2 05 _ n	n = 21 ... 25	20521	, 20525	, 1	
	3 05 _ n	n = 21 ... 25	30521	, 30525	, 1	
	4 05 _ n	n = 21 ... 25	40521	, 40525	, 1	
	5 05 _ n	n = 21 ... 25	50521	, 50525	, 1	
	6 05 _ n	n = 1 ... 25	60501	, 60525	, 1	
	7 05 _ n	n = 1 ... 25	70501	, 70525	, 1	
	8 05 _ n	n = 1 ... 25	80501	, 80525	, 1	
	9 05 _ n	n = 1 ... 25	90501	, 90525	, 1	
	10 05 _ n	n = 1 ... 25	100501	, 100525	, 1	
	1 05 _ n	n = 1 ... 2	10501	, 10502	, 1	
	2 05 _ n	n = 1 ... 2	20501	, 20502	, 1	
	3 05 _ n	n = 1 ... 2	30501	, 30502	, 1	
	4 05 _ n	n = 1 ... 2	40501	, 40502	, 1	
	5 05 _ n	n = 1 ... 2	50501	, 50502	, 1	
			**			
			*ELSET,ELSET=U			1 ,GENERATE
UP 1	1 05 _ n	n = 3 ... 20	10503	, 10520	, 1	
	2 05 _ n	n = 3 ... 20	20503	, 20520	, 1	
	3 05 _ n	n = 3 ... 20	30503	, 30520	, 1	
	4 05 _ n	n = 3 ... 20	40503	, 40520	, 1	
	5 05 _ n	n = 3 ... 20	50503	, 50520	, 1	
			**			
			*ELSET,ELSET=U			2 ,GENERATE
UP 2	1 05 _ n	n = 4 ... 20	10504	, 10520	, 1	
	2 05 _ n	n = 3 ... 20	20503	, 20520	, 1	
	3 05 _ n	n = 3 ... 20	30503	, 30520	, 1	
	4 05 _ n	n = 3 ... 20	40503	, 40520	, 1	
	5 05 _ n	n = 3 ... 20	50503	, 50520	, 1	
			**			
			*ELSET,ELSET=U			3 ,GENERATE
UP 3	1 05 _ n	n = 5 ... 20	10505	, 10520	, 1	
	2 05 _ n	n = 3 , 5 ... 20	20505	, 20520	, 1	
	3 05 _ n	n = 3 ... 20	30503	, 30520	, 1	
	4 05 _ n	n = 3 ... 20	40503	, 40520	, 1	
	5 05 _ n	n = 3 ... 20	50503	, 50520	, 1	
			20503	, 20503	, 1	
			**			
			*ELSET,ELSET=U			4 ,GENERATE
UP 4	1 05 _ n	n = 6 ... 20	10506	, 10520	, 1	
	2 05 _ n	n = 3 , 6 ... 20	20506	, 20520	, 1	
	3 05 _ n	n = 3 , 4 , 6 ... 20	30506	, 30520	, 1	
	4 05 _ n	n = 3 , 20	40503	, 40520	, 1	
	5 05 _ n	n = 3 ... 20	50503	, 50520	, 1	
			20503	, 20503	, 1	
			30503	, 30504	, 1	
			**			
			*ELSET,ELSET=U			5 ,GENERATE
UP 5	1 05 _ n	n = 7 ... 20	10507	, 10520	, 1	
	2 05 _ n	n = 3 , 7 ... 20	20507	, 20520	, 1	
	3 05 _ n	n = 3 , 4 , 7 ... 20	30507	, 30520	, 1	
	4 05 _ n	n = 3 ... 5 , 7 ... 20	40507	, 40520	, 1	
	5 05 _ n	n = 3 ... 20	50503	, 50520	, 1	
			20503	, 20503	, 1	
			30503	, 30504	, 1	
			40503	, 40505	, 1	
			**			
			*ELSET,ELSET=U			6 ,GENERATE
UP 6	1 05 _ n	n = 8 ... 20	10508	, 10520	, 1	
	2 05 _ n	n = 3 , 8 ... 20	20508	, 20520	, 1	
	3 05 _ n	n = 3 , 4 , 8 ... 20	30508	, 30520	, 1	
	4 05 _ n	n = 3 ... 5 , 8 ... 20	40508	, 40520	, 1	
	5 05 _ n	n = 3 ... 6 , 8 ... 20	50508	, 50520	, 1	
			20503	, 20503	, 1	
			30503	, 30504	, 1	
			40503	, 40505	, 1	
			50503	, 50506	, 1	
			**			
			*ELSET,ELSET=U			7 ,GENERATE
UP 7	1 05 _ n	n = 9 ... 20	10509	, 10520	, 1	
	2 05 _ n	n = 3 , 9 ... 20	20509	, 20520	, 1	
	3 05 _ n	n = 3 , 4 , 9 ... 20	30509	, 30520	, 1	
	4 05 _ n	n = 3 ... 5 , 9 ... 20	40509	, 40520	, 1	
	5 05 _ n	n = 3 ... 6 , 9 ... 20	50509	, 50520	, 1	
			20503	, 20503	, 1	
			30503	, 30504	, 1	
			40503	, 40505	, 1	
			50503	, 50506	, 1	
			**			

UP 8	1 0 5 _ n	n = 10 ... 20	*ELSET,ELSET=U	8 ,GENERATE
	2 0 5 _ n	n = 3 , 10 ... 20	10510 , 10520 , 1	
	3 0 5 _ n	n = 3 , 4 , 10 ... 20	20510 , 20520 , 1	
	4 0 5 _ n	n = 3 ... 5 , 10 ... 20	30510 , 30520 , 1	
	5 0 5 _ n	n = 3 ... 6 , 10 ... 20	40510 , 40520 , 1	
			50510 , 50520 , 1	
			20503 , 20503 , 1	
			30503 , 30504 , 1	
			40503 , 40505 , 1	
			50503 , 50506 , 1	
			**	
UP 9	1 0 5 _ n	n = 11 ... 20	*ELSET,ELSET=U	9 ,GENERATE
	2 0 5 _ n	n = 3 , 11 ... 20	10511 , 10520 , 1	
	3 0 5 _ n	n = 3 , 4 , 11 ... 20	20511 , 20520 , 1	
	4 0 5 _ n	n = 3 ... 5 , 11 ... 20	30511 , 30520 , 1	
	5 0 5 _ n	n = 3 ... 6 , 11 ... 20	40511 , 40520 , 1	
			50511 , 50520 , 1	
			20503 , 20503 , 1	
			30503 , 30504 , 1	
			40503 , 40505 , 1	
			50503 , 50506 , 1	
			**	
UP 10	1 0 5 _ n	n = 12 ... 20	*ELSET,ELSET=U	10 ,GENERATE
	2 0 5 _ n	n = 3 , 12 ... 20	10512 , 10520 , 1	
	3 0 5 _ n	n = 3 , 4 , 12 ... 20	20512 , 20520 , 1	
	4 0 5 _ n	n = 3 ... 5 , 12 ... 20	30512 , 30520 , 1	
	5 0 5 _ n	n = 3 ... 6 , 12 ... 20	40512 , 40520 , 1	
			50512 , 50520 , 1	
			20503 , 20503 , 1	
			30503 , 30504 , 1	
			40503 , 40505 , 1	
			50503 , 50506 , 1	
			**	
UP 11	1 0 5 _ n	n = 13 ... 20	*ELSET,ELSET=U	11 ,GENERATE
	2 0 5 _ n	n = 3 , 13 ... 20	10513 , 10520 , 1	
	3 0 5 _ n	n = 3 , 4 , 13 ... 20	20513 , 20520 , 1	
	4 0 5 _ n	n = 3 ... 5 , 13 ... 20	30513 , 30520 , 1	
	5 0 5 _ n	n = 3 ... 6 , 13 ... 20	40513 , 40520 , 1	
			50513 , 50520 , 1	
			20503 , 20503 , 1	
			30503 , 30504 , 1	
			40503 , 40505 , 1	
			50503 , 50506 , 1	
			**	
UP 12	1 0 5 _ n	n = 14 ... 20	*ELSET,ELSET=U	12 ,GENERATE
	2 0 5 _ n	n = 3 , 14 ... 20	10514 , 10520 , 1	
	3 0 5 _ n	n = 3 , 4 , 14 ... 20	20514 , 20520 , 1	
	4 0 5 _ n	n = 3 ... 5 , 14 ... 20	30514 , 30520 , 1	
	5 0 5 _ n	n = 3 ... 6 , 14 ... 20	40514 , 40520 , 1	
			50514 , 50520 , 1	
			20503 , 20503 , 1	
			30503 , 30504 , 1	
			40503 , 40505 , 1	
			50503 , 50506 , 1	
			**	
UP 13	1 0 5 _ n	n = 15 ... 20	*ELSET,ELSET=U	13 ,GENERATE
	2 0 5 _ n	n = 3 , 15 ... 20	10515 , 10520 , 1	
	3 0 5 _ n	n = 3 , 4 , 15 ... 20	20515 , 20520 , 1	
	4 0 5 _ n	n = 3 ... 5 , 15 ... 20	30515 , 30520 , 1	
	5 0 5 _ n	n = 3 ... 6 , 15 ... 20	40515 , 40520 , 1	
			50515 , 50520 , 1	
			20503 , 20503 , 1	
			30503 , 30504 , 1	
			40503 , 40505 , 1	
			50503 , 50506 , 1	
			**	
UP 14	1 0 5 _ n	n = 16 ... 20	*ELSET,ELSET=U	14 ,GENERATE
	2 0 5 _ n	n = 3 , 16 ... 20	10516 , 10520 , 1	
	3 0 5 _ n	n = 3 , 4 , 16 ... 20	20516 , 20520 , 1	
	4 0 5 _ n	n = 3 ... 5 , 16 ... 20	30516 , 30520 , 1	
	5 0 5 _ n	n = 3 ... 6 , 16 ... 20	40516 , 40520 , 1	
			50516 , 50520 , 1	
			20503 , 20503 , 1	
			30503 , 30504 , 1	
			40503 , 40505 , 1	
			50503 , 50506 , 1	
			**	

UP 15	1 05 _ n	n = 17 ... 20	*ELSET,ELSET=U	15 ,GENERATE
	2 05 _ n	n = 3 , 17 ... 20	10517 , 10520 , 1	
	3 05 _ n	n = 3 , 4 , 17 ... 20	20517 , 20520 , 1	
	4 05 _ n	n = 3 ... 5 , 17 ... 20	30517 , 30520 , 1	
	5 05 _ n	n = 3 ... 6 , 17 ... 20	40517 , 40520 , 1	
			50517 , 50520 , 1	
			20503 , 20503 , 1	
			30503 , 30504 , 1	
			40503 , 40505 , 1	
			50503 , 50506 , 1	
			**	
			*ELSET,ELSET=U	16 ,GENERATE
UP 16	1 05 _ n	n = 18 ... 20	10518 , 10520 , 1	
	2 05 _ n	n = 3 , 18 ... 20	20518 , 20520 , 1	
	3 05 _ n	n = 3 , 4 , 18 ... 20	30518 , 30520 , 1	
	4 05 _ n	n = 3 ... 5 , 18 ... 20	40518 , 40520 , 1	
	5 05 _ n	n = 3 ... 6 , 18 ... 20	50518 , 50520 , 1	
			20503 , 20503 , 1	
			30503 , 30504 , 1	
			40503 , 40505 , 1	
			50503 , 50506 , 1	
			**	
			*ELSET,ELSET=U	17 ,GENERATE
UP 17	1 05 _ n	n = 19 , 20	10519 , 10520 , 1	
	2 05 _ n	n = 3 , 19 , 20	20519 , 20520 , 1	
	3 05 _ n	n = 3 , 4 , 19 , 20	30519 , 30520 , 1	
	4 05 _ n	n = 3 ... 5 , 19 , 20	40519 , 40520 , 1	
	5 05 _ n	n = 3 ... 6 , 19 , 20	50519 , 50520 , 1	
			20503 , 20503 , 1	
			30503 , 30504 , 1	
			40503 , 40505 , 1	
			50503 , 50506 , 1	
			**	
			*ELSET,ELSET=U	18 ,GENERATE
UP 18	1 05 _ n	n = 20	10520 , 10520 , 1	
	2 05 _ n	n = 3 , 20	20520 , 20520 , 1	
	3 05 _ n	n = 3 , 4 , 20	30520 , 30520 , 1	
	4 05 _ n	n = 3 ... 5 , 20	40520 , 40520 , 1	
	5 05 _ n	n = 3 ... 6 , 20	50520 , 50520 , 1	
			20503 , 20503 , 1	
			30503 , 30504 , 1	
			40503 , 40505 , 1	
			50503 , 50506 , 1	
			**	
			*ELSET,ELSET=U	19 ,GENERATE
UP 19	1 05 _ n		20503 , 20503 , 1	
	2 05 _ n	n = 3	30503 , 30504 , 1	
	3 05 _ n	n = 3 , 4	40503 , 40505 , 1	
	4 05 _ n	n = 3 ... 5	50503 , 50506 , 1	
	5 05 _ n	n = 3 ... 6		

File “elemsets4”

				*ELSET,ELSET=SUBD			.GENERATE
SUBD	1 0 1 _n	n = 1 ... 25		10101	,	10125	, 1
	2 0 1 _n	n = 1 ... 25		20101	,	20125	, 1
	3 0 1 _n	n = 1 ... 25		30101	,	30125	, 1
	4 0 1 _n	n = 1 ... 25		40101	,	40125	, 1
	5 0 1 _n	n = 1 ... 25		50101	,	50125	, 1
	6 0 1 _n	n = 1 ... 25		60101	,	60125	, 1
	7 0 1 _n	n = 1 ... 25		70101	,	70125	, 1
	8 0 1 _n	n = 1 ... 25		80101	,	80125	, 1
	9 0 1 _n	n = 1 ... 25		90101	,	90125	, 1
	10 0 1 _n	n = 1 ... 25		100101	,	100125	, 1
				**			
				**			
				**			
SUBS	n_ 1 0 1	n = 1 ... 10		*ELSET,ELSET=SUBS			
	n_ 2 0 1	n = 1 ... 10		10101	,	100101	, 10000
	n_ 3 0 1	n = 1 ... 10		10201	,	100201	, 10000
	n_ 4 0 1	n = 1 ... 10		10301	,	100301	, 10000
	n_ 5 0 1	n = 1 ... 10		10401	,	100401	, 10000
				10501	,	100501	, 10000
				**			
				**			
				**			
SUBN	n_ 1 2 5	n = 1 ... 10		*ELSET,ELSET=SUBN			
	n_ 2 2 5	n = 1 ... 10		10125	,	100125	, 10000
	n_ 3 2 5	n = 1 ... 10		10225	,	100225	, 10000
	n_ 4 2 5	n = 1 ... 10		10325	,	100325	, 10000
	n_ 5 2 5	n = 1 ... 10		10425	,	100425	, 10000
				10525	,	100525	, 10000
				**			
				**			
				**			
SUBW	1 0 1 _n	n = 1 ... 25		*ELSET,ELSET=SUBW			
	1 0 2 _n	n = 1 ... 25		10101	,	10125	, 1
	1 0 3 _n	n = 1 ... 25		10201	,	10225	, 1
	1 0 4 _n	n = 1 ... 25		10301	,	10325	, 1
	1 0 5 _n	n = 1 ... 25		10401	,	10425	, 1
				10501	,	10525	, 1
				**			
				**			
				**			
SUBE	10 0 1 _n	n = 1 ... 25		*ELSET,ELSET=SUBE			
	10 0 2 _n	n = 1 ... 25		100101	,	100125	, 1
	10 0 3 _n	n = 1 ... 25		100201	,	100225	, 1
	10 0 4 _n	n = 1 ... 25		100301	,	100325	, 1
	10 0 5 _n	n = 1 ... 25		100401	,	100425	, 1
				100501	,	100525	, 1

File "elemsets_upn"

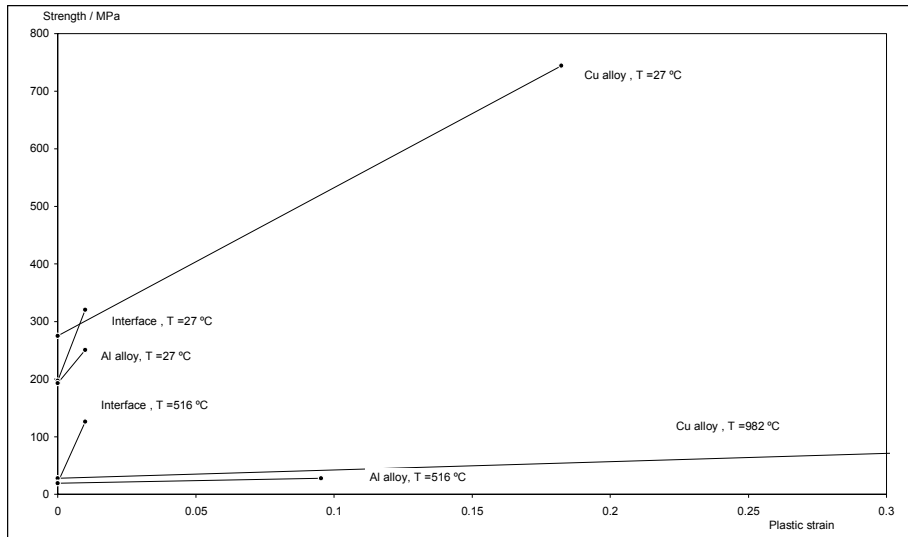
UP 1	1 0 5 _n n = 3 ... 20 2 0 5 _n n = 3 ... 20 3 0 5 _n n = 3 ... 20 4 0 5 _n n = 3 ... 20 5 0 5 _n n = 3 ... 20	
UP 2	1 0 5 _n n = 4 ... 20 2 0 5 _n n = 3 ... 20 3 0 5 _n n = 3 ... 20 4 0 5 _n n = 3 ... 20 5 0 5 _n n = 3 ... 20	
UP 3	1 0 5 _n n = 5 ... 20 2 0 5 _n n = 3 , 5 ... 20 3 0 5 _n n = 3 ... 20 4 0 5 _n n = 3 ... 20 5 0 5 _n n = 3 ... 20	
UP 4	1 0 5 _n n = 6 ... 20 2 0 5 _n n = 3 , 6 ... 20 3 0 5 _n n = 3 , 4 , 6 ... 20 4 0 5 _n n = 3 , 20 5 0 5 _n n = 3 ... 20	
UP 5	1 0 5 _n n = 7 ... 20 2 0 5 _n n = 3 , 7 ... 20 3 0 5 _n n = 3 , 4 , 7 ... 20 4 0 5 _n n = 3 ... 5 , 7 ... 20 5 0 5 _n n = 3 ... 20	
UP 6	1 0 5 _n n = 8 ... 20 2 0 5 _n n = 3 , 8 ... 20 3 0 5 _n n = 3 , 4 , 8 ... 20 4 0 5 _n n = 3 ... 5 , 8 ... 20 5 0 5 _n n = 3 ... 6 , 8 ... 20	
UP 7	1 0 5 _n n = 9 ... 20 2 0 5 _n n = 3 , 9 ... 20 3 0 5 _n n = 3 , 4 , 9 ... 20 4 0 5 _n n = 3 ... 5 , 9 ... 20 5 0 5 _n n = 3 ... 6 , 9 ... 20	
UP 8	1 0 5 _n n = 10 ... 20 2 0 5 _n n = 3 , 10 ... 20 3 0 5 _n n = 3 , 4 , 10 ... 20 4 0 5 _n n = 3 ... 5 , 10 ... 20 5 0 5 _n n = 3 ... 6 , 10 ... 20	
UP 9	1 0 5 _n n = 11 ... 20 2 0 5 _n n = 3 , 11 ... 20 3 0 5 _n n = 3 , 4 , 11 ... 20 4 0 5 _n n = 3 ... 5 , 11 ... 20 5 0 5 _n n = 3 ... 6 , 11 ... 20	
UP 10	1 0 5 _n n = 12 ... 20 2 0 5 _n n = 3 , 12 ... 20 3 0 5 _n n = 3 , 4 , 12 ... 20 4 0 5 _n n = 3 ... 5 , 12 ... 20 5 0 5 _n n = 3 ... 6 , 12 ... 20	
UP 11	1 0 5 _n n = 13 ... 20 2 0 5 _n n = 3 , 13 ... 20 3 0 5 _n n = 3 , 4 , 13 ... 20 4 0 5 _n n = 3 ... 5 , 13 ... 20 5 0 5 _n n = 3 ... 6 , 13 ... 20	
UP 12	1 0 5 _n n = 14 ... 20 2 0 5 _n n = 3 , 14 ... 20 3 0 5 _n n = 3 , 4 , 14 ... 20 4 0 5 _n n = 3 ... 5 , 14 ... 20 5 0 5 _n n = 3 ... 6 , 14 ... 20	
UP 13	1 0 5 _n n = 15 ... 20 2 0 5 _n n = 3 , 15 ... 20 3 0 5 _n n = 3 , 4 , 15 ... 20 4 0 5 _n n = 3 ... 5 , 15 ... 20 5 0 5 _n n = 3 ... 6 , 15 ... 20	
UP 14	1 0 5 _n n = 16 ... 20 2 0 5 _n n = 3 , 16 ... 20 3 0 5 _n n = 3 , 4 , 16 ... 20 4 0 5 _n n = 3 ... 5 , 16 ... 20 5 0 5 _n n = 3 ... 6 , 16 ... 20	
UP 15	1 0 5 _n n = 17 ... 20 2 0 5 _n n = 3 , 17 ... 20 3 0 5 _n n = 3 , 4 , 17 ... 20 4 0 5 _n n = 3 ... 5 , 17 ... 20 5 0 5 _n n = 3 ... 6 , 17 ... 20	
UP 16	1 0 5 _n n = 18 ... 20 2 0 5 _n n = 3 , 18 ... 20 3 0 5 _n n = 3 , 4 , 18 ... 20 4 0 5 _n n = 3 ... 5 , 18 ... 20 5 0 5 _n n = 3 ... 6 , 18 ... 20	
UP 17	1 0 5 _n n = 19 ... 20 2 0 5 _n n = 3 , 19 ... 20 3 0 5 _n n = 3 , 4 , 19 ... 20 4 0 5 _n n = 3 ... 5 , 19 ... 20 5 0 5 _n n = 3 ... 6 , 19 ... 20	
UP 18	1 0 5 _n n = 20 2 0 5 _n n = 3 , 20 3 0 5 _n n = 3 , 4 , 20 4 0 5 _n n = 3 ... 5 , 20 5 0 5 _n n = 3 ... 6 , 20	
UP 19	1 0 5 _n 2 0 5 _n n = 3 3 0 5 _n n = 3 , 4 4 0 5 _n n = 3 ... 5 5 0 5 _n n = 3 ... 6	

Appendix B. Materials properties

Composition	
Cu Alloy (C95700)	75 % Cu, 12% Mn, 8% Al, 3% Fe, 2% Ni
Precipitate (Al2Cu)	
Interface	Al alloy with f=20% Al2Cu
Al alloy (AA333)	Al, 8-10% Si, 1% Fe, 3-4% Cu, 0.5% Mn, 0.05-0.5% Mg, 0.5% Ni, 1% Zn, 0.25% Ti

Plastic properties

log Plastic strain	nominal Plastic strain	nominal strength	True Strength/ MPa	Reference	
		Cu alloy	Cu alloy		
0.00	0.00	275.0	275.0	[Metals H. vol2, 1990, p. 386]	27 °C
0.18	0.20	620.0	744.0	[Metals H. vol2, 1990, p. 386]	27 °C
				(b)	950 °C
0.00	0.00	27.5	27.5		950 °C
1.10	2.00	62.0	186.0		
		Interface	Interface		
0.00	0.00	197.0	197.0	[Mura, 1993, p.217, 218, Mori-Tanaka theory]	27 °C
0.01	0.01	317.0	320.2	[Mura, 1993, p.217, 218, Mori-Tanaka theory]	27 °C
0.00	0.00	20.0	20.0	[Mura, 1993, p.217, 218, Mori-Tanaka theory]	516 °C
0.01	0.01	125.0	126.3	[Mura, 1993, p.217, 218, Mori-Tanaka theory]	516 °C
		Al alloy	Al alloy		
0.00	0.00	193.0	193.0	[Metals H. vol2, 1990, p. 161]	27 °C
0.01	0.01	248.0	250.5	[Metals H. vol2, 1990, p. 161]	27 °C
				(b)	516 °C
0.00	0.00	19.0	19.0		516 °C
0.10	0.10	25.0	27.5		516 °C



Remarks

After the last reported value, data is taken as constant
 (b) value at solidus temp. taken as 10 % of room temp. value

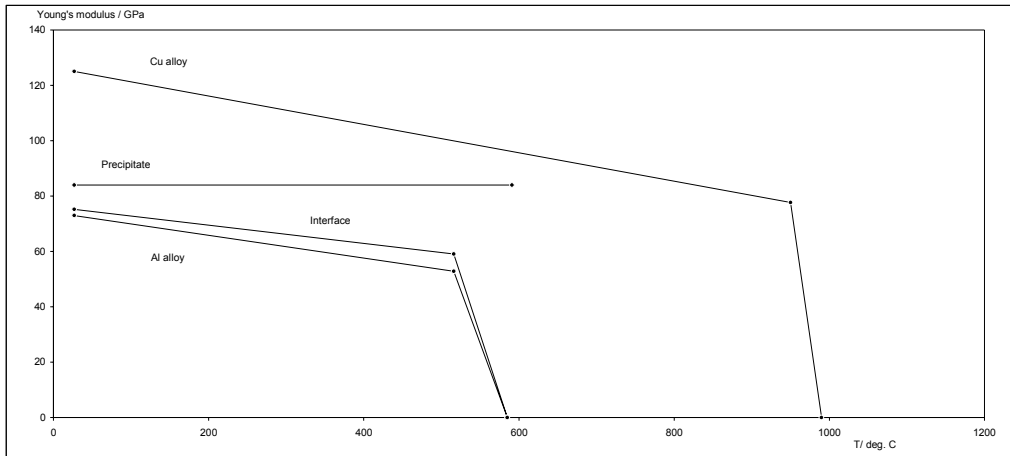
Elastic properties

Temperature/C	Young's Modulus/ GPa	Reference
Cu alloy		
27	125.0	[Metals H. vol2, 1990, p. 386]
950	77.7	[dE/dT from Pao, 1991]
990	1.0E-06	(d)
Precipitate		
27	84.0	[Otterloo, 1995]
591	84.0	(c)
Interface		
27	75.2	f=20% -> 0.2
516	59.1	[Mura, 1993, p. 422. Voigt approx.]
585	1.0E-06	(d)
Al alloy		
27	73.0	[Holt, 1996]
516	52.8	[dE/dT from Pao, 1991]
585	1.0E-06	(d)

	Poisson's ratio	Reference
Cu alloy	0.33	[Metals H. vol2, 1990, p. 386]
Precipitate	0.33	(f)
Interface	0.33	(f)
Al alloy	0.34	[Pao, 1991]

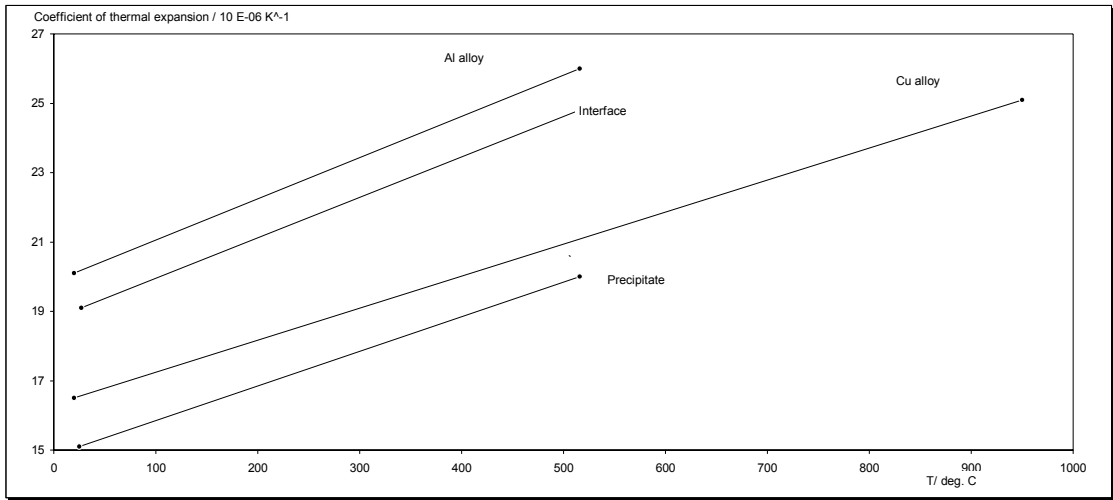
Remarks

After the last reported value, data is taken as constant
(c) Extrapolated
(d) To account for zero stress above liquidus
(f) Assumed



Thermal expansion

Temperature/C	Th. Exp. Coeff./ 10E-06 K ⁻¹	Reference
Cu alloy		
20	16.5	[Touloukian, vol. 12]
950	25.1	[Touloukian, vol. 12]
Precipitate		
25	15.1	[Touloukian, vol. 12]
516	20.0	[Touloukian, vol. 12]
Interface		
27	19.1	f=20% -> 0.2 rule of mixtures
516	24.8	
Al alloy		
20	20.1	[Touloukian, vol. 12]
516	26.0	[Touloukian, vol. 12]

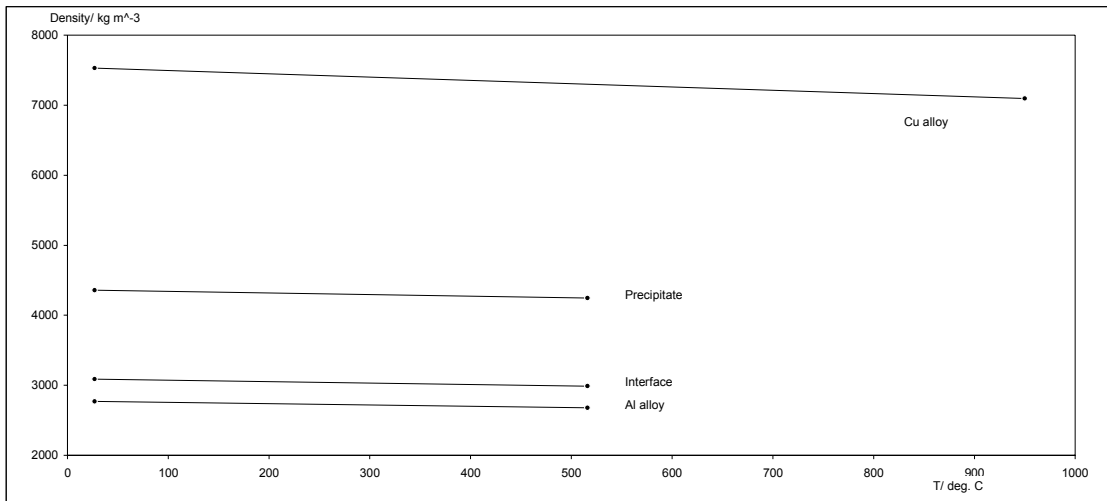


Remarks

After the last reported value, data is taken as constant

Density

Temperature/C	Density/ kg m ⁻³	Reference
	Cu alloy	
27	7530.0	[Metals H. vol2, 1990, p. 161, 386]
950	7096.3	(e)
	Precipitate	
27	4356.0	[TAPP software]
516	4243.9	(e)
	Interface	
27	3087.2	f=20% -> 0.2
516	2989.8	rule of mixtures
	Al alloy	
27	2770.0	[SAE report]
516	2676.3	(e)



Remarks

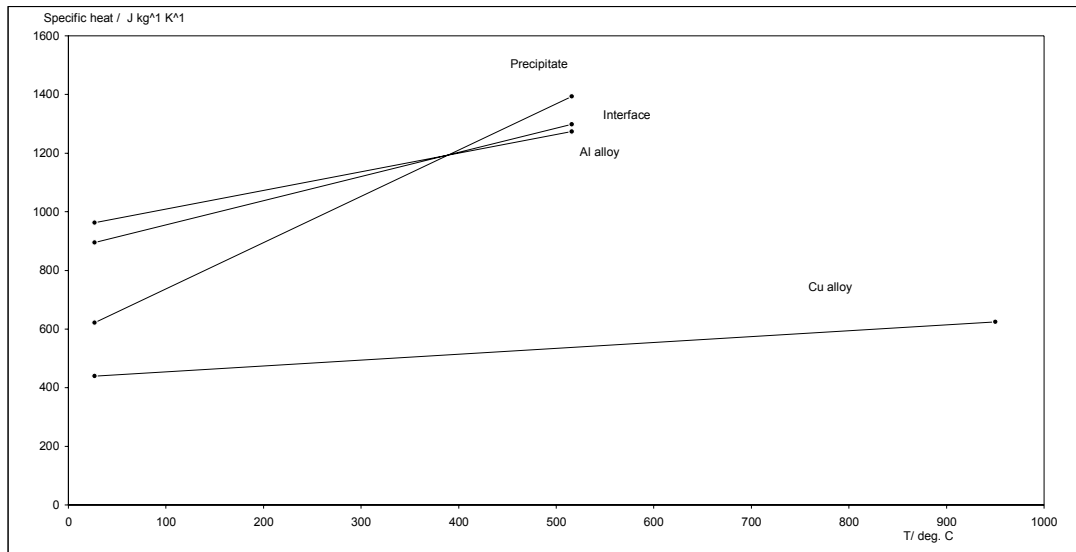
After the last reported value, data is taken as constant

(e) Calculated from: $\text{dens}(T) = \text{dens}(T_0) * [(1 - 3 * \text{CTE} * (T - T_0))]$

(T: temperature; dens: density, CTE: average thermal expansion coefficient)

Thermal properties

Temperature/C	Specific Heat/ J kg ⁻¹ K ⁻¹	Reference
Cu alloy		
27	440.0	[Metals H. vol2, 1990, p. 386]
950	624.6	[dCp/dT from Toulouk. Vol 4]
Precipitate		
27	622.0	[TAPP]
516	1393.0	[dCp/dT from Toulouk. Vol 4]
Interface		
27	894.8	f=20% -> 0.2
516	1297.8	rule of mixtures
Al alloy		
27	963.0	[Holt, 1996]
516	1274.0	[dCp/dT from Toulouk. Vol 4]



Remarks

After the last reported value, data is taken as constant

	Latent heat KJ/kg	Reference
Cu alloy	205	[Poirier]
Precipitate	205	estim.
Al alloy	398	[Poirier]

Temperature/C	Thermal Conductivity/ J kg ⁻¹ K ⁻¹	Reference
	Cu alloy	
20	72.4	[Toulouk. Vol 1]
200	93.7	[Toulouk. Vol 1]
	Precipitate same as Cu alloy	estim.
	Al alloy	
27	104	[SAE report]

Heat transfer coefficient / W m ⁻² K ⁻¹	location	Reference
100	melt pool (forced convection)	[Incropera]
1	bottom surface of substrate	estim.
10	elsewhere (free convection)	[Incropera]

Emissivity (total hemisph.)	Reference
0.04	[Incropera]

Appendix C. Sample Abaqus™ input files

```

Input file for 2D
temperature

*HEADING
**
** ABAQUS INPUT FILE
UPGRADE: This input file
was upgraded from
** version 5.8 or later
to version 6.3 with 20
warning(s) and 0
** error(s).
**
** Search the input file
for **WARNING.
  2D LASER CLADDING
**al22
**
**
** MESH GEN
**
** *NODE,NSET=P1
101,0.000000,0.000000
**
**
** *NODE,NSET=P2
1101,0.000000,0.006670
**
**
** *NODE,NSET=P3
2101,0.002578,0.007959
**
**
** *NODE,NSET=P4
2121,0.005000,0.007959
**
**
** *NODE,NSET=P5
1121,0.006502,0.006670
**
**
** *NODE,NSET=P6
121,0.006502,0.000000
**
**
** *NODE,NSET=P7
721,0.006502,0.006410
**
**
** *NODE,NSET=P8
701,0.000000,0.006410
**
**
** *NCOPY, CHANGE
NUMBER=100, OLDSET=P5, SHIF
T, NEW SET=ROT1,
MULTIPLE=9
**
**
** 0., 0., 0.
0.005000, 0.006440, 0., 0.00
5000, 0.006440, 0.01, 7.90
**
**
** *NSET, NSET=R1
ROT1, P4, P5

*NFILL, NSET=R2
P2, P3, 10, 100
**
**
** *NFILL, NSET=R3A, BIAS=1.50
**
** P6, P7, 6, 100
**
**
** *NFILL, NSET=R4A, BIAS=1.50
**
** P1, P8, 6, 100
**
**
** *NFILL, NSET=R3B, BIAS=1.00
**
** P7, P5, 4, 100
**
**
** *NFILL, NSET=R4B, BIAS=1.00
**
** P8, P2, 4, 100
**
**
** *NSET, NSET=R3
R3A, R3B
**
**
** *NSET, NSET=R4
R4A, R4B
**
**
** *NSET, NSET=R5
R1, R3
** *NSET, NSET=R6
R2, R4
**
**
** *NFILL, NSET=S1, BIAS=1.00
**
** R6, R5, 20, 1
**
**
** *NCOPY, CHANGE
NUMBER=20, OLDSET=R5, SHIFT
, NEW SET=R7
**
**
** 0.005000, 0.
0., 0., 0., 0., 0.1, 0.
**
**
** *NFILL, NSET=S2
R5, R7, 20, 1
**
**
** *NCOPY, CHANGE
NUMBER=50, OLDSET=R6, SHIFT
, NEW SET=R8
**
**
** 0.050000, 0.
0., 0., 0., 0., 0.1, 0.
**
**
** *NFILL, NSET=S3, BIAS=0.60
**

R7, R8, 10, 1
**
**
** *NSET, NSET=SUB, GENERATE
101, 151, 1
**
**
** 201, 251, 1
**
**
** 301, 351, 1
**
**
** 401, 451, 1
**
**
** 501, 551, 1
**
**
** 601, 651, 1
**
**
** 701, 751, 1
**
**
** 801, 851, 1
**
**
** 901, 951, 1
**
**
** 1001, 1051, 1
**
**
** 1101, 1151, 1
** *NSET, NSET=CLD, GENERATE
1201, 1251, 1
**
**
** 1301, 1351, 1
**
**
** 1401, 1451, 1
**
**
** 1501, 1551, 1
**
**
** 1601, 1651, 1
**
**
** 1701, 1751, 1
**
**
** 1801, 1851, 1
**
**
** 1901, 1951, 1
**
**
** 2001, 2051, 1
**
**
** 2101, 2151, 1
**
**
**
** *NSET, NSET=ALL
SUB, CLD
** *ELEMENT, TYPE=DC2D4
101, 101, 102, 202, 201
**
**
** 1101, 1101, 1102, 1202, 1201
**
**
**
** #####
####
** element sets
**
** *ELGEN, ELSET=SUB
101, 50, 1, 1, 10, 100, 100
**
**
** *ELGEN, ELSET=CLD

```

```

1101,40,1,1,10,100,100
**
**
**
#####
###
**
*ELSET,ELSET=SUBU,GENERAT
E
1001,1002,1
1041,1050,1
**
**
*ELSET,ELSET=SUBD,GENERAT
E
101,150,1
**
**
*ELSET,ELSET=SUBW,GENERAT
E
101,1001,100
**
**
*ELSET,ELSET=SUBE,GENERAT
E
150,1050,100
**
**
*ELSET,ELSET=U1,GENERATE
1003,1040,1
*ELSET,ELSET=U2,GENERATE
1004,1040,1
*ELSET,ELSET=U3,GENERATE
1005,1040,1
*ELSET,ELSET=U4,GENERATE
1006,1040,1
*ELSET,ELSET=U5,GENERATE
1007,1040,1
*ELSET,ELSET=U6,GENERATE
1008,1040,1
*ELSET,ELSET=U7,GENERATE
1009,1040,1
*ELSET,ELSET=U8,GENERATE
1010,1040,1
*ELSET,ELSET=U9,GENERATE
1011,1040,1
*ELSET,ELSET=U10,GENERATE
1012,1040,1
*ELSET,ELSET=U11,GENERATE
1013,1040,1
*ELSET,ELSET=U12,GENERATE
1014,1040,1
*ELSET,ELSET=U13,GENERATE
1015,1040,1
*ELSET,ELSET=U14,GENERATE
1016,1040,1
*ELSET,ELSET=U15,GENERATE
1017,1040,1
*ELSET,ELSET=U16,GENERATE
1018,1040,1
*ELSET,ELSET=U17,GENERATE
1019,1040,1
*ELSET,ELSET=U18,GENERATE
1020,1040,1
*ELSET,ELSET=U19,GENERATE
1021,1040,1
*ELSET,ELSET=U20,GENERATE
1022,1040,1
*ELSET,ELSET=U21,GENERATE
1023,1040,1
*ELSET,ELSET=U22,GENERATE

1024,1040,1
*ELSET,ELSET=U23,GENERATE
1025,1040,1
*ELSET,ELSET=U24,GENERATE
1026,1040,1
*ELSET,ELSET=U25,GENERATE
1027,1040,1
*ELSET,ELSET=U26,GENERATE
1028,1040,1
*ELSET,ELSET=U27,GENERATE
1029,1040,1
*ELSET,ELSET=U28,GENERATE
1030,1040,1
*ELSET,ELSET=U29,GENERATE
1031,1040,1
*ELSET,ELSET=U30,GENERATE
1032,1040,1
*ELSET,ELSET=U31,GENERATE
1033,1040,1
*ELSET,ELSET=U32,GENERATE
1034,1040,1
*ELSET,ELSET=U33,GENERATE
1035,1040,1
*ELSET,ELSET=U34,GENERATE
1036,1040,1
*ELSET,ELSET=U35,GENERATE
1037,1040,1
*ELSET,ELSET=U36,GENERATE
1038,1040,1
*ELSET,ELSET=U37,GENERATE
1039,1040,1
*ELSET,ELSET=U38
1040
*ELSET,ELSET=E2
1103
*ELSET,ELSET=E3,GENERATE
1104,1204,100
*ELSET,ELSET=E4,GENERATE
1105,1305,100
*ELSET,ELSET=E5,GENERATE
1106,1406,100
*ELSET,ELSET=E6,GENERATE
1107,1507,100
*ELSET,ELSET=E7,GENERATE
1108,1608,100
*ELSET,ELSET=E8,GENERATE
1109,1709,100
*ELSET,ELSET=E9,GENERATE
1110,1810,100
*ELSET,ELSET=E10,GENERATE
1111,1911,100
*ELSET,ELSET=E11,GENERATE
1112,2012,100
*ELSET,ELSET=E12,GENERATE
1113,2013,100
*ELSET,ELSET=E13,GENERATE
1114,2014,100
*ELSET,ELSET=E14,GENERATE
1115,2015,100
*ELSET,ELSET=E15,GENERATE
1116,2016,100
*ELSET,ELSET=E16,GENERATE
1117,2017,100
*ELSET,ELSET=E17,GENERATE
1118,2018,100
*ELSET,ELSET=E18,GENERATE
1119,2019,100
*ELSET,ELSET=E19,GENERATE
1120,2020,100
*ELSET,ELSET=E20,GENERATE
1121,2021,100

*ELSET,ELSET=E21,GENERATE
1122,2022,100
*ELSET,ELSET=E22,GENERATE
1123,2023,100
*ELSET,ELSET=E23,GENERATE
1124,2024,100
*ELSET,ELSET=E24,GENERATE
1125,2025,100
*ELSET,ELSET=E25,GENERATE
1126,2026,100
*ELSET,ELSET=E26,GENERATE
1127,2027,100
*ELSET,ELSET=E27,GENERATE
1128,2028,100
*ELSET,ELSET=E28,GENERATE
1129,2029,100
*ELSET,ELSET=E29,GENERATE
1130,2030,100
*ELSET,ELSET=E30,GENERATE
1131,2031,100
*ELSET,ELSET=E31,GENERATE
1132,2032,100
*ELSET,ELSET=E32,GENERATE
1133,2033,100
*ELSET,ELSET=E33,GENERATE
1134,2034,100
*ELSET,ELSET=E34,GENERATE
1135,2035,100
*ELSET,ELSET=E35,GENERATE
1136,2036,100
*ELSET,ELSET=E36,GENERATE
1137,2037,100
*ELSET,ELSET=E37,GENERATE
1138,2038,100
*ELSET,ELSET=E38,GENERATE
1139,2039,100
*ELSET,ELSET=E39,GENERATE
1140,2040,100
*ELSET,ELSET=V2
1103
*ELSET,ELSET=V3,GENERATE
1203,1204,1
*ELSET,ELSET=V4,GENERATE
1303,1305,1
*ELSET,ELSET=V5,GENERATE
1403,1406,1
*ELSET,ELSET=V6,GENERATE
1503,1507,1
*ELSET,ELSET=V7,GENERATE
1603,1608,1
*ELSET,ELSET=V8,GENERATE
1703,1709,1
*ELSET,ELSET=V9,GENERATE
1803,1810,1
*ELSET,ELSET=V10,GENERATE
1903,1911,1
*ELSET,ELSET=V11,GENERATE
2003,2012,1
*ELSET,ELSET=V12,GENERATE
2003,2013,1
*ELSET,ELSET=V13,GENERATE
2003,2014,1
*ELSET,ELSET=V14,GENERATE
2003,2015,1
*ELSET,ELSET=V15,GENERATE
2003,2016,1
*ELSET,ELSET=V16,GENERATE
2003,2017,1
*ELSET,ELSET=V17,GENERATE
2003,2018,1
*ELSET,ELSET=V18,GENERATE

```

2003,2019,1	*ELSET,ELSET=W16,GENERATE	701,702,1
*ELSET,ELSET=V19,GENERATE	1103,2003,100	**
2003,2020,1	*ELSET,ELSET=W17,GENERATE	742,750,1
*ELSET,ELSET=V20,GENERATE	1103,2003,100	**
2003,2021,1	*ELSET,ELSET=W18,GENERATE	**
*ELSET,ELSET=V21,GENERATE	1103,2003,100	601,650,1
2003,2022,1	*ELSET,ELSET=W19,GENERATE	**
*ELSET,ELSET=V22,GENERATE	1103,2003,100	501,550,1
2003,2023,1	*ELSET,ELSET=W20,GENERATE	**
*ELSET,ELSET=V23,GENERATE	1103,2003,100	401,450,1
2003,2024,1	*ELSET,ELSET=W21,GENERATE	**
*ELSET,ELSET=V24,GENERATE	1103,2003,100	301,350,1
2003,2025,1	*ELSET,ELSET=W22,GENERATE	**
*ELSET,ELSET=V25,GENERATE	1103,2003,100	201,250,1
2003,2026,1	*ELSET,ELSET=W23,GENERATE	**
*ELSET,ELSET=V26,GENERATE	1103,2003,100	101,150,1
2003,2027,1	*ELSET,ELSET=W24,GENERATE	**
*ELSET,ELSET=V27,GENERATE	1103,2003,100	**
2003,2028,1	*ELSET,ELSET=W25,GENERATE	*ELSET,ELSET=MOD1
*ELSET,ELSET=V28,GENERATE	1103,2003,100	SUB
2003,2029,1	*ELSET,ELSET=W26,GENERATE	*ELSET,ELSET=MOD2
*ELSET,ELSET=V29,GENERATE	1103,2003,100	MOD1, E2, V2
2003,2030,1	*ELSET,ELSET=W27,GENERATE	*ELSET,ELSET=MOD3
*ELSET,ELSET=V30,GENERATE	1103,2003,100	MOD2, E3, V3
2003,2031,1	*ELSET,ELSET=W28,GENERATE	*ELSET,ELSET=MOD4
*ELSET,ELSET=V31,GENERATE	1103,2003,100	MOD3, E4, V4
2003,2032,1	*ELSET,ELSET=W29,GENERATE	*ELSET,ELSET=MOD5
*ELSET,ELSET=V32,GENERATE	1103,2003,100	MOD4, E5, V5
2003,2033,1	*ELSET,ELSET=W30,GENERATE	*ELSET,ELSET=MOD6
*ELSET,ELSET=V33,GENERATE	1103,2003,100	MOD5, E6, V6
2003,2034,1	*ELSET,ELSET=W31,GENERATE	*ELSET,ELSET=MOD7
*ELSET,ELSET=V34,GENERATE	1103,2003,100	MOD6, E7, V7
2003,2035,1	*ELSET,ELSET=W32,GENERATE	*ELSET,ELSET=MOD8
*ELSET,ELSET=V35,GENERATE	1103,2003,100	MOD7, E8, V8
2003,2036,1	*ELSET,ELSET=W33,GENERATE	*ELSET,ELSET=MOD9
*ELSET,ELSET=V36,GENERATE	1103,2003,100	MOD8, E9, V9
2003,2037,1	*ELSET,ELSET=W34,GENERATE	*ELSET,ELSET=MOD10
*ELSET,ELSET=V37,GENERATE	1103,2003,100	MOD9, E10, V10
2003,2038,1	*ELSET,ELSET=W35,GENERATE	*ELSET,ELSET=MOD11
*ELSET,ELSET=V38,GENERATE	1103,2003,100	MOD10, E11, V11
2003,2039,1	*ELSET,ELSET=W36,GENERATE	*ELSET,ELSET=MOD12
*ELSET,ELSET=V39,GENERATE	1103,2003,100	MOD11, E12
2003,2040,1	*ELSET,ELSET=W37,GENERATE	*ELSET,ELSET=MOD13
*ELSET,ELSET=W2	1103,2003,100	MOD12, E13
1103	*ELSET,ELSET=W38,GENERATE	*ELSET,ELSET=MOD14
*ELSET,ELSET=W3,GENERATE	1103,2003,100	MOD13, E14
1103,1203,100	*ELSET,ELSET=W39,GENERATE	*ELSET,ELSET=MOD15
*ELSET,ELSET=W4,GENERATE	1103,2003,100	MOD14, E15
1103,1303,100	*ELSET,ELSET=INT,	*ELSET,ELSET=MOD16
*ELSET,ELSET=W5,GENERATE	GENERATE	MOD15, E16
1103,1403,100	1003,1041,1	*ELSET,ELSET=MOD17
*ELSET,ELSET=W6,GENERATE	**	MOD16, E17
1103,1503,100	903,941,1	*ELSET,ELSET=MOD18
*ELSET,ELSET=W7,GENERATE	**	MOD17, E18
1103,1603,100	803,841,1	*ELSET,ELSET=MOD19
*ELSET,ELSET=W8,GENERATE	**	MOD18, E19
1103,1703,100	703,741,1	*ELSET,ELSET=MOD20
*ELSET,ELSET=W9,GENERATE	*ELSET,ELSET=BAS,	MOD19, E20
1103,1803,100	GENERATE	*ELSET,ELSET=MOD21
*ELSET,ELSET=W10,GENERATE	1001,1002,1	MOD20, E21
1103,1903,100	**	*ELSET,ELSET=MOD22
*ELSET,ELSET=W11,GENERATE	1042,1050,1	MOD21, E22
1103,2003,100	**	*ELSET,ELSET=MOD23
*ELSET,ELSET=W12,GENERATE	901,902,1	MOD22, E23
1103,2003,100	**	*ELSET,ELSET=MOD24
*ELSET,ELSET=W13,GENERATE	942,950,1	MOD23, E24
1103,2003,100	**	*ELSET,ELSET=MOD25
*ELSET,ELSET=W14,GENERATE	801,802,1	MOD24, E25
1103,2003,100	**	*ELSET,ELSET=MOD26
*ELSET,ELSET=W15,GENERATE	842,850,1	MOD25, E26
1103,2003,100	**	*ELSET,ELSET=MOD27

```

MOD26, E27
*ELSET,ELSET=MOD28
MOD27, E28
*ELSET,ELSET=MOD29
MOD28, E29
*ELSET,ELSET=MOD30
MOD29, E30
*ELSET,ELSET=MOD31
MOD30, E31
*ELSET,ELSET=MOD32
MOD31, E32
*ELSET,ELSET=MOD33
MOD32, E33
*ELSET,ELSET=MOD34
MOD33, E34
*ELSET,ELSET=MOD35
MOD34, E35
*ELSET,ELSET=MOD36
MOD35, E36
*ELSET,ELSET=MOD37
MOD36, E37
*ELSET,ELSET=MOD38
MOD37, E38
*ELSET,ELSET=MOD39
MOD38, E39
*ELSET,ELSET=MOD40
MOD39
**
**
*ELSET,ELSET=HIST,
GENERATE
509,1709,400
519,1719,400
529,1729,400
539,1739,400
**
**
#####
###
**
**
*INITIAL
CONDITIONS,TYPE=TEMPERATU
RE
SUB,27.
CLD,1550.
**INITIAL
CONDITIONS,TYPE=MASS FLOW
RATE
**SUB,-75.42
**CLD,-49.25
** MATERIALS PROPERTIES
**
*SOLID
SECTION,ELSET=BAS,MATERIA
L=ALBAS
*SOLID
SECTION,ELSET=INT,MATERIA
L=ALBAS
*SOLID
SECTION,ELSET=CLD,MATERIA
L=CUBAS
**
** insert properties
**
**
** -----
-----|
*MATERIAL,NAME=ALBAS
*ELASTIC
73.0E9,0.34,27.
52.8E9,0.34,516.
1.E3,0.34,585.
*PLASTIC,HARDENING=KINEMA
TIC
193.E6,0.,27.
250.5E6,0.01,27.
19.E6,0.,516.
27.5E6,0.1,516.
18.9E6,0.,516.1
18.9E6,0.1,516.1
*ANNEAL TEMPERATURE
516.1
*EXPANSION,ZERO=27.
20.1E-6,27.
26.0E-6,516.
*CONDUCTIVITY
117.,27.
*DENSITY
2770.,27.
2676.,516.
*LATENT HEAT
389000.,516.,585.
*SPECIFIC HEAT
963.,27.
1274.,516.
** -----
-----|
*MATERIAL,NAME=INTER
*ELASTIC
75.2E9,0.33,27.
59.1E9,0.33,516.
1.E3,0.33,585.
*PLASTIC,HARDENING=KINEMA
TIC
197.E6,0.,27.
320.E6,.01,27.
20.E6,0.,516.
126.E6,.01,516.
19.9E6,0.,516.1
19.9E6,0.01,516.1
*ANNEAL TEMPERATURE
516.1
*EXPANSION,ZERO=27.
19.1E-6,27.
24.8E-6,516.
*CONDUCTIVITY
117.,27.
*DENSITY
3087.,27.
2990.,516.
*LATENT HEAT
389000.,516.,585.
*SPECIFIC HEAT
895.,27.
1298.,516.
** -----
-----|
*MATERIAL,NAME=CUBAS
*ELASTIC
125.0E9,0.33,27.
77.7E9,0.33,950.
1.E3,0.33,990.
*PLASTIC,HARDENING=KINEMA
TIC
275.E6,0.,27.
744.E6,0.18,27.
27.5E6,0.,950.
186.E6,1.1,950.
27.4E6,0.,950.1
27.4E6,2.,950.1
*ANNEAL TEMPERATURE
950.1
*EXPANSION,ZERO=27.
16.5E-6,27.
25.1E-6,950.
*CONDUCTIVITY
12.1,27.
85.9,950.
*DENSITY
7530.,27.
7096.,950.
*LATENT HEAT
205000.,950.,990.
*SPECIFIC HEAT
440.,27.
625.,950.
**
**
**RESTART,WRITE,FREQUENCY=
1000
**
**
**
#####
#####
**
**
** ----- BEGINNING
OF STEP 1 -----
----
*physical constants,
stefan boltzmann=1.0,
absolute zero=-273.
*STEP,INC=10000
*HEAT TRANSFER,DELTMX=20.
0.000001,0.072013615
*MODEL CHANGE,REMOVE
CLD
**
**
FFFFFFFFFFFFFFFFFFFFFFFF
FFFF
**
F
*FILM,OP=NEW
** SUBD: reduced heat
loss due to
** contact with ground
SUBD,F1,27.,1.
SUBU,F3,27.,10.
SUBW,F4,27.,10.
SUBE,F2,27.,10.
**
U1,F3,27.,10.
**
F
**
FFFFFFFFFFFFFFFFFFFFFFFF
FFFF
**
**
RRRRRRRRRRRRRRRRRRRRRR
RRRR
**
R
** **WARNING: The
*RADIATE option requires
emissivity instead of the
radiation

```

```

**          constant A.
Hence, the Stefan-
Boltzmann constant S is
required. A fictitious
**          value of the
Stefan-Boltzmann constant
of 1.0 was entered on the
*PHYSICAL
**          CONSTANTS
option.
**
**
**RADIATE,OP=NEW
SUBU,R3,27.,0.2268E-8
SUBW,R4,27.,0.2268E-8
SUBE,R2,27.,0.2268E-8
**
U1,R3,27.,0.2268E-8
**
R
**
RRRRRRRRRRRRRRRRRRRRRRRRRRRRRR
RRRR
**
**
SSSSSSSSSSSSSSSSSSSSSSSSSSSS
SSSS
**
S
*DFLUX,OP=NEW
SUBU,S3NU
**
U1,S3NU
**
S
**
SSSSSSSSSSSSSSSSSSSSSSSSSSSS
SSSS
**
** OUTPUT
*NODE FILE
NT
*OUTPUT, FIELD,
FREQUENCY=10
*ELEMENT OUTPUT,
ELSET=MOD1
TEMP
**
*OUTPUT, HISTORY,
FREQUENCY=10
*ELEMENT OUTPUT,
ELSET=HIST
TEMP
**
**
*END STEP
** ----- END OF
STEP 1 -----
-
**
**
#####
#####
**
**
** ----- BEGINNING
OF STEP2 -----
*STEP, INC=10000
*HEAT TRANSFER, DELTMX=20.
0.000001, 0.02606808
*MODEL CHANGE, ADD

```

```

E2,V2
**
**
FFFFFFFFFFFFFFFFFFFFFFFFFFFF
FFFF
**
F
*FILM,OP=NEW
** SUBD: reduced heat
loss due to
** contact with ground
SUBD,F1,27.,1.
SUBU,F3,27.,10.
SUBW,F4,27.,10.
SUBE,F2,27.,10.
**
U2,F3,27.,10.
V2,F3,27.,10.
E2,F2,27.,100.
W2,F4,27.,10.
** En: enhanced heat
transfer due to
** shielding gas
**
**
F
**
FFFFFFFFFFFFFFFFFFFFFFFFFFFF
FFFF
**
**
RRRRRRRRRRRRRRRRRRRRRRRRRRRRRR
RRRR
**
R
**
**WARNING: The
*RADIATE option requires
emissivity instead of the
radiation
**          constant A.
Hence, the Stefan-
Boltzmann constant S is
required. A fictitious
**          value of the
Stefan-Boltzmann constant
of 1.0 was entered on the
*PHYSICAL
**          CONSTANTS
option.
**
**
**RADIATE,OP=NEW
SUBU,R3,27.,0.2268E-8
SUBW,R4,27.,0.2268E-8
SUBE,R2,27.,0.2268E-8
**
U2,R3,27.,0.2268E-8
V2,R3,27.,0.2268E-8
E2,R2,27.,0.2268E-8
W2,R4,27.,0.2268E-8
**
R
**
RRRRRRRRRRRRRRRRRRRRRRRRRRRRRR
RRRR
**
**
SSSSSSSSSSSSSSSSSSSSSSSSSSSS
SSSS

```

```

**
S
*DFLUX,OP=NEW
SUBU,S3NU
**
U2,S3NU
V2,S3NU
E2,S2NU
W2,S4NU
**
S
**
S
**
SSSSSSSSSSSSSSSSSSSSSSSSSSSS
SSSS
**
** OUTPUT
*NODE FILE
NT
*OUTPUT, FIELD,
FREQUENCY=10, OP=ADD
*ELEMENT OUTPUT,
ELSET=MOD2
TEMP
**
**
*OUTPUT, HISTORY,
FREQUENCY=10
*ELEMENT OUTPUT,
ELSET=HIST
TEMP
**
**
*END STEP
** ----- END OF
STEP 2 -----
-
**
**
(...)
**
#####
#####
**
**
** ----- BEGINNING
OF STEP39 -----
*STEP, INC=10000
*HEAT TRANSFER, DELTMX=20.
0.000001, 0.02
*MODEL CHANGE, ADD
E39
**
**
FFFFFFFFFFFFFFFFFFFFFFFFFFFF
FFFF
**
F
*FILM,OP=NEW
** SUBD: reduced heat
loss due to
** contact with ground
SUBD,F1,27.,1.
SUBU,F3,27.,10.
SUBW,F4,27.,10.
SUBE,F2,27.,10.
**
V39,F3,27.,10.
E39,F2,27.,100.

```

```

W39,F4,27.,10.
** En: enhanced heat
transfer due to
** shielding gas
**
**
F
**
FFFFFFFFFFFFFFFFFFFFFFFFFFFF
FFFF
**
**
**
RRRRRRRRRRRRRRRRRRRRRRRRRR
RRRR
**
R
**      **WARNING: The
*RADIATE option requires
emissivity instead of the
radiation
**          constant A.
Hence, the Stefan-
Boltzmann constant S is
required. A fictitious
**          value of the
Stefan-Boltzmann constant
of 1.0 was entered on the
*PHYSICAL
**          CONSTANTS
option.
**
**
**
*RADIATE,OP=NEW
SUBU,R3,27.,0.2268E-8
SUBW,R4,27.,0.2268E-8
SUBE,R2,27.,0.2268E-8
**
V39,R3,27.,0.2268E-8
E39,R2,27.,0.2268E-8
W39,R4,27.,0.2268E-8
**
R
**
RRRRRRRRRRRRRRRRRRRRRRRRRR
RRRR
**
**
SSSSSSSSSSSSSSSSSSSSSSSSSS
SSSS
**
S
*DFLUX,OP=NEW
SUBU,S3NU
**
V39,S3NU
E39,S2NU
W39,S4NU
**
S
**
S
**
SSSSSSSSSSSSSSSSSSSSSSSSSS
SSSS
**
** OUTPUT
*NODE FILE
NT
*OUTPUT, FIELD,
FREQUENCY=10, OP=ADD

```

```

*ELEMENT OUTPUT,
ELSET=MOD39
TEMP
**
**
*OUTPUT, HISTORY,
FREQUENCY=10
*ELEMENT OUTPUT,
ELSET=HIST
TEMP
**
**
*END STEP
** ----- END OF
STEP 39 -----
--
**
**
#####
#####
**
**
** ----- BEGINNING
OF STEP40 -----
*STEP,INC=10000
*HEAT TRANSFER,DELTMX=20.
0.000001,14400.
**
**
**
FFFFFFFFFFFFFFFFFFFFFFFFFFFF
FFFF
**
F
*FILM,OP=NEW
** SUBD: reduced heat
loss due to
** contact with ground
SUBD,F1,27.,1.
SUBU,F3,27.,10.
SUBW,F4,27.,10.
SUBE,F2,27.,10.
**
V39,F3,27.,10.
E39,F2,27.,10.
W39,F4,27.,10.
** En: no more enhanced
heat transfer due to
** shielding gas
**
**
F
**
**
FFFFFFFFFFFFFFFFFFFFFFFFFFFF
FFFF
**
**
RRRRRRRRRRRRRRRRRRRRRRRRRR
RRRR
**
R
**      **WARNING: The
*RADIATE option requires
emissivity instead of the
radiation
**          constant A.
Hence, the Stefan-
Boltzmann constant S is
required. A fictitious
**          value of the
Stefan-Boltzmann constant

```

```

of 1.0 was entered on the
*PHYSICAL
**          CONSTANTS
option.
**
**
*RADIATE,OP=NEW
SUBU,R3,27.,0.2268E-8
SUBW,R4,27.,0.2268E-8
SUBE,R2,27.,0.2268E-8
**
V39,R3,27.,0.2268E-8
E39,R2,27.,0.2268E-8
W39,R4,27.,0.2268E-8
**
R
**
RRRRRRRRRRRRRRRRRRRRRRRRRR
RRRR
**
**
SSSSSSSSSSSSSSSSSSSSSSSSSS
SSSS
**
S
*DFLUX,OP=NEW
**
**
S
**
S
**
SSSSSSSSSSSSSSSSSSSSSSSSSS
SSSS
**
** OUTPUT
*NODE FILE
NT
*OUTPUT, FIELD,
FREQUENCY=1, OP=ADD
*ELEMENT OUTPUT,
ELSET=MOD40
TEMP
**
**
*END STEP
** ----- END OF
STEP 40 -----
--
**
**
#####
#####
**
**

```

**Input file for 2D
temperature with
properties dependent on
composition**

```

*HEADING
**
** ABAQUS INPUT FILE
UPGRADE: This input file
was upgraded from
** version 5.8 or later
to version 6.3 with 20
warning(s) and 0
** error(s).
**
** Search the input file
for **WARNING.
  2D LASER CLADDING
**al25
**
**
** MESH GEN
**
** *NODE,NSET=P1
101,0.000000,0.000000
**
**
** *NODE,NSET=P2
1101,0.000000,0.006670
**
**
** *NODE,NSET=P3
2101,0.002578,0.007959
**
**
** *NODE,NSET=P4
2121,0.005000,0.007959
**
**
** *NODE,NSET=P5
1121,0.006502,0.006670
**
**
** *NODE,NSET=P6
121,0.006502,0.000000
**
**
** *NODE,NSET=P7
721,0.006502,0.006410
**
**
** *NODE,NSET=P8
701,0.000000,0.006410
**
**
** *NCOPY, CHANGE
NUMBER=100, OLDSET=P5, SHIF
T, NEW SET=ROT1,
MULTIPLE=9
**
**
** 0., 0., 0.
0.005000, 0.006440, 0., 0.00
5000, 0.006440, 0.01, 7.90
**
**
** *NSET, NSET=R1
ROT1, P4, P5
** *NFILL, NSET=R2
P2, P3, 10, 100

```

```

**
**
** *NFILL, NSET=R3A, BIAS=1.50
**
** P6, P7, 6, 100
**
**
** *NFILL, NSET=R4A, BIAS=1.50
**
** P1, P8, 6, 100
**
**
** *NFILL, NSET=R3B, BIAS=1.00
**
** P7, P5, 4, 100
**
**
** *NFILL, NSET=R4B, BIAS=1.00
**
** P8, P2, 4, 100
**
**
** *NSET, NSET=R3
R3A, R3B
**
** *NSET, NSET=R4
R4A, R4B
**
**
** *NSET, NSET=R5
R1, R3
** *NSET, NSET=R6
R2, R4
**
**
** *NFILL, NSET=S1, BIAS=1.00
**
** R6, R5, 20, 1
**
**
** *NCOPY, CHANGE
NUMBER=20, OLDSET=R5, SHIFT
, NEW SET=R7
**
**
** 0.005000, 0.
0., 0., 0., 0., 0., 0.1, 0.
**
**
**
** *NFILL, NSET=S2
R5, R7, 20, 1
**
**
** *NCOPY, CHANGE
NUMBER=50, OLDSET=R6, SHIFT
, NEW SET=R8
**
**
** 0.050000, 0.
0., 0., 0., 0., 0., 0.1, 0.
**
**
**
** *NFILL, NSET=S3, BIAS=0.60
**
** R7, R8, 10, 1
**
**
** *NSET, NSET=SUB, GENERATE
101, 151, 1
**
** 201, 251, 1

```

```

**
** 301, 351, 1
**
** 401, 451, 1
**
** 501, 551, 1
**
** 601, 651, 1
**
** 701, 751, 1
**
** 801, 851, 1
**
** 901, 951, 1
**
** 1001, 1051, 1
**
** 1101, 1151, 1
** *NSET, NSET=CLD, GENERATE
1201, 1251, 1
**
** 1301, 1351, 1
**
** 1401, 1451, 1
**
** 1501, 1551, 1
**
** 1601, 1651, 1
**
** 1701, 1751, 1
**
** 1801, 1851, 1
**
** 1901, 1951, 1
**
** 2001, 2051, 1
**
** 2101, 2151, 1
**
**
** *NSET, NSET=ALL
SUB, CLD
** *ELEMENT, TYPE=DC2D4
101, 101, 102, 202, 201
**
**
** 1101, 1101, 1102, 1202, 1201
**
**
**
** #####
####
** element sets
**
** *ELGEN, ELSET=SUB
101, 50, 1, 1, 10, 100, 100
**
**
** *ELGEN, ELSET=CLD
1101, 40, 1, 1, 10, 100, 100
**
**
**
** #####
####
** *ELSET, ELSET=SUBU, GENERAT
E
1001, 1002, 1
1041, 1050, 1
**

```

```

**
*ELSET, ELSET=SUBD, GENERATE
E
101, 150, 1
**
**
*ELSET, ELSET=SUBW, GENERATE
E
101, 1001, 100
**
**
*ELSET, ELSET=SUBE, GENERATE
E
150, 1050, 100
**
**
*ELSET, ELSET=U1, GENERATE
1003, 1040, 1
*ELSET, ELSET=U2, GENERATE
1004, 1040, 1
*ELSET, ELSET=U3, GENERATE
1005, 1040, 1
*ELSET, ELSET=U4, GENERATE
1006, 1040, 1
*ELSET, ELSET=U5, GENERATE
1007, 1040, 1
*ELSET, ELSET=U6, GENERATE
1008, 1040, 1
*ELSET, ELSET=U7, GENERATE
1009, 1040, 1
*ELSET, ELSET=U8, GENERATE
1010, 1040, 1
*ELSET, ELSET=U9, GENERATE
1011, 1040, 1
*ELSET, ELSET=U10, GENERATE
1012, 1040, 1
*ELSET, ELSET=U11, GENERATE
1013, 1040, 1
*ELSET, ELSET=U12, GENERATE
1014, 1040, 1
*ELSET, ELSET=U13, GENERATE
1015, 1040, 1
*ELSET, ELSET=U14, GENERATE
1016, 1040, 1
*ELSET, ELSET=U15, GENERATE
1017, 1040, 1
*ELSET, ELSET=U16, GENERATE
1018, 1040, 1
*ELSET, ELSET=U17, GENERATE
1019, 1040, 1
*ELSET, ELSET=U18, GENERATE
1020, 1040, 1
*ELSET, ELSET=U19, GENERATE
1021, 1040, 1
*ELSET, ELSET=U20, GENERATE
1022, 1040, 1
*ELSET, ELSET=U21, GENERATE
1023, 1040, 1
*ELSET, ELSET=U22, GENERATE
1024, 1040, 1
*ELSET, ELSET=U23, GENERATE
1025, 1040, 1
*ELSET, ELSET=U24, GENERATE
1026, 1040, 1
*ELSET, ELSET=U25, GENERATE
1027, 1040, 1
*ELSET, ELSET=U26, GENERATE
1028, 1040, 1
*ELSET, ELSET=U27, GENERATE
1029, 1040, 1
*ELSET, ELSET=U28, GENERATE
1030, 1040, 1
*ELSET, ELSET=U29, GENERATE
1031, 1040, 1
*ELSET, ELSET=U30, GENERATE
1032, 1040, 1
*ELSET, ELSET=U31, GENERATE
1033, 1040, 1
*ELSET, ELSET=U32, GENERATE
1034, 1040, 1
*ELSET, ELSET=U33, GENERATE
1035, 1040, 1
*ELSET, ELSET=U34, GENERATE
1036, 1040, 1
*ELSET, ELSET=U35, GENERATE
1037, 1040, 1
*ELSET, ELSET=U36, GENERATE
1038, 1040, 1
*ELSET, ELSET=U37, GENERATE
1039, 1040, 1
*ELSET, ELSET=U38
1040
*ELSET, ELSET=E2
1103
*ELSET, ELSET=E3, GENERATE
1104, 1204, 100
*ELSET, ELSET=E4, GENERATE
1105, 1305, 100
*ELSET, ELSET=E5, GENERATE
1106, 1406, 100
*ELSET, ELSET=E6, GENERATE
1107, 1507, 100
*ELSET, ELSET=E7, GENERATE
1108, 1608, 100
*ELSET, ELSET=E8, GENERATE
1109, 1709, 100
*ELSET, ELSET=E9, GENERATE
1110, 1810, 100
*ELSET, ELSET=E10, GENERATE
1111, 1911, 100
*ELSET, ELSET=E11, GENERATE
1112, 2012, 100
*ELSET, ELSET=E12, GENERATE
1113, 2013, 100
*ELSET, ELSET=E13, GENERATE
1114, 2014, 100
*ELSET, ELSET=E14, GENERATE
1115, 2015, 100
*ELSET, ELSET=E15, GENERATE
1116, 2016, 100
*ELSET, ELSET=E16, GENERATE
1117, 2017, 100
*ELSET, ELSET=E17, GENERATE
1118, 2018, 100
*ELSET, ELSET=E18, GENERATE
1119, 2019, 100
*ELSET, ELSET=E19, GENERATE
1120, 2020, 100
*ELSET, ELSET=E20, GENERATE
1121, 2021, 100
*ELSET, ELSET=E21, GENERATE
1122, 2022, 100
*ELSET, ELSET=E22, GENERATE
1123, 2023, 100
*ELSET, ELSET=E23, GENERATE
1124, 2024, 100
*ELSET, ELSET=E24, GENERATE
1125, 2025, 100
*ELSET, ELSET=E25, GENERATE
1126, 2026, 100
*ELSET, ELSET=E26, GENERATE
1127, 2027, 100
*ELSET, ELSET=E27, GENERATE
1128, 2028, 100
*ELSET, ELSET=E28, GENERATE
1129, 2029, 100
*ELSET, ELSET=E29, GENERATE
1130, 2030, 100
*ELSET, ELSET=E30, GENERATE
1131, 2031, 100
*ELSET, ELSET=E31, GENERATE
1132, 2032, 100
*ELSET, ELSET=E32, GENERATE
1133, 2033, 100
*ELSET, ELSET=E33, GENERATE
1134, 2034, 100
*ELSET, ELSET=E34, GENERATE
1135, 2035, 100
*ELSET, ELSET=E35, GENERATE
1136, 2036, 100
*ELSET, ELSET=E36, GENERATE
1137, 2037, 100
*ELSET, ELSET=E37, GENERATE
1138, 2038, 100
*ELSET, ELSET=E38, GENERATE
1139, 2039, 100
*ELSET, ELSET=E39, GENERATE
1140, 2040, 100
*ELSET, ELSET=V2
1103
*ELSET, ELSET=V3, GENERATE
1203, 1204, 1
*ELSET, ELSET=V4, GENERATE
1303, 1305, 1
*ELSET, ELSET=V5, GENERATE
1403, 1406, 1
*ELSET, ELSET=V6, GENERATE
1503, 1507, 1
*ELSET, ELSET=V7, GENERATE
1603, 1608, 1
*ELSET, ELSET=V8, GENERATE
1703, 1709, 1
*ELSET, ELSET=V9, GENERATE
1803, 1810, 1
*ELSET, ELSET=V10, GENERATE
1903, 1911, 1
*ELSET, ELSET=V11, GENERATE
2003, 2012, 1
*ELSET, ELSET=V12, GENERATE
2003, 2013, 1
*ELSET, ELSET=V13, GENERATE
2003, 2014, 1
*ELSET, ELSET=V14, GENERATE
2003, 2015, 1
*ELSET, ELSET=V15, GENERATE
2003, 2016, 1
*ELSET, ELSET=V16, GENERATE
2003, 2017, 1
*ELSET, ELSET=V17, GENERATE
2003, 2018, 1
*ELSET, ELSET=V18, GENERATE
2003, 2019, 1
*ELSET, ELSET=V19, GENERATE
2003, 2020, 1
*ELSET, ELSET=V20, GENERATE
2003, 2021, 1
*ELSET, ELSET=V21, GENERATE
2003, 2022, 1
*ELSET, ELSET=V22, GENERATE
2003, 2023, 1
*ELSET, ELSET=V23, GENERATE
2003, 2024, 1
*ELSET, ELSET=V24, GENERATE

```

2003,2025,1	*ELSET,ELSET=W22,GENERATE	**
*ELSET,ELSET=V25,GENERATE	1103,2003,100	201,250,1
2003,2026,1	*ELSET,ELSET=W23,GENERATE	**
*ELSET,ELSET=V26,GENERATE	1103,2003,100	101,150,1
2003,2027,1	*ELSET,ELSET=W24,GENERATE	**
*ELSET,ELSET=V27,GENERATE	1103,2003,100	**
2003,2028,1	*ELSET,ELSET=W25,GENERATE	*ELSET,ELSET=MOD1
*ELSET,ELSET=V28,GENERATE	1103,2003,100	SUB
2003,2029,1	*ELSET,ELSET=W26,GENERATE	*ELSET,ELSET=MOD2
*ELSET,ELSET=V29,GENERATE	1103,2003,100	MOD1, E2, V2
2003,2030,1	*ELSET,ELSET=W27,GENERATE	*ELSET,ELSET=MOD3
*ELSET,ELSET=V30,GENERATE	1103,2003,100	MOD2, E3, V3
2003,2031,1	*ELSET,ELSET=W28,GENERATE	*ELSET,ELSET=MOD4
*ELSET,ELSET=V31,GENERATE	1103,2003,100	MOD3, E4, V4
2003,2032,1	*ELSET,ELSET=W29,GENERATE	*ELSET,ELSET=MOD5
*ELSET,ELSET=V32,GENERATE	1103,2003,100	MOD4, E5, V5
2003,2033,1	*ELSET,ELSET=W30,GENERATE	*ELSET,ELSET=MOD6
*ELSET,ELSET=V33,GENERATE	1103,2003,100	MOD5, E6, V6
2003,2034,1	*ELSET,ELSET=W31,GENERATE	*ELSET,ELSET=MOD7
*ELSET,ELSET=V34,GENERATE	1103,2003,100	MOD6, E7, V7
2003,2035,1	*ELSET,ELSET=W32,GENERATE	*ELSET,ELSET=MOD8
*ELSET,ELSET=V35,GENERATE	1103,2003,100	MOD7, E8, V8
2003,2036,1	*ELSET,ELSET=W33,GENERATE	*ELSET,ELSET=MOD9
*ELSET,ELSET=V36,GENERATE	1103,2003,100	MOD8, E9, V9
2003,2037,1	*ELSET,ELSET=W34,GENERATE	*ELSET,ELSET=MOD10
*ELSET,ELSET=V37,GENERATE	1103,2003,100	MOD9, E10, V10
2003,2038,1	*ELSET,ELSET=W35,GENERATE	*ELSET,ELSET=MOD11
*ELSET,ELSET=V38,GENERATE	1103,2003,100	MOD10, E11, V11
2003,2039,1	*ELSET,ELSET=W36,GENERATE	*ELSET,ELSET=MOD12
*ELSET,ELSET=V39,GENERATE	1103,2003,100	MOD11, E12
2003,2040,1	*ELSET,ELSET=W37,GENERATE	*ELSET,ELSET=MOD13
*ELSET,ELSET=W2	1103,2003,100	MOD12, E13
1103	*ELSET,ELSET=W38,GENERATE	*ELSET,ELSET=MOD14
*ELSET,ELSET=W3,GENERATE	1103,2003,100	MOD13, E14
1103,1203,100	*ELSET,ELSET=W39,GENERATE	*ELSET,ELSET=MOD15
*ELSET,ELSET=W4,GENERATE	1103,2003,100	MOD14, E15
1103,1303,100	*ELSET,ELSET=INT,	*ELSET,ELSET=MOD16
*ELSET,ELSET=W5,GENERATE	GENERATE	MOD15, E16
1103,1403,100	1003,1041,1	*ELSET,ELSET=MOD17
*ELSET,ELSET=W6,GENERATE	**	MOD16, E17
1103,1503,100	903,941,1	*ELSET,ELSET=MOD18
*ELSET,ELSET=W7,GENERATE	**	MOD17, E18
1103,1603,100	803,841,1	*ELSET,ELSET=MOD19
*ELSET,ELSET=W8,GENERATE	**	MOD18, E19
1103,1703,100	703,741,1	*ELSET,ELSET=MOD20
*ELSET,ELSET=W9,GENERATE	*ELSET,ELSET=BAS,	MOD19, E20
1103,1803,100	GENERATE	*ELSET,ELSET=MOD21
*ELSET,ELSET=W10,GENERATE	1001,1002,1	MOD20, E21
1103,1903,100	**	*ELSET,ELSET=MOD22
*ELSET,ELSET=W11,GENERATE	1042,1050,1	MOD21, E22
1103,2003,100	**	*ELSET,ELSET=MOD23
*ELSET,ELSET=W12,GENERATE	901,902,1	MOD22, E23
1103,2003,100	**	*ELSET,ELSET=MOD24
*ELSET,ELSET=W13,GENERATE	942,950,1	MOD23, E24
1103,2003,100	**	*ELSET,ELSET=MOD25
*ELSET,ELSET=W14,GENERATE	801,802,1	MOD24, E25
1103,2003,100	**	*ELSET,ELSET=MOD26
*ELSET,ELSET=W15,GENERATE	842,850,1	MOD25, E26
1103,2003,100	**	*ELSET,ELSET=MOD27
*ELSET,ELSET=W16,GENERATE	701,702,1	MOD26, E27
1103,2003,100	**	*ELSET,ELSET=MOD28
*ELSET,ELSET=W17,GENERATE	742,750,1	MOD27, E28
1103,2003,100	**	*ELSET,ELSET=MOD29
*ELSET,ELSET=W18,GENERATE	**	MOD28, E29
1103,2003,100	601,650,1	*ELSET,ELSET=MOD30
*ELSET,ELSET=W19,GENERATE	**	MOD29, E30
1103,2003,100	501,550,1	*ELSET,ELSET=MOD31
*ELSET,ELSET=W20,GENERATE	**	MOD30, E31
1103,2003,100	401,450,1	*ELSET,ELSET=MOD32
*ELSET,ELSET=W21,GENERATE	**	MOD31, E32
1103,2003,100	301,350,1	*ELSET,ELSET=MOD33

```

MOD32, E33          1.E3,0.33,585.,0.9          *DEPVAR
*ELSET,ELSET=MOD34 125.0E9,0.33,27.,1.          6
MOD33, E34          77.7E9,0.33,950.,1.          ** LC *USER DEFINED FIELD
*ELSET,ELSET=MOD35 1.E3,0.33,990.,1.          **
MOD34, E35          *PLASTIC,HARDENING=KINEMA          **
*ELSET,ELSET=MOD36 TIC,DEPENDENCIES=1          **
MOD35, E36          193.E6,0.,27.,0.          *RESTART,WRITE,FREQUENCY=
*ELSET,ELSET=MOD37 250.5E6,0.01,27.,0.          1000
MOD36, E37          19.E6,0.,516.,0.          **
*ELSET,ELSET=MOD38 27.5E6,0.1,516.,0.          **
MOD37, E38          18.9E6,0.,516.1,0.          **
*ELSET,ELSET=MOD39 18.9E6,0.1,516.1,0.          #####
MOD38, E39          197.E6,0.,27.,0.9          #####
*ELSET,ELSET=MOD40 320.E6,.01,27.,0.9          **
MOD39               20.E6,0.,516.,0.9          **
**               126.E6,.01,516.,0.9          ** ----- BEGINNING
**               19.9E6,0.,516.1,0.9          OF STEP 1 -----
*ELSET,ELSET=HIST, 19.9E6,0.01,516.1,0.9          ----
GENERATE           275.E6,0.,27.,1.          (...)
509,1709,400       744.E6,0.18,27.,1.
**519,1719,400     27.5E6,0.,950.,1.
529,1729,400       186.E6,1.1,950.,1.
**539,1739,400     27.4E6,0.,950.1,1.
**               27.4E6,2.,950.1,1.
**               *ANNEAL
#####           TEMPERATURE,DEPENDENCIES=
####            1
**             516.1,0.
*INITIAL        516.1,0.9
CONDITIONS,TYPE=SOLUTION, 950.1,1.
USER           *EXPANSION,ZERO=27.,DEPEN
*INITIAL       DENCIES=1
CONDITIONS,TYPE=FIELD,VAR 20.1E-6,27.,0.
TABLE=1        26.0E-6,516.,0.
SUB,0.0        19.1E-6,27.,0.9
CLD,1.0        24.8E-6,516.,0.9
**            16.5E-6,27.,1.
*INITIAL       25.1E-6,950.,1.
CONDITIONS,TYPE=TEMPERATU *CONDUCTIVITY,DEPENDENCIE
RE             S=1
SUB,27.        117.,27.,0.
CLD,2000.     117.,27.,0.9
**INITIAL     12.1,27.,1.
CONDITIONS,TYPE=MASS FLOW 85.9,950.,1.
RATE          *DENSITY,DEPENDENCIES=1
**SUB,-75.42  2770.,27.,0.
**CLD,-49.25  2676.,516.,0.
** MATERIALS PROPERTIES  3087.,27.,0.9
**           2990.,516.,0.9
*SOLID        7530.,27.,1.
SECTION,ELSET=BAS,MATERIA 7096.,950.,1.
L=ALB         **LATENT
*SOLID        HEAT,DEPENDENCIES=1
SECTION,ELSET=INT,MATERIA **389000.,516.,585.,0.
L=ALB         **389000.,516.,585.,0.9
*SOLID        **205000.,950.,990.,1.
SECTION,ELSET=CLD,MATERIA *SPECIFIC
L=ALB         HEAT,DEPENDENCIES=1
**           963.,27.,0.
** insert properties 1274.,516.,0.
**           895.,27.,0.9
** -----|          1298.,516.,0.9
*MATERIAL,NAME=ALB     440.,27.,1.
*USER DEFINED FIELD    625.,950.,1.
*ELASTIC,DEPENDENCIES=1 **
73.0E9,0.34,27.,0.     ** -----|
52.8E9,0.34,516.,0.   **
1.E3,0.34,585.,0.     *****
75.2E9,0.33,27.,0.9   *****
59.1E9,0.33,516.,0.9 **

```

Input file for 2D stress

```
*HEADING
**
** ABAQUS INPUT FILE
UPGRADE: This input file
was upgraded from
** version 5.8 or later
to version 6.3 with 0
warning(s) and 1
** error(s).
**
** Search the input file
for **ERROR.
  2D LASER CLADDING
**bl22
**
**
** MESH GEN
**
** generalized plane
strain
**
**
** extra nodes
*NODE
10,0.01,0.
**20,0.,1.
**
*NODE,NSET=P1
101,0.000000,0.000000
**
**
*NODE,NSET=P2
1101,0.000000,0.006670
**
**
*NODE,NSET=P3
2101,0.002578,0.007959
**
**
*NODE,NSET=P4
2121,0.005000,0.007959
**
**
*NODE,NSET=P5
1121,0.006502,0.006670
**
**
*NODE,NSET=P6
121,0.006502,0.000000
**
**
*NODE,NSET=P7
721,0.006502,0.006410
**
**
*NODE,NSET=P8
701,0.000000,0.006410
**
**
*NCOPY,CHANGE
NUMBER=100,OLDSET=P5,SHIF
T,NEW SET=ROT1,
MULTIPLE=9
**
**
0.,0.,0.
0.005000,0.006440,0.,0.00
5000,0.006440,0.01,7.90
**
```

```
**
*NSET,NSET=R1
ROT1,P4,P5
*NFILL,NSET=R2
P2,P3,10,100
**
**
*NFILL,NSET=R3A,BIAS=1.50
**
P6,P7,6,100
**
**
*NFILL,NSET=R4A,BIAS=1.50
**
P1,P8,6,100
**
**
*NFILL,NSET=R3B,BIAS=1.00
**
P7,P5,4,100
**
**
*NFILL,NSET=R4B,BIAS=1.00
**
P8,P2,4,100
**
**
*NSET,NSET=R3
R3A,R3B
**
**
*NSET,NSET=R4
R4A,R4B
**
**
*NSET,NSET=R5
R1,R3
*NSET,NSET=R6
R2,R4
**
**
*NFILL,NSET=S1,BIAS=1.00
**
R6,R5,20,1
**
**
**
*NCOPY,CHANGE
NUMBER=20,OLDSET=R5,SHIFT
,NEW SET=R7
**
**
0.005000,0.
0.,0.,0.,0.,0.,0.1,0.
**
**
*NFILL,NSET=S2
R5,R7,20,1
**
**
*NCOPY,CHANGE
NUMBER=50,OLDSET=R6,SHIFT
,NEW SET=R8
**
**
0.050000,0.
0.,0.,0.,0.,0.,0.1,0.
**
**
*NFILL,NSET=S3,BIAS=0.60
**
R7,R8,10,1
**
```

```
**
*NSET,NSET=SUB,GENERATE
101,151,1
**
201,251,1
**
301,351,1
**
401,451,1
**
501,551,1
**
601,651,1
**
701,751,1
**
801,851,1
**
901,951,1
**
1001,1051,1
**
1101,1151,1
*NSET,NSET=CLD,GENERATE
1201,1251,1
**
1301,1351,1
**
1401,1451,1
**
1501,1551,1
**
1601,1651,1
**
1701,1751,1
**
1801,1851,1
**
1901,1951,1
**
2001,2051,1
**
2101,2151,1
**
**
*NSET,NSET=ALL
SUB,CLD
**
**
**ERROR: Then name
of CGPEn elements has
been changed to CPEGn.
The two
**
additional
nodes listed in the
connectivity have been
replaced by a single node
**
defined with
the REF NODE parameter on
the corresponding *SOLID
SECTION option.
**
These changes
need to be made manually.
**
**
*ELEMENT,TYPE=CPEG4
101,101,102,202,201
**
**
1101,1101,1102,1202,1201
**
```

```

**
**
#####
####
**      element sets
**
*ELGEN,ELSET=SUB
101,50,1,1,10,100,100
**
**
*ELGEN,ELSET=CLD
1101,40,1,1,10,100,100
**
**
**
#####
####
**
*ELSET,ELSET=SUBU,GENERAT
E
1001,1002,1
1041,1050,1
**
**
*ELSET,ELSET=SUBD,GENERAT
E
101,150,1
**
**
*ELSET,ELSET=SUBW,GENERAT
E
101,1001,100
**
**
*ELSET,ELSET=SUBE,GENERAT
E
150,1050,100
**
**
*ELSET,ELSET=U1,GENERATE
1003,1040,1
*ELSET,ELSET=U2,GENERATE
1004,1040,1
*ELSET,ELSET=U3,GENERATE
1005,1040,1
*ELSET,ELSET=U4,GENERATE
1006,1040,1
*ELSET,ELSET=U5,GENERATE
1007,1040,1
*ELSET,ELSET=U6,GENERATE
1008,1040,1
*ELSET,ELSET=U7,GENERATE
1009,1040,1
*ELSET,ELSET=U8,GENERATE
1010,1040,1
*ELSET,ELSET=U9,GENERATE
1011,1040,1
*ELSET,ELSET=U10,GENERATE
1012,1040,1
*ELSET,ELSET=U11,GENERATE
1013,1040,1
*ELSET,ELSET=U12,GENERATE
1014,1040,1
*ELSET,ELSET=U13,GENERATE
1015,1040,1
*ELSET,ELSET=U14,GENERATE
1016,1040,1
*ELSET,ELSET=U15,GENERATE
1017,1040,1
*ELSET,ELSET=U16,GENERATE
1018,1040,1

*ELSET,ELSET=U17,GENERATE
1019,1040,1
*ELSET,ELSET=U18,GENERATE
1020,1040,1
*ELSET,ELSET=U19,GENERATE
1021,1040,1
*ELSET,ELSET=U20,GENERATE
1022,1040,1
*ELSET,ELSET=U21,GENERATE
1023,1040,1
*ELSET,ELSET=U22,GENERATE
1024,1040,1
*ELSET,ELSET=U23,GENERATE
1025,1040,1
*ELSET,ELSET=U24,GENERATE
1026,1040,1
*ELSET,ELSET=U25,GENERATE
1027,1040,1
*ELSET,ELSET=U26,GENERATE
1028,1040,1
*ELSET,ELSET=U27,GENERATE
1029,1040,1
*ELSET,ELSET=U28,GENERATE
1030,1040,1
*ELSET,ELSET=U29,GENERATE
1031,1040,1
*ELSET,ELSET=U30,GENERATE
1032,1040,1
*ELSET,ELSET=U31,GENERATE
1033,1040,1
*ELSET,ELSET=U32,GENERATE
1034,1040,1
*ELSET,ELSET=U33,GENERATE
1035,1040,1
*ELSET,ELSET=U34,GENERATE
1036,1040,1
*ELSET,ELSET=U35,GENERATE
1037,1040,1
*ELSET,ELSET=U36,GENERATE
1038,1040,1
*ELSET,ELSET=U37,GENERATE
1039,1040,1
*ELSET,ELSET=U38
1040
*ELSET,ELSET=E2
1103
*ELSET,ELSET=E3,GENERATE
1104,1204,100
*ELSET,ELSET=E4,GENERATE
1105,1305,100
*ELSET,ELSET=E5,GENERATE
1106,1406,100
*ELSET,ELSET=E6,GENERATE
1107,1507,100
*ELSET,ELSET=E7,GENERATE
1108,1608,100
*ELSET,ELSET=E8,GENERATE
1109,1709,100
*ELSET,ELSET=E9,GENERATE
1110,1810,100
*ELSET,ELSET=E10,GENERATE
1111,1911,100
*ELSET,ELSET=E11,GENERATE
1112,2012,100
*ELSET,ELSET=E12,GENERATE
1113,2013,100
*ELSET,ELSET=E13,GENERATE
1114,2014,100
*ELSET,ELSET=E14,GENERATE
1115,2015,100
*ELSET,ELSET=E15,GENERATE
1116,2016,100
*ELSET,ELSET=E16,GENERATE
1117,2017,100
*ELSET,ELSET=E17,GENERATE
1118,2018,100
*ELSET,ELSET=E18,GENERATE
1119,2019,100
*ELSET,ELSET=E19,GENERATE
1120,2020,100
*ELSET,ELSET=E20,GENERATE
1121,2021,100
*ELSET,ELSET=E21,GENERATE
1122,2022,100
*ELSET,ELSET=E22,GENERATE
1123,2023,100
*ELSET,ELSET=E23,GENERATE
1124,2024,100
*ELSET,ELSET=E24,GENERATE
1125,2025,100
*ELSET,ELSET=E25,GENERATE
1126,2026,100
*ELSET,ELSET=E26,GENERATE
1127,2027,100
*ELSET,ELSET=E27,GENERATE
1128,2028,100
*ELSET,ELSET=E28,GENERATE
1129,2029,100
*ELSET,ELSET=E29,GENERATE
1130,2030,100
*ELSET,ELSET=E30,GENERATE
1131,2031,100
*ELSET,ELSET=E31,GENERATE
1132,2032,100
*ELSET,ELSET=E32,GENERATE
1133,2033,100
*ELSET,ELSET=E33,GENERATE
1134,2034,100
*ELSET,ELSET=E34,GENERATE
1135,2035,100
*ELSET,ELSET=E35,GENERATE
1136,2036,100
*ELSET,ELSET=E36,GENERATE
1137,2037,100
*ELSET,ELSET=E37,GENERATE
1138,2038,100
*ELSET,ELSET=E38,GENERATE
1139,2039,100
*ELSET,ELSET=E39,GENERATE
1140,2040,100
*ELSET,ELSET=V2
1103
*ELSET,ELSET=V3,GENERATE
1203,1204,1
*ELSET,ELSET=V4,GENERATE
1303,1305,1
*ELSET,ELSET=V5,GENERATE
1403,1406,1
*ELSET,ELSET=V6,GENERATE
1503,1507,1
*ELSET,ELSET=V7,GENERATE
1603,1608,1
*ELSET,ELSET=V8,GENERATE
1703,1709,1
*ELSET,ELSET=V9,GENERATE
1803,1810,1
*ELSET,ELSET=V10,GENERATE
1903,1911,1
*ELSET,ELSET=V11,GENERATE
2003,2012,1
*ELSET,ELSET=V12,GENERATE
2003,2013,1

```

*ELSET, ELSET=V13, GENERATE	1103, 1903, 100	**
2003, 2014, 1	*ELSET, ELSET=W11, GENERATE	1042, 1050, 1
*ELSET, ELSET=V14, GENERATE	1103, 2003, 100	**
2003, 2015, 1	*ELSET, ELSET=W12, GENERATE	901, 902, 1
*ELSET, ELSET=V15, GENERATE	1103, 2003, 100	**
2003, 2016, 1	*ELSET, ELSET=W13, GENERATE	942, 950, 1
*ELSET, ELSET=V16, GENERATE	1103, 2003, 100	**
2003, 2017, 1	*ELSET, ELSET=W14, GENERATE	801, 802, 1
*ELSET, ELSET=V17, GENERATE	1103, 2003, 100	**
2003, 2018, 1	*ELSET, ELSET=W15, GENERATE	842, 850, 1
*ELSET, ELSET=V18, GENERATE	1103, 2003, 100	**
2003, 2019, 1	*ELSET, ELSET=W16, GENERATE	701, 702, 1
*ELSET, ELSET=V19, GENERATE	1103, 2003, 100	**
2003, 2020, 1	*ELSET, ELSET=W17, GENERATE	742, 750, 1
*ELSET, ELSET=V20, GENERATE	1103, 2003, 100	**
2003, 2021, 1	*ELSET, ELSET=W18, GENERATE	**
*ELSET, ELSET=V21, GENERATE	1103, 2003, 100	601, 650, 1
2003, 2022, 1	*ELSET, ELSET=W19, GENERATE	**
*ELSET, ELSET=V22, GENERATE	1103, 2003, 100	501, 550, 1
2003, 2023, 1	*ELSET, ELSET=W20, GENERATE	**
*ELSET, ELSET=V23, GENERATE	1103, 2003, 100	401, 450, 1
2003, 2024, 1	*ELSET, ELSET=W21, GENERATE	**
*ELSET, ELSET=V24, GENERATE	1103, 2003, 100	301, 350, 1
2003, 2025, 1	*ELSET, ELSET=W22, GENERATE	**
*ELSET, ELSET=V25, GENERATE	1103, 2003, 100	201, 250, 1
2003, 2026, 1	*ELSET, ELSET=W23, GENERATE	**
*ELSET, ELSET=V26, GENERATE	1103, 2003, 100	101, 150, 1
2003, 2027, 1	*ELSET, ELSET=W24, GENERATE	**
*ELSET, ELSET=V27, GENERATE	1103, 2003, 100	**
2003, 2028, 1	*ELSET, ELSET=W25, GENERATE	*ELSET, ELSET=MOD1
*ELSET, ELSET=V28, GENERATE	1103, 2003, 100	SUB
2003, 2029, 1	*ELSET, ELSET=W26, GENERATE	*ELSET, ELSET=MOD2
*ELSET, ELSET=V29, GENERATE	1103, 2003, 100	MOD1, E2, V2
2003, 2030, 1	*ELSET, ELSET=W27, GENERATE	*ELSET, ELSET=MOD3
*ELSET, ELSET=V30, GENERATE	1103, 2003, 100	MOD2, E3, V3
2003, 2031, 1	*ELSET, ELSET=W28, GENERATE	*ELSET, ELSET=MOD4
*ELSET, ELSET=V31, GENERATE	1103, 2003, 100	MOD3, E4, V4
2003, 2032, 1	*ELSET, ELSET=W29, GENERATE	*ELSET, ELSET=MOD5
*ELSET, ELSET=V32, GENERATE	1103, 2003, 100	MOD4, E5, V5
2003, 2033, 1	*ELSET, ELSET=W30, GENERATE	*ELSET, ELSET=MOD6
*ELSET, ELSET=V33, GENERATE	1103, 2003, 100	MOD5, E6, V6
2003, 2034, 1	*ELSET, ELSET=W31, GENERATE	*ELSET, ELSET=MOD7
*ELSET, ELSET=V34, GENERATE	1103, 2003, 100	MOD6, E7, V7
2003, 2035, 1	*ELSET, ELSET=W32, GENERATE	*ELSET, ELSET=MOD8
*ELSET, ELSET=V35, GENERATE	1103, 2003, 100	MOD7, E8, V8
2003, 2036, 1	*ELSET, ELSET=W33, GENERATE	*ELSET, ELSET=MOD9
*ELSET, ELSET=V36, GENERATE	1103, 2003, 100	MOD8, E9, V9
2003, 2037, 1	*ELSET, ELSET=W34, GENERATE	*ELSET, ELSET=MOD10
*ELSET, ELSET=V37, GENERATE	1103, 2003, 100	MOD9, E10, V10
2003, 2038, 1	*ELSET, ELSET=W35, GENERATE	*ELSET, ELSET=MOD11
*ELSET, ELSET=V38, GENERATE	1103, 2003, 100	MOD10, E11, V11
2003, 2039, 1	*ELSET, ELSET=W36, GENERATE	*ELSET, ELSET=MOD12
*ELSET, ELSET=V39, GENERATE	1103, 2003, 100	MOD11, E12
2003, 2040, 1	*ELSET, ELSET=W37, GENERATE	*ELSET, ELSET=MOD13
*ELSET, ELSET=W2	1103, 2003, 100	MOD12, E13
1103	*ELSET, ELSET=W38, GENERATE	*ELSET, ELSET=MOD14
*ELSET, ELSET=W3, GENERATE	1103, 2003, 100	MOD13, E14
1103, 1203, 100	*ELSET, ELSET=W39, GENERATE	*ELSET, ELSET=MOD15
*ELSET, ELSET=W4, GENERATE	1103, 2003, 100	MOD14, E15
1103, 1303, 100	*ELSET, ELSET=INT,	*ELSET, ELSET=MOD16
*ELSET, ELSET=W5, GENERATE	GENERATE	MOD15, E16
1103, 1403, 100	1003, 1041, 1	*ELSET, ELSET=MOD17
*ELSET, ELSET=W6, GENERATE	**	MOD16, E17
1103, 1503, 100	903, 941, 1	*ELSET, ELSET=MOD18
*ELSET, ELSET=W7, GENERATE	**	MOD17, E18
1103, 1603, 100	803, 841, 1	*ELSET, ELSET=MOD19
*ELSET, ELSET=W8, GENERATE	**	MOD18, E19
1103, 1703, 100	703, 741, 1	*ELSET, ELSET=MOD20
*ELSET, ELSET=W9, GENERATE	*ELSET, ELSET=BAS,	MOD19, E20
1103, 1803, 100	GENERATE	*ELSET, ELSET=MOD21
*ELSET, ELSET=W10, GENERATE	1001, 1002, 1	MOD20, E21

```

*ELSET,ELSET=MOD22
MOD21, E22
*ELSET,ELSET=MOD23
MOD22, E23
*ELSET,ELSET=MOD24
MOD23, E24
*ELSET,ELSET=MOD25
MOD24, E25
*ELSET,ELSET=MOD26
MOD25, E26
*ELSET,ELSET=MOD27
MOD26, E27
*ELSET,ELSET=MOD28
MOD27, E28
*ELSET,ELSET=MOD29
MOD28, E29
*ELSET,ELSET=MOD30
MOD29, E30
*ELSET,ELSET=MOD31
MOD30, E31
*ELSET,ELSET=MOD32
MOD31, E32
*ELSET,ELSET=MOD33
MOD32, E33
*ELSET,ELSET=MOD34
MOD33, E34
*ELSET,ELSET=MOD35
MOD34, E35
*ELSET,ELSET=MOD36
MOD35, E36
*ELSET,ELSET=MOD37
MOD36, E37
*ELSET,ELSET=MOD38
MOD37, E38
*ELSET,ELSET=MOD39
MOD38, E39
*ELSET,ELSET=MOD40
MOD39
**
**
*ELSET,ELSET=HIST,
GENERATE
509,1709,400
519,1719,400
529,1729,400
539,1739,400
**
**
#####
####
**
**
*PHYSICAL CONSTANTS,
ABSOLUTE ZERO=-273.
**INITIAL
CONDITIONS,TYPE=TEMPERATU
RE
**SUB,27.
**CLD,27.
**INITIAL
CONDITIONS,TYPE=MASS FLOW
RATE
**SUB,-75.42
**CLD,-49.25
** MATERIALS PROPERTIES
**
*SOLID SECTION,REF
NODE=10,
ELSET=BAS,MATERIAL=ALBAS

```

```

*SOLID SECTION,REF
NODE=10,
ELSET=INT,MATERIAL=ALBAS
*SOLID SECTION,REF
NODE=10,
ELSET=CLD,MATERIAL=CUBAS
**
** insert properties
**
**
** -----
-----|
*MATERIAL,NAME=ALBAS
*ELASTIC
73.0E9,0.34,27.
52.8E9,0.34,516.
1.E3,0.34,585.
*PLASTIC,HARDENING=KINEMA
TIC
193.E6,0.,27.
250.5E6,0.01,27.
19.E6,0.,516.
27.5E6,0.1,516.
18.9E6,0.,516.1
18.9E6,0.1,516.1
*ANNEAL TEMPERATURE
516.1
*EXPANSION,ZERO=27.
20.1E-6,27.
26.0E-6,516.
*CONDUCTIVITY
117.,27.
*DENSITY
2770.,27.
2676.,516.
*LATENT HEAT
389000.,516.,585.
*SPECIFIC HEAT
963.,27.
1274.,516.
** -----
-----|
*MATERIAL,NAME=INTER
*ELASTIC
75.2E9,0.33,27.
59.1E9,0.33,516.
1.E3,0.33,585.
*PLASTIC,HARDENING=KINEMA
TIC
197.E6,0.,27.
320.E6,.01,27.
20.E6,0.,516.
126.E6,.01,516.
19.9E6,0.,516.1
19.9E6,0.01,516.1
*ANNEAL TEMPERATURE
516.1
*EXPANSION,ZERO=27.
19.1E-6,27.
24.8E-6,516.
*CONDUCTIVITY
117.,27.
*DENSITY
3087.,27.
2990.,516.
*LATENT HEAT
389000.,516.,585.
*SPECIFIC HEAT
895.,27.
1298.,516.

```

```

** -----
-----|
*MATERIAL,NAME=CUBAS
*ELASTIC
125.0E9,0.33,27.
77.7E9,0.33,950.
1.E3,0.33,990.
*PLASTIC,HARDENING=KINEMA
TIC
275.E6,0.,27.
744.E6,0.18,27.
27.5E6,0.,950.
186.E6,1.1,950.
27.4E6,0.,950.1
27.4E6,2.,950.1
*ANNEAL TEMPERATURE
950.1
*EXPANSION,ZERO=27.
16.5E-6,27.
25.1E-6,950.
*CONDUCTIVITY
12.1,27.
85.9,950.
*DENSITY
7530.,27.
7096.,950.
*LATENT HEAT
205000.,950.,990.
*SPECIFIC HEAT
440.,27.
625.,950.
**
**
*BOUNDARY
101,2,6
151,ENCASTRE
*RESTART,WRITE,FREQUENCY=
1000
**
**
#####
#####
**
**
** ----- BEGINNING
OF STEP 1 -----
----
*STEP,INC=10000
*STATIC
1.0E-10,0.072013615
*MODEL CHANGE,REMOVE
CLD
*TEMPERATURE,FILE=a122,BS
TEP=1,ESTEP=1
**
*OUTPUT, FIELD,
FREQUENCY=20
*ELEMENT OUTPUT,
ELSET=MOD1
S,E,PEEQ,PEMAG,THE,PE
*NODE OUTPUT
U
**
*OUTPUT, HISTORY,
FREQUENCY=20
*ELEMENT OUTPUT,
ELSET=HIST
S11,MISES
**
**

```

```

*END STEP
** ----- END OF
STEP 1 -----
-
**
#####
#####
**
**
** ----- BEGINNING
OF STEP2 -----
*STEP, INC=10000
*STATIC
1.0E-10, 0.026006808
*MODEL CHANGE, ADD
E2, V2
*TEMPERATURE, FILE=a122, BS
TEP=2, ESTEP=2
*OUTPUT, FIELD,
FREQUENCY=20, OP=ADD
*ELEMENT OUTPUT,
ELSET=MOD2
S, E, PEEQ, PEMAG, THE, PE
*NODE OUTPUT
U
**
**
*OUTPUT, HISTORY,
FREQUENCY=20
*ELEMENT OUTPUT,
ELSET=HIST
S11, MISES
**
*END STEP
** ----- END OF
STEP 2 -----
-
**
**
#####
#####
**
**
**

```

Input file for 3D temperature

*HEADING
 **
 ** ABAQUS INPUT FILE
 UPGRADE: This input file was upgraded from
 ** version 5.8 or later to version 6.3 with 20 warning(s) and 0 error(s).
 **
 ** Search the input file for **WARNING.
 3D LASER CLADDING
 **c511
 **
 ** MESH GEN
 **
 *NODE,NSET=P1
 10101,0.000000,0.000000,0.000000
 .000000
 **
 **
 *NODE,NSET=P2
 10601,0.000000,0.006670,0.000000
 **
 **
 *NODE,NSET=P3
 11101,0.000000,0.007959,0.000000
 **
 **
 *NODE,NSET=P4
 11111,0.005000,0.007959,0.000000
 **
 **
 *NODE,NSET=P5
 10611,0.006502,0.006670,0.000000
 **
 **
 *NODE,NSET=P6
 10111,0.006502,0.000000,0.000000
 **
 **
 *NCOPY,CHANGE
 NUMBER=100,OLDSET=P5,SHIFT,NEW SET=ROT1,
 MULTIPLE=4
 **
 **
 0.,0.,0.
 0.005000,0.006440,0.,0.005000,0.006440,0.01,14.00
 **
 **
 *NSET,NSET=R1
 ROT1,P4,P5
 *NFILL,NSET=R2
 P2,P3,5,100
 **
 **
 *NFILL,NSET=R3,BIAS=2.7
 **
 **
 P6,P5,5,100

**
 **
 *NFILL,NSET=R4,BIAS=2.7
 **
 P1,P2,5,100
 **
 **
 *NSET,NSET=R5
 R1,R3
 *NSET,NSET=R6
 R2,R4
 **
 *NFILL,NSET=S1,BIAS=1.1
 **
 R6,R5,10,1
 **
 **
 *NCOPY,CHANGE
 NUMBER=10,OLDSET=R5,SHIFT,NEW SET=R7
 **
 **
 0.005000,0.,0.
 0.,0.,0.,0.,0.,0.1,0.
 **
 **
 *NFILL,NSET=S2
 R5,R7,10,1
 **
 **
 *NCOPY,CHANGE
 NUMBER=25,OLDSET=R6,SHIFT,NEW SET=R8
 **
 **
 0.020000,0.,0.
 0.,0.,0.,0.,0.,0.1,0.
 **
 **
 *NFILL,NSET=S3,BIAS=0.45
 **
 R7,R8,5,1
 **
 **
 *NSET,NSET=SUB,GENERATE
 10601,10626,1
 10501,10526,1
 10401,10426,1
 10301,10326,1
 10201,10226,1
 10101,10126,1
 *NSET,NSET=CLD,GENERATE
 11101,11121,1
 11001,11021,1
 10901,10921,1
 10801,10821,1
 10701,10721,1
 **
 *NCOPY,CHANGE
 NUMBER=10000,OLDSET=CLD,SHIFT,NEW SET=ROT2,
 MULTIPLE=4
 **
 **
 0.,0.,0.
 0.000000,0.006670,0.000000,0.006502,0.006670,0.000000,18.00
 **
 **
 *NSET,NSET=CD

ROT2, CLD
 **
 **
 *NSET,NSET=LL1,GENERATE
 10701,10721,1
 *NSET,NSET=LL2,GENERATE
 10801,10821,1
 *NSET,NSET=LL3,GENERATE
 10901,10921,1
 *NSET,NSET=LL4,GENERATE
 11001,11021,1
 *NSET,NSET=LL5,GENERATE
 11101,11121,1
 *NCOPY,CHANGE
 NUMBER=9900,OLDSET=LL1,SHIFT,NEW SET=LM1,
 MULTIPLE=1
 **
 **
 0.,0.,0.
 **
 **
 0.00,0.00667,0.00,0.0065017,0.00667,0.00,90.00
 **
 **
 *NCOPY,CHANGE
 NUMBER=19800,OLDSET=LL2,SHIFT,NEW SET=LM2,
 MULTIPLE=1
 **
 **
 0.,0.,0.
 **
 **
 0.00,0.00667,0.00,0.0065017,0.00667,0.00,90.00
 **
 **
 *NCOPY,CHANGE
 NUMBER=29700,OLDSET=LL3,SHIFT,NEW SET=LM3,
 MULTIPLE=1
 **
 **
 0.,0.,0.
 **
 **
 0.00,0.00667,0.00,0.0065017,0.00667,0.00,90.00
 **
 **
 *NCOPY,CHANGE
 NUMBER=39600,OLDSET=LL4,SHIFT,NEW SET=LM4,
 MULTIPLE=1
 **
 **
 0.,0.,0.
 **
 **
 0.00,0.00667,0.00,0.0065017,0.00667,0.00,90.00
 **
 **
 *NCOPY,CHANGE
 NUMBER=49500,OLDSET=LL5,SHIFT,NEW SET=LM5,
 MULTIPLE=1
 **
 **
 0.,0.,0.
 **
 **

```

0.00,0.00667,0.00,0.00650
17,0.00667,0.00,90.00
**
*NSET,NSET=LMM
LM1,
LM2,
LM3,
LM4,
LM5
**
*NCOPY,CHANGE NUMBER=-
500,OLDSET=LMM,SHIFT,NEW
SET=LMN
0.,-0.006670,0.
0.,0.,0.,0.,0.,0.1,0.
**
**
*NFILL,NSET=MM,BIAS=2.7
LMN,LMM,5,100
**
**
*NCOPY,CHANGE
NUMBER=100000,OLDSET=SUB,
SHIFT,
NEW SET=ST1
0.,0.,0.007500
0.,0.,0.,0.,0.,0.1,0.
**
**
*NSET,NSET=XX1,GENERATE
60101,60121,1
60201,60221,1
60301,60321,1
60401,60421,1
60501,60521,1
60601,60621,1
*NSET,NSET=XX2,GENERATE
**
110101,110121,1
110201,110221,1
110301,110321,1
110401,110421,1
110501,110521,1
110601,110621,1
**
**
*NFILL,NSET=MN,BIAS=0.550
XX1,XX2,5,10000
**
**
*NSET,NSET=YY1,GENERATE
10101,10601,100
20101,20601,100
30101,30601,100
40101,40601,100
50101,50601,100
60101,60601,100
70101,70601,100
80101,80601,100
90101,90601,100
100101,100601,100
110101,110601,100
**
**
*NCOPY,CHANGE
NUMBER=25,OLDSET=YY1,SHIF
T,NEW SET=YY2
**
0.020000,0.,0.
0.,0.,0.,0.,0.,0.1,0.
**
**
*NSET,NSET=YY3,GENERATE
10121,10621,100
20121,20621,100
30121,30621,100
40121,40621,100
50121,50621,100
60121,60621,100
70121,70621,100
80121,80621,100
90121,90621,100
100121,100621,100
110121,110621,100
**
**
*NFILL,NSET=MO,BIAS=0.650
YY3,YY2,5,1
**
**
*NSET,NSET=SB
MM,MN,MO,SUB
**
**
*NSET,NSET=ALL
SB,CD
**
**
*ELEMENT,TYPE=DC3D8
10101,10101,10102,10202,1
0201,20101,20102,20202,20
201
**
**
10701,10701,10702,10802,1
0801,20701,20702,20802,20
801
**
**
**
#####
####
**      element sets
**
*ELGEN,ELSET=SB
10101,25,1,1,5,100,100,10
,10000,10000
**
**
*ELGEN,ELSET=CD1
10701,20,1,1,4,100,100,4,
10000,10000
**
**
*ELEMENT,TYPE=DC3D8
20601,20601,20602,50702,5
0701,30601,30602,50802,50
801
30601,30601,30602,50802,5
0801,40601,40602,50902,50
901
40601,40601,40602,50902,5
0901,50601,50602,51002,51
001
50601,50601,50602,51002,5
1001,60601,60602,51102,51
101
**
**
*ELEMENT,TYPE=DC3D6
101,10601,50701,20601,106
02,50702,20602
201,10601,40701,50701,106
02,40702,50702
301,10601,30701,40701,106
02,30702,40702
401,10601,20701,30701,106
02,20702,30702
501,10601,10701,20701,106
02,10702,20702
**
**
*ELGEN,ELSET=CD2
20601,20,1,1,0,100,100,0,
10000,10000
**
**
*ELGEN,ELSET=CD3
30601,
20,1,1,0,100,100,0,10000,
10000
**
**
*ELGEN,ELSET=CD4
40601,
20,1,1,0,100,100,0,10000,
10000
**
**
*ELGEN,ELSET=CD5
50601,
20,1,1,0,100,100,0,10000,
10000
**
**
*ELGEN,ELSET=CT1
101,
20,1,1,0,100,100,0,10000,
10000
**
**
*ELGEN,ELSET=CT2
201,
20,1,1,0,100,100,0,10000,
10000
**
**
*ELGEN,ELSET=CT3
301,
20,1,1,0,100,100,0,10000,
10000
**
**
*ELGEN,ELSET=CT4
401,
20,1,1,0,100,100,0,10000,
10000
**
**
*ELGEN,ELSET=CT5
501,
20,1,1,0,100,100,0,10000,
10000
**
**
*ELSET,ELSET=CD
CD1,CT1
**
**
CD2,CT2
**
**
CD3,CT3
**
**

```

CD4,CT4	40508,40520,1	50503,50506,1
**	50508,50520,1	**
**	20503,20503,1	*ELSET,ELSET=U13,GENERATE
CD5,CT5	30503,30504,1	10515,10520,1
**	40503,40505,1	20515,20520,1
*ELSET,ELSET=SUBU,GENERATE	50503,50506,1	30515,30520,1
E	**	40515,40520,1
10501,10502,1	*ELSET,ELSET=U7,GENERATE	50515,50520,1
20501,20502,1	10509,10520,1	20503,20503,1
30501,30502,1	20509,20520,1	30503,30504,1
40501,40502,1	30509,30520,1	40503,40505,1
50501,50502,1	40509,40520,1	50503,50506,1
**	50509,50520,1	**
10521,10525,1	20503,20503,1	*ELSET,ELSET=U14,GENERATE
20521,20525,1	30503,30504,1	10516,10520,1
30521,30525,1	40503,40505,1	20516,20520,1
40521,40525,1	50503,50506,1	30516,30520,1
50521,50525,1	**	40516,40520,1
**	*ELSET,ELSET=U8,GENERATE	50516,50520,1
60501,60525,1	10510,10520,1	20503,20503,1
70501,70525,1	20510,20520,1	30503,30504,1
80501,80525,1	30510,30520,1	40503,40505,1
90501,90525,1	40510,40520,1	50503,50506,1
100501,100525,1	50510,50520,1	**
**	20503,20503,1	*ELSET,ELSET=U15,GENERATE
**	30503,30504,1	10517,10520,1
*ELSET,ELSET=U1,GENERATE	40503,40505,1	20517,20520,1
10503,10520,1	50503,50506,1	30517,30520,1
20503,20520,1	**	40517,40520,1
30503,30520,1	*ELSET,ELSET=U9,GENERATE	50517,50520,1
40503,40520,1	10511,10520,1	20503,20503,1
50503,50520,1	20511,20520,1	30503,30504,1
**	30511,30520,1	40503,40505,1
*ELSET,ELSET=U2,GENERATE	40511,40520,1	50503,50506,1
10504,10520,1	50511,50520,1	**
20503,20520,1	20503,20503,1	*ELSET,ELSET=U16,GENERATE
30503,30520,1	30503,30504,1	10518,10520,1
40503,40520,1	40503,40505,1	20518,20520,1
50503,50520,1	50503,50506,1	30518,30520,1
**	**	40518,40520,1
*ELSET,ELSET=U3,GENERATE	*ELSET,ELSET=U10,GENERATE	50518,50520,1
10505,10520,1	10512,10520,1	20503,20503,1
20505,20520,1	20512,20520,1	30503,30504,1
30503,30520,1	30512,30520,1	40503,40505,1
40503,40520,1	40512,40520,1	50503,50506,1
50503,50520,1	50512,50520,1	**
20503,20503,1	20503,20503,1	*ELSET,ELSET=U17,GENERATE
**	30503,30504,1	10519,10520,1
*ELSET,ELSET=U4,GENERATE	40503,40505,1	20519,20520,1
10506,10520,1	50503,50506,1	30519,30520,1
20506,20520,1	**	40519,40520,1
30506,30520,1	*ELSET,ELSET=U11,GENERATE	50519,50520,1
40503,40520,1	10513,10520,1	20503,20503,1
50503,50520,1	20513,20520,1	30503,30504,1
20503,20503,1	30513,30520,1	40503,40505,1
30503,30504,1	40513,40520,1	50503,50506,1
**	50513,50520,1	**
*ELSET,ELSET=U5,GENERATE	20503,20503,1	*ELSET,ELSET=U18,GENERATE
10507,10520,1	30503,30504,1	10520,10520,1
20507,20520,1	40503,40505,1	20520,20520,1
30507,30520,1	50503,50506,1	30520,30520,1
40507,40520,1	**	40520,40520,1
50503,50520,1	*ELSET,ELSET=U12,GENERATE	50520,50520,1
20503,20503,1	10514,10520,1	20503,20503,1
30503,30504,1	20514,20520,1	30503,30504,1
40503,40505,1	30514,30520,1	40503,40505,1
**	40514,40520,1	50503,50506,1
*ELSET,ELSET=U6,GENERATE	50514,50520,1	**
10508,10520,1	20503,20503,1	*ELSET,ELSET=U19,GENERATE
20508,20520,1	30503,30504,1	20503,20503,1
30508,30520,1	40503,40505,1	30503,30504,1

```

40503,40505,1
50503,50506,1
**
**
*ELSET,ELSET=SUBD,GENERAT
E
10101,10125,1
20101,20125,1
30101,30125,1
40101,40125,1
50101,50125,1
**
60101,60125,1
70101,70125,1
80101,80125,1
90101,90125,1
100101,100125,1
**
*ELSET,ELSET=SUBS,GENERAT
E
10101,100101,10000
10201,100201,10000
10301,100301,10000
10401,100401,10000
10501,100501,10000
**
*ELSET,ELSET=SUBN,GENERAT
E
10125,100125,10000
10225,100225,10000
10325,100325,10000
10425,100425,10000
10525,100525,10000
**
*ELSET,ELSET=SUBW,GENERAT
E
10101,10125,1
10201,10225,1
10301,10325,1
10401,10425,1
10501,10525,1
**
*ELSET,ELSET=SUBE,GENERAT
E
100101,100125,1
100201,100225,1
100301,100325,1
100401,100425,1
100501,100525,1
**
**
** -----
-
**
*ELSET,ELSET=AA2,
GENERATE
503,503,1
*ELSET,ELSET=BA2,
GENERATE
103,503,100
*ELSET,ELSET=BC2
BA2
*ELSET,ELSET=CA2,
GENERATE
103,503,100
**
** -----
-
**
*ELSET,ELSET=AA3,
GENERATE
503,504,1
*ELSET,ELSET=AB3,
GENERATE
10704,10704,1
*ELSET,ELSET=BA3,
GENERATE
104,504,100
*ELSET,ELSET=BB3,
GENERATE
10704,10704,100
20704,20704,100
30704,30704,100
40704,40704,100
*ELSET,ELSET=BC3,
GENERATE
20604,20604,10000
*ELSET,ELSET=BD3
BA3,BB3,BC3
*ELSET,ELSET=CA3,
GENERATE
103,503,100
*ELSET,ELSET=CB3,
GENERATE
10704,40704,10000
*ELSET,ELSET=CC3,
GENERATE
20604,20604,1
**
** -----
-
**
*ELSET,ELSET=AA4,
GENERATE
503,505,1
*ELSET,ELSET=AB4,
GENERATE
10704,10705,1
10805,10805,1
*ELSET,ELSET=BA4,
GENERATE
105,505,100
*ELSET,ELSET=BB4,
GENERATE
10705,10805,100
20705,20805,100
30705,30805,100
40705,40805,100
*ELSET,ELSET=BC4,
GENERATE
20605,30605,10000
*ELSET,ELSET=BD4
BA4,BB4,BC4
*ELSET,ELSET=CA4,
GENERATE
103,503,100
*ELSET,ELSET=CB4,
GENERATE
10704,40704,10000
10805,40805,10000
*ELSET,ELSET=CC4,
GENERATE
20604,20604,1
30605,30605,1
**
** -----
-
**
*ELSET,ELSET=AA5,
GENERATE
503,506,1
*ELSET,ELSET=AB5,
GENERATE
10704,10706,1
10805,10806,1
10906,10906,1
*ELSET,ELSET=BA5,
GENERATE
106,506,100
*ELSET,ELSET=BB5,
GENERATE
10706,10906,100
20706,20906,100
30706,30906,100
40706,40906,100
*ELSET,ELSET=BC5,
GENERATE
20606,40606,10000
*ELSET,ELSET=BD5
BA5,BB5,BC5
*ELSET,ELSET=CA5,
GENERATE
103,503,100
*ELSET,ELSET=CB5,
GENERATE
10704,40704,10000
10805,40805,10000
10906,40906,10000
*ELSET,ELSET=CC5,
GENERATE
20604,20604,1
30605,30605,1
40606,40606,1
**
** -----
-
**
*ELSET,ELSET=AA6,
GENERATE
503,507,1
*ELSET,ELSET=AB6,
GENERATE
10704,10707,1
10805,10807,1
10906,10907,1
11007,11007,1
*ELSET,ELSET=BA6,
GENERATE
107,507,100
*ELSET,ELSET=BB6,
GENERATE
10707,11007,100
20707,21007,100
30707,31007,100
40707,41007,100
*ELSET,ELSET=BC6,
GENERATE
20607,50607,10000
*ELSET,ELSET=BD6
BA6,BB6,BC6
*ELSET,ELSET=CA6,
GENERATE
103,503,100
*ELSET,ELSET=CB6,
GENERATE
10704,40704,10000
10805,40805,10000
10906,40906,10000
11007,41007,10000
*ELSET,ELSET=CC6,
GENERATE
20604,20604,1

```

```

30605,30605,1
40606,40606,1
50607,50607,1
**
** -----
-
**
*ELSET,ELSET=AA7,
GENERATE
503,508,1
*ELSET,ELSET=AB7,
GENERATE
10704,10708,1
10805,10808,1
10906,10908,1
11007,11008,1
*ELSET,ELSET=BA7,
GENERATE
108,508,100
*ELSET,ELSET=BB7,
GENERATE
10708,11008,100
20708,21008,100
30708,31008,100
40708,41008,100
*ELSET,ELSET=BC7,
GENERATE
20608,50608,10000
*ELSET,ELSET=BD7
BA7,BB7,BC7
*ELSET,ELSET=CA7,
GENERATE
103,503,100
*ELSET,ELSET=CB7,
GENERATE
10704,40704,10000
10805,40805,10000
10906,40906,10000
11007,41007,10000
*ELSET,ELSET=CC7,
GENERATE
20604,20604,1
30605,30605,1
40606,40606,1
50607,50607,1
*ELSET,ELSET=DB7
11008,21008,31008,41008
*ELSET,ELSET=DC7
50608
**
** -----
-
**
*ELSET,ELSET=AA8,
GENERATE
503,509,1
*ELSET,ELSET=AB8,
GENERATE
10704,10709,1
10805,10809,1
10906,10909,1
11007,11009,1
*ELSET,ELSET=BA8,
GENERATE
109,509,100
*ELSET,ELSET=BB8,
GENERATE
10709,11009,100
20709,21009,100
30709,31009,100
40709,41009,100

*ELSET,ELSET=BC8,
GENERATE
20609,50609,10000
*ELSET,ELSET=BD8
BA8,BB8,BC8
*ELSET,ELSET=CA8,
GENERATE
103,503,100
*ELSET,ELSET=CB8,
GENERATE
10704,40704,10000
10805,40805,10000
10906,40906,10000
11007,41007,10000
*ELSET,ELSET=CC8,
GENERATE
20604,20604,1
30605,30605,1
40606,40606,1
50607,50607,1
*ELSET,ELSET=DB8
11009,21009,31009,41009,D
B7
*ELSET,ELSET=DC8
50609,DC7
**
** -----
-
**
*ELSET,ELSET=AA9,
GENERATE
503,510,1
*ELSET,ELSET=AB9,
GENERATE
10704,10710,1
10805,10810,1
10906,10910,1
11007,11010,1
*ELSET,ELSET=BA9,
GENERATE
110,510,100
*ELSET,ELSET=BB9,
GENERATE
10710,11010,100
20710,21010,100
30710,31010,100
40710,41010,100
*ELSET,ELSET=BC9,
GENERATE
20610,50610,10000
*ELSET,ELSET=BD9
BA9,BB9,BC9
*ELSET,ELSET=CA9,
GENERATE
103,503,100
*ELSET,ELSET=CB9,
GENERATE
10704,40704,10000
10805,40805,10000
10906,40906,10000
11007,41007,10000
*ELSET,ELSET=CC9,
GENERATE
20604,20604,1
30605,30605,1
40606,40606,1
50607,50607,1
*ELSET,ELSET=DB9
11010,21010,31010,41010,D
B8
*ELSET,ELSET=DC9

50610,DC8
**
** -----
-
**
*ELSET,ELSET=AA10,
GENERATE
503,511,1
*ELSET,ELSET=AB10,
GENERATE
10704,10711,1
10805,10811,1
10906,10911,1
11007,11011,1
*ELSET,ELSET=BA10,
GENERATE
111,511,100
*ELSET,ELSET=BB10,
GENERATE
10711,11011,100
20711,21011,100
30711,31011,100
40711,41011,100
*ELSET,ELSET=BC10,
GENERATE
20611,50611,10000
*ELSET,ELSET=BD10
BA10,BB10,BC10
*ELSET,ELSET=CA10,
GENERATE
103,503,100
*ELSET,ELSET=CB10,
GENERATE
10704,40704,10000
10805,40805,10000
10906,40906,10000
11007,41007,10000
*ELSET,ELSET=CC10,
GENERATE
20604,20604,1
30605,30605,1
40606,40606,1
50607,50607,1
*ELSET,ELSET=DB10
11011,21011,31011,41011,D
B9
*ELSET,ELSET=DC10
50611,DC9
**
** -----
-
**
*ELSET,ELSET=AA11,
GENERATE
503,512,1
*ELSET,ELSET=AB11,
GENERATE
10704,10712,1
10805,10812,1
10906,10912,1
11007,11012,1
*ELSET,ELSET=BA11,
GENERATE
112,512,100
*ELSET,ELSET=BB11,
GENERATE
10712,11012,100
20712,21012,100
30712,31012,100
40712,41012,100

```

```

*ELSET,ELSET=BC11,
GENERATE
20612,50612,10000
*ELSET,ELSET=BD11
BA11,BB11,BC11
*ELSET,ELSET=CA11,
GENERATE
103,503,100
*ELSET,ELSET=CB11,
GENERATE
10704,40704,10000
10805,40805,10000
10906,40906,10000
11007,41007,10000
*ELSET,ELSET=CC11,
GENERATE
20604,20604,1
30605,30605,1
40606,40606,1
50607,50607,1
*ELSET,ELSET=DB11
11012,21012,31012,41012,D
B10
*ELSET,ELSET=DC11
50612,DC10
**
** -----
-
**
*ELSET,ELSET=AA12,
GENERATE
503,513,1
*ELSET,ELSET=AB12,
GENERATE
10704,10713,1
10805,10813,1
10906,10913,1
11007,11013,1
*ELSET,ELSET=BA12,
GENERATE
113,513,100
*ELSET,ELSET=BB12,
GENERATE
10713,11013,100
20713,21013,100
30713,31013,100
40713,41013,100
*ELSET,ELSET=BC12,
GENERATE
20613,50613,10000
*ELSET,ELSET=BD12
BA12,BB12,BC12
*ELSET,ELSET=CA12,
GENERATE
103,503,100
*ELSET,ELSET=CB12,
GENERATE
10704,40704,10000
10805,40805,10000
10906,40906,10000
11007,41007,10000
*ELSET,ELSET=CC12,
GENERATE
20604,20604,1
30605,30605,1
40606,40606,1
50607,50607,1
*ELSET,ELSET=DB12
11013,21013,31013,41013,D
B11
*ELSET,ELSET=DC12

```

```

50613,DC11
**
** -----
-
**
*ELSET,ELSET=AA13,
GENERATE
503,514,1
*ELSET,ELSET=AB13,
GENERATE
10704,10714,1
10805,10814,1
10906,10914,1
11007,11014,1
*ELSET,ELSET=BA13,
GENERATE
114,514,100
*ELSET,ELSET=BB13,
GENERATE
10714,11014,100
20714,21014,100
30714,31014,100
40714,41014,100
*ELSET,ELSET=BC13,
GENERATE
20614,50614,10000
*ELSET,ELSET=BD13
BA13,BB13,BC13
*ELSET,ELSET=CA13,
GENERATE
103,503,100
*ELSET,ELSET=CB13,
GENERATE
10704,40704,10000
10805,40805,10000
10906,40906,10000
11007,41007,10000
*ELSET,ELSET=CC13,
GENERATE
20604,20604,1
30605,30605,1
40606,40606,1
50607,50607,1
*ELSET,ELSET=DB13
11014,21014,31014,41014,D
B12
*ELSET,ELSET=DC13
50614,DC12
**
** -----
-
**
*ELSET,ELSET=AA14,
GENERATE
503,515,1
*ELSET,ELSET=AB14,
GENERATE
10704,10715,1
10805,10815,1
10906,10915,1
11007,11015,1
*ELSET,ELSET=BA14,
GENERATE
115,515,100
*ELSET,ELSET=BB14,
GENERATE
10715,11015,100
20715,21015,100
30715,31015,100
40715,41015,100

```

```

*ELSET,ELSET=BC14,
GENERATE
20615,50615,10000
*ELSET,ELSET=BD14
BA14,BB14,BC14
*ELSET,ELSET=CA14,
GENERATE
103,503,100
*ELSET,ELSET=CB14,
GENERATE
10704,40704,10000
10805,40805,10000
10906,40906,10000
11007,41007,10000
*ELSET,ELSET=CC14,
GENERATE
20604,20604,1
30605,30605,1
40606,40606,1
50607,50607,1
*ELSET,ELSET=DB14
11015,21015,31015,41015,D
B13
*ELSET,ELSET=DC14
50615,DC13
**
** -----
-
**
*ELSET,ELSET=AA15,
GENERATE
503,516,1
*ELSET,ELSET=AB15,
GENERATE
10704,10716,1
10805,10816,1
10906,10916,1
11007,11016,1
*ELSET,ELSET=BA15,
GENERATE
116,516,100
*ELSET,ELSET=BB15,
GENERATE
10716,11016,100
20716,21016,100
30716,31016,100
40716,41016,100
*ELSET,ELSET=BC15,
GENERATE
20616,50616,10000
*ELSET,ELSET=BD15
BA15,BB15,BC15
*ELSET,ELSET=CA15,
GENERATE
103,503,100
*ELSET,ELSET=CB15,
GENERATE
10704,40704,10000
10805,40805,10000
10906,40906,10000
11007,41007,10000
*ELSET,ELSET=CC15,
GENERATE
20604,20604,1
30605,30605,1
40606,40606,1
50607,50607,1
*ELSET,ELSET=DB15
11016,21016,31016,41016,D
B14
*ELSET,ELSET=DC15

```

```

50616,DC14
**
** -----
-
**
*ELSET,ELSET=AA16,
GENERATE
503,517,1
*ELSET,ELSET=AB16,
GENERATE
10704,10717,1
10805,10817,1
10906,10917,1
11007,11017,1
*ELSET,ELSET=BA16,
GENERATE
117,517,100
*ELSET,ELSET=BB16,
GENERATE
10717,11017,100
20717,21017,100
30717,31017,100
40717,41017,100
*ELSET,ELSET=BC16,
GENERATE
20617,50617,10000
*ELSET,ELSET=BD16
BA16,BB16,BC16
*ELSET,ELSET=CA16,
GENERATE
103,503,100
*ELSET,ELSET=CB16,
GENERATE
10704,40704,10000
10805,40805,10000
10906,40906,10000
11007,41007,10000
*ELSET,ELSET=CC16,
GENERATE
20604,20604,1
30605,30605,1
40606,40606,1
50607,50607,1
*ELSET,ELSET=DB16
11017,21017,31017,41017,D
B15
*ELSET,ELSET=DC16
50617,DC15
**
** -----
-
**
*ELSET,ELSET=AA17,
GENERATE
503,518,1
*ELSET,ELSET=AB17,
GENERATE
10704,10718,1
10805,10818,1
10906,10918,1
11007,11018,1
*ELSET,ELSET=BA17,
GENERATE
118,518,100
*ELSET,ELSET=BB17,
GENERATE
10718,11018,100
20718,21018,100
30718,31018,100
40718,41018,100

```

```

*ELSET,ELSET=BC17,
GENERATE
20618,50618,10000
*ELSET,ELSET=BD17
BA17,BB17,BC17
*ELSET,ELSET=CA17,
GENERATE
103,503,100
*ELSET,ELSET=CB17,
GENERATE
10704,40704,10000
10805,40805,10000
10906,40906,10000
11007,41007,10000
*ELSET,ELSET=CC17,
GENERATE
20604,20604,1
30605,30605,1
40606,40606,1
50607,50607,1
*ELSET,ELSET=DB17
11018,21018,31018,41018,D
B16
*ELSET,ELSET=DC17
50618,DC16
**
** -----
-
**
*ELSET,ELSET=AA18,
GENERATE
503,519,1
*ELSET,ELSET=AB18,
GENERATE
10704,10719,1
10805,10819,1
10906,10919,1
11007,11019,1
*ELSET,ELSET=BA18,
GENERATE
119,519,100
*ELSET,ELSET=BB18,
GENERATE
10719,11019,100
20719,21019,100
30719,31019,100
40719,41019,100
*ELSET,ELSET=BC18,
GENERATE
20619,50619,10000
*ELSET,ELSET=BD18
BA18,BB18,BC18
*ELSET,ELSET=CA18,
GENERATE
103,503,100
*ELSET,ELSET=CB18,
GENERATE
10704,40704,10000
10805,40805,10000
10906,40906,10000
11007,41007,10000
*ELSET,ELSET=CC18,
GENERATE
20604,20604,1
30605,30605,1
40606,40606,1
50607,50607,1
*ELSET,ELSET=DB18
11019,21019,31019,41019,D
B17
*ELSET,ELSET=DC18

```

```

50619,DC17
**
** -----
-
**
*ELSET,ELSET=AA19,
GENERATE
503,520,1
*ELSET,ELSET=AB19,
GENERATE
10704,10720,1
10805,10820,1
10906,10920,1
11007,11020,1
*ELSET,ELSET=BA19,
GENERATE
120,520,100
*ELSET,ELSET=BB19,
GENERATE
10720,11020,100
20720,21020,100
30720,31020,100
40720,41020,100
*ELSET,ELSET=BC19,
GENERATE
20620,50620,10000
*ELSET,ELSET=BD19
BA19,BB19,BC19
*ELSET,ELSET=CA19,
GENERATE
103,503,100
*ELSET,ELSET=CB19,
GENERATE
10704,40704,10000
10805,40805,10000
10906,40906,10000
11007,41007,10000
*ELSET,ELSET=CC19,
GENERATE
20604,20604,1
30605,30605,1
40606,40606,1
50607,50607,1
*ELSET,ELSET=DB19
11020,21020,31020,41020,D
B18
*ELSET,ELSET=DC19
50620,DC18
**
*ELSET,ELSET=INT,GENERATE
10503,10520,1
10403,10420,1
20504,20520,1
20404,20420,1
30505,30520,1
30405,30420,1
40506,40520,1
40406,40420,1
50507,50520,1
50407,50420,1
60507,60520,1
60407,60420,1
**
*ELSET,ELSET=MOD1
SB
*ELSET,ELSET=MOD2
MOD1, BA2
*ELSET,ELSET=MOD3
MOD2, BD3
*ELSET,ELSET=MOD4
MOD3, BD4

```



```

**
**
*RADIATE,OP=NEW
SUBU,R5,27.,0.2268E-8
SUBS,R6,27.,0.2268E-8
SUBN,R4,27.,0.2268E-8
** SUBW,R1,27.,0.2268E-8
SUBE,R2,27.,0.2268E-8
**
U1,R5,27.,0.2268E-8
**
R
**
RRRRRRRRRRRRRRRRRRRRRRRRRRRRRR
RRRR
**
**
SSSSSSSSSSSSSSSSSSSSSSSSSSSSSS
SSSS
**
S
*DFLUX,OP=NEW
SUBU,S5NU
SUBW,S1,0.0
**
U1,S5NU
**
S
**
SSSSSSSSSSSSSSSSSSSSSSSSSSSSSS
SSSS
**
** OUTPUT
*NODE FILE
NT
*NODE PRINT, FREQUENCY=0
*EL PRINT, FREQUENCY=0
**
*END STEP
** ----- END OF
STEP 1 -----
-
**
**
#####
#####
**
** ----- BEGINNING
OF STEP 2 -----
-----
*STEP,INC=10000
*HEAT
TRANSFER,DELTMX=200.
0.000001, 0.052014
*MODEL CHANGE,ADD
BA2
**
**
FFFFFFFFFFFFFFFFFFFFFFFFFFFF
FFFF
**
F
*FILM,OP=NEW
** SUBD: reduced heat
loss due to
** contact with ground
SUBD,F3,27.,1.
SUBU,F5,27.,10.
SUBS,F6,27.,10.
SUBN,F4,27.,10.
** SUBW,F1,27.,10.

```

```

SUBE,F2,27.,10.
**
U2,F5,27.,10.
BA2,F2,27.,100.
CA2,F4,27.,10.
CA2,F1,27.,10.
**
F
**
FFFFFFFFFFFFFFFFFFFFFFFFFFFF
FFFF
**
**
RRRRRRRRRRRRRRRRRRRRRRRRRRRRRR
RRRR
**
**
R
**
**WARNING: The
*RADIATE option requires
emissivity instead of the
radiation
**
** constant A.
Hence, the Stefan-
Boltzmann constant S is
required. A fictitious
**
** value of the
Stefan-Boltzmann constant
of 1.0 was entered on the
*PHYSICAL
**
** CONSTANTS
option.
**
**
*RADIATE,OP=NEW
SUBU,R5,27.,0.2268E-8
SUBS,R6,27.,0.2268E-8
SUBN,R4,27.,0.2268E-8
** SUBW,R1,27.,0.2268E-8
SUBE,R2,27.,0.2268E-8
U2,R5,27.,0.2268E-8
BA2,R2,27.,0.2268E-8
CA2,R4,27.,0.2268E-8
CA2,R1,27.,0.2268E-8
**
**
R
**
RRRRRRRRRRRRRRRRRRRRRRRRRRRRRR
RRRR
**
**
SSSSSSSSSSSSSSSSSSSSSSSSSSSSSS
SSSS
**
**
S
*DFLUX,OP=NEW
SUBU,S5NU
SUBW,S1,0.0
**
U2,S5NU
BA2,S2NU
CA2,S4NU
CA2,S1NU
**
**
S
**
SSSSSSSSSSSSSSSSSSSSSSSSSSSSSS
SSSS
**
** OUTPUT

```

```

*NODE FILE
NT
*NODE PRINT, FREQUENCY=0
*EL PRINT, FREQUENCY=0
**
*END STEP
** ----- END OF
STEP 2 -----
-
**
**
#####
#####
**
** ----- BEGINNING
OF STEP 19 -----
-----
*STEP,INC=10000
*HEAT
TRANSFER,DELTMX=200.
0.00000001, 0.04
*MODEL CHANGE,ADD
BD19
**
**
FFFFFFFFFFFFFFFFFFFFFFFFFFFF
FFFF
**
**
F
*FILM,OP=NEW
** SUBD: reduced heat
loss due to
** contact with ground
SUBD,F3,27.,1.
SUBU,F5,27.,10.
SUBS,F6,27.,10.
SUBN,F4,27.,10.
** SUBW,F1,27.,10.
SUBE,F2,27.,10.
**
U19,F5,27.,10.
BA19,F2,27.,100.
BB19,F4,27.,100.
BC19,F4,27.,100.
CA19,F4,27.,10.
CA19,F1,27.,10.
CB19,F5,27.,10.
CB19,F6,27.,10.
CC19,F2,27.,10.
CC19,F6,27.,10.
DB19,F5,27.,10.
DC19,F2,27.,10.
**
**
F
**
FFFFFFFFFFFFFFFFFFFFFFFFFFFF
FFFF
**
**
RRRRRRRRRRRRRRRRRRRRRRRRRRRRRR
RRRR
**
**
R
**
**WARNING: The
*RADIATE option requires
emissivity instead of the
radiation

```

```

**          constant A.
Hence, the Stefan-
Boltzmann constant S is
required. A fictitious
**          value of the
Stefan-Boltzmann constant
of 1.0 was entered on the
*PHYSICAL
**          CONSTANTS
option.
**
*RADIATE,OP=NEW
SUBU,R5,27.,0.2268E-8
SUBS,R6,27.,0.2268E-8
SUBN,R4,27.,0.2268E-8
** SUBW,R1,27.,0.2268E-8
SUBE,R2,27.,0.2268E-8
U19,R5,27.,0.2268E-8
BA19,R2,27.,0.2268E-8
BB19,R4,27.,0.2268E-8
BC19,R4,27.,0.2268E-8
CA19,R4,27.,0.2268E-8
CA19,R1,27.,0.2268E-8
CB19,R5,27.,0.2268E-8
CB19,R6,27.,0.2268E-8
CC19,R2,27.,0.2268E-8
CC19,R6,27.,0.2268E-8
DB19,R5,27.,0.2268E-8
DC19,R2,27.,0.2268E-8
**
**
R
**
RRRRRRRRRRRRRRRRRRRRRRRRRRRRRR
RRRR
**
**
SSSSSSSSSSSSSSSSSSSSSSSSSSSS
SSSS
**
S
*DFLUX,OP=NEW
SUBU,S5NU
SUBW,S1,0.0
**
U19,S5NU
BA19,S2NU
BB19,S4NU
BC19,S4NU
CA19,S4NU
CA19,S1NU
CB19,S5NU
CB19,S6NU
CC19,S2NU
CC19,S6NU
DB19,S5NU
DC19,S2NU
**
**
S
**
SSSSSSSSSSSSSSSSSSSSSSSSSSSS
SSSS
**
** OUTPUT
*NODE FILE
NT
*NODE PRINT, FREQUENCY=0
*EL PRINT, FREQUENCY=0
**
*END STEP

```

```

** ----- END OF
STEP 19 -----
---
**
**
#####
#####
**
** ----- BEGINNING
OF STEP 20 -----
-----
*STEP, INC=10000
*HEAT
TRANSFER, DELTMX=200.
0.00000001, 3600.
**
**
FFFFFFFFFFFFFFFFFFFFFFFFFFFF
FFFF
**
F
*FILM,OP=NEW
** SUBD: reduced heat
loss due to
** contact with ground
SUBD,F3,27.,1.
SUBU,F5,27.,10.
SUBS,F6,27.,10.
SUBN,F4,27.,10.
** SUBW,F1,27.,10.
SUBE,F2,27.,10.
**
U19,F5,27.,10.
BA19,F2,27.,10.
BB19,F4,27.,10.
BC19,F4,27.,10.
CA19,F4,27.,10.
CA19,F1,27.,10.
CB19,F5,27.,10.
CB19,F6,27.,10.
CC19,F2,27.,10.
CC19,F6,27.,10.
DB19,F5,27.,10.
DC19,F2,27.,10.
**
**
F
**
FFFFFFFFFFFFFFFFFFFFFFFFFFFF
FFFF
**
**
RRRRRRRRRRRRRRRRRRRRRRRRRRRRRR
RRRR
**
**
R
**          **WARNING: The
*RADIATE option requires
emissivity instead of the
radiation
**          constant A.
Hence, the Stefan-
Boltzmann constant S is
required. A fictitious
**          value of the
Stefan-Boltzmann constant
of 1.0 was entered on the
*PHYSICAL
**          CONSTANTS
option.

```

```

**
**
*RADIATE,OP=NEW
SUBU,R5,27.,0.2268E-8
SUBS,R6,27.,0.2268E-8
SUBN,R4,27.,0.2268E-8
** SUBW,R1,27.,0.2268E-8
SUBE,R2,27.,0.2268E-8
U19,R5,27.,0.2268E-8
BA19,R2,27.,0.2268E-8
BB19,R4,27.,0.2268E-8
BC19,R4,27.,0.2268E-8
CA19,R4,27.,0.2268E-8
CA19,R1,27.,0.2268E-8
CB19,R5,27.,0.2268E-8
CB19,R6,27.,0.2268E-8
CC19,R2,27.,0.2268E-8
CC19,R6,27.,0.2268E-8
DB19,R5,27.,0.2268E-8
DC19,R2,27.,0.2268E-8
**
**
R
**
RRRRRRRRRRRRRRRRRRRRRRRRRRRRRR
RRRR
**
**
SSSSSSSSSSSSSSSSSSSSSSSSSSSS
SSSS
**
**
S
*DFLUX,OP=NEW
** SUBU,S5NU
SUBW,S1,0.0
**
**
S
**
SSSSSSSSSSSSSSSSSSSSSSSSSSSS
SSSS
**
** OUTPUT
*NODE FILE
NT
*NODE PRINT, FREQUENCY=0
*EL PRINT, FREQUENCY=0
**
**
*END STEP
** ----- END OF
STEP 20 -----
---
**
**
#####
#####
**
**

```

Input file for 3D stress

```
*HEADING
  3D LASER CLADDING
** dn513
**
** MESH GEN
**
*NODE,NSET=P1
10101,0.000000,0.000000,0
.000000
**
**
*NODE,NSET=P2
10601,0.000000,0.006670,0
.000000
**
**
*NODE,NSET=P3
11101,0.000000,0.007959,0
.000000
**
**
*NODE,NSET=P4
11111,0.005000,0.007959,0
.000000
**
**
*NODE,NSET=P5
10611,0.006502,0.006670,0
.000000
**
**
*NODE,NSET=P6
10111,0.006502,0.000000,0
.000000
**
**
*NCOPY, CHANGE
NUMBER=100, OLDSET=P5, SHIF
T, NEW SET=ROT1,
MULTIPLE=4
**
**
0.,0.,0.
0.005000,0.006440,0.,0.00
5000,0.006440,0.01,14.00
**
**
*NSET,NSET=R1
ROT1,P4,P5
*NFILL,NSET=R2
P2,P3,5,100
**
**
*NFILL,NSET=R3,BIAS=2.7
**
**
P6,P5,5,100
**
**
*NFILL,NSET=R4,BIAS=2.7
**
**
P1,P2,5,100
**
**
*NSET,NSET=R5
R1,R3
*NSET,NSET=R6
R2,R4
**
```

```
*NFILL,NSET=S1,BIAS=1.1
**
R6,R5,10,1
**
**
*NCOPY, CHANGE
NUMBER=10, OLDSET=R5, SHIF
T, NEW SET=R7
**
**
0.005000,0.,0.
0.,0.,0.,0.,0.,0.1,0.
**
**
*NFILL,NSET=S2
R5,R7,10,1
**
**
*NCOPY, CHANGE
NUMBER=25, OLDSET=R6, SHIF
T, NEW SET=R8
**
**
0.020000,0.,0.
0.,0.,0.,0.,0.,0.1,0.
**
**
*NFILL,NSET=S3,BIAS=0.45
**
R7,R8,5,1
**
**
*NSET,NSET=SUB, GENERATE
10601,10626,1
10501,10526,1
10401,10426,1
10301,10326,1
10201,10226,1
10101,10126,1
*NSET,NSET=CLD, GENERATE
11101,11121,1
11001,11021,1
10901,10921,1
10801,10821,1
10701,10721,1
**
**
*NCOPY, CHANGE
NUMBER=10000, OLDSET=CLD, S
HIFT, NEW SET=ROT2,
MULTIPLE=4
**
**
0.,0.,0.
0.000000,0.006670,0.00000
0,0.006502,0.006670,0.000
00,18.00
**
**
*NSET,NSET=CD
ROT2, CLD
**
**
*NSET,NSET=LL1, GENERATE
10701,10721,1
*NSET,NSET=LL2, GENERATE
10801,10821,1
*NSET,NSET=LL3, GENERATE
10901,10921,1
*NSET,NSET=LL4, GENERATE
11001,11021,1
*NSET,NSET=LL5, GENERATE
```

```
11101,11121,1
*NCOPY, CHANGE
NUMBER=9900, OLDSET=LL1, S
HIFT, NEW SET=LM1,
MULTIPLE=1
**
**
0.,0.,0.
**
**
0.00,0.00667,0.00,0.00650
17,0.00667,0.00,90.00
**
**
*NCOPY, CHANGE
NUMBER=19800, OLDSET=LL2, S
HIFT, NEW SET=LM2,
MULTIPLE=1
**
**
0.,0.,0.
**
**
0.00,0.00667,0.00,0.00650
17,0.00667,0.00,90.00
**
**
*NCOPY, CHANGE
NUMBER=29700, OLDSET=LL3, S
HIFT, NEW SET=LM3,
MULTIPLE=1
**
**
0.,0.,0.
**
**
0.00,0.00667,0.00,0.00650
17,0.00667,0.00,90.00
**
**
*NCOPY, CHANGE
NUMBER=39600, OLDSET=LL4, S
HIFT, NEW SET=LM4,
MULTIPLE=1
**
**
0.,0.,0.
**
**
0.00,0.00667,0.00,0.00650
17,0.00667,0.00,90.00
**
**
*NCOPY, CHANGE
NUMBER=49500, OLDSET=LL5, S
HIFT, NEW SET=LM5,
MULTIPLE=1
**
**
0.,0.,0.
**
**
0.00,0.00667,0.00,0.00650
17,0.00667,0.00,90.00
**
**
*NSET,NSET=LMM
LM1,
LM2,
LM3,
LM4,
LM5
**
**
*NCOPY, CHANGE NUMBER=-
500, OLDSET=LMM, SHIF, NEW
SET=LMN
```

```

0., -0.006670,0.
0.,0.,0.,0.,0.,0.1,0.
**
**
*NFILL,NSET=MM,BIAS=2.7
LMN,LMM,5,100
**
**
*NCOPY,CHANGE
NUMBER=100000,OLDSET=SUB,
SHIFT,
NEW SET=ST1
0.,0.,0.007500
0.,0.,0.,0.,0.,0.1,0.
**
*NSET,NSET=XX1,GENERATE
60101,60121,1
60201,60221,1
60301,60321,1
60401,60421,1
60501,60521,1
60601,60621,1
*NSET,NSET=XX2,GENERATE
**
110101,110121,1
110201,110221,1
110301,110321,1
110401,110421,1
110501,110521,1
110601,110621,1
**
**
*NFILL,NSET=MN,BIAS=0.550
XX1,XX2,5,10000
**
**
*NSET,NSET=YY1,GENERATE
10101,10601,100
20101,20601,100
30101,30601,100
40101,40601,100
50101,50601,100
60101,60601,100
70101,70601,100
80101,80601,100
90101,90601,100
100101,100601,100
110101,110601,100
**
**
*NCOPY,CHANGE
NUMBER=25,OLDSET=YY1,SHIF
T,NEW SET=YY2
**
0.020000,0.,0.
0.,0.,0.,0.,0.,0.1,0.
**
**
*NSET,NSET=YY3,GENERATE
10121,10621,100
20121,20621,100
30121,30621,100
40121,40621,100
50121,50621,100
60121,60621,100
70121,70621,100
80121,80621,100
90121,90621,100
100121,100621,100
110121,110621,100
**
**

*NFILL,NSET=MO,BIAS=0.650
YY3,YY2,5,1
**
**
*NSET,NSET=SB
MM,MN,MO,SUB
**
**
*NSET,NSET=ALL
SB,CD
**
**
*ELEMENT,TYPE=C3D8
10101,10101,10102,10202,1
0201,20101,20102,20202,20
201
**
**
10701,10701,10702,10802,1
0801,20701,20702,20802,20
801
**
#####
###
**
element sets
**
**
*ELGEN,ELSET=SB
10101,25,1,1,5,100,100,10
,10000,10000
**
**
*ELGEN,ELSET=CD1
10701,20,1,1,4,100,100,4,
10000,10000
**
**
*ELEMENT,TYPE=C3D8
20601,20601,20602,50702,5
0701,30601,30602,50802,50
801
30601,30601,30602,50802,5
0801,40601,40602,50902,50
901
40601,40601,40602,50902,5
0901,50601,50602,51002,51
001
50601,50601,50602,51002,5
1001,60601,60602,51102,51
101
**
**
*ELEMENT,TYPE=C3D6
101,10601,50701,20601,106
02,50702,20602
201,10601,40701,50701,106
02,40702,50702
301,10601,30701,40701,106
02,30702,40702
401,10601,20701,30701,106
02,20702,30702
501,10601,10701,20701,106
02,10702,20702
**
**
*ELGEN,ELSET=CD2
20601,20,1,1,0,100,100,0,
10000,10000
**
**
*ELGEN,ELSET=CD3
30601,
20,1,1,0,100,100,0,10000,
10000
**
**

*ELGEN,ELSET=CD4
40601,
20,1,1,0,100,100,0,10000,
10000
**
**
*ELGEN,ELSET=CD5
50601,
20,1,1,0,100,100,0,10000,
10000
**
**
*ELGEN,ELSET=CT1
101,
20,1,1,0,100,100,0,10000,
10000
**
**
*ELGEN,ELSET=CT2
201,
20,1,1,0,100,100,0,10000,
10000
**
**
*ELGEN,ELSET=CT3
301,
20,1,1,0,100,100,0,10000,
10000
**
**
*ELGEN,ELSET=CT4
401,
20,1,1,0,100,100,0,10000,
10000
**
**
*ELGEN,ELSET=CT5
501,
20,1,1,0,100,100,0,10000,
10000
**
**
*ELSET,ELSET=CD
CD1,CT1
**
**
CD2,CT2
**
**
CD3,CT3
**
**
CD4,CT4
**
**
CD5,CT5
**
**
*ELSET,ELSET=SUBU,GENERAT
E
10501,10502,1
20501,20502,1
30501,30502,1
40501,40502,1
50501,50502,1
**
10521,10525,1
20521,20525,1
30521,30525,1
40521,40525,1
50521,50525,1
**
60501,60525,1

```

```

70501,70525,1
80501,80525,1
90501,90525,1
100501,100525,1
**
**
*ELSET,ELSET=U1,GENERATE
10503,10520,1
20503,20520,1
30503,30520,1
40503,40520,1
50503,50520,1
**
*ELSET,ELSET=U2,GENERATE
10504,10520,1
20503,20520,1
30503,30520,1
40503,40520,1
50503,50520,1
**
*ELSET,ELSET=U3,GENERATE
10505,10520,1
20505,20520,1
30503,30520,1
40503,40520,1
50503,50520,1
20503,20503,1
**
*ELSET,ELSET=U4,GENERATE
10506,10520,1
20506,20520,1
30506,30520,1
40503,40520,1
50503,50520,1
20503,20503,1
30503,30504,1
30503,30504,1
**
*ELSET,ELSET=U5,GENERATE
10507,10520,1
20507,20520,1
30507,30520,1
40507,40520,1
50503,50520,1
20503,20503,1
30503,30504,1
40503,40505,1
**
*ELSET,ELSET=U6,GENERATE
10508,10520,1
20508,20520,1
30508,30520,1
40508,40520,1
50508,50520,1
20503,20503,1
30503,30504,1
40503,40505,1
50503,50506,1
**
*ELSET,ELSET=U7,GENERATE
10509,10520,1
20509,20520,1
30509,30520,1
40509,40520,1
50509,50520,1
20503,20503,1
30503,30504,1
40503,40505,1
50503,50506,1
**
*ELSET,ELSET=U8,GENERATE
10510,10520,1
20510,20520,1
30510,30520,1
40510,40520,1
50510,50520,1
20503,20503,1
30503,30504,1
40503,40505,1
50503,50506,1
**
*ELSET,ELSET=U9,GENERATE
10511,10520,1
20511,20520,1
30511,30520,1
40511,40520,1
50511,50520,1
20503,20503,1
30503,30504,1
40503,40505,1
50503,50506,1
**
*ELSET,ELSET=U10,GENERATE
10512,10520,1
20512,20520,1
30512,30520,1
40512,40520,1
50512,50520,1
20503,20503,1
30503,30504,1
40503,40505,1
50503,50506,1
**
*ELSET,ELSET=U11,GENERATE
10513,10520,1
20513,20520,1
30513,30520,1
40513,40520,1
50513,50520,1
20503,20503,1
30503,30504,1
40503,40505,1
50503,50506,1
**
*ELSET,ELSET=U12,GENERATE
10514,10520,1
20514,20520,1
30514,30520,1
40514,40520,1
50514,50520,1
20503,20503,1
30503,30504,1
40503,40505,1
50503,50506,1
**
*ELSET,ELSET=U13,GENERATE
10515,10520,1
20515,20520,1
30515,30520,1
40515,40520,1
50515,50520,1
20503,20503,1
30503,30504,1
40503,40505,1
50503,50506,1
**
*ELSET,ELSET=U14,GENERATE
10516,10520,1
20516,20520,1
30516,30520,1
40516,40520,1
50516,50520,1
20503,20503,1
30503,30504,1
40503,40505,1
50503,50506,1
**
*ELSET,ELSET=U15,GENERATE
10517,10520,1
20517,20520,1
30517,30520,1
40517,40520,1
50517,50520,1
20503,20503,1
30503,30504,1
40503,40505,1
50503,50506,1
**
*ELSET,ELSET=U16,GENERATE
10518,10520,1
20518,20520,1
30518,30520,1
40518,40520,1
50518,50520,1
20503,20503,1
30503,30504,1
40503,40505,1
50503,50506,1
**
*ELSET,ELSET=U17,GENERATE
10519,10520,1
20519,20520,1
30519,30520,1
40519,40520,1
50519,50520,1
20503,20503,1
30503,30504,1
40503,40505,1
50503,50506,1
**
*ELSET,ELSET=U18,GENERATE
10520,10520,1
20520,20520,1
30520,30520,1
40520,40520,1
50520,50520,1
20503,20503,1
30503,30504,1
40503,40505,1
50503,50506,1
**
*ELSET,ELSET=U19,GENERATE
20503,20503,1
30503,30504,1
40503,40505,1
50503,50506,1
**
*ELSET,ELSET=SUBD,GENERAT
E
10101,10125,1
20101,20125,1
30101,30125,1
40101,40125,1
50101,50125,1
**
60101,60125,1
70101,70125,1
80101,80125,1
90101,90125,1
100101,100125,1
**
*ELSET,ELSET=SUBS,GENERAT
E

```

```

10101,100101,10000
10201,100201,10000
10301,100301,10000
10401,100401,10000
10501,100501,10000
**
*ELSET,ELSET=SUBN,GENERAT
E
10125,100125,10000
10225,100225,10000
10325,100325,10000
10425,100425,10000
10525,100525,10000
**
*ELSET,ELSET=SUBW,GENERAT
E
10101,10125,1
10201,10225,1
10301,10325,1
10401,10425,1
10501,10525,1
**
*ELSET,ELSET=SUBE,GENERAT
E
100101,100125,1
100201,100225,1
100301,100325,1
100401,100425,1
100501,100525,1
**
**
** -----
-
**
*ELSET,ELSET=AA2,
GENERATE
503,503,1
*ELSET,ELSET=BA2,
GENERATE
103,503,100
*ELSET,ELSET=BC2
BA2
*ELSET,ELSET=CA2,
GENERATE
103,503,100
**
** -----
-
**
*ELSET,ELSET=AA3,
GENERATE
503,504,1
*ELSET,ELSET=AB3,
GENERATE
10704,10704,1
*ELSET,ELSET=BA3,
GENERATE
104,504,100
*ELSET,ELSET=BB3,
GENERATE
10704,10704,100
20704,20704,100
30704,30704,100
40704,40704,100
*ELSET,ELSET=BC3,
GENERATE
20604,20604,10000
*ELSET,ELSET=BD3
BA3,BB3,BC3
*ELSET,ELSET=CA3,
GENERATE
103,503,100
*ELSET,ELSET=CB3,
GENERATE
10704,40704,10000
*ELSET,ELSET=CC3,
GENERATE
20604,20604,1
**
** -----
-
**
*ELSET,ELSET=AA4,
GENERATE
503,505,1
*ELSET,ELSET=AB4,
GENERATE
10704,10705,1
10805,10805,1
*ELSET,ELSET=BA4,
GENERATE
105,505,100
*ELSET,ELSET=BB4,
GENERATE
10705,10805,100
20705,20805,100
30705,30805,100
40705,40805,100
*ELSET,ELSET=BC4,
GENERATE
20605,30605,10000
*ELSET,ELSET=BD4
BA4,BB4,BC4
*ELSET,ELSET=CA4,
GENERATE
103,503,100
*ELSET,ELSET=CB4,
GENERATE
10704,40704,10000
10805,40805,10000
*ELSET,ELSET=CC4,
GENERATE
20604,20604,1
30605,30605,1
**
** -----
-
**
*ELSET,ELSET=AA5,
GENERATE
503,506,1
*ELSET,ELSET=AB5,
GENERATE
10704,10706,1
10805,10806,1
10906,10906,1
*ELSET,ELSET=BA5,
GENERATE
106,506,100
*ELSET,ELSET=BB5,
GENERATE
10706,10906,100
20706,20906,100
30706,30906,100
40706,40906,100
*ELSET,ELSET=BC5,
GENERATE
20606,40606,10000
*ELSET,ELSET=BD5
BA5,BB5,BC5
*ELSET,ELSET=CA5,
GENERATE
103,503,100
*ELSET,ELSET=CB5,
GENERATE
10704,40704,10000
10805,40805,10000
10906,40906,10000
*ELSET,ELSET=CC5,
GENERATE
20604,20604,1
30605,30605,1
40606,40606,1
**
** -----
-
**
*ELSET,ELSET=AA6,
GENERATE
503,507,1
*ELSET,ELSET=AB6,
GENERATE
10704,10707,1
10805,10807,1
10906,10907,1
11007,11007,1
*ELSET,ELSET=BA6,
GENERATE
107,507,100
*ELSET,ELSET=BB6,
GENERATE
10707,11007,100
20707,21007,100
30707,31007,100
40707,41007,100
*ELSET,ELSET=BC6,
GENERATE
20607,50607,10000
*ELSET,ELSET=BD6
BA6,BB6,BC6
*ELSET,ELSET=CA6,
GENERATE
103,503,100
*ELSET,ELSET=CB6,
GENERATE
10704,40704,10000
10805,40805,10000
10906,40906,10000
11007,41007,10000
*ELSET,ELSET=CC6,
GENERATE
20604,20604,1
30605,30605,1
40606,40606,1
50607,50607,1
**
** -----
-
**
*ELSET,ELSET=AA7,
GENERATE
503,508,1
*ELSET,ELSET=AB7,
GENERATE
10704,10708,1
10805,10808,1
10906,10908,1
11007,11008,1
*ELSET,ELSET=BA7,
GENERATE
108,508,100
*ELSET,ELSET=BB7,
GENERATE

```

```

10708,11008,100
20708,21008,100
30708,31008,100
40708,41008,100
*ELSET,ELSET=BC7,
GENERATE
20608,50608,10000
*ELSET,ELSET=BD7
BA7,BB7,BC7
*ELSET,ELSET=CA7,
GENERATE
103,503,100
*ELSET,ELSET=CB7,
GENERATE
10704,40704,10000
10805,40805,10000
10906,40906,10000
11007,41007,10000
*ELSET,ELSET=CC7,
GENERATE
20604,20604,1
30605,30605,1
40606,40606,1
50607,50607,1
*ELSET,ELSET=DB7
11008,21008,31008,41008
*ELSET,ELSET=DC7
50608
**
** -----
-
**
*ELSET,ELSET=AA8,
GENERATE
503,509,1
*ELSET,ELSET=AB8,
GENERATE
10704,10709,1
10805,10809,1
10906,10909,1
11007,11009,1
*ELSET,ELSET=BA8,
GENERATE
109,509,100
*ELSET,ELSET=BB8,
GENERATE
10709,11009,100
20709,21009,100
30709,31009,100
40709,41009,100
*ELSET,ELSET=BC8,
GENERATE
20609,50609,10000
*ELSET,ELSET=BD8
BA8,BB8,BC8
*ELSET,ELSET=CA8,
GENERATE
103,503,100
*ELSET,ELSET=CB8,
GENERATE
10704,40704,10000
10805,40805,10000
10906,40906,10000
11007,41007,10000
*ELSET,ELSET=CC8,
GENERATE
20604,20604,1
30605,30605,1
40606,40606,1
50607,50607,1
*ELSET,ELSET=DB8

11009,21009,31009,41009,D
B7
*ELSET,ELSET=DC8
50609,DC7
**
** -----
-
**
*ELSET,ELSET=AA9,
GENERATE
503,510,1
*ELSET,ELSET=AB9,
GENERATE
10704,10710,1
10805,10810,1
10906,10910,1
11007,11010,1
*ELSET,ELSET=BA9,
GENERATE
110,510,100
*ELSET,ELSET=BB9,
GENERATE
10710,11010,100
20710,21010,100
30710,31010,100
40710,41010,100
*ELSET,ELSET=BC9,
GENERATE
20610,50610,10000
*ELSET,ELSET=BD9
BA9,BB9,BC9
*ELSET,ELSET=CA9,
GENERATE
103,503,100
*ELSET,ELSET=CB9,
GENERATE
10704,40704,10000
10805,40805,10000
10906,40906,10000
11007,41007,10000
*ELSET,ELSET=CC9,
GENERATE
20604,20604,1
30605,30605,1
40606,40606,1
50607,50607,1
*ELSET,ELSET=DB9
11010,21010,31010,41010,D
B8
*ELSET,ELSET=DC9
50610,DC8
**
** -----
-
**
*ELSET,ELSET=AA10,
GENERATE
503,511,1
*ELSET,ELSET=AB10,
GENERATE
10704,10711,1
10805,10811,1
10906,10911,1
11007,11011,1
*ELSET,ELSET=BA10,
GENERATE
111,511,100
*ELSET,ELSET=BB10,
GENERATE
10711,11011,100
20711,21011,100

30711,31011,100
40711,41011,100
*ELSET,ELSET=BC10,
GENERATE
20611,50611,10000
*ELSET,ELSET=BD10
BA10,BB10,BC10
*ELSET,ELSET=CA10,
GENERATE
103,503,100
*ELSET,ELSET=CB10,
GENERATE
10704,40704,10000
10805,40805,10000
10906,40906,10000
11007,41007,10000
*ELSET,ELSET=CC10,
GENERATE
20604,20604,1
30605,30605,1
40606,40606,1
50607,50607,1
*ELSET,ELSET=DB10
11011,21011,31011,41011,D
B9
*ELSET,ELSET=DC10
50611,DC9
**
** -----
-
**
*ELSET,ELSET=AA11,
GENERATE
503,512,1
*ELSET,ELSET=AB11,
GENERATE
10704,10712,1
10805,10812,1
10906,10912,1
11007,11012,1
*ELSET,ELSET=BA11,
GENERATE
112,512,100
*ELSET,ELSET=BB11,
GENERATE
10712,11012,100
20712,21012,100
30712,31012,100
40712,41012,100
*ELSET,ELSET=BC11,
GENERATE
20612,50612,10000
*ELSET,ELSET=BD11
BA11,BB11,BC11
*ELSET,ELSET=CA11,
GENERATE
103,503,100
*ELSET,ELSET=CB11,
GENERATE
10704,40704,10000
10805,40805,10000
10906,40906,10000
11007,41007,10000
*ELSET,ELSET=CC11,
GENERATE
20604,20604,1
30605,30605,1
40606,40606,1
50607,50607,1
*ELSET,ELSET=DB11

```

```

11012,21012,31012,41012,D
B10
*ELSET,ELSET=DC11
50612,DC10
**
** -----
-
**
*ELSET,ELSET=AA12,
GENERATE
503,513,1
*ELSET,ELSET=AB12,
GENERATE
10704,10713,1
10805,10813,1
10906,10913,1
11007,11013,1
*ELSET,ELSET=BA12,
GENERATE
113,513,100
*ELSET,ELSET=BB12,
GENERATE
10713,11013,100
20713,21013,100
30713,31013,100
40713,41013,100
*ELSET,ELSET=BC12,
GENERATE
20613,50613,10000
*ELSET,ELSET=BD12
BA12,BB12,BC12
*ELSET,ELSET=CA12,
GENERATE
103,503,100
*ELSET,ELSET=CB12,
GENERATE
10704,40704,10000
10805,40805,10000
10906,40906,10000
11007,41007,10000
*ELSET,ELSET=CC12,
GENERATE
20604,20604,1
30605,30605,1
40606,40606,1
50607,50607,1
*ELSET,ELSET=DB12
11013,21013,31013,41013,D
B11
*ELSET,ELSET=DC12
50613,DC11
**
** -----
-
**
*ELSET,ELSET=AA13,
GENERATE
503,514,1
*ELSET,ELSET=AB13,
GENERATE
10704,10714,1
10805,10814,1
10906,10914,1
11007,11014,1
*ELSET,ELSET=BA13,
GENERATE
114,514,100
*ELSET,ELSET=BB13,
GENERATE
10714,11014,100
20714,21014,100
30714,31014,100
40714,41014,100
*ELSET,ELSET=BC13,
GENERATE
20614,50614,10000
*ELSET,ELSET=BD13
BA13,BB13,BC13
*ELSET,ELSET=CA13,
GENERATE
103,503,100
*ELSET,ELSET=CB13,
GENERATE
10704,40704,10000
10805,40805,10000
10906,40906,10000
11007,41007,10000
*ELSET,ELSET=CC13,
GENERATE
20604,20604,1
30605,30605,1
40606,40606,1
50607,50607,1
*ELSET,ELSET=DB13
11014,21014,31014,41014,D
B12
*ELSET,ELSET=DC13
50614,DC12
**
** -----
-
**
*ELSET,ELSET=AA14,
GENERATE
503,515,1
*ELSET,ELSET=AB14,
GENERATE
10704,10715,1
10805,10815,1
10906,10915,1
11007,11015,1
*ELSET,ELSET=BA14,
GENERATE
115,515,100
*ELSET,ELSET=BB14,
GENERATE
10715,11015,100
20715,21015,100
30715,31015,100
40715,41015,100
*ELSET,ELSET=BC14,
GENERATE
20615,50615,10000
*ELSET,ELSET=BD14
BA14,BB14,BC14
*ELSET,ELSET=CA14,
GENERATE
103,503,100
*ELSET,ELSET=CB14,
GENERATE
10704,40704,10000
10805,40805,10000
10906,40906,10000
11007,41007,10000
*ELSET,ELSET=CC14,
GENERATE
20604,20604,1
30605,30605,1
40606,40606,1
50607,50607,1
*ELSET,ELSET=DB14
11015,21015,31015,41015,D
B13
*ELSET,ELSET=DC14
50615,DC13
**
** -----
-
**
*ELSET,ELSET=AA15,
GENERATE
503,516,1
*ELSET,ELSET=AB15,
GENERATE
10704,10716,1
10805,10816,1
10906,10916,1
11007,11016,1
*ELSET,ELSET=BA15,
GENERATE
116,516,100
*ELSET,ELSET=BB15,
GENERATE
10716,11016,100
20716,21016,100
30716,31016,100
40716,41016,100
*ELSET,ELSET=BC15,
GENERATE
20616,50616,10000
*ELSET,ELSET=BD15
BA15,BB15,BC15
*ELSET,ELSET=CA15,
GENERATE
103,503,100
*ELSET,ELSET=CB15,
GENERATE
10704,40704,10000
10805,40805,10000
10906,40906,10000
11007,41007,10000
*ELSET,ELSET=CC15,
GENERATE
20604,20604,1
30605,30605,1
40606,40606,1
50607,50607,1
*ELSET,ELSET=DB15
11016,21016,31016,41016,D
B14
*ELSET,ELSET=DC15
50616,DC14
**
** -----
-
**
*ELSET,ELSET=AA16,
GENERATE
503,517,1
*ELSET,ELSET=AB16,
GENERATE
10704,10717,1
10805,10817,1
10906,10917,1
11007,11017,1
*ELSET,ELSET=BA16,
GENERATE
117,517,100
*ELSET,ELSET=BB16,
GENERATE
10717,11017,100
20717,21017,100

```

```

30717,31017,100
40717,41017,100
*ELSET,ELSET=BC16,
GENERATE
20617,50617,10000
*ELSET,ELSET=BD16
BA16,BB16,BC16
*ELSET,ELSET=CA16,
GENERATE
103,503,100
*ELSET,ELSET=CB16,
GENERATE
10704,40704,10000
10805,40805,10000
10906,40906,10000
11007,41007,10000
*ELSET,ELSET=CC16,
GENERATE
20604,20604,1
30605,30605,1
40606,40606,1
50607,50607,1
*ELSET,ELSET=DB16
11017,21017,31017,41017,D
B15
*ELSET,ELSET=DC16
50617,DC15
**
** -----
-
**
*ELSET,ELSET=AA17,
GENERATE
503,518,1
*ELSET,ELSET=AB17,
GENERATE
10704,10718,1
10805,10818,1
10906,10918,1
11007,11018,1
*ELSET,ELSET=BA17,
GENERATE
118,518,100
*ELSET,ELSET=BB17,
GENERATE
10718,11018,100
20718,21018,100
30718,31018,100
40718,41018,100
*ELSET,ELSET=BC17,
GENERATE
20618,50618,10000
*ELSET,ELSET=BD17
BA17,BB17,BC17
*ELSET,ELSET=CA17,
GENERATE
103,503,100
*ELSET,ELSET=CB17,
GENERATE
10704,40704,10000
10805,40805,10000
10906,40906,10000
11007,41007,10000
*ELSET,ELSET=CC17,
GENERATE
20604,20604,1
30605,30605,1
40606,40606,1
50607,50607,1
*ELSET,ELSET=DB17

11018,21018,31018,41018,D
B16
*ELSET,ELSET=DC17
50618,DC16
**
** -----
-
**
*ELSET,ELSET=AA18,
GENERATE
503,519,1
*ELSET,ELSET=AB18,
GENERATE
10704,10719,1
10805,10819,1
10906,10919,1
11007,11019,1
*ELSET,ELSET=BA18,
GENERATE
119,519,100
*ELSET,ELSET=BB18,
GENERATE
10719,11019,100
20719,21019,100
30719,31019,100
40719,41019,100
*ELSET,ELSET=BC18,
GENERATE
20619,50619,10000
*ELSET,ELSET=BD18
BA18,BB18,BC18
*ELSET,ELSET=CA18,
GENERATE
103,503,100
*ELSET,ELSET=CB18,
GENERATE
10704,40704,10000
10805,40805,10000
10906,40906,10000
11007,41007,10000
*ELSET,ELSET=CC18,
GENERATE
20604,20604,1
30605,30605,1
40606,40606,1
50607,50607,1
*ELSET,ELSET=DB18
11019,21019,31019,41019,D
B17
*ELSET,ELSET=DC18
50619,DC17
**
** -----
-
**
*ELSET,ELSET=AA19,
GENERATE
503,520,1
*ELSET,ELSET=AB19,
GENERATE
10704,10720,1
10805,10820,1
10906,10920,1
11007,11020,1
*ELSET,ELSET=BA19,
GENERATE
120,520,100
*ELSET,ELSET=BB19,
GENERATE
10720,11020,100
20720,21020,100

30720,31020,100
40720,41020,100
*ELSET,ELSET=BC19,
GENERATE
20620,50620,10000
*ELSET,ELSET=BD19
BA19,BB19,BC19
*ELSET,ELSET=CA19,
GENERATE
103,503,100
*ELSET,ELSET=CB19,
GENERATE
10704,40704,10000
10805,40805,10000
10906,40906,10000
11007,41007,10000
*ELSET,ELSET=CC19,
GENERATE
20604,20604,1
30605,30605,1
40606,40606,1
50607,50607,1
*ELSET,ELSET=DB19
11020,21020,31020,41020,D
B18
*ELSET,ELSET=DC19
50620,DC18
**
*ELSET,ELSET=INT,GENERATE
10503,10520,1
10403,10420,1
20504,20520,1
20404,20420,1
30505,30520,1
30405,30420,1
40506,40520,1
40406,40420,1
50507,50520,1
50407,50420,1
60507,60520,1
60407,60420,1
**
**
*ELSET,ELSET=MOD1
SB
*ELSET,ELSET=MOD2
MOD1, BA2
*ELSET,ELSET=MOD3
MOD2, BD3
*ELSET,ELSET=MOD4
MOD3, BD4
*ELSET,ELSET=MOD5
MOD4, BD5
*ELSET,ELSET=MOD6
MOD5, BD6
*ELSET,ELSET=MOD7
MOD6, BD7
*ELSET,ELSET=MOD8
MOD7, BD8
*ELSET,ELSET=MOD9
MOD8, BD9
*ELSET,ELSET=MOD10
MOD9, BD10
*ELSET,ELSET=MOD11
MOD10, BD11
*ELSET,ELSET=MOD12
MOD11, BD12
*ELSET,ELSET=MOD13
MOD12, BD13
*ELSET,ELSET=MOD14
MOD13, BD14

```

```

*ELSET,ELSET=MOD15
MOD14, BD15
*ELSET,ELSET=MOD16
MOD15, BD16
*ELSET,ELSET=MOD17
MOD16, BD17
*ELSET,ELSET=MOD18
MOD17, BD18
*ELSET,ELSET=MOD19
MOD18, BD19
*ELSET,ELSET=MOD20
MOD19
**
** -----
-
**
*** *****
**
*PHYSICAL CONSTANTS,
ABSOLUTE ZERO=-273.
** MATERIALS PROPERTIES
**
*SOLID
SECTION,ELSET=SB,MATERIAL
=ALBAS
*SOLID
SECTION,ELSET=CD,MATERIAL
=CUBAS
*SOLID
SECTION,ELSET=INT,MATERIA
L=ALBAS
**
** -----
-----|
*MATERIAL,NAME=ALBAS
*ELASTIC
73.0E9,0.34,27.
52.8E9,0.34,516.
1.E3,0.34,585.
*PLASTIC,HARDENING=KINEMA
TIC
193.E6,0.,27.
250.5E6,0.01,27.
19.E6,0.,516.
27.5E6,0.1,516.
18.9E6,0.,516.1
18.9E6,0.1,516.1
*ANNEAL TEMPERATURE
516.1
*EXPANSION,ZERO=27.
20.1E-6,27.
26.0E-6,516.
*CONDUCTIVITY
117.,27.
*DENSITY
2770.,27.
2676.,516.
*LATENT HEAT
389000.,516.,585.
*SPECIFIC HEAT
963.,27.
1274.,516.
** -----
-----|
*MATERIAL,NAME=INTER
*ELASTIC
75.2E9,0.33,27.
59.1E9,0.33,516.
1.E3,0.33,585.
*PLASTIC,HARDENING=KINEMA
TIC
197.E6,0.,27.
320.E6,.01,27.
20.E6,0.,516.
126.E6,.01,516.
19.9E6,0.,516.1
19.9E6,0.01,516.1
*ANNEAL TEMPERATURE
516.1
*EXPANSION,ZERO=27.
19.1E-6,27.
24.8E-6,516.
*CONDUCTIVITY
117.,27.
*DENSITY
3087.,27.
2990.,516.
*LATENT HEAT
389000.,516.,585.
*SPECIFIC HEAT
895.,27.
1298.,516.
** -----
-----|
*MATERIAL,NAME=CUBAS
*ELASTIC
125.0E9,0.33,27.
77.7E9,0.33,950.
1.E3,0.33,990.
*PLASTIC,HARDENING=KINEMA
TIC
275.E6,0.,27.
744.E6,0.18,27.
27.5E6,0.,950.
186.E6,1.1,950.
27.4E6,0.,950.1
27.4E6,2.,950.1
*ANNEAL TEMPERATURE
950.1
*EXPANSION,ZERO=27.
16.5E-6,27.
25.1E-6,950.
*CONDUCTIVITY
12.1,27.
85.9,950.
*DENSITY
7530.,27.
7096.,950.
*LATENT HEAT
205000.,950.,990.
*SPECIFIC HEAT
440.,27.
625.,950.
**
*BOUNDARY
10101, 2
110101, 2
10126, 2
110126,ENCASTRE
SUB, ZSYMM
CLD, ZSYMM
**
*RESTART,WRITE,FREQUENCY=
10000
**
#####
#####
**
** ----- BEGINNING
OF STEP 1 -----
----
**STEP,INC=10000, NLGEOM
*STEP,INC=10000
*STATIC
1.00E-10, 0.124027, 1.0E-
20
**MODEL CHANGE, ACTIVATE
*CONTROLS,PARAMETER=FIELD
0.03, 0.03
*MODEL CHANGE,REMOVE
CD
**
*TEMPERATURE,FILE=cn511,B
STEP=1,ESTEP=1
*NODE PRINT, FREQUENCY=0
*EL PRINT, FREQUENCY=0
*OUTPUT, FIELD,
VARIABLE=PRESELECT,FREQUE
NCY=50
**
**OUTPUT, HISTORY,
FREQUENCY=50
**ELEMENT OUTPUT
**S
**
*END STEP
** ----- END OF
STEP 1 -----
-
**
#####
#####
**
** ----- BEGINNING
OF STEP 2 -----
----
*STEP,INC=10000
*STATIC
1.00E-10, 0.052014, 1.0E-
20
*MODEL CHANGE,ADD
BA2
**
*TEMPERATURE,FILE=cn511,B
STEP=2,ESTEP=2
*NODE PRINT, FREQUENCY=0
*EL PRINT, FREQUENCY=0
**
*END STEP
** ----- END OF
STEP 2 -----
-

```


Fortran file for 2D temperature:

```
      SUBROUTINE DFLUX (FLUX, SOL, KSTEP, KINC, TIME, NOEL, NPT,  
$COORDS, JLTYP, TEMP, PRESS, SNAME)  
      INCLUDE 'ABA_PARAM_DP.INC'  
C      IMPLICIT DOUBLE PRECISION (A-H,O-Z)  
      DIMENSION FLUX(2), TIME(2), COORDS(3)  
      CHARACTER*80 SNAME  
C      INCLUDE 'ABA_PARAM.INC'  
C  
C      V= BEAM velocity (m/s)  
C      STIM= STILL-LASER HEAT-UP TIME (s)  
C      RBEAM= beam radius (m)  
C      ABS= ABSORPTIVITY  
C      QTOT= total POWER available to the PART.(W)  
C      Q= heat flux at the BEAM center,R=0 (W/m2)  
C      XM= x-coordinate w.r.t. the traveling BEAM (m)  
C      YM= Y-coordinate w.r.t. the traveling BEAM (m)  
C      XI= INITIAL x-coordinate OF the traveling BEAM (m)  
C      YI= INITIAL y-coordinate OF the traveling BEAM (m)  
C      R= distance of a point on the plate surface from  
C      the beam in xy-surface plane (m)  
C      C= exponent of the exponential(e) to calculate heat  
C      flux at a point on the surface of the plate.  
C  
      TIM=TIME(2)  
      STIM= 0.100000  
      FLUX(1)=0.  
      FLUX(2)=0.  
      QPD=0.  
      IF (TIM.GE.100000.0) GO TO 10  
      V= 0.012500  
      RBEAM= 0.001000  
      ABS= 0.250000  
      QTOT= 600. - QPD  
      Q=2.0*ABS*QTOT/(3.1416*(RBEAM*RBEAM))  
      XI= 0.001000  
C      XI=0.034+REAL(KSTEP-1)*0.0025
```

```

C      YI=0.03
C      XM=COORDS(1)-XI
C
      IF (TIM.LT.STIM) THEN
          XM=COORDS(1)-XI
      ELSE
          XM=COORDS(1)-V*(TIM-STIM)-XI
      ENDIF
C
C      YM=COORDS(2)-YI
      R=SQRT(XM*XM)
C      IF (R.GT.RBEAM) GO TO 10
      C=2.*(R*R)/(RBEAM*RBEAM)
      FLUX(1)=Q*EXP(-C)
10 RETURN
      END

```

Fortran file for 2D temperature with properties dependent on composition:

```
      SUBROUTINE DFLUX (FLUX, SOL, KSTEP, KINC, TIME, NOEL, NPT,
$COORDS, JLTYP, TEMP, PRESS, SNAME)
      INCLUDE 'ABA_PARAM_DP.INC'
C      IMPLICIT DOUBLE PRECISION (A-H,O-Z)
      DIMENSION FLUX(2), TIME(2), COORDS(3)
      CHARACTER*80 SNAME
C      INCLUDE 'ABA_PARAM.INC'
C
C      V= BEAM velocity (m/s)
C      STIM= STILL-LASER HEAT-UP TIME (s)
C      RBEAM= beam radius (m)
C      ABS= ABSORPTIVITY
C      QTOT= total POWER available to the PART.(W)
C      Q= heat flux at the BEAM center,R=0 (W/m2)
C      XM= x-coordinate w.r.t. the traveling BEAM (m)
C      YM= Y-coordinate w.r.t. the traveling BEAM (m)
C      XI= INITIAL x-coordinate OF the traveling BEAM (m)
C      YI= INITIAL y-coordinate OF the traveling BEAM (m)
C      R= distance of a point on the plate surface from
C      the beam in xy-surface plane (m)
C      C= exponent of the exponential(e) to calculate heat
C      flux at a point on the surface of the plate.
C
      TIM=TIME(2)
      STIM= 0.100000
      FLUX(1)=0.
      FLUX(2)=0.
      QPD=0.
      IF (TIM.GE.100000.0) GO TO 10
      V= 0.012500
      RBEAM= 0.001000
      ABS= 0.250000
      QTOT= 800. - QPD
      Q=2.0*ABS*QTOT/(3.1416*(RBEAM*RBEAM))
      XI= 0.001000
C      XI=0.034+REAL(KSTEP-1)*0.0025
```

```

C      YI=0.03
C      XM=COORDS(1)-XI
C
C      IF (TIM.LT.STIM) THEN
C          XM=COORDS(1)-XI
C      ELSE
C          XM=COORDS(1)-V*(TIM-STIM)-XI
C      ENDIF
C
C      YM=COORDS(2)-YI
C      R=SQRT(XM*XM)
C      IF (R.GT.RBEAM) GO TO 10
C      C=2.*(R*R)/(RBEAM*RBEAM)
C      FLUX(1)=Q*EXP(-C)
10 RETURN
C      END
C
C      SUBROUTINE SDVINI (STATEV, COORDS, NSTATV, NCRDS, NOEL, NPT,
C          $LAYER, KSPT)
C
C      INCLUDE 'ABA_PARAM_DP.INC'
C
C      DIMENSION STATEV(NSTATV), COORDS(NCRDS)
C
C
C      HSUB = 0.006670
C      HSUB is the substrate height, ie the yy coordinate
C      of node P2
C
C      IF (COORDS(2).GT.HSUB) THEN
C          STATEV(1)=1.0
C          STATEV(2)=0.0
C          STATEV(2)=(27.-27.)/(990.-27.) = DTini / DTmeltClad
C          STATEV(2)=0.02749
C          STATEV(2)=27./990. = Tini / TmeltClad
C      ELSE
C          STATEV(1)=0.0

```

```

STATEV(2)=0.0
C STATEV(2)= (27.-27.)/ (585.-27.) = DTini / DTmeltSub
C STATEV(2)=0.04615
C STATEV(2)=27./585. = Tini / TmeltSub
ENDIF
C
STATEV(3)=27.
C
STATEV(4)=0.000001
C
STATEV(5)=0.0
C
STATEV(6)=0.0
C
C statev(1) - composition variable, equals to
C 1.0 for clad
C 0.0 for substrate
C intermediate values,
C for the substrate zone, according to the
C local peak temperature that was attained
C in relation to the melting temperature
C difference between clad and substrate
C
C
C statev(2) - reduced temperature, ie,
C (temperature - 27)/ (local melting temperature - 27)
C
C stetev(3) - temperature at previous timestep
C
C statev(4) - time increment
C
C statev(5) - cooling rate = - dT/dt
C
C statev(6) - temperature gradient
C
RETURN
END
C

```

```

C
    SUBROUTINE USDFLD (FIELD, STATEV, PNEWDT, DIRECT, T, CELENT,
$TIME, DTIME, CMNAME, ORNAME, NFIELD, NSTATV, NOEL, NPT, LAYER,
$KSPT, KSTEP, KINC, NDI, NSHR, COORD, JMAC, JMATYP, MATLAYO, LACCFLA)
C
    INCLUDE 'ABA_PARAM_DP.INC'
C
    CHARACTER*80 CMNAME, ORNAME
    CHARACTER*3 FLGRAY (15)
    DIMENSION FIELD (NFIELD), STATEV (NSTATV), DIRECT (3, 3),
$T (3, 3), TIME (2)
    DIMENSION ARRAY (15), JARRAY (15), JMAC (*), JMATYP (*), COORD (*)
C
C
    CALL GETVRM ('HFL', ARRAY, JARRAY, FLGRAY, JRCD, JMAC, JMATYP,
$MATLAYO, LACCFLA)
    FLUXO=ARRAY (1)
C
C
    CALL GETVRM ('TEMP', ARRAY, JARRAY, FLGRAY, JRCD, JMAC, JMATYP,
$MATLAYO, LACCFLA)
C
    ST1=(ARRAY (1) -585.) /405.
C
    IF (ST1.GT.STATEV (1)) THEN
        STATEV (1)=ST1
    ELSE
        CONTINUE
    ENDIF
    IF (STATEV (1) .GT.1.0) THEN
        STATEV (1)=1.0
    ELSE
        CONTINUE
    ENDIF
C
C
    IF (STATEV (1) .GT.0.99999) THEN
        TMEL=963.

```

```

ELSE
    TMEL=558.
ENDIF
C
C
STATEV(2)=(ARRAY(1)-27.)/TMEL
C
STATEV(5)=(STATEV(3)-ARRAY(1))/STATEV(4)
C
C ***** definition of thermal conductivity ***
C
IF(ARRAY(1).GT.950.) THEN
    TCCU=85.9
ELSE
    TCCU=12.1+0.079957*(ARRAY(1)-27.)
ENDIF
C
TCAL=117.
C
IF(STATEV(1).GE.0.9) THEN
    TCM=STATEV(1)*TCCU+(1.0-STATEV(1))*TCAL
ELSE
    TCM=TCAL
ENDIF
C
STATEV(6)=FLUXO/TCM
C
C
C ***** variable updates*****
C
FIELD(1)=STATEV(1)
C
STATEV(4)=DTIME
C
STATEV(3)=ARRAY(1)
C
RETURN
END

```

Fortran file for 3D temperature:

```
      SUBROUTINE DFLUX (FLUX, TEMP, KSTEP, KINC, TIME, NOEL, NPT,  
$COORDS, JLTYP)  
      IMPLICIT DOUBLE PRECISION (A-H,O-Z)  
      DIMENSION COORDS (3), TIME (2)  
C      INCLUDE 'ABA_PARAM.INC'  
C  
C      V= BEAM velocity (m/s)  
C      STIM= STILL-LASER HEAT-UP TIME (s)  
C      RBEAM= beam radius (m)  
C      ABS= ABSORPTIVITY  
C      QTOT= total POWER available to the PART.(W)  
C      Q= heat flux at the BEAM center,R=0 (W/m**2)  
C      XM= x-coordinate w.r.t. the traveling BEAM (m)  
C      YM= Y-coordinate w.r.t. the traveling BEAM (m)  
C      XI= INITIAL x-coordinate OF the traveling BEAM (m)  
C      YI= INITIAL y-coordinate OF the traveling BEAM (m)  
C      R= distance of a point on the plate surface from  
C      the beam in xy-surface plane (m)  
C      C= exponent of the exponential(e) to calculate heat  
C      flux at a point on the surface of the plate.  
C  
      TIM=TIME (2)  
      STIM= 0.100000  
      FLUX=0.  
      QPD=0.  
      IF (TIM.GE.100000.0) GO TO 10  
      V= 0.012500  
      RBEAM= 0.001000  
      ABS= 0.250000  
      QTOT= 800. - QPD  
      Q=2.0*ABS*QTOT/(3.1416*(RBEAM*RBEAM))  
      XI= 0.001000  
C      XI=0.034+REAL (KSTEP-1) *0.0025  
C      YI=0.03  
C      XM=COORDS (1) -XI  
C
```

```

      IF (TIM.LT.STIM) THEN
        XM=COORDS(1)-XI
      ELSE
        XM=COORDS(1)-V*(TIM-STIM)-XI
      ENDIF
      ZM= COORDS(3)
C
C      YM=COORDS(2)-YI
      R=SQRT(XM*XM+ZM*ZM)
C      IF (R.GT.RBEAM) GO TO 10
      C=2.*(R*R)/(RBEAM*RBEAM)
      FLUX=Q*EXP(-C)
10 RETURN
      END

```

Appendix D. Computer runs

File	Dimension and analysis type	Comment	Number of elements	Number of nodes	Processor	Cpu time /s	Laser power /W	T_3^{clad} /°C	Interface composition	L_c /mm	h_s /mm	L_s /mm	w_s /mm
al120	2D Temp	Substrate only, coarse mesh	125	156	Intel	51.6	600	---	Cu alloy	---	6.67	50.	---
al220	2D Temp	Substrate only, mid-grade mesh	500	561	Intel	138.0	600	---	Cu alloy	---	6.67	50.	---
al320	2D Temp	Substrate only, fine mesh	1900	2016	Intel	326.4	600	---	Cu alloy	---	6.67	50.	---
cl220	2D Temp	Substrate only, mid-grade mesh	500	561	Intel	145.8	600	---	Cu alloy	---	25.4	40.	---
bl120	2D Stress	Substrate only, coarse mesh	125	157	Intel	54.2	600	---	Cu alloy	---	6.67	50.	---
bl220	2D Stress	Substrate only, mid-grade mesh	500	562	Intel	312.8	600	---	Cu alloy	---	6.67	50.	---
bl320	2D Stress	Substrate only, fine mesh	1900	2017	Intel	3367.6	600	---	Cu alloy	---	6.67	50.	---
dl220	2D Stress	Substrate only, mid-grade mesh	500	562	Intel	190.7	600	---	Cu alloy	---	25.4	40.	---
al22	2D Temp	Substrate and clad, mid mesh	900	971	Intel	642.9	600	1550	Al alloy	10.	6.67	50.	---
al23	2D Temp	Substrate and clad, mid mesh	900	971	Intel	837.	700	1775	Cu alloy	10.	6.67	50.	---
al24	2D Temp	Substrate and clad, mid mesh	900	971	Intel	756.5	700	1775	Composite	10.	6.67	50.	---
al25	2D Temp	Substrate and clad, mid mesh	900	971	Intel	2820.5	800	2000	Variable	10.	6.67	50.	---
al26	2D Temp	Substrate and clad, mid mesh	900	971	Intel SGI	2500.1 8078.4	700	1775	Variable	10.	6.67	50.	---
bl22	2D Stress	Generalized plane strain, large thickness	900	972	Intel	7662	600	1550	Al alloy	10.	6.67	50.	Large
bc22	2D Stress	Generalized plane strain, small thickness	900	972	Intel	4312.1	600	1550	Al alloy	10.	6.67	50.	25.0 / 1.289
bh22	2D Stress	Generalized plane strain, smaller thickness	900	972	Intel	4201.5	600	1550	Al alloy	10.	6.67	50.	10.0 / 1.289
bi22	2D Stress	Plane stress	900	971	Intel	3557.0	600	1550	Al alloy	10.	6.67	50.	10.0 / 1.289
bi22	2D Stress	Generalized plane strain for substrate, plane stress for clad	900	972	Intel	3047.8	600	1550	Al alloy	10.	6.67	50.	10.0 / 1.289
cl22	2D Temp	Thick substrate, short clad bead	900	971	Intel	838.2	600	1550	Al alloy	10.	25.4	40.	---
cl24	2D Temp	Thick substrate, short clad bead	900	971	Intel	810.4	700	1775	Composite	10.	25.4	40.	---
el22	2D Temp	Thick substrate, long clad bead	1700	1811	Intel	2802.5	600	1550	Al alloy	20.	25.4	40.	---
el24	2D Temp	Thick substrate, long clad bead	1700	1811	Intel	2766.8	700	1775	Composite	20.	25.4	40.	---
dl22	2D Stress	Thick substrate, short clad bead	900	972	Intel	5278.8	600	1550	Al alloy	10.	25.4	40.	---
dl24	2D Stress	Thick substrate, short clad bead	900	972	Intel	4556.7	700	1775	Composite	10.	25.4	40.	---
fl24	2D Stress	Thick substrate, long clad bead	1700	1811	Intel	25175	700	1775	Composite	20.	25.4	40.	---
cn511	3D Temp	Curved shape	1750	2241	SGI	4650.4	800	27	Al alloy	10.	6.67	20.	7.5
cn521	3D Temp	Curved shape	1750	2241	SGI	4440.	800	27	Al alloy	10.	25.4	20.	7.5
cg533	3D Temp	Curved shape	1750	2241	SGI	25564.	1400	1550	Variable	10.	25.4	40.	25.
dn513	3D Stress	Curved shape	1750	2241	SGI	27804.	800	27	Al alloy	10.	6.67	20.	7.5
dn523	3D Stress	Curved shape	1750	2241	SGI	27212.	800	27	Al alloy	10.	25.4	20.	7.5
dn531	3D Stress	Curved shape	1750	2241	SGI	30821.	850	27	Al alloy	10.	25.4	40.	25.
lc141	3D Temp	Planar shape	1120	1607	Intel	934.5	1400	1550	Al alloy	12.89	29.6	38.7	28.3
lc131	3D Temp	Planar shape	1120	1607	Intel	2661.8	1400	1550	Variable	12.89	29.6	38.7	28.3
mc141	3D Stress	Planar shape	1120	1607	Intel	1265.8	1400	1550	Al alloy	12.89	29.6	38.7	28.3
mc131	3D Stress	Planar shape	1120	1607	Intel	2361.7	1400	1550	Variable	12.89	29.6	38.7	28.3

Vita

Augusto Moita de Deus was born in Grandola, Portugal on August 13th, 1966. He entered the University of Lisbon (UL), where he graduated in Physics in 1989. In 1989 he became a member of the Materials Engin. Dept. of Instituto Superior Tecnico (IST), Technical University of Lisbon, as an Assistant Lecturer, where since then and up to the present he has taught a number of undergraduate courses: Materials Science, Solid State Physics, Surfaces and Interfaces, Physical Metallurgy, Polymer Processing and Mechanics of Materials. He also joined the Laser Materials Processing Group of Professor R. Vilar. In 1993 he received his M.Sc. (APCC) degree in Materials Engin., with the thesis "*Analytical solutions for the calculation of the temperature field in laser irradiated materials*". In 1994 he joined the Center for Laser Aided Materials Processing of Professor J. Mazumder at the UIUC. He moved to Ann Arbor, MI, in 1997 where he became a member of the Center for Laser Aided Intelligent Manufacturing at the University of Michigan. In 1999 he returned to Portugal to resume his teaching duties at IST. Besides the topic of his dissertation, he has pursued research in other fields: he collaborated in a study of liquid foams and developed an analytical model of grain growth; he is also currently involved in developing FE models to estimate tempering effects in steel parts produced by laser cladding. (A resumé that includes published work can be found at www.eecs.umich.edu/~dedeus/resumamd.html.) He is pursuing to extend his academic career at IST, where he is to become an Assistant Professor upon completion of his dissertation. There he plans to develop and expand Modeling research in Materials Science and Mechanics of Materials. He is a member of ASME. He is married since 1989 with Alexandra, who is a Biology teacher and who is also involved in research activities at the Education Department, University of Lisbon. They have two children, Filipa, 12, and Miguel, 7.